

Gnathia bermudensis (Crustacea, Isopoda, Gnathiidae), a new species from the mesophotic reefs of Bermuda, with a key to *Gnathia* from the Greater Caribbean biogeographic region

Kerry A. Hadfield¹, Nikolaos V. Schizas², Tapas Chatterjee³, Nico J. Smit¹

1 Water Research Group, Unit for Environmental Sciences and Management, North-West University, Private Bag X6001, Potchefstroom, 2520, South Africa **2** University of Puerto Rico at Mayagüez, Department of Marine Sciences, PO Box 9000, Mayagüez, Puerto Rico, 00681, USA **3** Crescent International School, Bario, Govindpur, Dhanbad 828109, Jharkhand, India

Corresponding author: Kerry A. Hadfield (kerry.malherbe@nwu.ac.za)

Academic editor: T. Horton | Received 30 August 2019 | Accepted 21 October 2019 | Published 21 November 2019

<http://zoobank.org/82F35276-BF62-47A2-BCF6-5045351EB6F3>

Citation: Hadfield KA, Schizas NV, Chatterjee T, Smit NJ (2019) *Gnathia bermudensis* (Crustacea, Isopoda, Gnathiidae), a new species from the mesophotic reefs of Bermuda, with a key to *Gnathia* from the Greater Caribbean biogeographic region. ZooKeys 891: 1–16. <https://doi.org/10.3897/zookeys.891.39564>

Abstract

Gnathia bermudensis sp. nov. is described from mesophotic coral ecosystems in Bermuda; it is distinguished by pronounced and pointed supraocular lobes, two superior frontolateral processes and a weak bifid mediofrontal process, pereonite 1 not fused dorsally with the cephalosome, and large eyes. This is the first record of a species of *Gnathia* from Bermuda. A synopsis and key to the other *Gnathia* species from the Greater Caribbean biogeographic region is provided.

Keywords

Atlantic Ocean, benthic, ectoparasite, Nekton Mission, taxonomy

Introduction

Gnathiid isopods are temporary ectoparasites that occur in a variety of habitats ranging in depth, water currents, temperature, climate and salinity (Smit and Davies 2004). The parasitic juveniles feed on the blood and lymph of their fish hosts, while the non-feeding free-living adults are usually hidden in cavities, corals, or sponges (Hadfield et al. 2009). The taxonomic classification of these isopods is based almost exclusively on the morphology of the adult males, and this makes studies reliant on accurate species identification problematic as males can be difficult to obtain. Currently, there are 12 genera in the family Gnathiidae Leach, 1814 (Smit et al. 2019). Of these, the most speciose genus is *Gnathia* Leach, 1814, with 126 valid species (Boyko et al. 2008 onwards). To date, there are 14 known species of *Gnathia* from the Greater Caribbean biogeographic region (see Table 1 for a summary of known information on these species). In 1993, Müller (1993) proposed *Gnathia puertoricensis* Menzies & Glynn, 1968 as a junior synonym for *G. virginalis* Monod, 1926 based on the variation in the characters that separated these two species (granulation and tubercles on the anterior pereonites and cephalon). Although not recognised in subsequent publications on gnathiids from this region (George 2003; Farquharson et al. 2012), this synonymisation appears to still be valid and the information regarding both species is combined in Table 1.

Recently, there has been a growing interest in gnathiids from this region specifically regarding their role in cleaner interactions (Artim et al. 2017), food web ecology (Demopoulos and Sikkell 2015), and their role as potential vectors of blood parasites (Cook et al. 2015). However, all of this work has focused on a single species, *G. marleyi* Farquharson, Smit & Sikkell, 2012, and therefore it is also the only species from this region with known hosts for the parasitic larval stage. These host fishes include *Acanthurus bahianus* Castelnau, 1855; *Chaetodon capistratus* Linnaeus, 1758; *Epinephelus guttatus* (Linnaeus, 1758); *Haemulon flavolineatum* (Desmarest, 1823); *H. plumieri* (Lacepede, 1801); *H. sciurus* (Shaw, 1803); *Holocentrus rufus* (Walbaum, 1792); *Lutjanus apodus* (Walbaum, 1792); *L. griseus* (Linnaeus, 1758); *Scarus taeniopterus* Desmarest, 1831; *Sparisoma aurofrenatum* (Valenciennes, 1840); *Stegastes diencaeus* (Jordan & Rutter, 1897); and *S. planifrons* (Cuvier, 1830) (see Farquharson et al. 2012).

Bermuda forms part of this Greater Caribbean biogeographic region in the North Atlantic Ocean (Robertson and Cramer 2014). It is situated on the western side of the Sargasso Sea (high salinity, high temperatures and high biodiversity), and has the most northern coral reef system in the world. As part of the Nekton Foundation/XL-Catlin Deep-Ocean Survey – Mission 1 (www.nektonmission.org), fish (Stefanoudis et al. 2019a), zooplankton (Stefanoudis et al. 2019b), black corals (Wagner and Shuler 2017), macroalgae (Schneider et al. 2018, 2019) and other benthic communities (NVS pers. obs.) were studied. Macrofaunal collections from mesophotic reef ecosystems of Bermuda (MCEs) contained several specimens of a gnathiid isopod that did not correspond to currently described species. This isopod is here described as a new species of *Gnathia* and is the first gnathiid isopod to be recorded from Bermuda.

Table 1. Summary of the location, depth, size and references of 15 *Gnathia* species from the Greater Caribbean biogeographic region, including the 14 previously known species and the new species, *Gnathia bermudensis* sp. nov.

Species	Location	Depth (m)	Size (mm)	Substratum	References
<i>G. beethoveni</i> Paul & Menzies, 1971	Venezuela	95	3	mangrove roots; muddy and sandy bottoms; algae; seaweed; tunicates; seagrass	Paul and Menzies 1971; Dias et al. 2013
	Colombia (Santa Marta)	13–30		coral rubble	Müller 1988a
	Tobago				Kensley and Schotte 1994
	Mexico (Puerto Morelos)	3–12	1.8	coral rubble	Monroy-Velázquez and Alvarez 2016; Monroy-Velázquez et al. 2017
<i>G. bermudensis</i> sp. nov.	Bermuda	56–90	1.7–2.2	loose gravel and sediment (associated with corals); algae; sponges; rodoliths	Present study
<i>G. brucei</i> George, 2003	USA (North Carolina)	1000–1020	2.8–3.2		George 2003
<i>G. calsi</i> Müller, 1993	Martinique, French Antilles	0–2	1.9	dead corals	Müller 1993
<i>G. gonzalezi</i> Müller, 1988	Colombia (Santa Marta)	12–30	1.5	coral rubble	Müller 1988a
<i>G. hewinguayi</i> Ortiz & Lalana, 1997	Cuba (Cojimar Bay)	2	3	wood pile	Ortiz and Lalana 1997
<i>G. johanna</i> Monod, 1926	US Virgin Islands (St. John)	29–46	2–2.16		Monod 1926; Müller 1988b
	Colombia				Kensley and Schotte 1990
	Venezuela			seagrass beds; muddy bottom	Dias et al. 2013
<i>G. magdalenensis</i> Müller, 1988	Colombia (Santa Marta)	6–30	2.8	coral rubble	Müller 1988a
	Belize				Kensley and Schotte 1989
<i>G. marleyi</i> Farquharson, Smit & Sikkel, 2012	Mexico (Puerto Morelos)	3–12		coral rubble	Monroy-Velázquez et al. 2017
	St. John, US Virgin Islands; Bahamas; British Virgin Islands (Guana Island); Puerto Rico; Saba (Lesser Antilles)	3–5	2.6–3.7	several host fish	Farquharson et al. 2012
	Cuba (Cayo Matias)	20	2.6–3.3	algae	Ortiz et al. 2012
<i>G. micheli</i> Ortiz, Winfield & Varela, 2012	Cuba (Cayo Matias)	20	2.6–3.3	algae	Ortiz et al. 2012
<i>G. rathi</i> Kensley, 1984	Belize (Carrie Bow Cay)	0.5–128	1.6–1.9	rubble	Kensley 1984
<i>G. samariensis</i> Müller, 1988	Colombia (Santa Marta)	30	1.7	coral rubble	Müller 1988a
<i>G. triospathiona</i> Boone, 1918	USA (Florida)	200	8.8		Boone 1918
<i>G. vellosa</i> Müller, 1988	Colombia (Santa Marta)	25–30	1.5	sponges and hydroids	Müller 1988a
	Venezuela			seagrass beds; mangrove roots; algae	Dias et al. 2013
	Mexico (Puerto Morelos)	6–12	2.7	coral rubble	Monroy-Velázquez and Alvarez 2016; Monroy-Velázquez et al. 2017
<i>G. virginalis</i> Monod, 1926 Syn: <i>G. puertoricensis</i> Menzies & Glynn, 1968	US Virgin Islands	29	2.2		Monod 1926
	Puerto Rico	0–3	3		Menzies and Glynn 1968
	Cuba				Ortiz 1983; Müller 1988a
	Belize (Carrie Bow Cay)			rubble	Kensley 1984
	Colombia (Santa Marta)	0–30	2	coral rubble; under stones; fouling on harbour pilings	Müller 1988a
	Martinique, French Antilles	0.5–2		seagrass beds; dead corals; under stones	Müller 1993
	Venezuela			mangrove roots; seagrass beds; muddy bottom; algae	Dias et al. 2013
	Mexico (Puerto Morelos)	6–12	2.2	coral rubble	Monroy-Velázquez and Alvarez 2016; Monroy-Velázquez et al. 2017

Materials and methods

All benthic samples were collected from 17 July to 14 August 2016 aboard the R/V “Baseline Explorer”. Mesophotic benthic surveys and sampling were conducted using Trimix rebreathing divers from the Global Underwater Explorers (GUE) down to 94 m around the edge of the Bermuda platform. The sampling sites North Northeast (NNE), Plantagenet Bank, Spittal, and Tiger, were selected along the northeast, southeast and southern slopes of the Bermuda platform, respectively (Figure 1). During the same mission, two two-person Triton Class Submersibles (Nomad and Nemo; Vero Beach, FL, United States) equipped with an arm manipulator assisted in sample collection down to 300 m. Divers collected macroalgae, loose gravel, bottom sediment, rhodoliths, sponges, and hard and soft corals to characterise the biodiversity of the Bermudian mesophotic reefs. The depth range for each sample was noted. Once the substrata were brought onto the research vessel, they were placed on a 0.063 μm sieve and washed thoroughly with filtered water. Meiofauna and macrofauna associated with the substrata were captured on the 0.063 μm sieve and preserved in > 95 % ethanol. The preserved samples were sorted, placed in 95 % ethanol, and stored at -20 °C until further processing. Research permits for Bermuda were issued by the Department of Environment and Natural Resources, Bermuda (No. 2016070751).

From these samples, several gnathiids were cleaned and prepared for scanning electron microscopy (SEM; PhenomWorld). Gnathiids were also observed and drawn using an Olympus BX41 compound microscope and an Olympus SZX7 dissecting microscope with a camera lucida. Appendages were removed with the aid of dissecting needles and forceps and stained using lignin pink.

The species description was prepared in DELTA (DEscriptive Language for TAXonomy) using a general Gnathiidae character set (as used in Svavarsson and Bruce 2012). The description is based on the adult male gnathiid. Terminology follows Monod (1926), Cohen and Poore (1994) and Svavarsson and Bruce (2012, 2019). Isopod classification follows that of Brandt and Poore (2003).

Material is deposited in the Natural History Museum of Bermuda.

Taxonomy

Suborder Cymothoida Wägele, 1989

Superfamily Cymothooidea Leach, 1814

Family Gnathiidae Leach, 1814

Genus *Gnathia* Leach, 1814, restricted syn.

Gnathia Leach, 1814: 386–402; Monod 1926: 326–329 (part); Cohen and Poore 1994: 343–346.

Anceus Risso, 1816: 8.

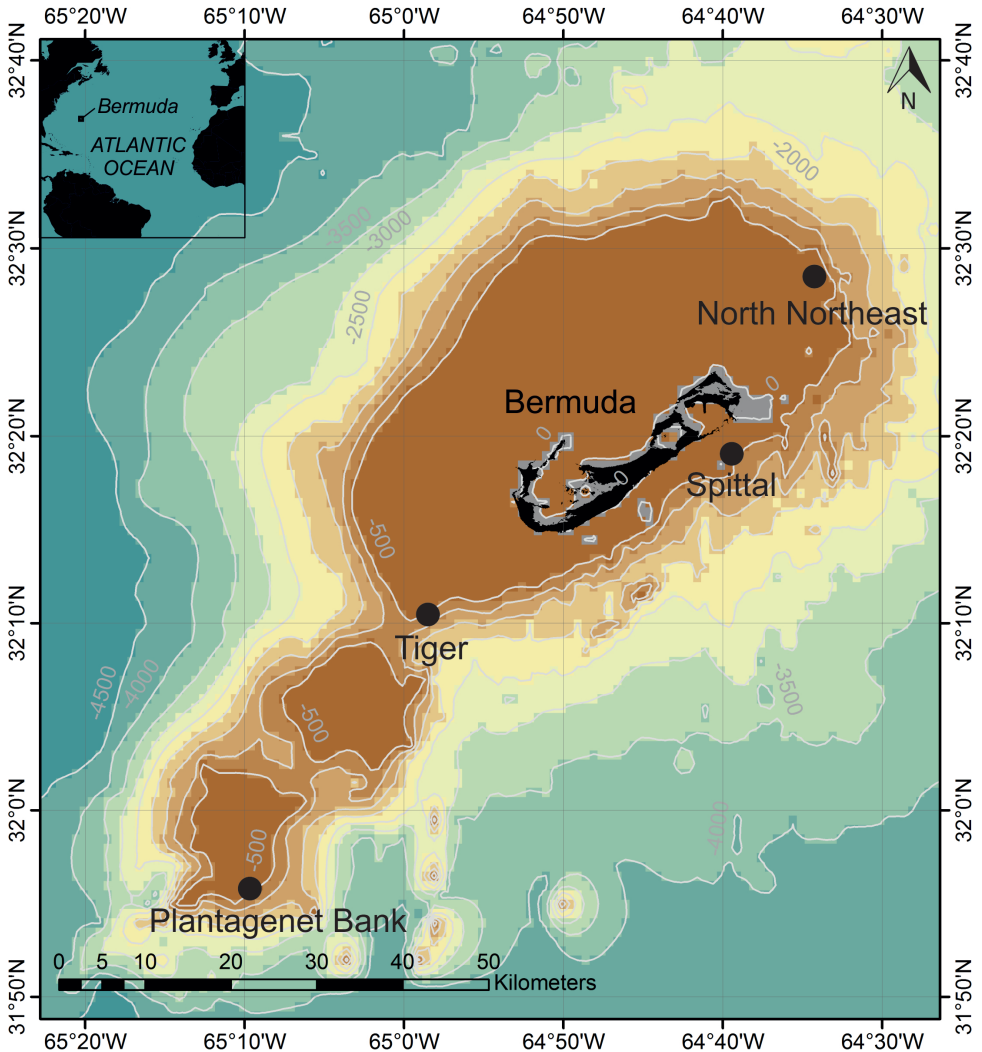


Figure 1. Map of collection sites around Bermuda. Data overlay GEBCO_2014 Grid which provides 30 arc-second global grid of elevations. Depth contours in meters.

Praniza Latreille, 1817: 54.

Zuphea Risso, 1826: 104.

Gnathia (*Gnathia*) s.s.: Monod 1926: 329 (part).

Gnathia (*Perignathia*): Monod 1926: 554–555 (not *Perignathia* Monod, 1922).

Type species. *Gnathia termitoides* Leach, 1814, by monotypy (see Cohen and Poore 1994).

Diagnosis. Frontal margin of cephalosome generally straight (not deeply excavated), with frontal processes. Mandibles not elongate, usually with mandibular incisor and dentate mandibular blade. Paraocular ornamentation and/or a dorsal sulcus may

be present on cephalosome. Pereonite 1 possibly immersed in cephalosome. Pylopod broad and distinct, with two or three articles, operculate; article 1 enlarged, generally with dense external margin of plumose setae; article 3 reduced or absent.

Remarks. *Gnathia* can be identified by the presence of frontal processes, a straight frontal border, a broad 2 or 3 articulated pylopod, and non-extended mandibles with a dentate blade.

It is the most speciose genus in the family Gnathiidae (currently with 126 valid species). *Gnathia* is a cosmopolitan genus, commonly found in coral-reef habitats, and its parasitic larvae have been reported from both teleost and elasmobranch hosts (Smit and Davies 2004). The most recent revision of this genus was by Cohen and Poore (1994).

***Gnathia bermudensis* sp. nov.**

<http://zoobank.org/5FD1EC92-2EE5-40E8-8BB8-0C47255A73A2>

Figures 2–4

Material examined. Holotype. BERMUDA • 1 ♂ (2.2 mm TL); Plantagenet Bank (31°56.55'N, 65°09.29'W); 56 m; 12 Aug 2016; Diver 2, from sediment; Sample ID BEX 2016-449 (BAMZ 2016-338-147).

Paratypes. BERMUDA • 3 ♂♂ (1.9–2.1 mm TL) (one dissected), 1 ♂ used for SEM (1.8 mm TL), 1 ♀ (1.6 mm TL); same info as holotype (BAMZ 2016-338-148).

Other material. BERMUDA • 4 ♂♂ (1.8–1.9 mm TL) (one dissected); Spittal (32°19.119'N, 64°39.437'W); 45 m; 3 Aug 2016; sediment from *Montastraea cavernosa* (Linnaeus, 1767) corals, Divers 39; Sample ID BEX 2016-227, Parent BEX2016-225 (sediment from several *Montastraea cavernosa* colonies) (BAMZ 2016-338-149) • 1 ♂ (2.0 mm TL); NNE (32°28.59'N, 64°34.46'W); 90 m; 4 Aug 2016; Event Divers; Sample ID BEX 2016-250, Parent BEX2016-248 (BAMZ 2016-338-150) • 1 zuphea (Z1) (0.45 mm TL); NNE (32°28.59'N, 64°34.46'W); 4 Aug 2016; algae substrate; Sample ID BEX 2016-251 • 1 ♂ used for SEM (1.7 mm TL); Spittal (32°19.119'N, 64°39.437'W); from rhodolith collected between 82–152 m; 7 Aug 2016; Dive 22, Nomad 1 (a Triton Submersible); Sample ID BEX 2016-299, Parent BEX2016-0265 • 1 ♂ (2.0 mm TL), 1 ♀ (1.9 mm TL), 1 zuphea (0.8 mm TL); Tiger 4 (32°11.17'N, 64°58.36'W); 7 Aug 2016; Divers 12, from sediment; Sample ID BEX 2016-304, Parent BEX2016-0282 (rhodolith with red encrusting sponge, > 40 m) (BAMZ 2016-338-151) • 2 ♂♂ (1.9–2.0 mm TL); Spittal (32°19.119'N, 64°39.437'W); 77 m; 11 Aug 2016; wash from rhodolith; Sample ID BEX 2016-428 • 1 ♂ (2.0 mm TL), 1 praniza (P3) (2.3 mm TL), 1 zuphea (Z1) (0.5 mm TL); Spittal (32°19.119'N, 64°39.437'W); 77 m; 11 Aug 2016; Diver 30; Sample ID BEX 2016-430 • 4 zuphea (Z1) (0.5 mm TL); Plantagenet Bank (31°56.55'N, 65°09.29'W); 56 m; 12 Aug 2016; Divers 2; Sample ID BEX 2016-450 • 2 ♂♂ (1.7–1.9 mm TL) (one used for SEM); Plantagenet Bank (31°56.55'N, 65°09.29'W); 56 m; 12 Aug 2016; Divers 6; Sample ID BEX 2016-451. All samples were collected by GUE technical divers except Sample ID BEX 2016-299, Parent BEX2016-0265, which was collected by a Triton Submersible.

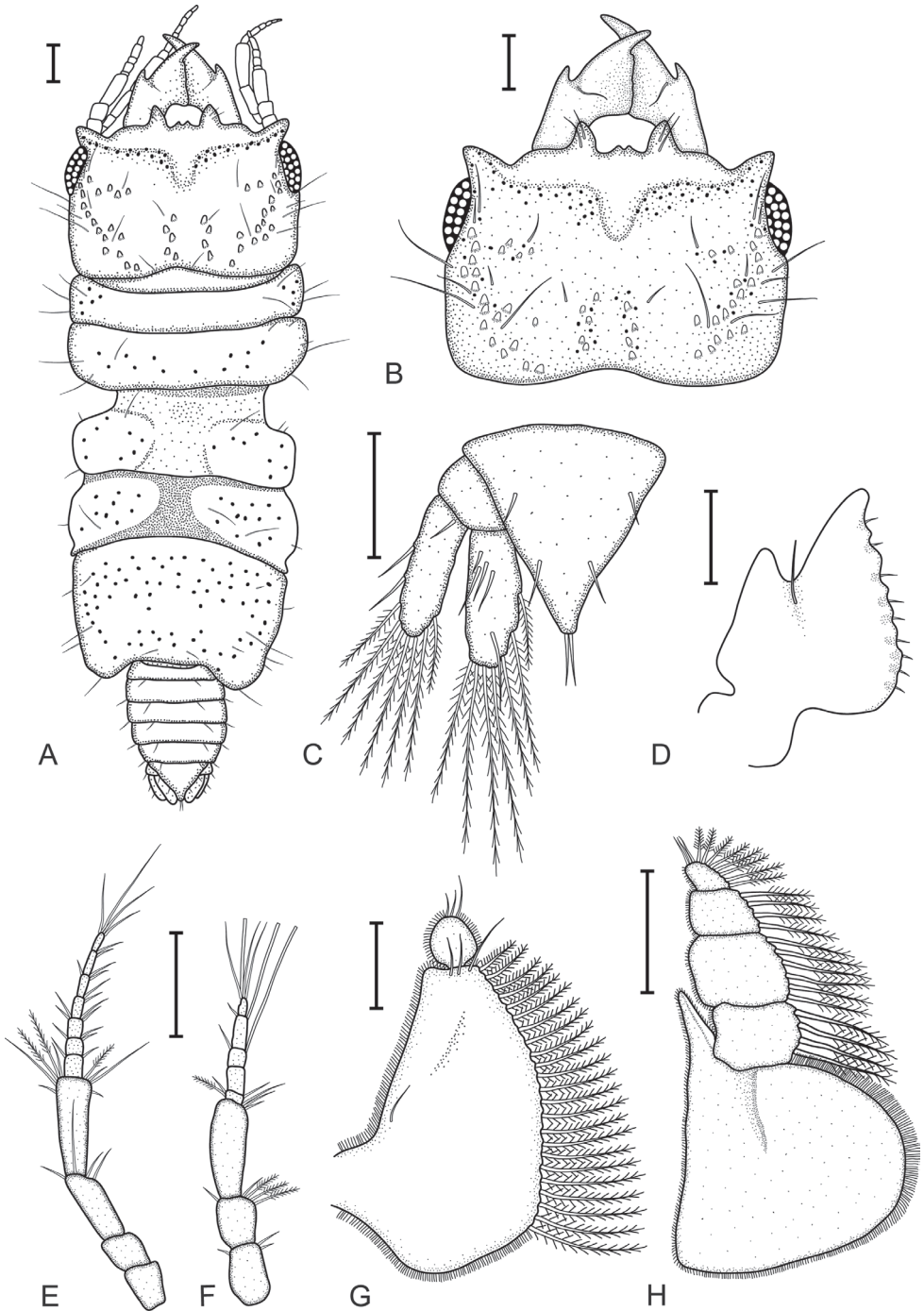


Figure 2. *Gnathia bermudensis* sp. nov. (BAMZ 2016-338-147), male holotype (2.2 mm TL) **A** dorsal view **B** dorsal view of cephalosome **C** dorsal view of pleotelson and uropods **D** dorsal view of mandible **E** antenna **F** antennula **G** pylopod **H** maxilliped. Scale bars: 100 μ m.

Description of male. *Body* 2.3 times as long as greatest width, widest at pereonite 3; dorsal surfaces sparsely punctate, sparsely setose. *Cephalosome* quadrate, 0.7 as long as wide, lateral margins sub-parallel; dorsal surface with sparse granules; dorsal sulcus narrow, shallow, short; translucent region absent; paraocular ornamentation strongly developed, posteromedian tubercle present. *Frontolateral processes* present. *Frontal margin* slightly produced. *External scissura* present, wide, shallow. *Mediofrontal process* present, weak, bifid, without fine setae. *Supraocular lobe* pronounced, pointed; accessory supraocular lobe not pronounced. *Superior frontolateral process* present, single, strong, conical, with two long simple setae. *Inferior frontolateral process* absent. *Mesioventral margin* concave. *Eyes* present, elongate, 0.3 times as long as cephalosome length, bulbous, standing out from head surface, ommatidia arranged in rows, eye colour black.

Pereon lateral margins subparallel, with few setae; anteriorly with sparse fine granules. *Pereonite 1* not fused dorsally with cephalosome; dorsolateral margins fully obscured by cephalosome. *Pereonite 2* wider than pereonite 1. *Areae laterales* present on pereonite 5. *Pereonite 6* without lobi laterales; lobuii weak, globular. *Pleon* covered in pectinate scales, epimera not dorsally visible on all pleonites. *Pleonite 1* lateral margins with one pair of simple setae, with one pair of simple setae medially. *Pleotelson* as long as anterior width, covered in pectinate scales. Pleotelson lateral margins finely serrate, anterolateral margins weakly convex, with two submarginal setae; posterolateral margin distally weakly concave, with two submarginal setae; apex with two setae.

Antennula peduncle article 2 0.8 times as long as article 1; article 3 1.9 times as long as article 2, 2.7 times as long as wide; flagellum 1.1 times as long as article 3, with five articles; article 3 with one aesthetasc seta and one simple seta; article 4 with one aesthetasc seta and one simple seta; article 5 terminating with one aesthetasc seta and three simple setae. *Antenna* peduncle article 4 2.5 times as long as wide, twice as long as article 3, and four simple setae; article 5 1.3 times as long as article 4, 2.8 times as long as wide, inferior margin with three penicillate setae, with six simple setae; flagellum 1.5 times as long as article 5, with seven articles.

Mandible 0.4 as long as width of cephalosome, triangular, weakly curved, evenly; apex 42% total length; mandibular seta present. *Incisor* dentate. *Blade* present, dentate, weakly convex, dentate along 100% of margin. *Pseudoblade* absent; internal lobe absent; dorsal lobe absent; basal neck short; erisma present.

Maxilliped 5-articled; article 1 lateral margin with continuous marginal scale-setae; article 2 lateral margin with four plumose setae; article 3 lateral margin with six plumose setae; article 4 lateral margin with four plumose setae; article 5 with eight plumose setae; endite extending to mid-margin of article 3; without coupling setae.

Pylod first article 1.5 as long as wide, without distolateral lobe; posterior and lateral margins forming rounded curve; lateral margin with 23 large plumose setae; mesial margin with continuous scale-setae; distal margin with three simple setae; second article 1.1 as long as wide.

Pereopods 2–6 with long simple setae and randomly covered in pectinate scales; pereopod 2 with tubercles on carpus and basis to ischium. *Pereopod 2 basis* 2.8 times as long as greatest width, superior margin with five setae, inferior margin with two setae; ischium 0.6 times as long as basis, 2.6 as long as wide, superior margin with one seta,

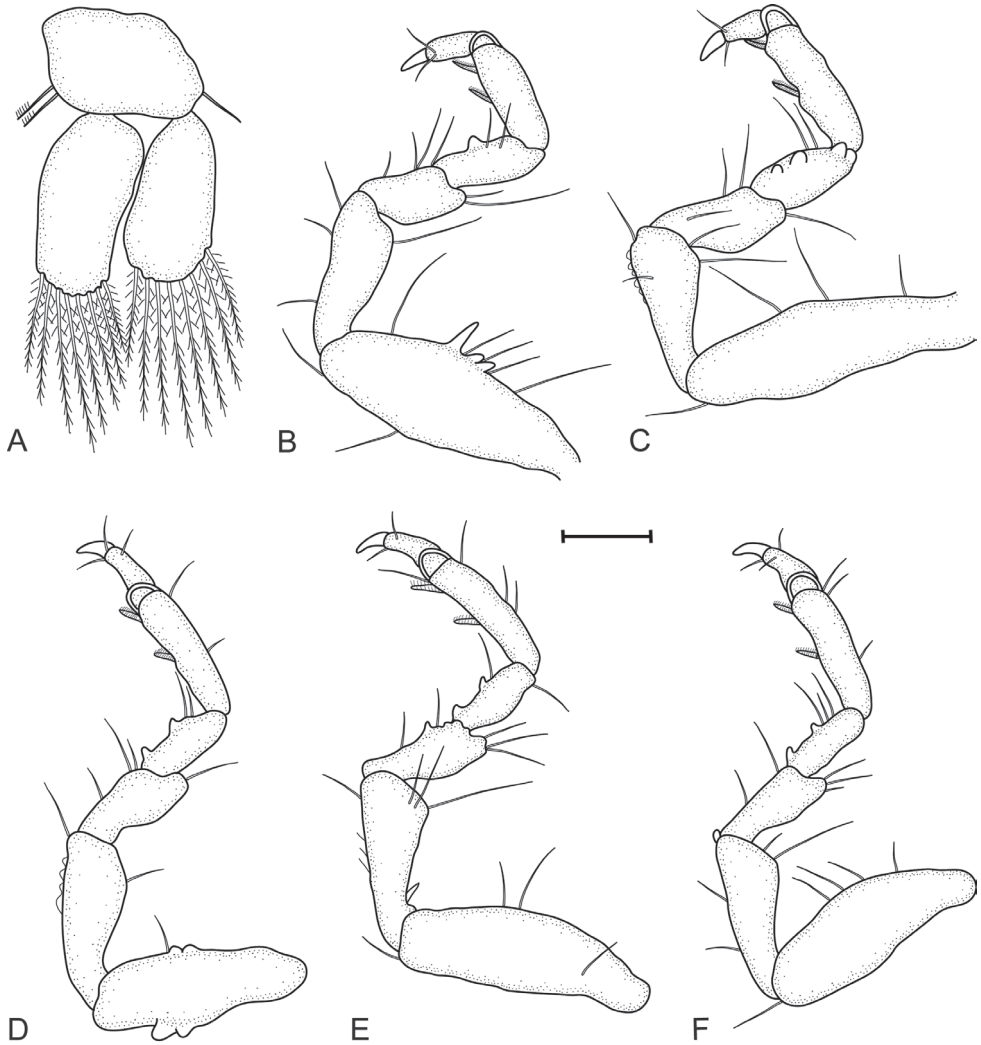


Figure 3. *Gnathia bermudensis* sp. nov. (BAMZ 2016-338-147), male holotype (2.2 mm TL) **A** pleopod 2 **B–F** pereopods 2–6, respectively. Scale bar: 100 μ m.

inferior margin with three setae; merus 0.5 as long as ischium, 1.5 as long as wide, superior margin with two setae, inferior margin with four setae; carpus 0.6 as long as ischium, 1.9 as long as wide, superior margin without setae, inferior margin with two setae; propodus 0.8 times as long as ischium, 2.8 times as long as wide, superior and inferior margins without setae, and two robust setae; dactylus 0.7 as long as propodus. *Pereopods 3 and 4* similar to pereopod 2. *Pereopod 5* similar to pereopod 6. *Pereopod 6* with tubercles on merus and carpus; basis 3.1 times as long as greatest width, superior margin with two setae, inferior margin with two setae; ischium 0.7 as long as basis, 2.7 as long as greatest width, superior margin with three setae, inferior margin with four setae; merus 0.6 as long as ischium, 2.1 times as long as wide, superior margin with three setae, inferior margin with two setae; carpus 0.6 as long as ischium, 1.7 times as

long as wide, superior margin and inferior margin with one seta; propodus 0.9 as long as ischium, 3.8 times as long as wide, superior margin with three setae, inferior margin with one seta, and two robust setae; dactylus 0.6 as long as propodus.

Penes opening flush with surface of sternite 7.

Pleopod 2 exopod 1.9 as long as wide, distally broadly rounded, with eight plumose setae; endopod 1.9 as long as wide, distally broadly rounded, with eight plumose setae; appendix masculina absent; peduncle 1.5 times as wide as long, mesial margin with two coupling setae, lateral margin with one simple seta.

Uropod rami extending beyond pleotelson, apices narrowly rounded. *Uropod endopod* 2.4 as long as greatest width, dorsally with five setae; lateral margin straight; proximomesial margin weakly convex, with seven long plumose setae. *Uropod exopod* not extending to end of endopod, 2.9 times as long as greatest width; lateral margin straight, with two simple setae; proximomesial margin straight, distally convex, mesio-distal margin with seven long plumose setae.

Etymology. The epithet *bermudensis* is for the country Bermuda, being the first *Gnathia* record from this island nation.

Distribution. Bermuda.

Hosts. Not known.

Remarks. *Gnathia bermudensis* sp. nov. may be identified by the produced frontal margin; presence of two superior frontolateral processes; a weak and bifid mediofrontal process; and pronounced and pointed supraocular lobes. The uropod rami extend past the posterior point of the pleotelson; pereonite 1 is not dorsally fused with the cephalosome; large eyes (0.3 as long as cephalosome length); and a weakly curved, dentate mandible.

This species is from a moderate depth of 56–90 m and was collected from several habitat types (algae, loose gravel, rhodoliths, sediment associated with scleractinian corals, muddy sand, and sponges) encompassing the mesophotic reef ecosystems of Bermuda. The Mesophotic Coral Ecosystems (MCEs) of Bermuda represent the most northern coral reef systems of the Atlantic; they are visually dominated by scleractinian corals at the upper depth limits, which are replaced gradually at greater depths by rhodoliths, macroalgae beds and fossilised reefs (Goodbody-Gringley et al. 2019). The new gnathiid species has been found on the mesophotic slopes of the main seamount (i.e., the main island of Bermuda) and the smaller seamount Plantagenet (Figure 1); therefore, it is expected to be found throughout the deeper reefs of Bermuda. Only four other species of *Gnathia* have been collected from greater depths in this region.

Gnathia bermudensis sp. nov. is most similar to *G. beethoveni* Paul & Menzies, 1971, *G. calsi* Müller, 1993, *G. johanna* Monod, 1926, *G. magdalenensis* Müller, 1988, and *G. virginialis* Monod, 1926 from the region. The frontal margin of *G. beethoveni* differs from *Gnathia bermudensis* in having less pronounced supraocular lobes, four frontolateral processes, a shallow median notch, and the cephalosome is lacking dorsal tubercles. *Gnathia calsi* also has a deeply notched mediofrontal process with two lobes (and setae), and well developed but angular supraocular lobes, not seen in *Gnathia bermudensis* sp. nov. *Gnathia johanna* is narrower than *Gnathia bermudensis* sp. nov., with less pronounced supraocular lobes and a single convex mediofrontal process (with setae) between the supe-

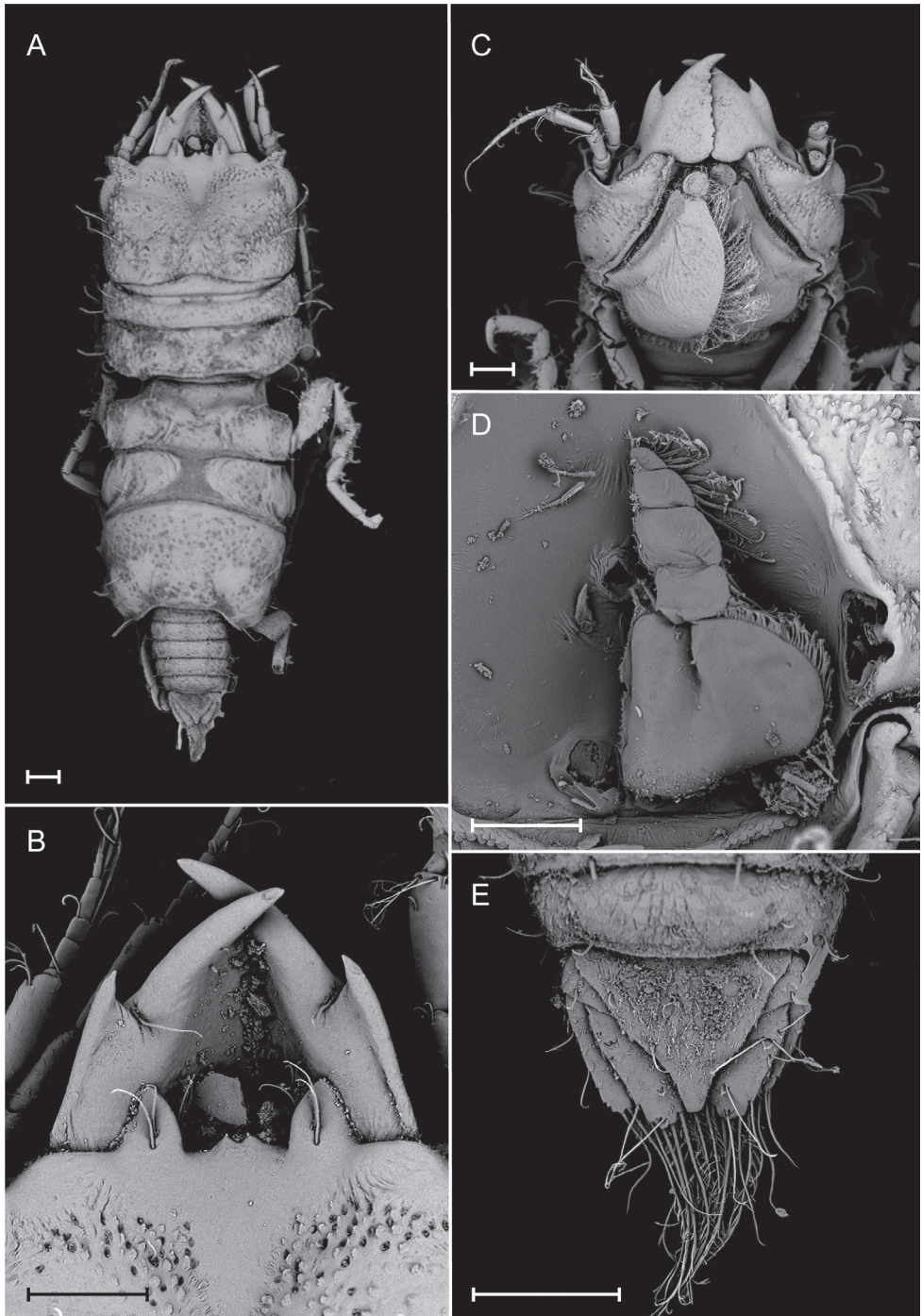


Figure 4. *Gnathia bermudensis* sp. nov. (BAMZ 2016-338-148), male paratype (1.8 mm TL) Scanning Electron Microscope (SEM) images. **A** dorsal view **B** frontal margin and mandibles **C** ventral view of cephalosome **D** maxilliped **E** dorsal view of pleotelson and uropods. Scale bars: 100 μ m.

rior frontolateral processes. *Gnathia magdalenensis* and *G. virginalis* differ from *Gnathia bermudensis* sp. nov. in having slightly pointed supraocular lobes, a single pointed medio-frontal process with setae, and a longer cephalosome that is fused with pereonite 1.

Although adult females and zuphea juveniles were collected with the males, they cannot be confidently linked to this species without molecular or ecological data. More collections and rearing of the gnathiid isopods would need to be made in the future for more information and validation of these different life stages, as well as to determine the hosts of the juvenile stages.

Key to members of the genus *Gnathia* known from the Greater Caribbean biogeographic region

This key is based on the morphological characters of the adult male:

- 1 Pereonite 5 elongate (quadrate); located in deeper waters (≥ 200 m); cephalon frontal border wavy (with 3 bifid frontal lobes or 3 tooth-like projections).....**2**
- Pereonite 5 similar in shape and size to pereonites 2–4; located in shallower waters (≤ 200 m); cephalon frontal border with regular frontal processes**3**
- 2 Frontal border produced with large quadrate projection; deep sea (> 1000 m); total body length measuring approximately 2.8–3.2 mm ***G. brucei***
- Frontal border with deep V-shaped groove; depths below 1000 m (approx. 200 m); total body length measuring approximately 8.8 mm.....
..... ***G. triospathiona***
- 3 Mediofrontal processes absent.....**4**
- Mediofrontal processes present**10**
- 4 Anterior margin of cephalon medially concave; robust body; cephalon wider than long and without granules or tubercles..... ***G. gonzalezi***
- Anterior margin of cephalon not medially concave; slender body; cephalon quadrate.....**5**
- 5 Only superior frontolateral processes present**6**
- Both superior and inferior frontolateral processes present**7**
- 6 Frontal margin slightly convex or straight; cephalon granular (tubercles)
..... ***G. rathi***
- Frontal margin convex with 4 medial setae; cephalon without tubercles.....
..... ***G. johanna***
- 7 Pylopod 2-articled; inferior frontolateral processes smaller in size than superior frontolateral processes ***G. micheli***
- Pylopod 3-articled; superior and inferior frontolateral processes similar in size.....**8**
- 8 Cephalon and body without granules or tubercles; sparsely setose
..... ***G. beethoveni***
- Cephalon with granules or tubercles; few to many slender setae over the body**9**

- 9 Supraocular lobes not well developed; narrow pleon and pleotelson longer than wide; pereonites 5 and 6 not clearly defined..... *G. hemingwayi*
- Supraocular lobes well developed; pleon with short setae and wider than long; pereonites 5 and 6 clearly defined *G. calsi*
- 10 Mediofrontal process bifid 11
- Mediofrontal process not bifid 12
- 11 Frontal margin medially concave; superior frontolateral processes weak with 3 or 4 simple setae on each process; supraocular lobe not pronounced.....
..... *G. marleyi*
- Frontal margin produced; superior frontolateral processes strong with 2 simple setae on each process; supraocular lobe pronounced and pointed
..... *G. bermudensis* sp. nov.
- 12 Cephalon with few or no granules or tubercles..... 13
- Cephalon with many small tubercles (finely granular)..... 14
- 13 Mediofrontal process with 2–4 simple setae; mandible with inner lobe.....
..... *G. magdalenensis*
- Mediofrontal process without any setae; mandible without inner lobe
..... *G. samariensis*
- 14 Cephalon approximately 1.7 times as wide as long; mandibular carina distally notched *G. vellosa*
- Cephalon approximately 1.2 times as wide as long; mandibular carina distally rounded *G. virginialis*

Acknowledgments

The authors and the Nekton Mission would like to thank SR Smith, J Pitt, T Trotts, and C Flook from the Bermudian Government for their assistance, advice and participation in the XL-Catlin Deep-Ocean Survey Bermuda Mission. We would also like to thank the crew and technicians of the Baseline Explorer, Brownies Global Logistics, and Triton Submersibles. This is contribution number 14 for Nekton and contribution number 355 for the NWU Water Research Group.

References

- Artim JM, Hook A, Grippo RS, Sikkil PC (2017) Predation on parasitic gnathiid isopods on coral reefs: a comparison of Caribbean cleaning gobies with non-cleaning microcarnivores. *Coral Reefs* 36: 1213–1223. <https://doi.org/10.1007/s00338-017-1613-6>
- Boone PL (1918) Description of ten new isopods. *Proceedings of the United States National Museum* 54: 591–604.
- Brandt A, Poore GCB (2003) Higher classification of the flabelliferan and related Isopoda based on a reappraisal of relationships. *Invertebrate Systematics* 17: 893–923. <https://doi.org/10.1071/IS02032>

- Boyko CB, Bruce NL, Hadfield KA, Merrin KL, Ota Y, Poore GCB, Taiti S, Schotte M, Wilson GDF (Eds) (2008 onwards) World Marine, Freshwater and Terrestrial Isopod Crustaceans database. *Gnathia* Leach, 1814. Accessed through: World Register of Marine Species. <http://www.marinespecies.org/aphia.php?p=taxdetails&id=118437> [on 2019-07-10]
- Cohen BF, Poore GCB (1994) Phylogeny and biogeography of the Gnathiidae (Crustacea: Isopoda) with descriptions of new genera and species, most from South-Eastern Australia. *Memoirs of the Museum of Victoria* 54: 271–397. <https://doi.org/10.24199/j.mmv.1994.54.13>
- Cook CA, Sikkel PC, Renoux LP, Smit NJ (2015) Blood parasite biodiversity of reef-associated fishes of the eastern Caribbean. *Marine Ecology Progress Series* 533: 1–13. <https://doi.org/10.3354/meps11430>
- Demopoulos AWJ, Sikkel PC (2015) Enhanced understanding of ectoparasite-host trophic linkages on coral reefs through stable isotope analysis. *International Journal for Parasitology: Parasites and Wildlife* 4: 125–134. <https://doi.org/10.1016/j.ijppaw.2015.01.002>
- Díaz YJ, Martín A, Herrera J (2013) Diversidad de isópodos (Crustacea: Isopoda) del Parque Nacional Morrocoy, Venezuela, y clave de identificación. *Boletín del Instituto Oceanográfico de Venezuela* 52: 33–60.
- Farquharson C, Smit NJ, Sikkel PC (2012) *Gnathia marleyi* sp. nov. (Crustacea, Isopoda, Gnathiidae) from the Eastern Caribbean. *Zootaxa* 3381: 47–61. <https://doi.org/10.11646/zootaxa.3381.1.3>
- George RY (2003) Two new species of gnathiid isopod Crustacea from the North Carolina coast. *Journal of the North Carolina Academy of Science* 119: 33–40.
- Goodbody-Gringley G, Noyes T, Smith SR (2019) Mesophotic Coral Ecosystems of Bermuda. In: Loya Y, Puglise KA, Bridge TCL (Eds) *Mesophotic Coral Ecosystems (MCEs)*. Springer International Publishing, 31–45. <https://doi.org/10.1007/978-3-319-92735-0>
- Hadfield KA, Smit NJ, Avenant-Oldewage (2009) Life cycle of the temporary fish parasite, *Gnathia pilosus* (Crustacea: Isopoda: Gnathiidae) from the east coast of South Africa. *Journal of the Marine Biological Association of the United Kingdom* 89: 1331–1339. <https://doi.org/10.1017/S0025315409000587>
- Kensley B (1984) *The Atlantic Barrier Reef Ecosystem at Carrie Bow Cay, Belize, III: New marine Isopoda*. Smithsonian Institution Press, Washington, DC, 81 pp. <https://doi.org/10.5479/si.01960768.24.1>
- Kensley B, Schotte M (1989) *Guide to the marine isopod crustaceans of the Caribbean*. Smithsonian Institution Press, Washington D.C., 308 pp. <https://doi.org/10.5962/bhl.title.10375>
- Kensley B, Schotte M (1994) Marine isopods from the Lesser Antilles and Colombia (Crustacea: Peracarida). *Proceedings of the Biological Society of Washington* 107: 482–510.
- Latreille PA (1817) Les Crustacés, les Arachnides, et les Insectes. In: Cuvier G (Ed.) *Le Règne Animal, distribué d'après son organisation, pour servir de base à l'histoire naturelle des animaux et d'introduction à l'anatomie comparée*. Vol. 3. D'Éterville, Paris, 653 pp. <https://doi.org/10.5962/bhl.title.41460>
- Leach WE (1814) Crustaceology. In: *Brewster's Edinburgh Encyclopedia*. 7: 383–437. <https://doi.org/10.5962/bhl.title.30911>
- Menzies RJ, Glynn PW (1968) *The common marine isopod Crustacea of Puerto Rico: A handbook for marine biologists*. Martinus Nijhoff, The Hague, Netherlands, 133 pp.

- Monod T (1926) Les Gnathiidae. Essai monographique (morphologie, biologie, systématique). Mémoires de la Société des Sciences Naturelles du Maroc 13: 1–668.
- Monroy-Velázquez V, Alvarez F (2016) New records of isopods (Crustacea: Peracarida: Isopoda) from the Mesoamerican Reef at Puerto Morelos, Quintana Roo, Mexico. Check List 12: 1938. <https://doi.org/10.15560/12.4.1938>
- Monroy-Velázquez V, Rodríguez-Martínez RE, Alvarez F (2017) Taxonomic richness and abundance of cryptic peracarid crustaceans in the Puerto Morelos Reef National Park, Mexico. PeerJ 5: e3411. <https://doi.org/10.7717/peerj.3411>
- Müller H-G (1988a) The genus *Gnathia* Leach (Isopoda) from the Santa Marta area, northern Colombia, with a review of Gnathiidea from the Caribbean Sea and Gulf of Mexico. Bijdragen tot de Dierkunde 58: 88–104. <https://doi.org/10.1163/26660644-05801008>
- Müller H-G (1988b) Redescription of *Gnathia johanna* Monod, 1926 (Isopoda) from St. John, Virgin Islands. Bulletin Zoölogisch Museum Universiteit van Amsterdam 11(15): 129–135.
- Müller H-G (1993) Marine Isopoda from Martinique, French Antilles: Cirolanidae and Gnathiidae (Crustacea: Cymothoidea). Cahiers de Biologie Marine 34: 29–42.
- Ortiz M (1983) Guía para la identificación de los isópodos y tanaidáceos (Crustacea: Peracarida), asociados a los pilotes de las aguas Cubanas. Revista de Investigaciones Marinas 4: 3–20.
- Ortiz M, Lalana R (1997) *Gnathia hemingwayi* especie nueva (Isopoda, Gnathiidea) de la costa noroccidental de Cuba. Revista de Investigaciones Marinas 18: 21–26.
- Ortiz M, Winfield I, Varela C (2012) First records of peracarid crustaceans from the Cayo Matias Ocean Blue Hole, SW Cuba, with the description of two new species. Zootaxa 3505: 53–66. <https://doi.org/10.11646/zootaxa.3505.1.4>
- Paul AZ, Menzies RJ (1971) Sub-tidal isopods of the Fosa de Cariaco, Venezuela, with descriptions of two new genera and twelve new species. Boletín de Instituto Universidade Oriente 10: 29–48.
- Risso A (1816) Histoire naturelle des Crustacés des environs de Nice. Paris: Librairie Grecque-Latine-Allemande. 175 pp. <https://doi.org/10.5962/bhl.title.8992>
- Risso A (1826) Histoire naturelle des principales productions de l'Europe méridionale et particulièrement de celles des environs de Nice et des Alpes Maritimes, vol. 5. FG Levrault, Paris, 403 pp. <https://doi.org/10.5962/bhl.title.58984>
- Robertson DR, Cramer KL (2014) Defining and dividing the Greater Caribbean: Insights from the biogeography of shorefishes. PLoS ONE 9(7): e102918. <https://doi.org/10.1371/journal.pone.0102918>
- Schneider CW, Lane CE, Saunders GW (2018) A revision of the genus *Cryptonemia* (Halymeniaceae, Rhodophyta) in Bermuda, western Atlantic Ocean, including five new species and *C. bermudensis* (Collins & M. Howe) comb. nov. European Journal of Phycology 53: 350–368. <https://doi.org/10.1080/09670262.2018.1452297>
- Schneider CW, Papolizio TR, Saunders GW (2019) Collections from the mesophotic zone off Bermuda reveal three species of Kallymeniaceae (Gigartinales, Rhodophyta) in genera with transoceanic distributions. Journal of Phycology 55: 414–424. <https://doi.org/10.1111/jpy.12828>
- Smit NJ, Davies AJ (2004) The curious life-style of the parasitic stages of gnathiid isopods. Advances in Parasitology 58: 289–391. [https://doi.org/10.1016/S0065-308X\(04\)58005-3](https://doi.org/10.1016/S0065-308X(04)58005-3)

- Smit NJ, Bruce NL, Hadfield KA (2019) Parasitic Crustacea: State of knowledge and future trends. Springer International Publishing, 481 pp. <https://doi.org/10.1007/978-3-030-17385-2>
- Stefanoudis PV, Gress E, Pitt JM, Smith SR, Kincaid T, Rivers M, Andradi-Brown DA, Rowlands G, Woodall LC, Rogers AD (2019a) Depth-dependent structuring of reef fish assemblages from the shallows to the rariphotic zone. *Frontiers in Marine Science* 6 p. 357. <https://doi.org/10.3389/fmars.2019.00307>
- Stefanoudis PV, Rivers M, Ford H, Yashayaev IM, Rogers AD, Woodall LC (2019b) Changes in zooplankton communities from epipelagic to lower mesopelagic waters. *Marine Environmental Research* 146: 1–11. <https://doi.org/10.1016/j.marenvres.2019.02.014>
- Svavarsson J, Bruce NL (2012) New and little-known gnathiid isopod crustaceans (Cymothoidea) from the northern Great Barrier Reef and the Coral Sea. *Zootaxa* 3380: 1–33. <https://doi.org/10.11646/zootaxa.3380.1.1>
- Svavarsson J, Bruce NL (2019) New gnathiid isopod crustaceans (Cymothoidea) from Heron Island and Wistari Reef, southern Great Barrier Reef. *Zootaxa* 4609: 31–67. <https://doi.org/10.11646/zootaxa.4609.1.2>
- Wagner D, Shuler A (2017) The black coral fauna (Cnidaria: Antipatharia) of Bermuda with new records. *Zootaxa* 4344: 367–379. <https://doi.org/10.11646/zootaxa.4344.2.11>

A new lapsiine jumping spider from North America, with a review of Simon's *Lapsias* species (Araneae, Salticidae, Spartaeinae)

Wayne P. Maddison¹

¹ *Departments of Zoology and Botany and Beaty Biodiversity Museum, University of British Columbia, 6270 University Boulevard, Vancouver, British Columbia, V6T 1Z4, Canada*

Corresponding author: *Wayne P. Maddison* (wayne.maddison@ubc.ca)

Academic editor: *J. Miller* | Received 26 July 2019 | Accepted 27 September 2019 | Published 21 November 2019

<http://zoobank.org/26724E9C-ABBB-41E9-85A2-87021244E574>

Citation: Maddison WP (2019) A new lapsiine jumping spider from North America, with a review of Simon's *Lapsias* species (Araneae, Salticidae, Spartaeinae). ZooKeys 891: 17–29. <https://doi.org/10.3897/zookeys.891.38563>

Abstract

A new spider genus and species from México and Guatemala, *Amilaps mayana* **gen. et sp. nov.**, is described, distinct from other members of the jumping spider tribe Lapsiini (subfamily Spartaeinae) by its four retromarginal cheliceral teeth and the large sclerite cradling the embolus. It is the first living lapsiine known outside of South America. This tribe has received attention recently for new species and genera in Ecuador and Brazil, but Simon's original four species of *Lapsias*, described from Venezuela in 1900 and 1901, remain relatively poorly known. Accordingly, new illustrations of Simon's type material are given, and a lectotype is designated for *L. cyrboides* Simon, 1900. The three forms of females in Simon's material from Colonia Tovar, Aragua, are reviewed and illustrated, and they are tentatively matched with the three male lectotypes of his species from the same location.

Keywords

Guatemala, jumping spider, Lapsiini, México, Venezuela

Introduction

For more than 100 years after Eugene Simon's (1900) description of the jumping spider genus *Lapsias* Simon, 1900, the only known species were the four he described from Venezuela (Simon, 1900, 1901). Indeed, these were the only species described of the broader group now recognized as the Lapsiini, one of only two salticid groups in the New World that fall outside the major subfamily Salticinae (the other being the Lyssomaninae). Considerably more lapsiine diversity has been revealed since 2006 through work by Maddison (2006, 2012), Makhan (2007), Ruiz and Maddison (2012), and Ruiz (2013), giving us now five described genera containing 21 species (WSC 2019). All of the living lapsiine species known to date are from South America, but recently García-Villafuerte (2018) described a fossil of *Galianora* Maddison, 2006 from Miocene amber in Chiapas, México.

Here I report the north-westernmost known living lapsiine, *Amilaps mayana* sp. nov., from southern México and Guatemala. In addition, new illustrations of Simon's four species of *Lapsias* from Venezuela are provided to supplement Galiano's (1963) redescrptions, and the matching of males and females is reconsidered.

Materials and methods

The preserved specimens were examined under both dissecting microscopes and a compound microscope with reflected light. Photographs were taken under an Olympus SZ61 stereo microscope (bodies) and a Nikon ME600L compound microscope (palpi) and focus stacked using Helicon Focus 4.2.7. Drawings were made with a drawing tube on an Olympus BH-2 compound microscope (*Amilaps mayana* sp. nov.) and a Nikon ME600L compound microscope (Simon's species).

Terminology is standard for Araneae. Measurements are given in millimetres. Carapace length was measured from the base of the anterior median eyes not including the lenses to the rear margin of the carapace medially; abdomen length to the end of the anal tubercle.

Abbreviations

AME	anterior median eyes;	PLE	posterior lateral eyes;
ALE	anterior lateral eyes;	RTA	retrolateral tibial apophysis.
PME	posterior median eyes;		

Museum abbreviations

MCZ	Museum of Comparative Zoology, Harvard University (G. Giribet);
AMNH	American Museum of Natural History, New York (L. Prendini);
MNHN	Muséum national d'Histoire naturelle, Paris (C. Rollard).

Taxonomy

Amilaps gen. nov.

<http://zoobank.org/AEE550A1-9490-41C9-8D0E-EAF544D338F0>

Type species. *Amilaps mayana* sp. nov.

Etymology. An arbitrary combination of letters, composed to contain a reference to the Mayan word for spider (“äm”, Christensen 1987) and to *Lapsias*, to be treated grammatically as feminine.

Diagnosis. Differs from all described lapsiines in having a large sclerite (**p** in Fig. 3) cradling the tip of the embolus, and in having four retromarginal teeth on the chelicerae (two in all others; see Ruiz and Maddison 2012, Maddison 2012, Ruiz 2013). Differs from *Lapsias*, *Soesiladeepakius*, and *Thrandina* in lacking a prolateral pre-embolic spermophore loop (see Ruiz and Maddison 2012), although the loop may be present on the retrolateral side (see below under “Relationships”). Unlike most *Lapsias* species, *Amilaps* has the PME displaced medially, as far as the medial edge of the ALE.

Relationships. The four retromarginal cheliceral teeth suggest that *Amilaps* is outside a clade including all previously described lapsiine genera, which share the synapomorphy of a reduction to two teeth (Ruiz and Maddison 2012) from the plurident condition in other Spartaeninae. There are no clear characters linking *Amilaps* to any particular lapsiines: it lacks the highly reduced RTA of *Lapsias*, the round tegulum of *Galianora*, the large PME and robust median apophysis of *Thrandina*, and the many peculiarities of *Soesiladeepakius* and *Lapsamita*. The spermophore of *Amilaps* appears to lack the pre-embolic loop approaching the median apophysis, widespread in lapsiines (e.g., Figs 14, 21, 30, 41; Maddison 2012: figs 7, 11, 12; see Ruiz and Maddison 2012: character 17). In *Amilaps mayana* the spermophore does in fact closely approach the median apophysis (MA), but on the retrolateral side of the bulb. In ventral view, it passes just retrolateral to the MA, but in retrolateral view it can be seen to be curved, reaching its ventralmost point just proximal to the MA. If this is the same pre-embolic loop but displaced retrolaterally, it hints to the possibility that the base of the embolus of *A. mayana* may be unusually large, occupying a large proportion of the prolateral side of the bulb.

If *Amilaps* is outside the clade of previous lapsiines, then an open question is whether it belongs with them at all. The tribe Lapsiini has no known morphological synapomorphies (Maddison 2015) other than the reduction in cheliceral teeth (Ruiz and Maddison 2012). Our understanding of morphology gives little reason to expect that salticids in the Americas left over once salticines and lyssomanines are removed would form a clade, but the molecular data suggests this, at least among those species studied (Maddison et al. 2014). *Amilaps* is exactly that: a generalized salticid that is not a salticine or lyssomanine. Were it to have been found in New Guinea, *Amilaps* would fit equally happily among the cocalodines according to our current knowledge. Thus, its current placement among the lapsiines is tentative.

***Amilaps mayana* sp. nov.**

<http://zoobank.org/154D15D5-3292-4465-B6C6-11768434EDD6>

Figs 1–11

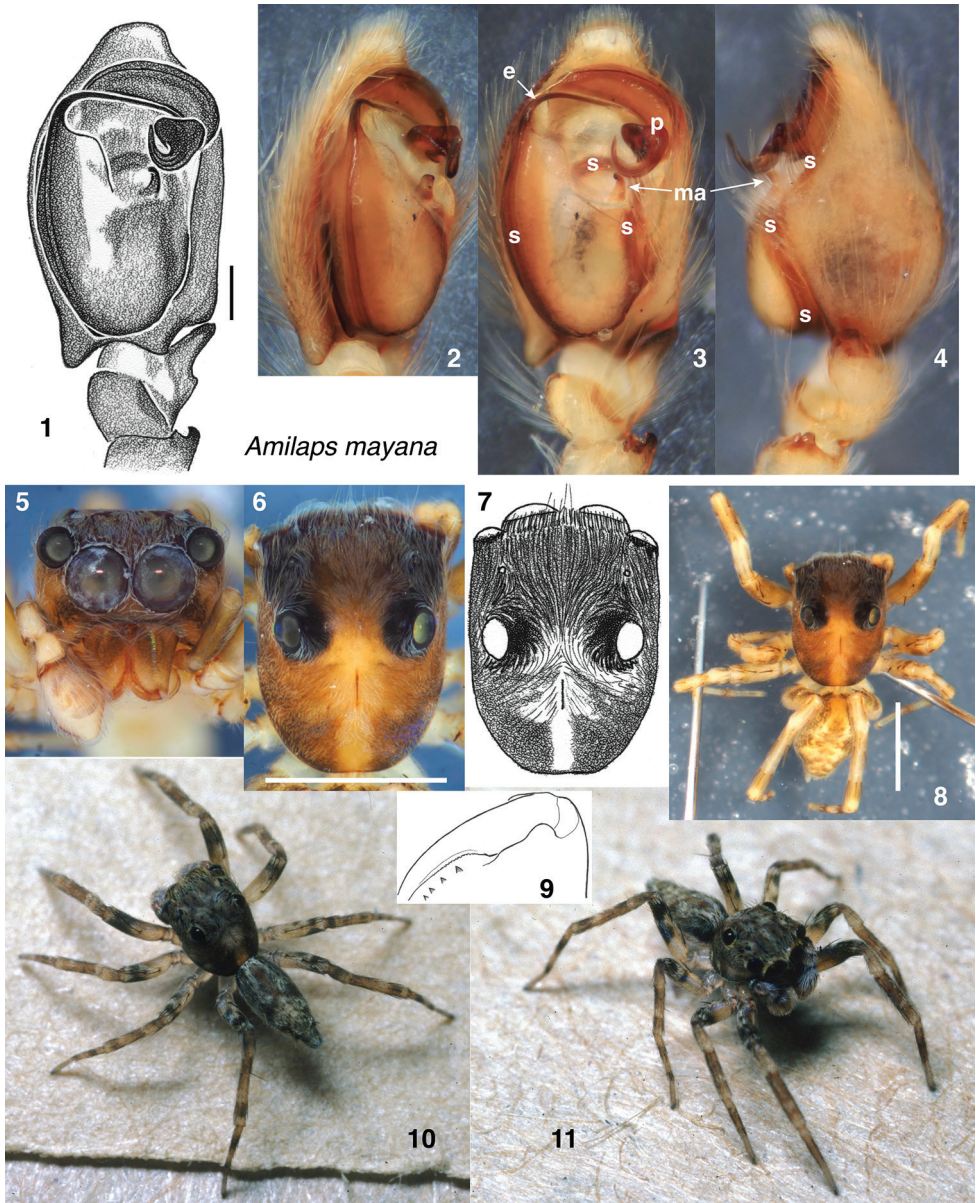
Type material. Holotype in MCZ: male, with label “MCZ, MEXICO: TABASCO: 2.4 km E of Teapa, Grutas de Cocona, ca. 17°33'N, 92°56'W 7 July 1983 W.Maddison 83-089 forested steep slope, ca. 250 ft. el.”. The recorded latitude is likely incorrect; the specimen was collected near the entrance to the Grutas, which is at ca. 17.564N, 92.929W.

Etymology. Refers to the distribution of this species in the lands of the Maya.

Description. Male (holotype). Carapace length 2.0; abdomen length 1.7. **Carapace** (Figs 6, 7) with long fovea; anterior eye row approx. as wide as carapace, and wider than posterior row. PME small, displaced medially to lie behind medial edge of ALE. Ocular area medium brown under alcohol and darker around eyes, dusted with dull brown and tan scales that are oriented concentrically around the unusually large PLE. Thoracic area brown, with paler medial longitudinal band, and paler spots just above each of the leg coxae. **Clypeus** (Fig. 5) narrow and with a few scattered whitish hairs and scales. **Chelicerae** vertical and relatively small. Four small but distinct teeth on retromargin of chelicerae (Fig. 9); promargin not observed (on the specimen from Guatemala, three promarginal teeth). **Palp** (Figs 1–4) with embolus arising on prolateral side, narrowing abruptly, then bending directly to the retrolateral, where it meets a large sclerotized projection (**p** in Fig. 3) that envelops it so completely that the terminal third of the embolus is most easily seen as a dark line within the projection; the tip of the embolus rests within the tip of the projection. The projection consists of a plate at the distal edge of the bulb, which then narrows before swelling and curving to a point that projects ventrally. (Regarding its homology to the conductor in *Lapsias*, see comments below.) Median apophysis distinct (separated from the tegulum by a membrane) but relatively small, almost hidden by the sclerotized projection. Cymbium with proximal prolateral conical projection. Retrolateral tibial apophysis a short flange (Fig. 4) whose ventral edge extends proximally and forms a round pocket facing retrolateral side. Patella with two retrolateral apophyses, the larger one being hooked. **Legs** (Figs 10, 11) pale honey-coloured, darkening to nearly black on distal half of femora, and with broad darker annuli on tibiae and metatarsi. First tibia macrosetae as follows: three pairs of ventral, two to three anterior lateral, two posterior lateral, and one dorsal. First metatarsus macrosetae as follows: two ventral pairs, two anterior lateral, and two posterior lateral. Fourth legs distinctly longest; leg formula 4132. **Abdomen** (Figs 8, 10) brown above, with paler undulating medial longitudinal pale band.

Additional material. Male in AMNH from Guatemala: Petén: Cueva de Olla, Poptún. 8 April 1989. A. Cobb. The specimen is missing legs and is mostly disarticulated, but its structure including the distinctive palp matches the holotype.

Data for material examined. MÉXICO • 1 ♂, holotype; Tabasco, 2.4 km E of Teapa, Grutas de Cocona; 17.564N, 92.929W; 7 Jul. 1983; W. Maddison leg.; collecting event WPM#83-089; MCZ. GUATEMALA • 1 ♂; Petén, Poptún, Cueva de Olla; 8 Apr. 1989; A. Cobb, leg.; AMNH.



Figures 1–11. *Amilaps mayana*, sp. nov, male holotype **1–4** palp **1** ventral view **2** prolateral view **3** ventral view **4** retrolateral view **5** face **6, 7** carapace, dorsal view **8** body in alcohol **9** posterior ventral view of chelicera showing four retromarginal teeth **10, 11** living specimen. Abbreviations: e embolus, s spermphore, ma median apophysis, p sclerotized projection serving as conductor. Scale bars: 0.1 mm (**1**); 1.0 mm (**6, 8**).

Natural history. My field notes for the holotype indicate it was found on a limestone rock face, and the back of the vial’s label says “on limestone cliff face on forested slope”. Both the holotype from México and the male from Guatemala (according to its locality) were associated with caves. The holotype was not in the cave, but on a cliff near the cave.

***Lapsias* Simon, 1900**

Type species. *Lapsias estebanensis* Simon, 1900, by original designation.

Although Galiano (1963) redescribed Simon's original four species, her illustrations are limited in number and detail. Thus, I give new figures of Simon's original four species, including the first published figures of their bodies and more detailed illustrations of their genitalia. Among Simon's specimens are three forms of female, only one of which (under *L. cyrboides* Simon, 1900) was described by Simon and Galiano. As these females are all from the same site (Colonia Tovar) from which the males of three *Lapsias* species were described, we are faced with a puzzle as to which females match which males. This is considered below under the notes for each species.

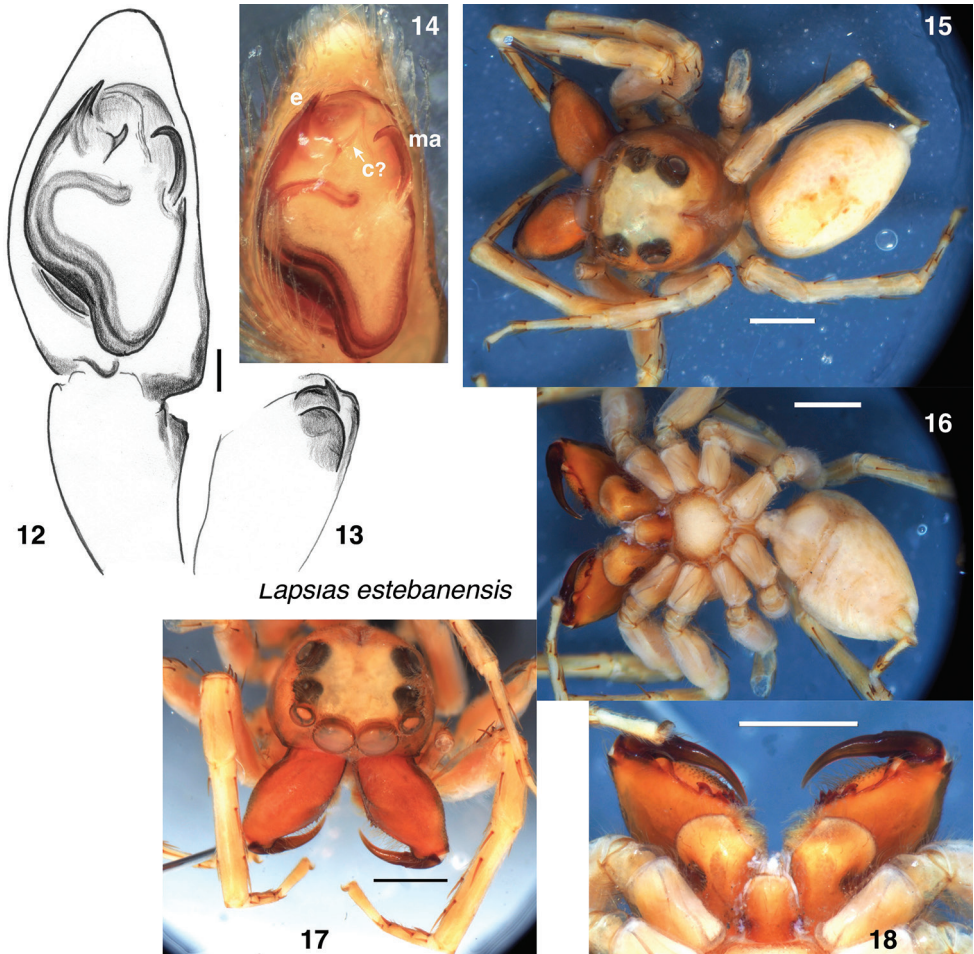
All four of Simon's species have two retromarginal teeth on the chelicera, and three pairs of ventral macrosetae on both the tibia and metatarsus of leg 1. The median apophysis of the palp is a long narrow blade, hooked at the tip and separated from the tegulum by a membrane. There is a small apophysis just retrolateral from the base of the embolus in *L. estebanensis*, *L. towarensis* Simon, 1901, and possibly *L. ciliatus* Simon, 1900 (see **c?** in Figs 14, 43) that by position is likely homologous to that called the conductor by Maddison (2012) in *L. canandea* Maddison, 2012 and in *Thrandina* species (see discussion by Ruiz 2013). The sclerite functioning as a conductor in *Amilaps mayana* (**p** in Fig. 3) is likely not homologous, given its more distal position outside the loop of the spermophore. The female spermathecae of all three species (Figs 28, 38, 49) are thick-walled and bear a pale rough-edged extension to the anterior (most easily seen in Fig. 28; partially hidden behind the fertilization ducts in Figs 38 and 49).

***Lapsias estebanensis* Simon, 1900**

Figs 12–18

Type material. In MNHN, 2 males from La Cumbre, San Esteban, Carabobo State, Venezuela, with label "21196 Laps. estebanensis E.S., S. Esteban! La Cumbre!". Galiano (1963) designated one male as lectotype, which I presume to be that in a separate microvial with her label "Typus? M.E. Galiano II 1959". The type vial also has a recent label "det Szűts 0015". Because the old handwritten label was fragile and fragmenting, I made a copy, which I added to the type vial.

Notes. This is the most robust of the four Venezuelan species, with males having enlarged chelicerae (Figs 15–17). The retromarginal tooth closest the fang is larger and curved (Fig. 18). The palp bears a close resemblance to that of *L. towarensis*, but differs in the shorter, straighter embolus and distinctly larger apophysis (**c?** in Fig. 14) accompanying the embolus.



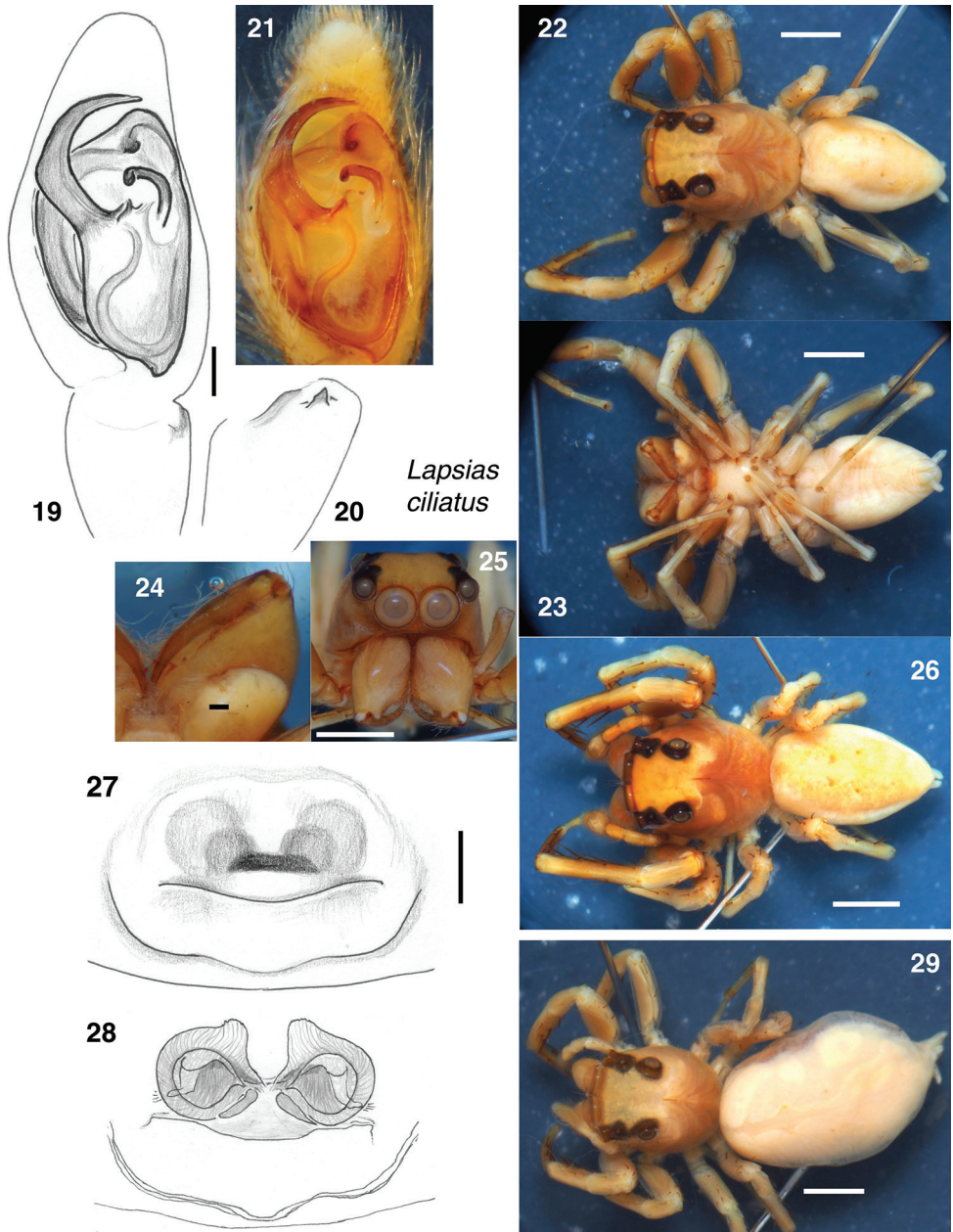
Lapsias estebanensis

Figures 12–18. *Lapsias estebanensis*, lectotype male **12–14** palp **12** ventral view **13** retrolateral view of tibia **14** ventral view **15** dorsal view of body **16** ventral view of body **17** oblique view of prosoma **18** chelicerae from below. Abbreviations: **e** embolus, **c?** scerite homologous to that of the conductor in other lapsiines, **ma** median apophysis. Scale bars: 0.1 mm (**12**); 1.0 mm (otherwise).

Lapsias ciliatus Simon, 1900

Figs 19–29

Type material. In MNHN Paris, 25 males from Colonia Tovar, Aragua State, Venezuela, most in a single vial with label “21083 Laps. ciliatus E.S., Tovar!” and more recent label “det Szűts 0012”. When I received the specimens from the MNHN, one male matching this species was in a separate vial without label except one in Galiano’s handwriting reading “Typus? M.E. Galiano II 1959” and another “det Szűts 0013”.



Figures 19–29. *Lapsias ciliatus*, lectotype male (19–25) paralectotype (26), and associated female (27–29). 19–21 Male palp 19 ventral view 20 retrolateral view of tibia 21 ventral view 22 male body from above 23 body from below 24 chelicera from below 25 face 26 paralectotype male body from above 27 epigyne from below 28 vulva from above 29 body of same female as 27, 28. Scale bars: 0.1 mm (19, 27); 1.0 mm (otherwise).

Insofar as Galiano (1963) indicated she designated a lectotype from the type vial, this specimen can be safely considered that specimen. I have therefore made a copy of the label “21083 Laps. ciliatus E.S., Tovar!” and placed it in that male lectotype’s vial. The same applies to a female separated and with only Galiano’s label “Allotypus ♀ det. M.E. Galiano II 1959”. The vial with most specimens also includes 7 females, which cannot be considered type material because Simon’s description makes no mention of females.

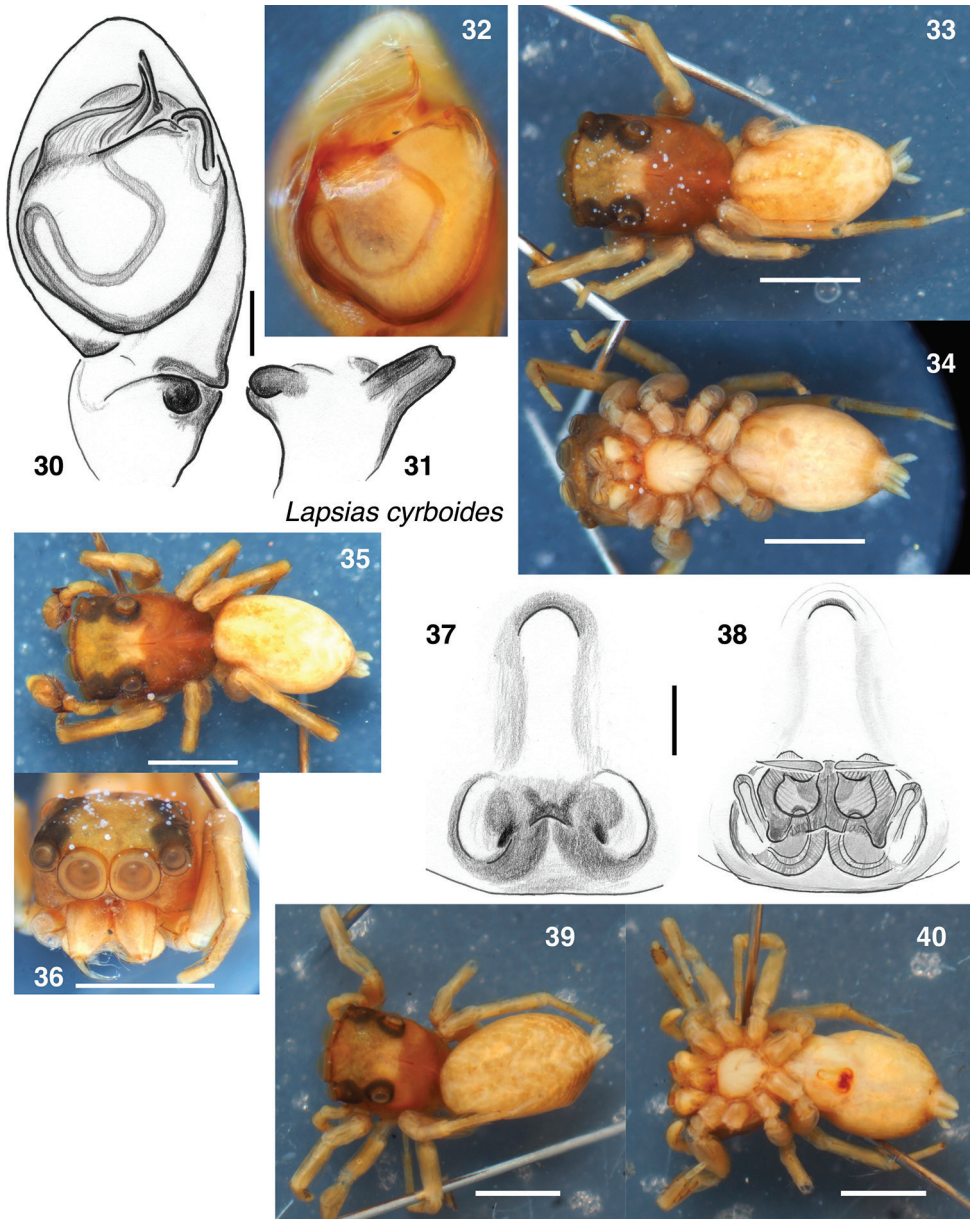
Notes. The female is illustrated for the first time in Figs 27–29. The epigynal openings are beneath a common central hood. Although Galiano separated off a female and labelled it as allotype, neither she nor Simon gave any acknowledgement or description of a female of *L. ciliatus*. The matching of these females to males of *L. ciliatus* is reasonably secure, even though three species of *Lapsias* occur at Colonia Tovar. The females of form shown in Figs 27–29 and the males matching the lectotype appear to have been abundant together, judging by the numbers of specimens. Both are larger and more robust, with wider carapaces, than the other two smaller, more delicate species from Colonia Tovar (*L. cyrboides* and *L. towarensis*). Both male and female show a faint pale spot just posterior to the PLE.

***Lapsias cyrboides* Simon, 1900**

Figs 30–40

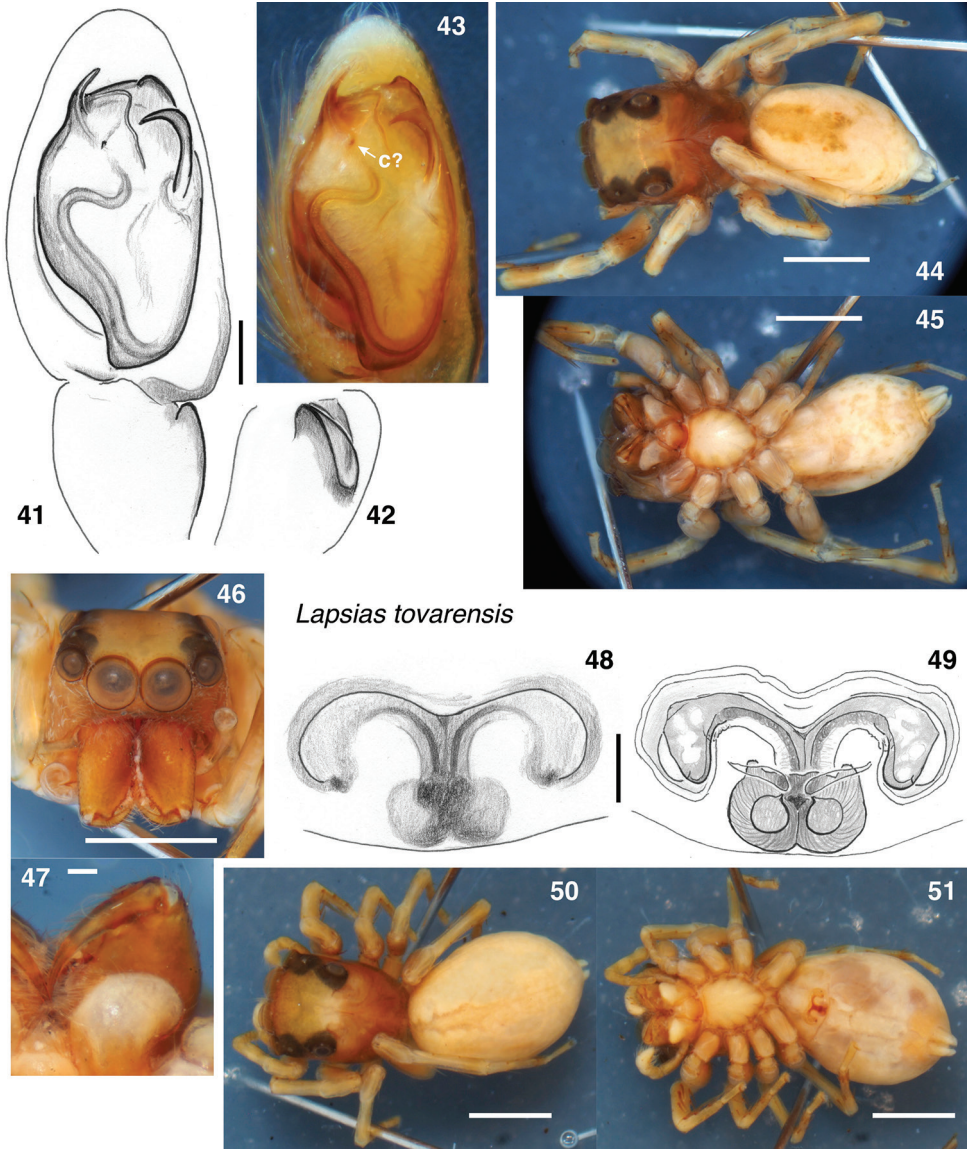
Type material. In MNHN, 3 males, 4 females, 3 juveniles from Colonia Tovar, Aragua State, Venezuela, in a vial with label “20924 Laps. cyrboides E.S., Tovar!” and a more recent label “det Szűts 0014”. Galiano (1963) designated one male as a lectotype, in separate microvial with her label “Typus? M.E. Galiano II 1959”. She mentions one female designated also as lectotype, but no female is separated and labelled as such. Because Galiano (incorrectly) designated two lectotypes, the name is not yet fixed to a single specimen. This ambiguity is resolved by designating her male lectotype as the only lectotype.

Notes. Simon (1900) described a male and female. However, as noted by Galiano (1963), there are two species of female among the four females in the type vial, similar in body but easily distinguished by the epigyne. Two of the females (Figs 37–40) have an anteriorly placed guide (Fig. 37), while the other two females (Figs 48–51) lack such a guide and instead show two wing-shaped atria extending laterally (Fig. 48). It is reasonable to assume that these two kinds of female belong to the two smaller-bodied *Lapsias* at Colonia Tovar, *L. cyrboides* and *L. towarensis*. Under *L. cyrboides* Simon described the female kind with anterior guide (“Plaga genitalis...longior quam latior”), but he did not justify this choice nor even mention the second form of female. Galiano followed Simon’s choice of matching female. The two forms of female are approximately the same size and carapace shape and are too faded to supply distinctive markings by which to match to the males. Nonetheless, I tentatively support Simon’s and Galiano’s matching based on an expected correlation between the form of the female’s



Figures 30–40. *Lapsias cyrboides* lectotype male (30–34, 36), paralectotype male (35), and female tentatively considered of this species (37–40). 30–32 Palp 30 ventral view 31 retrolateral view of tibia 32 ventral view 33 body from above 34 body from below 35 paralectotype male body from above 36 lectotype male face 37 epigyne from below 38 vulva from above 39 female body from above 40 body from below. Scale bars: 0.1 mm (30); 1.0 mm (otherwise).

guide and that of the male's RTA. An anterior guide is expected to be associated with an extraordinary RTA, for instance, as in *Papuanmyr ombifosa* Maddison & Szűts, 2019 (Maddison and Szűts 2019). Males of *L. ciliatus* and *L. tovarensis* have small RTAs,



Figures 41–51. *Lapsias tovarensis* lectotype male (41–47) and female tentatively considered of this species (48–51). 41–43 Palp 41 ventral view 42 retrolateral view of tibia 43 ventral view 44 body from above 45 body from below 46 face 47 chelicerae from below 48 epigyne from below 49 vulva from above 50 female body from above 51 body from below. Abbreviations: c? sclerite homologous to that called the conductor in other lapsiines. Scale bars: 0.1 mm (41); 1.0 mm (otherwise).

suggesting a simple or small guide along the epigastric furrow, as is common in salticids, while the male of *L. cyrboides* has an unusual dorsally projecting tibial apophysis, which predicts an unusually-placed female guide. Thus, the female with anterior guide is tentatively considered that of *L. cyrboides*, and the female with wing-shaped atria is considered that of *L. tovarensis*.

***Lapsias towarensis* Simon, 1901**

Figs 41–51

Type material. In MNHN, three males from Colonia Tovar, Aragua State, Venezuela, with label “21092 Laps. towarensis E.S., Tovar!”. Galiano (1963) designated one male as lectotype, in separate microvial with her label “Typus? M.E. Galiano II 1959”.

Notes. This is one of the two smaller-bodied species from Colonia Tovar. See the discussion under *L. estebanensis* for how to distinguish it from that species, and the discussion under *L. cyrboides* regarding the identity of the female.

Acknowledgements

I thank the curators of the MCZ, AMNH and MNHN for loaning material, and especially Christine Rollard for her patience. I thank G. Azarkina, G.B. Edwards, W. Galvis, G. Ruiz, and T. Yamasaki for suggestions that improved the paper. Yamasaki helpfully pointed out issues with the status of type material of *L. ciliatus* and *L. cyrboides*. Edwards and Ruiz gave convincing encouragement to accept Simon’s matching of female with male *L. cyrboides*. Funding was provided by an NSERC Discovery grant to the author.

References

- Christensen AJ (1987) K’iche’ – English dictionary and guide to pronunciation of the K’iche’-Maya alphabet. http://www.famsi.org/mayawriting/dictionary/christenson/quidic_complete.pdf [Accessed on 2019-07-15]
- Galiano ME (1963) Las especies americanas de arañas de la familia Salticidae descritas por Eugène Simon: Redescripciones basadas en los ejemplares típicos. *Physis, Revista de la Sociedad Argentina de Ciencias Naturales (C)* 23: 273–470.
- García-Villafuerte MA (2018) Primer registro fósil de un lapsino (Araneae, Salticidae) en el ámbar de Chiapas, México. *Boletín de la Sociedad Geológica Mexicana* 70: 689–708. <https://doi.org/10.18268/BSGM2018v70n3a6>
- Maddison WP (2006) New lapsiine jumping spiders from Ecuador (Araneae: Salticidae). *Zootaxa* 1255: 17–28.
- Maddison WP (2012) Five new species of lapsiine jumping spiders from Ecuador (Araneae: Salticidae). *Zootaxa* 3424: 51–65. <https://doi.org/10.11646/zootaxa.3424.1.3>
- Maddison WP (2015) A phylogenetic classification of jumping spiders (Araneae: Salticidae). *Journal of Arachnology* 43: 231–292. <https://doi.org/10.1636/ arac-43-03-231-292>
- Maddison WP, Li DQ, Bodner MR, Zhang JX, Xu X, Liu QQ, Liu FX (2014) The deep phylogeny of jumping spiders (Araneae, Salticidae). *ZooKeys* 440: 57–87. <https://doi.org/10.3897/zookeys.440.7891>

- Maddison WP, Szűts T (2019) Myrmarachnine jumping spiders of the new subtribe *Levieina* from Papua New Guinea (Araneae, Salticidae, Myrmarachnini). *ZooKeys* 842: 85–112. <https://doi.org/10.3897/zookeys.842.32970>
- Makhan D (2007) *Soesiladeepakius aschmae* gen. et sp. nov. and *Soesilarishius amrishi* gen. et sp. nov. from Suriname (Araneae: Salticidae). *Calodema Supplementary Paper* 60: 1–8.
- Ruiz GRS (2013) Proposal and phylogenetic relationships of *Lapsamita*, new genus of lapsiines, and description of a new species (Araneae, Salticidae). *PLoS ONE* 8(2): e56188, 1–5. <https://doi.org/10.1371/journal.pone.0056188>
- Ruiz GRS, Maddison WP (2012) DNA sequences corroborate *Soesiladeepakius* as a non-salticoid genus of jumping spiders: placement with lapsiines, phylogeny, and description of six new species (Araneae, Salticidae). *Zoological Journal of the Linnean Society* 165: 274–295. <https://doi.org/10.1111/j.1096-3642.2012.00815.x>
- Simon E (1900) Descriptions d'arachnides nouveaux de la famille des Attidae. *Annales de la Société Entomologique de Belgique* 44: 381–407.
- Simon E (1901) *Histoire naturelle des araignées*. Paris 2: 381–668.
- World Spider Catalog (2019) *World Spider Catalog Version 20.5* Natural History Museum Bern. <http://wsc.nmbe.ch> [Accessed on 2019-07-24]

Trichopolydesmidae from Cameroon, 2: A species-level reclassification of Afrotropical trichopolydesmids (Diplopoda, Polydesmida), with two new species and two new records from Cameroon, and two new species from the Nimba Mountains, Guinea

Sergei I. Golovatch¹, Armand Richard Nzoko Fiemapong^{2,3},
Didier VandenSpiegel⁴

1 Institute for Problems of Ecology and Evolution, Russian Academy of Sciences, Moscow, Russia **2** Laboratoire de Zoologie, Université Yaoundé 1, BP812, Cameroon **3** Laboratory of Zoology, Higher Teacher's Training College, University of Yaounde I, P.O.Box 47, Yaounde, Cameroon **4** Musée Royal de l'Afrique centrale, Tervuren, Belgium

Corresponding author: Sergei I. Golovatch (sgolovatch@yandex.ru)

Academic editor: Pavel Stoev | Received 1 October 2019 | Accepted 25 October 2019 | Published 21 November 2019

<http://zoobank.org/4B0C5A33-87F4-4B20-B837-6723C0BEA8B2>

Citation: Golovatch SI, Nzoko Fiemapong AR, VandenSpiegel D (2019) Trichopolydesmidae from Cameroon, 2: A species-level reclassification of Afrotropical trichopolydesmids (Diplopoda, Polydesmida), with two new species and two new records from Cameroon, and two new species from the Nimba Mountains, Guinea. ZooKeys 891: 31–59. <https://doi.org/10.3897/zookeys.891.46986>

Abstract

A revised classification of Afrotropical Trichopolydesmidae is presented. The fauna presently contains as many as 52 species in six recognized genera, with numerous new transfers/combinations involved: *Bactrodesmus* Cook, 1896 (3 species, including *B. grandis* **sp. nov.** from the Nimba Mountains, Guinea), *Eburodesmus* Schubart, 1955 (2 species), *Hemisphaeroparia* Schubart, 1955 (26 species, including one old species, *Polydesmus parvulus* Porat, 1894, revised from type material and provisionally assigned to *Hemisphaeroparia*, as well as two new records and two new species from Cameroon: *H. longibrachiata* **sp. nov.** and *H. avis* **sp. nov.**), *Mecistoparia* Brolemann, 1926 (3 species), *Physetoparia* Brolemann, 1920 (12 species, including *P. complexa* **sp. nov.** from the Nimba Mountains, Guinea), and *Sphaeroparia* Attems, 1909 (6 species). The hitherto enigmatic genus *Bactrodesmus* is redefined, but the monotypic *Trichozonus* Carl, 1905 still remains dubious.

Keywords

classification, millipede, new combination, new records, review, SEM iconography, taxonomy

Introduction

All Afrotropical genera of the millipede family Trichopolydesmidae have recently been reviewed based on their type species and a presumed scenario of gonopodal evolution (Golovatch et al. 2018). As a result, in addition to two still enigmatic genera, *Bactrodesmus* Cook, 1896 and *Trichozonus* Carl, 1905, only five genera have been regarded as currently recognizable: *Sphaeroparia* Attems, 1909, *Physetoparia* Brolemann, 1920, *Eburodesmus* Schubart, 1955, *Mecistoparia* Brolemann, 1926 and *Hemisphaeroparia* Schubart, 1955. The last genus listed is the sole trichopolydesmid to occur in Cameroon and is especially diverse (26 species).

The present contribution provides a species-level reclassification of Afrotropical Trichopolydesmidae and gives a new diagnosis of *Bactrodesmus* based on the discovery of a new species from the Nimba Mountains, Guinea. Two additional records and two new species of *Hemisphaeroparia* are described from Cameroon, while the sole old and still enigmatic species reported from that country, *Polydesmus parvulus* Porat, 1894, is revised from female syntypes and is tentatively assigned to *Hemisphaeroparia* as well. A new species of *Physetoparia* is also described from the Nimba Mountains, Guinea.

Material and methods

Most of the material treated here derives from the collection of the Musée Royal de l'Afrique Centrale (MRAC), Tervuren, Belgium, with only a few duplicates retained for the collections of the University of Yaounde 1 (UY1), Cameroon or donated to the Zoological Museum, State University of Moscow (ZMUM), Russia, as indicated below. The samples are stored in 70% ethanol. Specimens for scanning electron microscopy (SEM) were air-dried, mounted on aluminium stubs, coated with gold and studied using a JEOL JSM-6480LV scanning electron microscope. The colour pictures were taken using the focus stacking setup described by Brecko et al. (2014). Canon EOS Utility software was used to control the camera. Zerene Stacker was applied for stacking the individual pictures into one 'stacked image'.

The abbreviations used to denote gonopodal structures are explained directly in the text and figure captions.

Results

A revised list of Afrotropical Trichopolydesmidae, arranged in alphabetic order

Bactrodesmus Cook, 1896

1. *Bactrodesmus bicornis* (Demange & Mauriès, 1975), Mount Tonkoui, Côte d'Ivoire (Demange and Mauriès 1975), originally described as *Sphaeroparia bicornis* De-

- mange & Mauriès, 1975. Because it shows strongly enlarged ♂ legs 2 and 3, it definitely belongs to *Bactrodesmus*, thus representing a comb. nov. ex *Sphaeroparia*.
2. *Bactrodesmus claviger* Cook, 1896, the type species by subsequent monotypy, Liberia (Cook 1896b).
 3. *Bactrodesmus grandis* sp. nov., Nimba Mountains, Guinea (see below).

***Eburodesmus* Schubart, 1955**

1. *Eburodesmus cyrtus* Schubart, 1955, Mount Tonkoui, Côte d'Ivoire (Schubart 1955).
2. *Eburodesmus erectus* Schubart, 1955, the type species by original designation, Guinea and Côte d'Ivoire (Schubart 1955).

***Hemisphaeroparia* Schubart, 1955**

1. *Hemisphaeroparia avis* sp. nov., Cameroon (see below).
2. *Hemisphaeroparia bamboutos* Golovatch, Nzoko Fiemapong, Tamesse, Mauriès & VandenSpiegel, 2018, Cameroon (Golovatch et al. 2018).
3. *Hemisphaeroparia bangoulap* Golovatch, Nzoko Fiemapong, Tamesse, Mauriès & VandenSpiegel, 2018, Cameroon (Golovatch et al. 2018).
4. *Hemisphaeroparia boletiphora* (Mauriès, 1968), Gabon (Mauriès 1968). Originally described as *Mecistoparia (Mabocus) boletiphora* Mauriès, 1968, it definitely belongs to *Hemisphaeroparia* as it shows not only ♂ epicranial modifications and conspicuously enlarged spiracles next to coxa 1 or 2, but also clearly enlarged and globose gonocoxae, the telopodites being strongly sunken inside a deep gonocoel and leaving at least two exposed branches (Golovatch et al. 2018). This formally results in the following new transfer: *Hemisphaeroparia boletiphora* (Mauriès, 1968), comb. nov. ex *Mecistoparia*.
5. *Hemisphaeroparia bonakanda* Golovatch, Nzoko Fiemapong, Tamesse, Mauriès & VandenSpiegel, 2018, Cameroon (Golovatch et al. 2018).
6. *Hemisphaeroparia cumbula* Schubart, 1955, the type species by original designation, Nimba Mountains, Guinea and Mount Tonkoui, Côte d'Ivoire (Schubart 1955).
7. *Hemisphaeroparia digitifer* Golovatch, Nzoko Fiemapong, Tamesse, Mauriès & VandenSpiegel, 2018, Cameroon (Golovatch et al. 2018).
8. *Hemisphaeroparia falcata* Golovatch, Nzoko Fiemapong, Tamesse, Mauriès & VandenSpiegel, 2018, Cameroon (Golovatch et al. 2018, see also below).
9. *Hemisphaeroparia fusca* Golovatch, Nzoko Fiemapong, Tamesse, Mauriès & VandenSpiegel, 2018, Cameroon (Golovatch et al. 2018).
10. *Hemisphaeroparia galeata* (Mauriès, 1968), Gabon (Mauriès 1968). Originally described as *Mecistoparia (Mabocus) galeata* Mauriès, 1968, it definitely belongs to *Hemisphaeroparia* as it shows not only ♂ epicranial modifications and con-

- spicuously enlarged spiracles next to coxa 1 or 2, but also clearly enlarged and globose gonocoxae, the telopodites being strongly sunken inside a deep gonocoel and leaving at least two exposed branches (Golovatch et al. 2018). This formally results in the following new transfer: *Hemisphaeroparia galeata* (Mauriès, 1968), comb. nov. ex *Mecistoparia*.
11. *Hemisphaeroparia guerouti* Demange, 1967, Côte d'Ivoire (Demange 1967). Mauriès and Heymer (1996) transferred this species to *Sphaeroparia*, but we return it to *Hemisphaeroparia* herewith.
 12. *Hemisphaeroparia hallini* (Demange & Mauriès, 1975), Mount Tonkoui, Côte d'Ivoire Demange and Mauriès 1975). Originally described as *Sphaeroparia hallini* Demange & Mauriès, 1975, but it seems to fit better in *Hemisphaeroparia* because of enlarged and globose gonocoxae, coupled with each telopodite being strongly sunken inside a deep gonocoel and leaving one rather long branch partly exposed (Golovatch et al. 2018). This results in the following formal transfer: *Hemisphaeroparia hallini* (Demange & Mauriès, 1975), comb. nov. ex *Sphaeroparia*.
 13. *Hemisphaeroparia hexatracha* (Mauriès & Heymer, 1996), Kivu, the Democratic Republic of the Congo (Mauriès and Heymer 1996). Originally described as *Sphaeroparia (Physetoparia) hexatracha* Mauriès & Heymer, 1996, it seems best to assign to *Hemisphaeroparia* because of enlarged and globose gonocoxae, coupled with each telopodite being strongly sunken inside a deep gonocoel and leaving one rather long branch clearly exposed (Golovatch et al. 2018). This results in the following formal transfer: *Hemisphaeroparia hexatracha* (Mauriès & Heymer, 1996), comb. nov. ex *Sphaeroparia*.
 14. *Hemisphaeroparia integrata* (Porat, 1894), Cameroon (Porat 1894; Golovatch et al. 2018). This species was originally described as *Polydesmus integratus* Porat, 1894, but Golovatch et al. (2018), based on a revision of the ♂ holotype, re-described and transferred it to *Hemisphaeroparia*.
 15. *Hemisphaeroparia longibrachiata* sp. nov., Cameroon (see below).
 16. *Hemisphaeroparia mouanko* Golovatch, Nzoko Fiemapong, Tamesse, Mauriès & VandenSpiegel, 2018, Cameroon (Golovatch et al. 2018).
 17. *Hemisphaeroparia nyabitabae* (Mauriès & Heymer, 1996), Ruwenzori Mts, Uganda (Mauriès and Heymer 1996). Originally described as *Sphaeroparia (Physetoparia) nyabitabae* Mauriès & Heymer, 1996, it seems best to assign to *Hemisphaeroparia* because of enlarged and globose gonocoxae, coupled with each telopodite being strongly sunken inside a deep gonocoel and leaving one rather long branch clearly exposed (Golovatch et al. 2018). This results in the following formal transfer: *Hemisphaeroparia nyabitabae* (Mauriès & Heymer, 1996), comb. nov. ex *Sphaeroparia*.
 18. *Hemisphaeroparia ongot* Golovatch, Nzoko Fiemapong, Tamesse, Mauriès & VandenSpiegel, 2018, Cameroon (Golovatch et al. 2018).
 19. *Hemisphaeroparia parva* Golovatch, Nzoko Fiemapong, Tamesse, Mauriès & VandenSpiegel, 2018, Cameroon (Golovatch et al. 2018).
 20. *Hemisphaeroparia parvocristata* (Mauriès, 1968), Gabon (Mauriès 1968). Originally described as *Mecistoparia (Mabocus) parvocristata* Mauriès, 1968, it defi-

nately belongs to *Hemisphaeroparia* as it shows not only ♂ epicranial modifications and conspicuously enlarged spiracles next to coxa 1 or 2, but also clearly enlarged and globose gonocoxae, the telopodites being strongly sunken inside a deep gonocoel and leaving at least two exposed branches (Golovatch et al. 2018). This formally results in the following new transfer: *Hemisphaeroparia parvocristata* (Mauriès, 1968), comb. nov. ex *Mecistoparia*.

21. *Hemisphaeroparia parvula* (Porat, 1894), Cameroon (Porat 1894; Golovatch et al. 2018). This species was originally described as *Polydesmus parvulus* Porat, 1894, but Golovatch et al. (2018) tentatively transferred it to *Hemisphaeroparia*. Based on a revision of both ♀ syntypes, this combination is confirmed here (see below).
22. *Hemisphaeroparia pileata* (Mauriès, 1968), Gabon (Mauriès 1968). Originally described as *Mecistoparia (Mabocus) pileata* Mauriès, 1968, it definitely belongs to *Hemisphaeroparia* as it shows not only ♂ epicranial modifications and conspicuously enlarged spiracles next to coxa 1 or 2, but also clearly enlarged and globose gonocoxae, the telopodites being strongly sunken inside a deep gonocoel and leaving at least two exposed branches (Golovatch et al. 2018). This formally results in the following new transfer: *Hemisphaeroparia pileata* (Mauriès, 1968), comb. nov. ex *Mecistoparia*.
23. *Hemisphaeroparia pretzmanni* (Demange & Mauriès, 1975), Mount Tonkoui, Côte d'Ivoire (Demange and Mauriès 1975). Originally described as *Sphaeroparia pretzmanni* Demange & Mauriès, 1975, but it seems to fit best in the genus *Hemisphaeroparia* because of clearly showing enlarged and globose gonocoxae, coupled with each telopodite being strongly sunken inside a deep gonocoel and leaving one rather long branch partly exposed (Golovatch et al. 2018). This results in the following formal transfer: *Hemisphaeroparia pretzmanni* (Demange & Mauriès, 1975), comb. nov. ex *Sphaeroparia*.
24. *Hemisphaeroparia spiniger* Golovatch, Nzoko Fiemapong, Tamesse, Mauriès & VandenSpiegel, 2018, Cameroon (Golovatch et al. 2018, see also below).
25. *Hemisphaeroparia subfalcata* Golovatch, Nzoko Fiemapong, Tamesse, Mauriès & VandenSpiegel, 2018, Cameroon (Golovatch et al. 2018).
26. *Hemisphaeroparia zamakoe* Golovatch, Nzoko Fiemapong, Tamesse, Mauriès & VandenSpiegel, 2018, Cameroon (Golovatch et al. 2018).

***Mecistoparia* Brolemann, 1926**

1. *Mecistoparia cristata* Brolemann, 1926, Benin (Brolemann 1926).
2. *Mecistoparia lophocrania* Brolemann, 1926, the type species by original designation, Benin (Brolemann 1926).
3. *Mecistoparia pusilla* (Verhoeff, 1941), the type species of *Dendrobrachypus* Verhoeff, 1941 by monotypy, Fernando Po (Verhoeff 1941). Since the synonymization of both genera by Golovatch et al. (2018), the new transfer can be formalized as follows: *Mecistoparia pusilla* (Verhoeff, 1941), comb. nov. ex *Dendrobrachypus*.

***Physetoparia* Brolemann, 1920**

1. *Physetoparia beshkovi* (Mauriès & Heymer, 1996), Ruwenzori Mts, Uganda (Mauriès and Heymer 1996). Originally described as *Sphaeroparia* (*Sphaeroparia*) *beshkovi* Mauriès & Heymer, 1996, it actually belongs to *Physetoparia* as redefined by Golovatch et al. (2018): both gonopodal coxae and gonocoel medium-sized; telopodite usually less strongly exposed and less complex (when strongly exposed, then with a protective coxal apicolateral process), with two strong branches; seminal groove short and simple, solenomere relatively long, subspiniform. This results in the following formal transfer: *Physetoparia beshkovi* (Mauriès & Heymer, 1996), comb. nov. ex *Sphaeroparia*.
2. *Physetoparia complexa* sp. nov., Nimba Mountains, Guinea (see below).
3. *Physetoparia difficilis* (Kraus, 1958), the Democratic Republic of the Congo (Kraus 1958). Since the synonymization of *Mabocus* Chamberlin, 1951 with *Physetoparia* by Golovatch et al. (2018), the species must be referred to as *Physetoparia difficilis* (Kraus, 1958), comb. nov. ex *Mabocus*.
4. *Physetoparia edentula* (Attems, 1953), Kivu, the Democratic Republic of the Congo (Attems 1953). Originally described as *Elgonicola edentula*, since the synonymization of *Elgonicola* with *Physetoparia* by Golovatch et al. (2018), it must be referred to as *Physetoparia edentula* (Attems, 1953), comb. nov. ex *Elgonicola*.
5. *Physetoparia granulifer* (Chamberlin, 1951), the type species of *Mabocus* Chamberlin, 1951 by original designation, Angola (Chamberlin 1951; Kraus 1958). Since the synonymization of *Mabocus* with *Physetoparia* by Golovatch et al. (2018), the species must be referred to as *Physetoparia granulifer* (Attems, 1953), comb. nov. ex *Mabocus*.
6. *Physetoparia imbecilla* (Brolemann, 1920), the type species by monotypy, Mount Kinangop, Kenya (Brolemann 1920). Originally described as *Sphaeroparia* (*Physetoparia*) *imbecilla* Brolemann, 1920, it is to be referred to as *Physetoparia imbecilla* (Brolemann, 1920), comb. nov.
7. *Physetoparia jeanneli* (Attems, 1939), Mount Elgon, Uganda (Attems 1939). This is the type species of *Elgonicola* Attems, 1939 by original designation, the genus synonymized by Golovatch et al. (2018), formally resulting in *Physetoparia jeanneli* (Attems, 1939), comb. nov. ex *Elgonicola*.
8. *Physetoparia microchaeta* (Attems, 1939), Mount Elgon, Uganda (Attems 1939). Originally described as a subspecies of *Elgonicola jeanneli*, but the striking difference in the length of tergal setae between the two subspecies, let alone their strict sympatry (Mount Elgon) correctly allowed Mauriès and Heymer (1996) to elevate the rank of *microchaeta* to full species, formally resulting in *Physetoparia microchaeta* (Attems, 1939), comb. nov. ex *Elgonicola*.
9. *Physetoparia petarberoni* (Mauriès & Heymer, 1996), Ruwenzori Mts, Uganda (Mauriès and Heymer 1996). Originally described as *Sphaeroparia* (*Sphaeroparia*) *petarberoni* Mauriès & Heymer, 1996, it actually belongs to *Physetoparia* as redefined by Golovatch et al. (2018): both gonopodal coxae and gonocoel medium-sized; telopodite usually less strongly exposed and less complex (when strongly ex-

- posed, then with a protective coxal apicolateral process), with one strong branch; seminal groove short and simple, solenomere relatively short and subspiniform. This results in the following formal transfer: *Physetoparia petarberoni* (Mauriès & Heymer, 1996), comb. nov. ex *Sphaeroparia*.
10. *Physetoparia sangae* (Chamberlin, 1951), Angola (Chamberlin 1951; Kraus 1958). Since the synonymization of *Mabocus* Chamberlin, 1951 with *Physetoparia* by Golovatch et al. (2018), the species must be referred to as *Physetoparia sangae* (Attems, 1953), comb. nov. ex *Mabocus*.
 11. *Physetoparia villiersi* (Schubart, 1955), the type species *Heterosphaeroparia* Schubart, 1955 by original designation, Nimba Mountains, Guinea and Mount Tonkoui, Côte d'Ivoire (Schubart 1955; Demange and Mauriès 1975). This species was originally described in *Heterosphaeroparia* Schubart, 1955, then relegated to *Sphaeroparia* (Demange and Mauriès 1975; Mauriès and Heymer 1996), but since the synonymization of *Heterosphaeroparia* with *Physetoparia* by Golovatch et al. (2018), it must be transferred to *Physetoparia*, comb. nov. ex *Sphaeroparia*.
 12. *Physetoparia violantennae* (Mauriès & Heymer, 1996), Ruwenzori Mts, Uganda (Mauriès and Heymer 1996). Originally described as *Sphaeroparia* (*Sphaeroparia*) *violantennae* Mauriès & Heymer, 1996, it actually belongs to *Physetoparia* as redefined by Golovatch et al. (2018): both gonopodal coxae and gonocoel medium-sized; telopodite strongly exposed, but less complex, with a large apicolateral lobe, one strong branch and a strong spiniform solenomere. This results in the following formal transfer: *Physetoparia violantennae* (Mauriès & Heymer, 1996), comb. nov. ex *Sphaeroparia*.

***Sphaeroparia* Attems, 1909**

1. *Sphaeroparia attenuata* Brolemann, 1920, Mount Kilimanjaro, Tanzania (Brolemann 1920). Originally described as a subspecies of *minuta* (see below), but the differences noted by Brolemann (1920) between the two subspecies, especially those in the proportions and shapes of the various outgrowths of the gonopodal telopodites, allowed Mauriès and Heymer (1996) to correctly regard *attenuata* as a distinct species.
2. *Sphaeroparia lanceolata* Brolemann, 1920, Mount Kenya, Kenya (Brolemann 1920).
3. *Sphaeroparia lignivora* Brolemann, 1920, the type species of *Megaloparia* Brolemann, 1920 by subsequent designation by Attems (1940), Mount Kenya, Kenya (Brolemann 1920). *Megaloparia* has been synonymized with *Sphaeroparia* by Mauriès and Heymer (1996).
4. *Sphaeroparia minuta* Attems, 1909, the type species by monotypy, Mount Meru, Tanzania (Attems 1909).
5. *Sphaeroparia pygmaea* Brolemann, 1920, Shimoni, Kenya (Brolemann 1920). Originally described as *Sphaeroparia* (*Megaloparia*) *pygmaea*, but *Megaloparia* has been synonymized with *Sphaeroparia* by Mauriès and Heymer (1996).

6. *Sphaeroparia uncinata* Brolemann, 1920, Mount Kenya, Kenya (Brolemann 1920).

The above list contains 52 species, including 26 in *Hemisphaeroparia*, 12 in *Physetoparia*, six in *Sphaeroparia*, three each in *Mecistoparia* and *Bactrodesmus*, and two in *Eburodesmus*. One more species remains in the dubious genus *Trichozonus* (see below). We describe here another four new species in three genera and clarify the identity of *Bactrodesmus*. Additional records of two species recently described from Cameroon are also presented.

Species descriptions

Physetoparia complexa sp. nov.

<http://zoobank.org/C6BD407F-E50B-495E-A0E7-0402D0008563>

Figs 1A, 2, 3

Type material. *Holotype* ♂ (MRAC 22840), Guinea, Nimba Mountains, summit of Mount Nion, ca 1405 m a.s.l., forest litter, 28.V.2019, A. Henrard, D. VandenSpiegel, C. Allard et al. leg. (Nimba 2019-24). *Paratypes*: 1 ♂ (MRAC 22841), 9 ♀ (MRAC 22852), 1 ♂ (SEM, MRAC 22842), same locality and date, together with holotype.

Diagnosis. Differs from all other species of the genus by the unusually complex gonopodal structure, i.e. the presence of a particularly prominent, distolateral, gonocoxal lobe (lo) that protects a similarly clearly exposed telopodite, the latter being largely represented by a high apicomeral lobe/outgrowth (ab) that carries a highly peculiar, large, tube-shaped solenomere (tu). The gonocoel is shallow and conceals only the bases of the telopodites (Figs 2K, 3).

Name. To emphasize the complex gonopodal structure; adjective in feminine gender.

Description. Length of holotype ca 5 mm (♂), width of midbody pro- and metazonae 0.5 and 0.7 mm (♂), respectively. Length of paratypes ca 5 mm (♂) or 6–7 mm (♀), width of midbody pro- and metazonae 0.5 and 0.7 mm (♂) or 0.6–0.7 and 0.8–1.0 mm (♀), respectively. Coloration in alcohol marbled light or darker reddish brown, venter and legs light brown to nearly pallid (Fig. 1A).

Body with 20 segments in both sexes. Tegument very delicately micro-alveolate, mainly slightly shining. Head densely micropilose, devoid of epicranial modifications (Fig. 2A, B, E). Interantennal isthmus almost two times diameter of antennal socket. Antennae long and strongly clavate, reaching back past segment 3 when stretched dorsally. In length, antennomere 3 = 6 > 2 = 5 > 1 = 4 = 7; antennomere 6 the largest, antennomeres 5 and 6 each with a distinct, round, distodorsal field of sensilla. In width, collum < head < segments 2–4 < 5–16; thereafter body gradually tapering towards telson. Collum ellipsoid, transversely oval, like all following metaterga with three transverse, regular rows of setae on low, but evident, setigerous bosses. Tergal setae medium-sized, each ca 1/4–1/5 as long as metatergum, bacilliform and longitudinally ribbed, gradually growing longer towards telson, set on minute knobs (Fig. 2A–J), always 3+3 in each row on postcollum metaterga; 2–3 additional setae normally

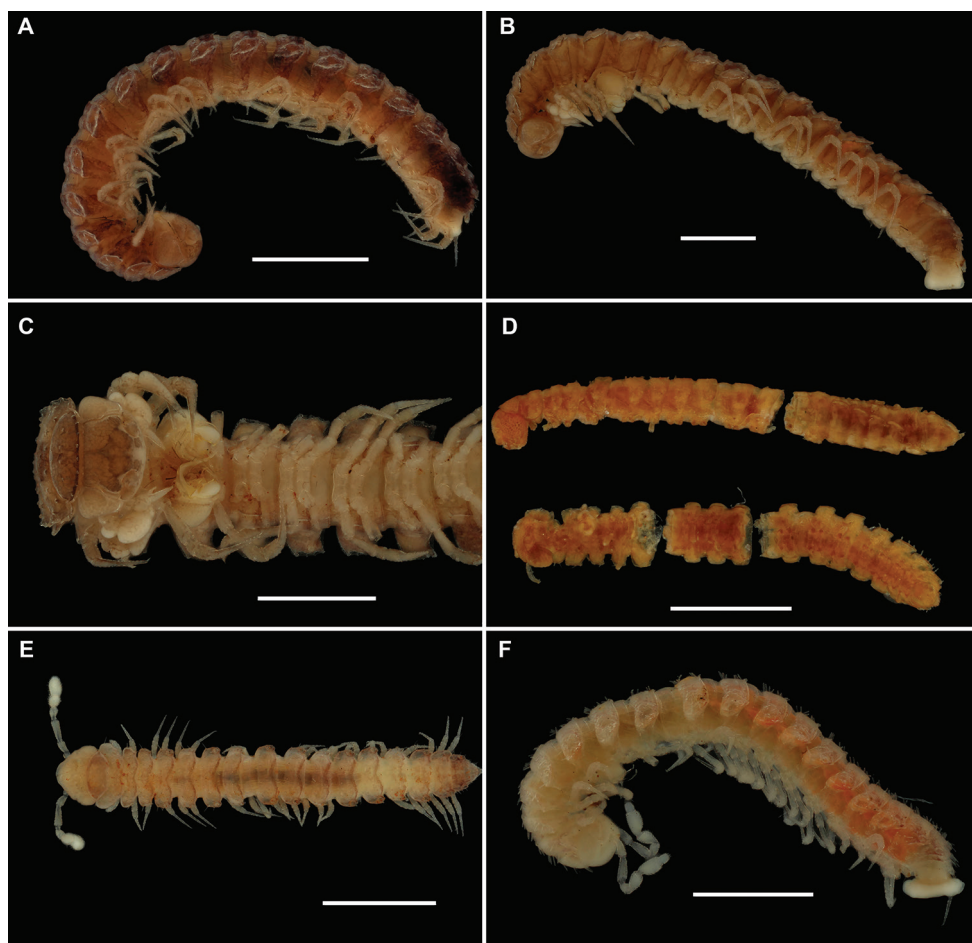


Figure 1. Habitus of **A** *Physetoparia complexa* sp. nov., ♂ holotype, lateral view **B, C** *Bactrodesmus grandis* sp. nov., ♂ paratype, lateral view of entire animal and its anterior body half, ventral view **D** *Hemisphaeroparia parvula* (Porat, 1894), both ♀ syntypes, lateral, subventral or sublateral view **E** *Hemisphaeroparia longibrachiata* sp. nov., ♂ holotype, dorsal view **F** *Hemisphaeroparia avis* sp. nov., ♂ paratype, lateral view. Scale bars: 1.0 mm.

present at lateral margin of paraterga. A faint, sinuate, transverse sulcus visible behind first row on most metaterga. Dorsum invariably regularly convex. Paraterga medium-sized, set at around upper 1/3 of metazonae (Fig. 2A–H), visible starting with collum, often slightly upturned caudally, faintly, but regularly rounded and bordered, lateral incisions almost absent. Caudal corner of paraterga mostly rounded, sharply truncate only in a few caudal segments (Fig. 2D, G). Pore formula normal: 5, 7, 9, 10, 12, 13, 15–19. Ozopores small, round, opening flush dorsally near caudal corner of poriferous paraterga. Stricture between pro- and metazonae wide, shallow. Limbus very finely microspiculate. All spiracles usual, simple. Pleurosternal carinae traceable as very faint lines on most segments (Fig. 2B, D). Epiproct short, conical, flattened dorsoventrally. Hypoproct semi-circular, setae strongly separated and borne on minute knobs.

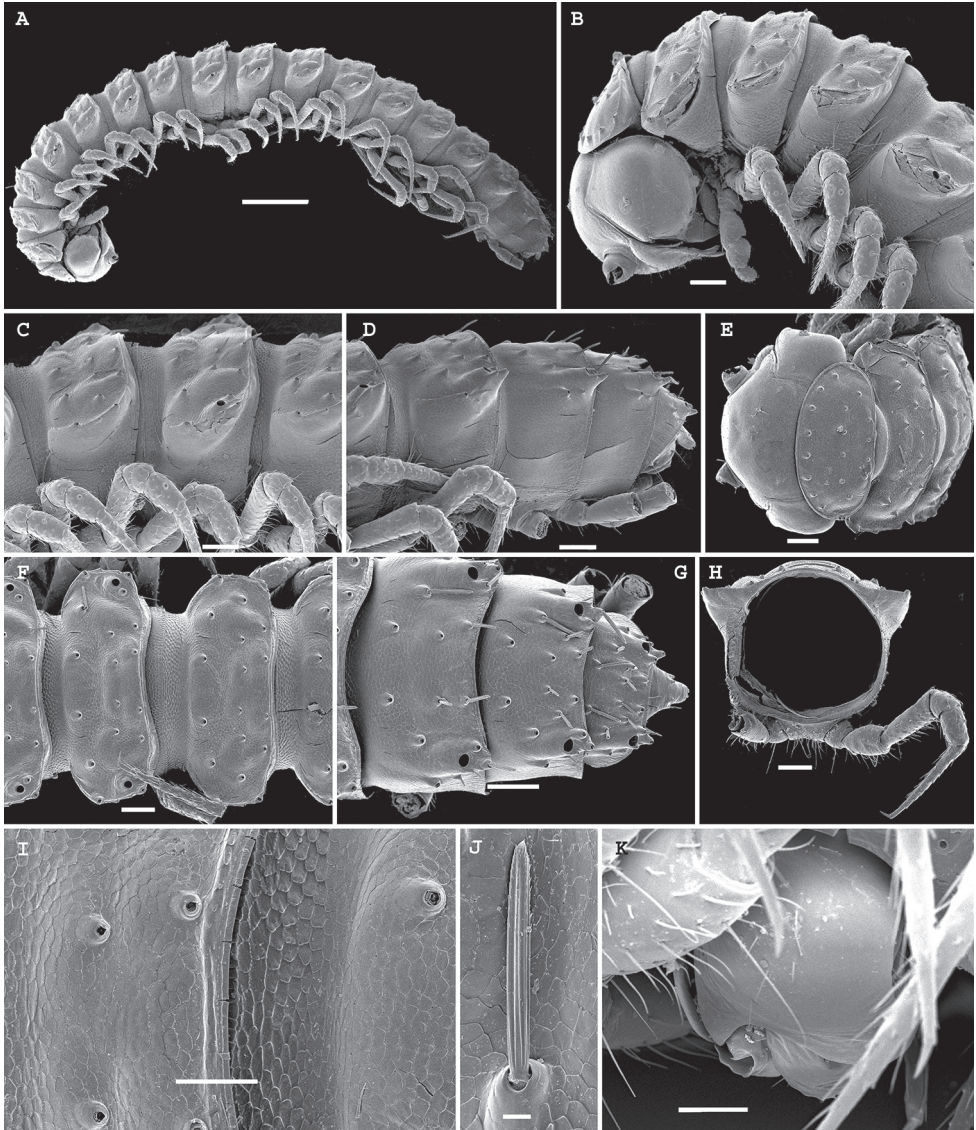


Figure 2. *Physetoparia complexa* sp. nov., SEM micrographs of ♂ paratype **A** habitus, lateral view **B, E** anterior part of body, lateral and dorsofrontal views, respectively **C, F** midbody segments, lateral and dorsal views, respectively **D, G** posterior part of body, lateral and dorsal views, respectively **H** cross-section of a midbody segment, caudal view **I** fine tergal structure, dorsal view **J** tergal seta, lateral view **K** gonopodal coxa in situ, lateral view. Scale bars: 0.5 mm (**A**), 0.1 mm (**B–H**), 0.05 mm (**I, K**), 0.01 mm (**J**).

Sterna wide, unmodified, setose. Legs rather long and slender, ca 1.2–1.3 (♂) or 1.0–1.1 (♀) times as long as midbody height; in length, tarsus > femur > prefemur > coxa = postfemur = tibia, the latter with a particularly long, tactile seta apicodorsally. Tarsal brushes absent.

Gonopods (Fig. 3) with large, subglobose, barely setose coxae, fused medially at base, each coxa carrying a very prominent, rounded, distolateral lobe (lo) and two very

strong setae near place of fusion. Telopodites very clearly exposed, but strongly protected by lo, bases only a little concealed inside a shallow gonocoel. Telopodites only slightly shorter than lo, each with only a single, large, subsecuriform, lobe-shaped, apicomeresal branch/outgrowth (ab) showing a microdentate apical margin, a peculiar tube (tu) with a large orifice (or), and a field of fimbriae at base of tu, both hidden between lo and ap; tu apparently functioning as a solenomere.

Remarks. This new species shows several clear-cut apomorphies in gonopodal characters (see Diagnosis above), but on balance it fits quite well the scope of *Physetoparia* as outlined by Golovatch et al. (2018). Especially distinct similarities concern the sole congener that has a marked apicolateral outgrowth/lobe on the gonopodal coxa to protect a likewise well exposed telopodite: *P. villiersi* (Schubart, 1955). However, the gonotelopodite in the latter species is tripartite, including a finger-shaped solenomere,

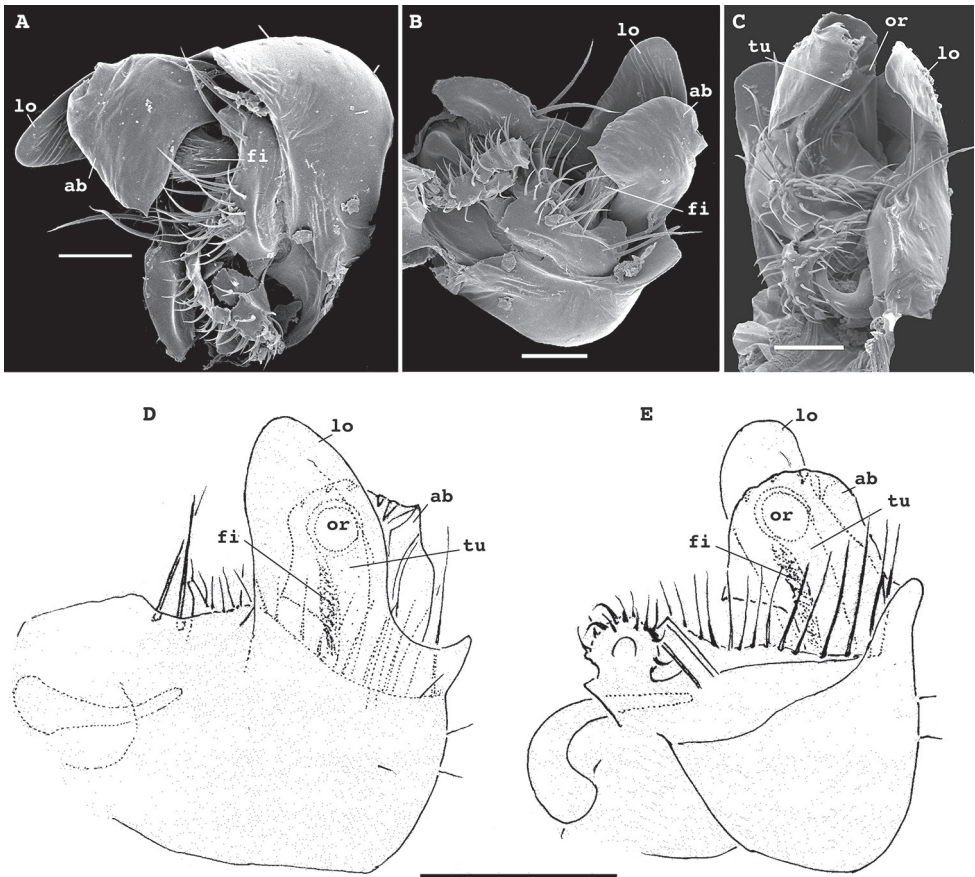


Figure 3. *Physetoparia complexa* sp. nov., gonopods of ♂ paratypes **A, B** left gonopod, lateral and ventrolateral views, respectively **C** right gonopod, ventrocaudal view **D, E** right gonopod, lateral and mesal views, respectively. Abbreviations: **lo** distolateral lobe of coxa, **ab** apicomeresal branch/outgrowth of telopodite, **tu** tube/solenomere between **lo** and **ab** with a broad orifice (**or**) and a field of filaments (**fi**) at base. Scale bars: 0.05 mm.

while the coxal lobe is much smaller and less conspicuous (Schubart 1955). In addition, both these species compared come from the same area, the Nimba Mountains which are shared by Liberia, Guinea and Côte d'Ivoire.

***Bactrodesmus* Cook, 1896**

Type species. *Bactrodesmus claviger* Cook, 1896, by subsequent monotypy, Liberia.

As reiterated recently (Golovatch et al. 2018), this genus was first proposed as a *nomen nudum* (Cook 1896a), but then properly typified (Cook 1896b). The sole useful information contained in the original description of *B. claviger*, which was accompanied by no illustrations, concerns its small size (7 mm long, 1 mm wide), typically micropolydesmid facies (small paraterga, large and clubbed tergal setae arranged in three transverse rows etc.), strongly enlarged gonocoxae that fully conceal the telopodites and, above all, ♂ legs 2, especially their tibiae, greatly enlarged compared to others (Cook 1896b). No number of body segments has been given.

Below we put on record a new *Bactrodesmus* coming from the Guinean portion of the Nimba Mountains. This allows us to unequivocally clarify the identity of the genus and provide a new diagnosis.

Diagnosis. At least ♂ tibiae 2, as well as both gonopodal coxae and gonocoel hypertrophied, telopodites being strongly sunken and their distal outgrowths remaining nearly fully concealed inside gonocoel. Only one prominent, basal fold/branch (bb = sp) present, albeit fully concealed as well; a simple and short solenomere branch (sl) protected by bb mesally and by a clearly 2-segmented lateral part laterally.

Remark. This genus is presumably among the most advanced representatives of Afrotropical Trichopolydesmidae in showing several autapomorphies.

***Bactrodesmus grandis* sp. nov.**

<http://zoobank.org/AF5E4B4D-7A9B-426D-A87D-16EC8FFB61BD>

Figs 1B, C, 4, 5

Type material. *Holotype* ♂ (MRAC 22843), Guinea, Nimba Mountains, near cave 2, Serengbara, camp 3, ca 1035 m a.s.l., litter, 2.V.2019, A. Henrard, D. VandenSpiegel, C. Allard et al. leg. (Nimba 2019-41). *Paratypes*: 1 ♀ (MRAC 22844), same locality, together with holotype: 2 ♂, 1 ♀ (MRAC 22845), 2 ♂ (MRAC 22862), 1 ♂ (SEM, MRAC 22846), 1 ♂ (ZMUM Rd 4628), same locality, forest; ca 975 m a.s.l., 2.V.2019, A. Henrard, D. VandenSpiegel, C. Allard et al. leg. (Nimba 2019-49).

Diagnosis. Differs from both other species of the genus by ♂ legs 1–3 being clearly enlarged and modified, vs. ♂ legs 2 or 2 and 3, from *B. bicornis* also by three (vs. two) transverse rows of tergal setae and the collum which is narrower than the head, from *B. claviger* by the considerably larger body.

Name. To emphasize the relatively large body and clearly enlarged ♂ legs 1–3; adjective.

Description. Length ca 8 (♂, including holotype) or 9 mm (♀), width of mid-body pro- and metazonae 1.0 and 1.3 mm (♂, including holotype) or 1.2 and 1.5 mm (♀), respectively. Coloration in alcohol marbled light brown to reddish brown, venter and legs usually lighter, light grey-brown to nearly pallid (Fig. 1B, C).

Body with 20 segments in both sexes. Tegument very delicately micro-alveolate, mainly slightly shining. Head densely micropilose, devoid of epicranial modifications, but genae roundly squarish and very strongly swollen laterally; gnathochilarium without modifications (Fig. 4G). Interantennal isthmus 1.8 times diameter of antennal socket. Antennae long and strongly clavate, reaching back past segment 3 (♂) when stretched dorsally. In length, antennomere 3 = 6 > 5 > 2 = 4 > 7 > 1; antennomere 6 the largest, antennomeres 5 and 6 each with a distinct, round, distodorsal field of minute sensilla. In width, collum < segments 2 and 3 < head = 4 < 5–16; thereafter body gradually tapering towards telson. Collum ellipsoid, transversely oval, like all following metaterga with three transverse, regular rows of setae. Tergal setae largely abraded, medium-sized, each ca 1/4–1/5 as long as metatergum, bacilliform and longitudinally ribbed, set on minute knobs, growing slightly longer toward telson, 3–4 additional setae present at lateral margin of paraterga (Fig. 4A–E, H), always 3+3 in each row on postcollum metaterga. Dorsal surface of metaterga nearly smooth, regularly convex. Paraterga medium-sized, set at around upper 1/3 of metazonae (Fig. 4A–C, E, H), visible starting with collum, often slightly upturned caudally, faintly, but regularly rounded and bordered, lateral incisions absent, with minute setigerous knobs present in their stead, including ones located at caudal corners. Paraterga 2 slightly enlarged, more strongly declined and broadly rounded compared to following ones (Fig. 4A). Starting with paraterga 5 or 6, caudal corner increasingly sharp and drawn back past rear tergal margin (Fig. 4A–C, H). Pore formula normal: 5, 7, 9, 10, 12, 13, 15–19. Ozopores small, round, opening flush dorsally near caudal corner of poriferous paraterga. Stricture between pro- and metazonae wide, shallow. Limbus very finely micro-spiculate. Spiracles very small, located on short cones (Fig. 4K). Pleurosternal carinae traceable as very faint ridges or lines on most segments (Fig. 4A, B). Epiproct short, conical, flattened dorsoventrally. Hypoproct semi-circular, setae strongly separated and borne on minute knobs.

Sterna wide, unmodified, setose. Legs rather long and slender, ca 1.3–1.4 (♂) or 1.1–1.2 times (♀) as long as midbody height; in length, tarsus > femur > prefemur > coxa = postfemur = tibia. Tarsal brushes present only on ♂ legs 1 and 2; ♂ legs 1–3 conspicuously enlarged (Fig. 4I): legs 1 (Fig. 4J) with increasingly inflated pretarsal podomeres; legs 2 (Fig. 4K, L) with each coxa caudally supplied with what seems to be a gland whose wide orifice is surrounded by a whorl of setae while the interior carries bundles of abundant, very long, sharp, distally entangled filaments; tibiae 2 particularly strongly swollen, while tarsi 2 somewhat shortened, dorsally flattened and spoon-shaped; legs 3 (Fig. 4K, M) resembling legs 1, but their prefemora and femora especially densely setose ventrally.

Gonopods (Fig. 5) complex, with particularly strongly enlarged, globose and nearly smooth coxae (cx), both forming a very deep gonocoel, both clearly rimmed apically and with 2+2 especially strong setae mediobasally near place of coxal fusion; one small

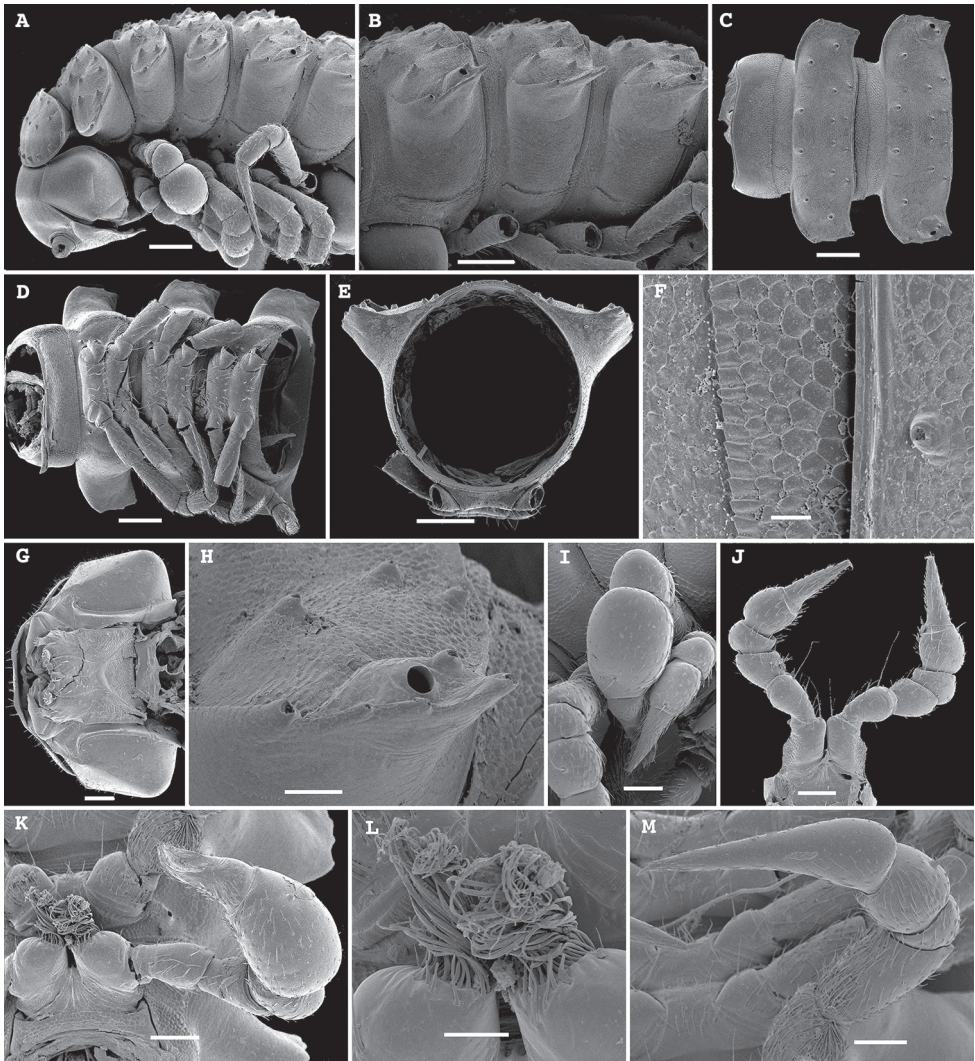


Figure 4. *Bactrodesmus grandis* sp. nov., SEM micrographs of a ♂ paratype **A** anterior part of body, lateral view **B–D** midbody segments, lateral, dorsal and ventral views, respectively **E** cross-section of a midbody segment, caudal view **F** fine tergal structure, dorsal view **G** head, ventral view **H** midbody paratergum, lateral view **I** from right to left, legs 1–3 in situ, lateral view **J** leg-pair 1, oral view **K** leg 2 and base of leg 3, frontoventral view **L** coxae 2, subventral view **M** leg 3 and bases of several following legs, frontoventral view. Scale bars: 0.2 mm (**A–E**), 0.1 mm (**G, I–K, M**), 0.05 mm (**I, L**), 0.02 mm (**F**).

rounded lobe each present on cx distolaterally (lol) and distomesally (lom); cannulae relatively small, as usual. Telopodites deeply sunken inside gonocoel, very poorly exposed beyond it, each starting with a setose funnel-shaped part (fu) marking the orifice for the cannula to enter and the beginning of a seminal groove, the latter quickly passing onto a short, stout, slightly curved, distad attenuating solenomere (sl) branch fully

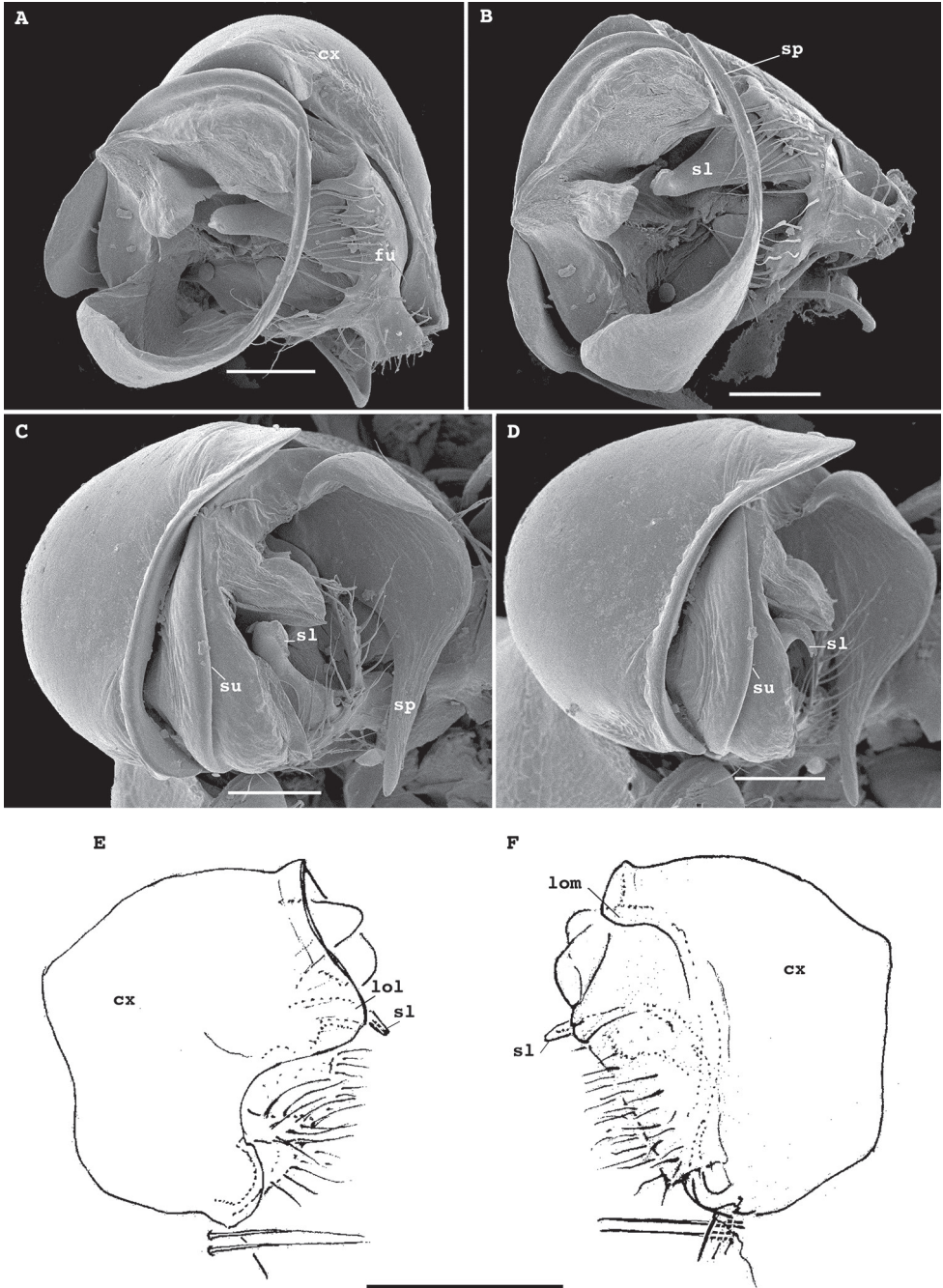


Figure 5. *Bactrodesmus grandis* sp. nov., gonopods of ♂ paratypes **A, B** left gonopod, subventral and ventromesal views, respectively **C, D** right gonopod, ventrolateral and ventral views, respectively **E, F** right gonopod, lateral and mesal views, respectively. Abbreviations: **cx** coxa, **lol** distolateral lobe of coxa, **lom** distomesal lobe of coxa, **fu** basal funnel of telopodite, **sl** solenomere, **sp** spine, **su** parabasal sulcus on telopodite. Scale bars: 0.1 mm.

concealed inside gonocoel; basal part of telopodite extended mesally along fu into a distinct fold turning apically into a long, gently and regularly curved, laterad directed spine (sp); lateral part of telopodite divided distally by a clear-cut suture (su) into two sections, both being simple and stout slabs, but distal one bearing a meso-central membranous sac to protect sl tip.

Remarks. The size, external structures and gonopodal conformation of *B. grandis* sp. nov. match closely those as described and depicted for *B. bicornis* by Demange and Mauriès (1975). The latter species is 8.0 mm long and 1.5 mm wide. Its hypertrophied gonopodal coxa is likewise nearly smooth and shows two small distal lobes, lol and lom. The short spiniform solenomere (sl), the long mesobasal spine (sp) and the two-segmented lateral part of the gonotelopodite look much like, and are located similarly in *B. grandis* sp. nov. Unfortunately, even though the gonopodal structure of *B. claviger* remains unknown, the genus *Bactrodesmus* can presently be redefined (see above).

***Hemisphaeroparia parvula* (Porat, 1894), comb. nov.**

Fig. 1D

Polydesmus parvulus Porat, 1894: 31 (original description).

Type material. Syntypes 2 ♀ (NHRM-GULI000069465), Kamerun, Yngve Sjöstedt leg.

Remarks. Porat (1894) described this species, based on two syntypes deriving from an unspecified locality in Cameroon. We have revised both syntypes and found them to be adult females, one incomplete, the other one complete and with 20 segments (Fig. 1D). Since Cameroon appears to support solely species of the trichopolydesmid genus *Hemisphaeroparia* (24 at the moment), we tentatively transfer the above species to *Hemisphaeroparia*, comb. nov., even though the spiracles located next to coxa 1 or 2 are not enlarged (Fig. 1D). Characteristically enlarged spiracles 1 appear to be restricted to far from all species of *Hemisphaeroparia* (see below under *H. spiniger*). We doubt though that the identity of this enigmatic species will ever be properly established, as superficially the females of most species of Trichopolydesmidae look very much alike. Only the everted vulvae of one of the syntypes might be helpful in the future, but first their comparative study must be accomplished.

***Hemisphaeroparia falcata* Golovatch, Nzoko Fiemapong, Tamesse, Mauriès & VandenSpiegel, 2018**

Figs 6, 7

Hemisphaeroparia falcata Golovatch et al., 2018: 84 (original description).

New material. 1 ♂ (MRAC 22847), 1 ♂ (SEM, MRAC 22848), Cameroon, Center Region, Mafou and Afamba Division, Mfou, cocoa plantation, 3°48'49.6"N, 11°40'49.6"E, 24.VII.2019, A.R. Nzoko Fiemapong leg.

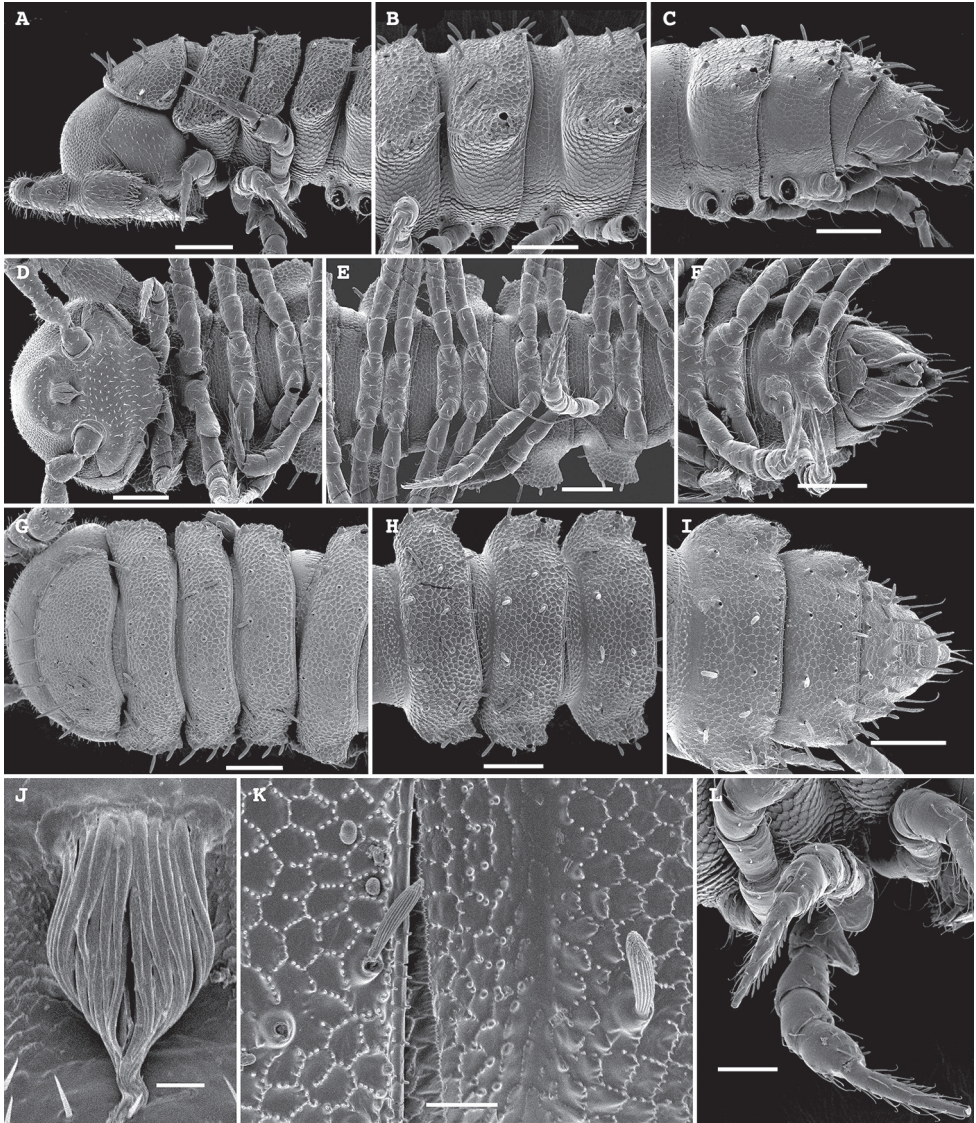


Figure 6. *Hemisphaeroparia falcata* Golovatch, Nzoko Fiemapong, Tamesse, Mauriès & VandenSpiegel, 2018, SEM micrographs of ♂ from Mfou **A, D, G** anterior part of body, lateral, ventral and dorsal views, respectively **B, E, H** midbody segments, lateral, ventral and dorsal views, respectively **C, F, I** posterior part of body, lateral, ventral and dorsal views, respectively **J** epicranial bundles of filaments, dorsal view **K** fine tergal structure with setae, dorsal view **L** anterior legs with a triangular ventral process on prefemur 1, lateral view. Scale bars: 0.1 mm (**A–I**), 0.05 mm (**L**), 0.02 mm (**K**), 0.01 mm (**J**).

Remarks. The new samples fully agree with the original description (Golovatch et al. 2018) and are again illustrated not only to confirm the species' identity (Figs 6, 7), including the unique, conspicuous, epicranial bundles of long filaments on the ♂ head (Fig. 6D, J), but also to note the presence of a marked ventrobasal process on each ♂ prefemur 1 (Fig. 6L), which is much like the one observed in *H. avis* sp. nov.

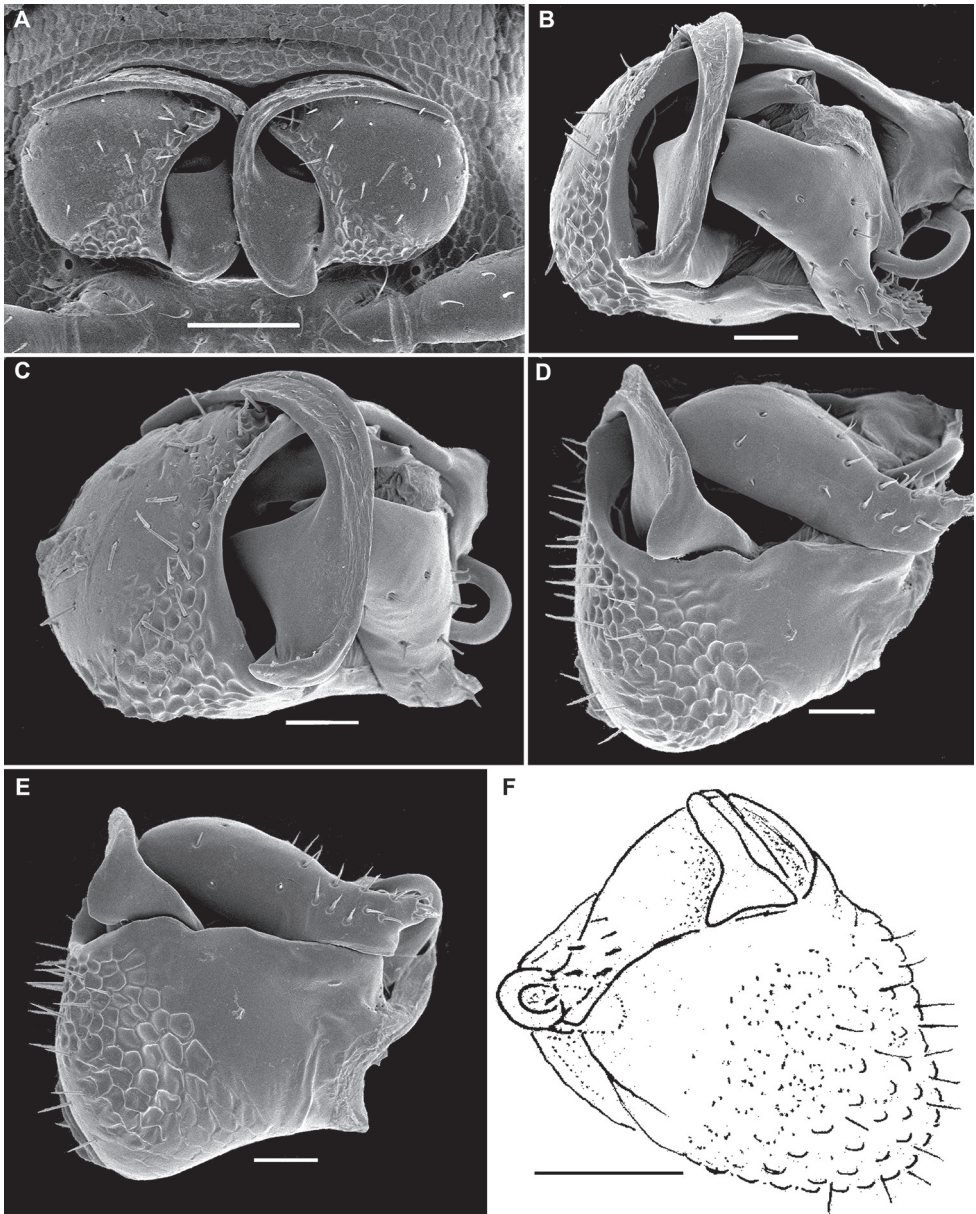


Figure 7. *Hemisphaeroparia falcata* Golovatch, Nzoko Fiemapong, Tamesse, Mauriès & VandenSpiegel, 2018, gonopods of ♂♂ from Mfou **A** both gonopods in situ, ventral view **B–E** left gonopod in various views **F** right gonopod, caudal view. Scale bars: 0.05 mm (**A, F**), 0.02 mm (**B–E**).

The new locality, Mfou, lies quite close to the type one, Awaé, both in the Central Region of Cameroon. Because Awaé represents a native woodland habitat, *H. falcata* might have been introduced to the cocoa plantation at Mfou.

***Hemisphaeroparia spiniger* Golovatch, Nzoko Fiemapong, Tamesse, Mauriès & VandenSpiegel, 2018**

Figs 8, 9

Hemisphaeroparia spiniger Golovatch et al., 2018: 64 (original description).

New material. 1 ♂ (MRAC 22860), 1 ♂ (SEM, MRAC 22861), Cameroon, Center Region, Mafou and Afamba Division, Mfou, cocoa plantation, 3°48'49.6"N, 11°40'49.6"E, 24.VII.2019, A.R. Nzoko Fiemapong leg.

Remarks. The new samples fully agree with the original description (Golovatch et al. 2018) and are again illustrated to confirm the species' identity (Figs 8, 9), including the remarkably enlarged spiracles 1.

The new locality, Mfou, lies quite close to the type one, campus of University Yaounde 1, both in the Central Region of Cameroon. Moreover, because both known localities/habitats represent artificial palm or cocoa plantations, *H. spiniger* could have been introduced there from some native woodlands still to be revealed or already vanished.

***Hemisphaeroparia longibrachiata* sp. nov.**<http://zoobank.org/2B3015B9-3869-471D-B387-C5B3B840FEB4>

Figs 1E, 10, 11

Type material. Holotype ♂ (MRAC 22857), Cameroon, West Region, Haut-Nkam Division; sacred forest, 5,313712N, 10,250323E, 28.V.2019, A.R. Nzoko Fiemapong leg.

Paratypes, 2 ♂, 2 ♀, 1 ♀ fragment (MRAC 22858), 1 ♂ (SEM, MRAC 22859), 1 ♂ (UY1), 1 ♂ (ZMUM Rd 4629), same locality, together with holotype.

Diagnosis. Differs from all other species of the genus by the presence of only 19 segments in both sexes, coupled with a distinct, central, setose pit with two paramedian pores at the bottom in the ♂ epicranium, and the particularly long, falcate, fully exposed branch/process ab on the gonopodal telopodite.

Name. To emphasize the particularly long branch/process ab on the gonopodal telopodite; adjective in feminine gender.

Description. Length of holotype ca 4 mm (♂), width of midbody pro- and metazonae 0.3 and 0.5 mm (♂), respectively. Length of paratypes 4–5 mm, width of midbody pro- and metazonae 0.3–0.4 and 0.5–0.6 mm (♂, ♀), respectively. Coloration in alcohol faintly marbled, light brown to brown, venter and legs light grey-brown (Fig. 1E).

Body with 19 segments in both sexes. Tegument very delicately micro-alveolate, mainly slightly shining. Head very densely micropilose, ♂ epicranium slightly elevated and supplied with a very distinct, central, oval, densely setose pit with two paramedian pores (Fig. 10G, K). Interantennal isthmus almost three times diameter of antennal socket. Antennae long and strongly clavate, reaching back past segment 4 (♂) or 3 (♀) when stretched dorsally. In length, antennomere 3 = 6 > 5 > 2 =

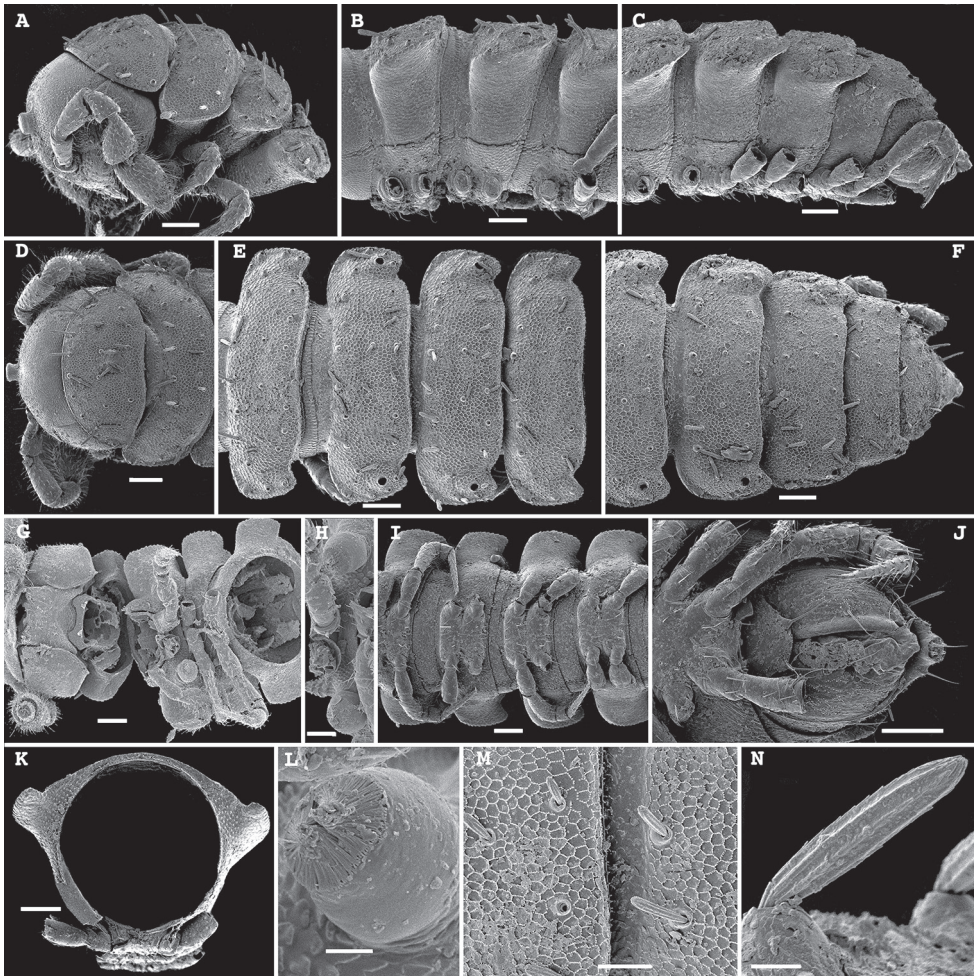


Figure 8. *Hemisphaeroparia spiniger* Golovatch, Nzoko Fiamapong, Tamesse, Mauriès & VandenSpiegel, 2018, SEM micrographs of ♂ from Mfou **A, D, G** anterior part of body, lateral, dorsal and ventral views, respectively **B, E, I** midbody segments, lateral, dorsal and ventral views, respectively **C, F, J** posterior part of body, lateral, dorsal and ventral views, respectively **H, L** enlarged spiracles near coxae 2, ventral view **K** cross-section of a midbody segment, caudal view **M** fine tergal structure with setae, dorsal view **N** tergal seta, enlarged. Scale bars: 0.1 mm (**A–G, I–K**), 0.05 mm (**H, M**), 0.02 mm (**L**), 0.01 mm (**N**).

$4 > 7 > 1$; antennomere 6 the largest, antennomeres 5 and 6 each with a distinct, round, distodorsal field of sensilla. In width, segments 5–15 $> 2 > \text{head} = \text{segments 3 and 4} > \text{collum}$; body gradually tapering towards telson on segments 16–19. Collum ellipsoid, transversely oval, like all following metaterga with three transverse, regular rows of setae; anterior row composed of somewhat longer setae. Tergal setae medium-sized, each ca $1/5$ as long as metatergum, bacilliform and longitudinally ribbed (Fig. 10A–E, I, M), always 3+3 in each row on postcollum metaterga; 2–3 additional setae at lateral margin of paraterga. Dorsum invariably regularly convex.

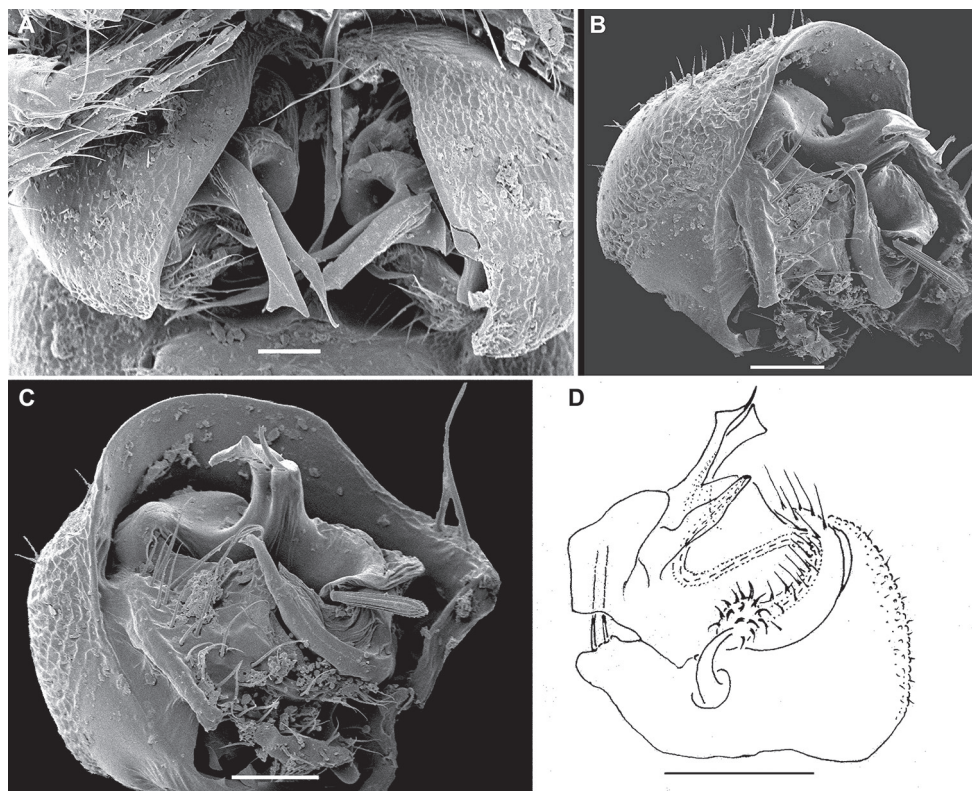


Figure 9. *Hemisphaeroparia spiniger* Golovatch, Nzoko Fiemapong, Tamesse, Mauriès & VandenSpiegel, 2018, gonopods of ♂♂ from Mfou **A** both gonopods in situ, ventral view **B, C** right gonopod, caudolateral and subcaudal views, respectively **D** left gonopod, mesal view. Scale bars: 0.1 mm (**D**), 0.05 mm (**A–C**).

Paraterga medium-sized, set at around upper 1/3 of metazonae (Fig. 10D–F), visible starting with collum, regularly rounded, lateral incisions absent. Caudal corner of paraterga mostly rounded, drawn back past rear tergal margin only on segments 16 and 17 (Fig. 10C, E). Pore formula normal: 5, 7, 9, 10, 12, 13, 15–18. Ozopores small, round, opening flush dorsally near caudal corner of poriferous paraterga. Stricture between pro- and metazonae wide, shallow. Limbus very finely microspiculate. Spiracles very small, as usual. Pleurosternal carinae traceable as very faint ridges or lines on most segments (Fig. 10D, E). Epiproct short, conical, flattened dorsoventrally. Hypoproct semi-circular, setae strongly separated and borne on minute knobs.

Sterna wide, unmodified, setose. Legs rather long and slender, ca 1.2–1.3 (♂) or 1.0–1.1 (♀) times as long as midbody height; in length, tarsus > femur > coxa = prefemur = postfemur = tibia, the latter with a particularly long, tactile seta apicodorsally. Tarsal brushes absent.

Gonopods (Fig. 11) with large, subglobose, clearly exposed, alveolate coxae, these rather densely setose nearly throughout, fused medially at base, each carrying two very

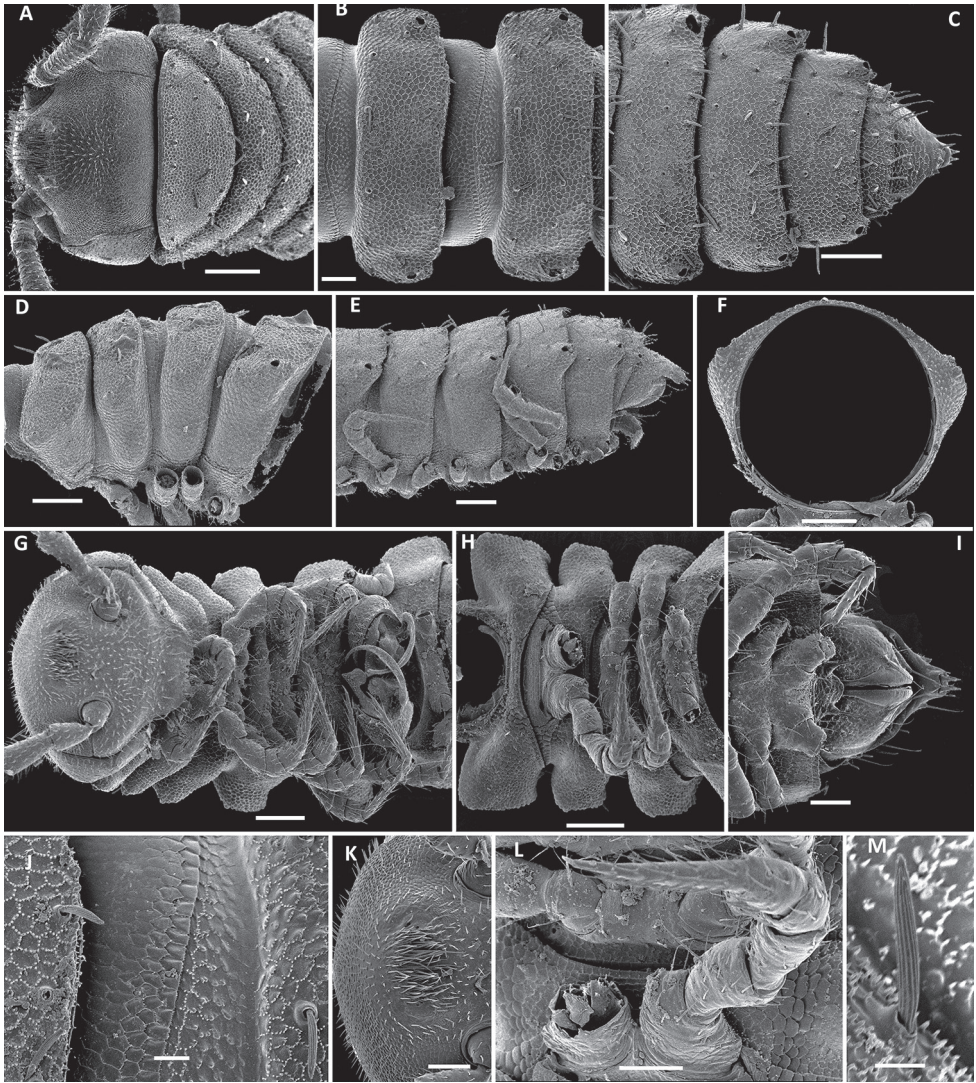


Figure 10. *Hemisphaeroparia longibrachiata* sp. nov., SEM micrographs of a ♂ paratype **A, G** anterior part of body, dorsal and ventral views, respectively **B, D, H** midbody segments, dorsal, lateral and ventral views, respectively **C, E, I** posterior part of body, dorsal, lateral and ventral views, respectively **F** cross-section of a midbody segment, caudal view **J** fine tergal structure with setae, dorsal view **K** epicranial pit, dorsal view **L** leg 2 with gonopore on coxa **M** limbus and tergal seta, enlarged. Scale bars: 0.1 mm (**A–G, I–K**), 0.05 mm (**H, M**), 0.02 mm (**L**), 0.01 mm (**N**)

long setae near place of fusion. Telopodites largely well exposed beyond a moderately deep gonocoel, each with two low bulges basal to anterior branch (ab), the latter extremely long, slightly coiled in basal third, falcate, gradually attenuating towards a narrowly rounded tip. No solenomere discernible at base of ab.

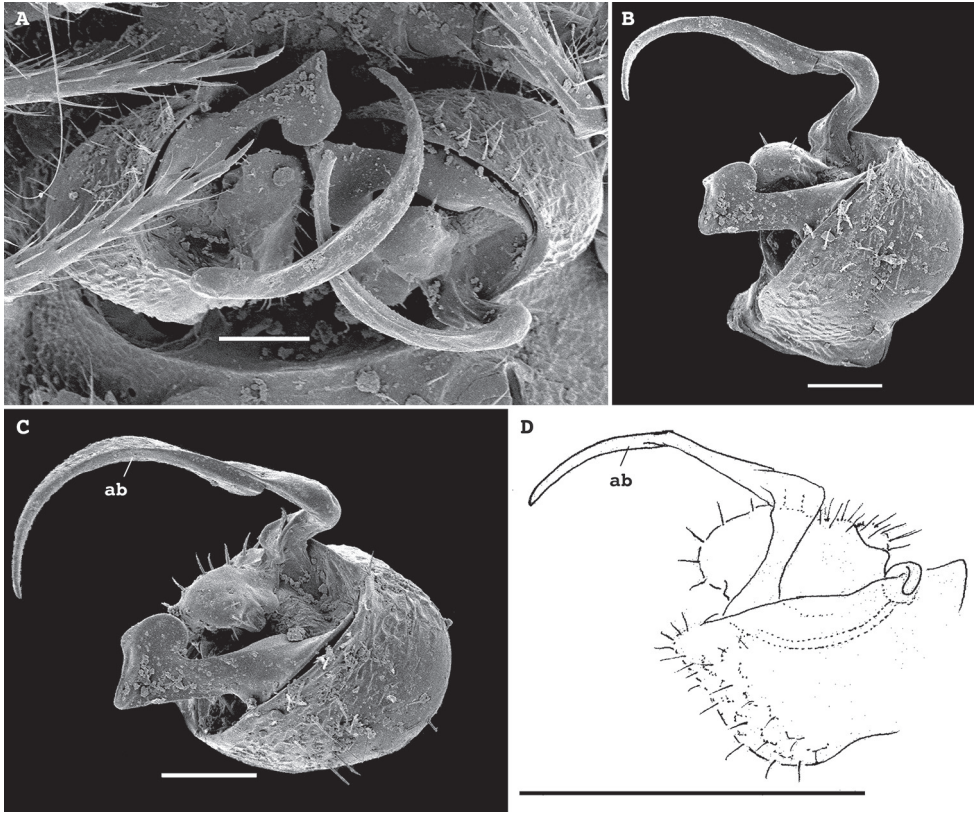


Figure 11. *Hemisphaeroparia longibrachiata* sp. nov., gonopods of ♂ paratypes **A** both gonopods in situ, ventral view **B, C** left gonopod, caudolateral and subcaudal views, respectively **D** right gonopod, mesal view. Abbreviation: **ab** apical branch. Scale bars: 0.1 mm (**D**), 0.05 mm (**A–C**).

***Hemisphaeroparia avis* sp. nov.**

<http://zoobank.org/3BEC5271-1547-4F69-9757-7629D354F257>

Figs 1F, 12, 13

Type material. *Holotype* ♂ (MRAC 22853), Cameroon, Center Region, Mafou and Afamba Division, Mfou, cocoa plantation, 3°48'49.6"N, 11°40'49.6"E, 24.VII.2019, A.R. Nzoko Fiemapong leg. *Paratypes*: 3 ♂, 12 ♀, 2 subadult ♀ (many fragmented) (MRAC 22854), 12 ♂ (MRAC 22855), 1 ♂ (SEM, MRAC 22856), 1 ♂, 1 ♀ (ZMUM Rd 4630), 1 ♂ (UY1), same locality, together with holotype.

Diagnosis. Differs from all other species of the genus by the presence of a boleti-form epicranial tubercle (♂) (Fig. 12D, K), coupled with the unusually large, disc-shaped spiracles next to coxae 1 or 2 (Fig. 12G, L), the strong, setose, subtriangular, distoventral process on ♂ prefemur (Fig. 12J), the densely setose sterna between ♂ coxae 2 and 3 (Fig. 12M), and the sole prominent, clearly exposed process (ab) with a bird's beak-shaped tip on the gonopodal telopodite (Fig. 13).

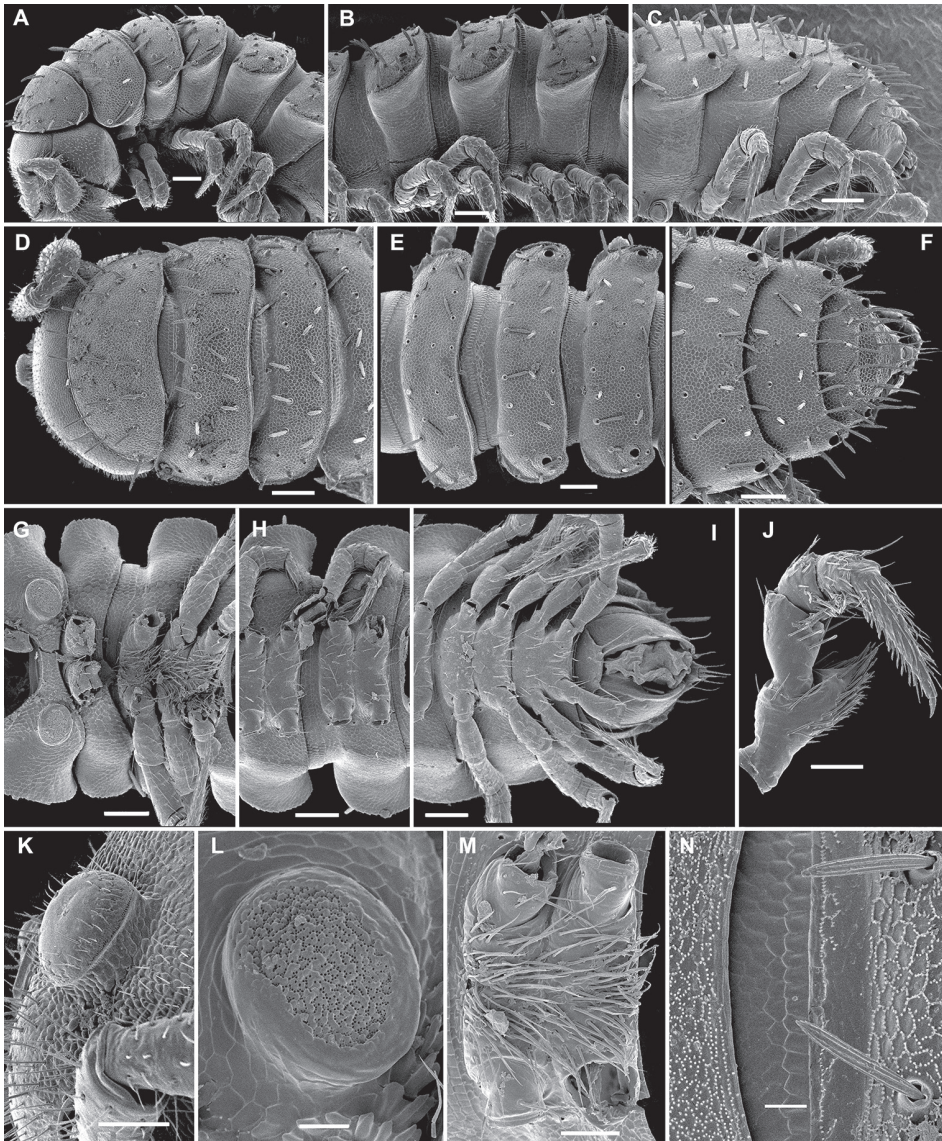


Figure 12. *Hemisphaeroparia avis* sp. nov., SEM micrographs of a ♂ paratype **A, D, G** anterior part of body, lateral, dorsal and ventral views, respectively **B, E, H** midbody segments, lateral, dorsal and ventral views, respectively **C, F, I** posterior part of body, lateral, dorsal and ventral views, respectively **J** telopodite 1 with a prominent process in prefemur **K, L** epicranial tubercle **M** densely setose sterna between coxae 2 and 3 **N** fine tergal structure with limbus and setae, dorsal view. Scale bars: 0.1 mm (**A–I**), 0.05 mm (**J, K, M**), 0.02 mm (**L, N**).

Name. From Latin *avis* (= bird), to emphasize the bird's beak-shaped tip of the sole process (ab) of the gonopodal telopodite; noun in apposition.

Description. Length of holotype ca 4.5 mm, width of midbody pro- and meta-zonae 0.45 and 0.6 mm (♂), respectively. Length of paratypes 4.0–5.5 mm, width of

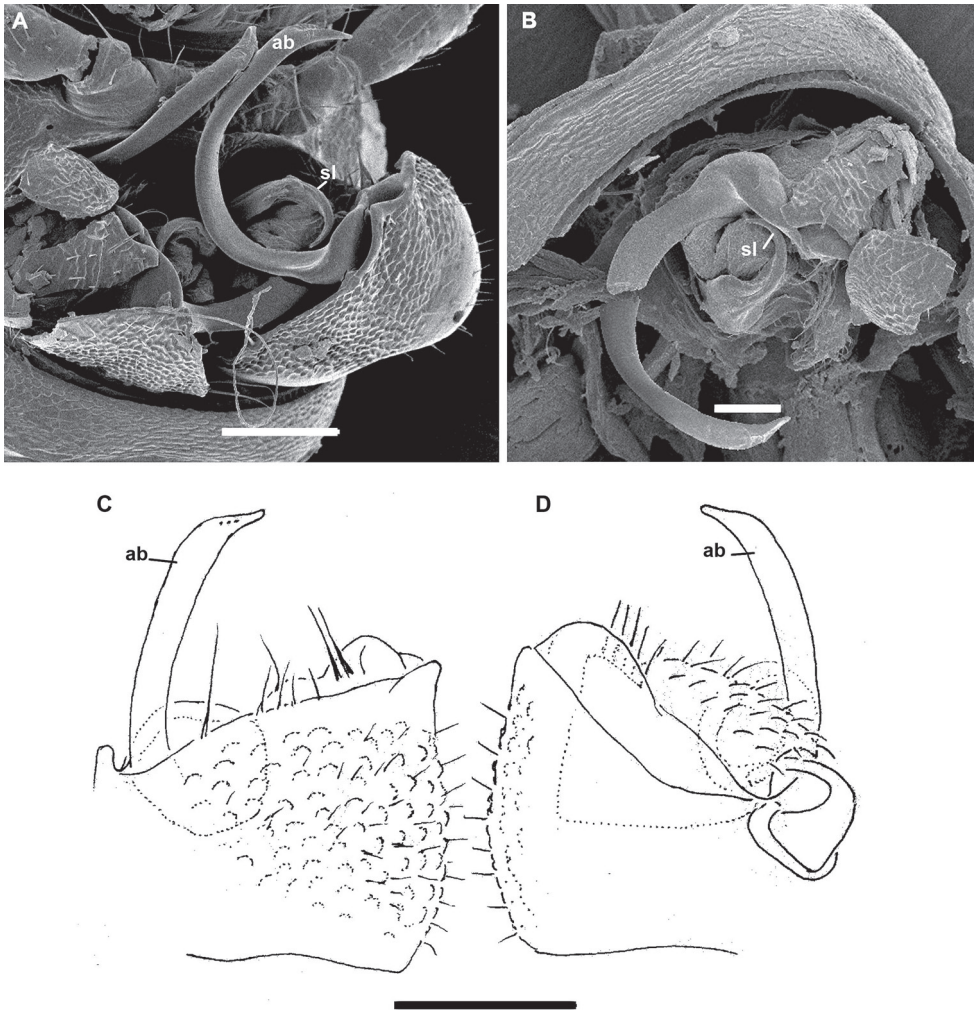


Figure 13. *Hemisphaeroparia avis* sp. nov., gonopods of ♂ paratypes **A** both gonopods in situ, ventral view **B–D** right gonopod, ventrocaudal, lateral and mesal views, respectively. Abbreviations: **ab** apical branch, **sl** solenomere. Scale bars: 0.1 mm (**A, C, D**), 0.05 mm (**B**).

midbody pro- and metazonae 0.45–0.5 and 0.6–0.7 (♂) or 0.6–0.8 mm (♀), respectively. Coloration in alcohol mostly uniformly reddish, apparently in part due to a thin earth crust coating most of the body (Fig. 1F); more rarely nearly pallid.

Body with 20 segments in both sexes. Tegument very delicately micro-alveolate, slightly shining to dull. Head very densely micropilose, with a very distinct, mushroom-like, frontal tubercle (♂) (Fig. 12D, K). Interantennal isthmus ca 1.3–1.4 times diameter of antennal socket. Antennae long and strongly clavate, reaching back up to segment 3 when stretched dorsally (♂, ♀). In length, antennomere 3 = 6 > 5 > 2 = 4 > 7 > 1; antennomere 6 the largest, antennomeres 5 and 6 each with a distinct, round, distodorsal field of minute sensilla. In width, collum < head < segments 2–4

< 5–16; thereafter body gradually tapering towards telson. Collum ellipsoid, transversely oval, like all following metaterga with three transverse, regular rows of setae. Tergal setae relatively long, each mostly ca 1/3–1.4 as long as metatergum, a little longer on collum and gradually reduced in size towards telson, bacilliform and longitudinally ribbed (Fig. 12A–F, N), always 3+3 in each row on postcollum metaterga. Dorsum invariably regularly convex. Paraterga medium-sized, set at around upper 1/3 of metazonae (Fig. 12A–C), visible starting with collum, often slightly upturned caudally, faintly, but regularly rounded and bordered, lateral incisions absent; but 2–3 setae or their insertion points present at lateral margin. Caudal corner of paraterga mostly rounded, drawn increasingly back, but faintly reaching past rear tergal margin only on segments 18 and 19 (Fig. 12C, F). Pore formula normal: 5, 7, 9, 10, 12, 13, 15–18. Ozopores small, round, opening flush dorsally near caudal corner of poriferous paraterga. Stricture between pro- and metazonae wide, shallow. Limbus very finely microspiculate. Spiracles next to coxae 1 or 2 unusually prominent, discoid and microporose (Fig. 12G, L); following ones small, inconspicuous, as usual. Pleurosternal carinae traceable as very faint ridges or lines on most segments (Fig. 12A–C). Epiproct short, conical, flattened dorsoventrally. Hypoproct semi-circular, setae strongly separated and borne on minute knobs.

Sterna wide, mostly unmodified and sparsely setose, unusually densely setose only between ♂ coxae 2 and 3 (Fig. 12M); each ♂ prefemur 1 with a prominent, densely setose, subtriangular, blunt, distoventral process (Fig. 12J) (much like in *H. falcata*); some setae on ♂ legs slightly modified, with flattened or branching tips. Legs rather long and slender, ca 1.2–1.3 (♂) or 1.0–1.1 (♀) times as long as midbody height; in length, tarsus > femur > coxa = prefemur = postfemur = tibia, the latter with a particularly long, tactile seta apicodorsally. Tarsal brushes absent.

Gonopods (Fig. 13) with large, subglobose, clearly exposed, alveolate coxae, these rather densely setose nearly throughout, fused medially at base, each carrying two very long setae near place of fusion. Telopodite bases clearly concealed inside a large gonocoel, each very densely setose along funnel-shaped mesal part, with only one strong, slightly curved, very distinctly exposed, ribbon-shaped, apically bird's beak-shaped branch (ab). Solenomere (sl) a short unciform branch located at and hidden by base of ab.

Remarks. Mfou, the type locality of *Hemisphaeroparia avis* sp. nov., is shared with as many as further two congeners, *H. spiniger* and *H. falcata*.

***Trichozonus* Carl, 1905**

Type species. *Trichozonus escalerae* Carl, 1905, the type species by monotypy, Equatorial Guinea (Carl 1905).

Description. Female. 20 segments, body length 8 mm; paraterga modest, tergal setae long and bacilliform.

Remarks. This genus is bound to remain dubious until a male topotypic sample from Fernando Po becomes available for study. The only other trichopolydesmid known from Fernando Po is *Dendrobrachypus pusillus* Verhoeff, 1941 (= *Mecistoparia pusilla*), which is only 5.0–5.5 mm long (Verhoeff 1941). Mauriès and Heymer (1996) tentatively synonymized *Trichozonus* with *Physetoparia*.

Discussion

Interestingly, based on the gonopodal conformations alone, all Afrotropical Trichopolydesmidae seem to represent a single lineage characterized by basically rounded, lens-shaped, oblong, relatively small gonotelopodites more or less deeply sunken into a gonocoel and showing, unlike the bulk of Euro-Mediterranean confamilial members (30 species in 17 genera, see Vagalinski et al. (2019)), no transversely oriented bases. The various outgrowths (usually 1–3) of the telopodites, if any, are typically not erect, but curved and directed caudomesad, while the solenomeres, if any, are mostly simple, short, fully mesal processes or lobes. In addition, most species in life tend to show different tinges of red, but are quick to fade in alcohol. Only one genus and species, *Simplogonopus rubellus* (Attems, 1902), also reddish *in vivo*, seems to be of the Afrotropical stock, but it occurs beyond tropical Africa. It has been recorded only from Crete, the Aegean islands of Kythnos and Chios, and northeastern Bulgaria (Vagalinski et al. 2019). Among the possible reasons to explain such a distribution, the following have been considered: (1) a palaeorelict survivor, (2) a human-caused introduction, and (3) recent migration. A combination of reasons cannot be excluded either (Vagalinski et al. 2019).

Previous knowledge of the trichopolydesmid fauna of Cameroon (Golovatch et al. 2018) seems to point to two interesting observations. Cameroon presently appears to be the country in Africa best known with regard to Trichopolydesmidae diversity, even though its trichopolydesmid fauna seems to be surprisingly monotonous, represented by species (16 of 26) of a single large genus, *Hemisphaeroparia*, which ranges from Guinea in the west to Uganda in the east. This has also permitted us to provisionally assign an old species described from Cameroon to that genus as well. The second observation is that there tend to be as many species as localities, meaning that each species has been encountered in a single place. Localities that support two species are rather exceptional (Golovatch et al. 2018).

Our present contribution partly disproves the latter observation, since two already described species have been found more widespread and occurring at least at localities other than the type ones. Moreover, the present paper reveals that one and the same locality can harbour as many as three congeners! It is quite clear that the diversity of Trichopolydesmidae in tropical Africa, despite all efforts, both past and present, remains grossly understudied. Many new taxa and records are undoubtedly still ahead, but we believe we have a sufficiently solid foundation to continue.

Acknowledgements

This research was partially supported by the “Société des Mines de Fer de Guinée”. Special thanks go to Sven Boström, the Keeper at the Swedish Royal Museum of Natural History (Naturhistoriska riksmuseet) in Stockholm, who sent us the type material of *Polydesmus parvulus* Porat, 1894 for restudy, as well as to both reviewers, Cathy Car (Western Australian Museum, Australia) and Henrik Enghoff (Natural History Museum of Denmark, Copenhagen, Denmark), whose thorough, constructive and positive critiques have allowed to considerably improve our paper. We are most grateful to the Administration of the MRAC for having invited SIG for 3 weeks to their museum for research in September 2019. Jonathan Brecko skillfully took and stacked all colour pictures.

References

- Attems CG (1909) 19. Myriopoda. Wissenschaftliche Ergebnisse der schwedischen zoologischen Expedition nach dem Kilimandjaro, dem Meru und den umgebenden Massasteppen Deutsch-Ostafrikas 1905–1906 unter Leitung von Prof. Dr. Yngve Sjöstedt, Stockholm, 64 pp.
- Attems C (1939) Myriopoda. Mission scientifique de l’Omo 5(55). Mémoires du Muséum national d’Histoire naturelle, NS 9: 303–318.
- Attems C (1940) Myriopoda 3. Polydesmoidea III. Fam. Polydesmidae, Vanhoeffeniidae, Cryptodesmidae, Oniscodesmidae, Sphaerotrichopidae, Peridontodesmidae, Rhachidesmidae, Macellophidae, Pandirodesmidae. Das Tierreich 70: 1–577. <https://doi.org/10.1515/9783111609645>
- Attems C (1953) Neue Myriopoden des Belgischen Congo. Annales du Musée Royal du Congo belge, série in 8, Sciences zoologiques 18: 1–139.
- Brecko J, Mathys A, Dekoninck W, Leponce M, VandenSpiegel D, Semal P (2014) Focus stacking: Comparing commercial top-end set-ups with a semi-automatic low budget approach. A possible solution for mass digitization of type specimens. ZooKeys 464: 1–23. <https://doi.org/10.3897/zookeys.464.8615>
- Brolemann HW (1920) Myriapodes III, Diplopoda. Voyage de Ch. Alluaud et R. Jeannel en Afrique orientale (1911–1912). Résultats scientifiques. Paris, L. Lhomme, 49–298.
- Brolemann HW (1926) Myriapodes recueillis en Afrique occidentale française par M. l’Administrateur en chef L. Duboscq. Archives de Zoologie expérimentale et générale 65: 1–159.
- Carl J (1905) Diplopodes de la Guinée espagnole. Memorias de la Sociedad española de Historia natural 1(15): 261–284.
- Chamberlin RV (1951) On Diplopoda of North-East Angola. Museu do Dundo, Estudos Diversos III. Lisboa, Publicações culturais da Companhia de diamantes de Angola (Diamang) 10: 65–93.
- Cook OF (1896a) A new diplopod fauna in Liberia. The American Naturalist, Entomology 30: 413–420. <https://doi.org/10.1086/276402>

- Cook OF (1896b) Summary of new Liberian Polydesmoidea. Proceedings of the Academy of Natural Sciences of Philadelphia 1896: 257–267.
- Demange JM (1967) Une nouvelle espèce du genre *Hemisphaeroparia* Schubart (Myriapoda, Diplopoda, Polydesmoidea). Bulletin de l'Institut français de l'Afrique noire, série A 29(1): 123–125.
- Demange JM, Mauriès JP (1975) Myriapodes-Diplopedes des monts Nimba et Tonkoui (Côte d'Ivoire, Guinée) récoltés par M. Lamotte et ses collaborateurs de 1942 à 1960. Annales du Musée Royal de l'Afrique Centrale, série in-8, Sciences zoologiques 212: 1–192.
- Golovatch SI, Nzoko Fiemapong AR, Tamesse JL, Mauriès JP, VandenSpiegel D (2018) Trichopolydesmidae from Cameroon, 1: The genus *Hemisphaeroparia* Schubart, 1955. With a genus-level reclassification of Afrotropical genera of the family (Diplopoda, Polydesmida) ZooKeys 785: 49–98. <https://doi.org/10.3897/zookeys.785.27422>
- Kraus O (1958) Diplopeden aus Angola. Museu do Dundo, Lisboa, Publicações culturais da Companhia de diamantes de Angola (Diamang) 38: 47–84.
- Mauriès JP (1968) Matériaux récoltés par M. H. Coiffait au Gabon: Myriapoda, Diplopoda. Biologia Gabonica 3(4): 361–401 [for 1967]
- Mauriès JP, Heymer A (1996) Nouveaux micropolydesmides d'Afrique centrale: essai de rassemblement pour une révision du genre *Sphaeroparia* (Diplopoda, Polydesmida, Fuhrmannodesmidae). Bulletin du Muséum national d'Histoire naturelle, 4e série 18 (Section A, Nos 1–2): 165–184.
- Porat O (1894) Zur Myriopodenfauna Kameruns. Bihang till Kungliga Svenska Vetenskaps-Akademie 20(4/5): 1–90.
- Schubart O (1955) Proterospermophora oder Polydesmoidea von Französisch West-Afrika (Diplopoda). Bulletin de l'Institut français de l'Afrique noire, série A 17(2): 377–443.
- Vagalinski B, Golovatch SI, Akkari N, Stoev P (2019) *Simplogonopus rubellus* (Attems, 1902) gen. n., comb. nov. (Diplopoda: Polydesmida: Trichopolydesmidae): Revealing the identity of an enigmatic Eastern-Mediterranean millipede. Acta Zoologica Bulgarica 71(3): 325–334.
- Verhoeff KW (1941) Myriapoden der Insel Fernando Po. Zoologischer Anzeiger 136(5/6): 89–98.

A new species of *Acorhinotermes* Emerson, 1949 (Blattodea, Isoptera, Rhinotermitidae) from Colombia, with a key to Neotropical Rhinotermitinae species based on minor soldiers

Daniel Castro¹, Rudolf H. Scheffrahn²

1 Instituto Amazónico de Investigaciones Científicas SINCHI, Avenida Vásquez Cobo Calles 15 y 16, Leticia, Amazonas, Colombia **2** Fort Lauderdale Research and Education Center, Institute for Food and Agricultural Sciences, University of Florida, 3205 College Avenue, Davie, Florida 33314, USA

Corresponding author: Daniel Castro (danielkaz80@gmail.com)

Academic editor: Eliana Canello | Received 19 June 2019 | Accepted 11 October 2019 | Published 21 November 2019

<http://zoobank.org/544A3082-EDF4-45C1-B611-2A845371D8CF>

Citation: Castro D, Scheffrahn RH (2019) A new species of *Acorhinotermes* Emerson, 1949 (Blattodea, Isoptera, Rhinotermitidae) from Colombia, with a key to Neotropical Rhinotermitinae species based on minor soldiers. ZooKeys 891: 61–70. <https://doi.org/10.3897/zookeys.891.37523>

Abstract

Acorhinotermes Emerson, 1949 is the only Neotropical Rhinotermitine genus with no major soldier. Herein *Acorhinotermes claritae* Castro & Scheffrahn, **sp. nov.** is described based on minor soldiers and an alate nymph collected in a secondary rain forest in the Colombian Amazon. The minor soldier of *A. claritae* Castro & Scheffrahn, **sp. nov.** has longer mandibular points and it is comparatively smaller than *A. subfusciceps*. An illustrated key to the minor soldiers of the Neotropical species of Rhinotermitinae is presented.

Keywords

Colombian Amazon, *Dolichorhinotermes*, *Rhinotermes*, taxonomy, termites

Introduction

The subfamily Rhinotermitinae Froggatt, 1897 comprises worldwide the genera *Par-rhinotermes* Holmgren, 1910, *Macrorhinotermes* Holmgren, 1913, *Schedorhinotermes* Silvestri, 1909, *Rhinotermes* Hagen, 1858, *Dolichorhinotermes* Snyder & Emerson, 1949, and *Acorhinotermes* Emerson, 1949. The last three genera are recorded from the Neotropical region (Maiti 2011; Krishna et al. 2013).

Acorhinotermes subfusciceps was originally described within the genus *Rhinotermes* (Emerson 1925; Snyder 1949). Emerson in Snyder (1949) transferred *Rhinotermes subfusciceps* to a new genus, *Acorhinotermes*, straightening the absence of the major soldier as a diagnostic characteristic of the genus.

Colombia has very few records of species of the subfamily Rhinotermitinae, only *Rhinotermes hispidus* Emerson, 1925 and *Rhinotermes marginalis* (Linnaeus, 1758) are reported (Pinzón et al. 2017; Constantino 2019). *Acorhinotermes* has been reported for Brazil, Guyana, French Guiana, Venezuela and Peru (Snyder 1949; Davies et al. 2003; Salick et al. 2013; Scheffrahn unpubl. data; Silva et al. 2019). Currently, only *Dolichorhinotermes japuraensis* Constantino, 1990 is endemic to the Amazon Basin (Constantino 1991). Additionally, all Rhinotermitinae species except *Dolichorhinotermes longidens* (Snyder, 1924) are found in the Amazon Region (Castro unpubl. data, Constantino 1992, Constantino and Canello 1992, Krishna et al. 2013).

In this paper, we describe a new species *Acorhinotermes claritae* sp. nov. based on characters from the minor soldier and alate nymph. We provide as well as an illustrated key for the Neotropical Rhinotermitinae based on the minor soldier caste, which would be very helpful when major soldiers or imagoes are not represented in the collected samples.

Materials and methods

Specimens of *Acorhinotermes claritae* sp. nov. were collected in trucks of dead trees with aspirators, at weat season (July 12–19, 2018), in the southern state of Amazonas, Colombia, and preserved in 95% ethanol. The holotype and paratypes are deposited in the “Colección de Artrópodos Terrestres de la Amazonía Colombiana”, SINCHI Amazon Institute of Scientific Research, Leticia, Amazonas, Colombia (CATAC). Paratypes are also deposited in the Termite Collection, Fort Lauderdale Research and Education Center, University of Florida, Davie, Florida, United States of America (UF).

Additional material examined for the Rhinotermitine species key is deposited in the UF and the CATAC, as follows: *Acorhinotermes subfusciceps*, PERU, (-9.05222, -75.57818), 30/05/2014, R. Scheffrahn col., 376 m (PN.799.0); *Dolichorhinotermes lanciaris* Engel & Krishna, 2007, PERU, (-11.06414, -74.71955), 25/05/2014, R. Scheffrahn col., 602 m (PN.104.0); *Dolichorhinotermes longidens*, PANAMA, (9.34349, -79.77382), 4/06/2005, R. Scheffrahn col., 216 m (PN.684.0); *Dolichorhinotermes longilabius* (Emerson, 1924), FRENCH GUYANA, (5.03784, -52.95580), 7/02/2008, J.

Krêcêk col., 87 m (FG.181.0); *Rhinotermes hispidus*, BOLIVIA (-16.99937, -65.62736), 26/05/2013, R. Scheffrahn col., 491 m (BO. 163.0); *Rhinotermes marginalis*, BOLIVIA, (-16.97043, -65.21001), 26/05/2013, col. R. Scheffrahn, 231 m (BO. 76.0); *Dolichorhinotermes longilabius*, COLOMBIA, (4.343416, -69.98627), col. L. Pinedo, 101 m (CATAC-03314); *Rhinotermes hispidus*, COLOMBIA (3.8210, -67.81041), 16/03/2019, col. J. Chase, 98 m (CATAC-03687); *Rhinotermes marginalis*, COLOMBIA, (-3.80044, -70.31533), col. J. Chase, 76 m (CATAC-03558). In the other hand, Emerson (1925), Constantino (1990), Snyder (1924), Snyder (1926) and Desneux (1904) were consulted for those species not represented in the UF or CATAC collections.

Morphological characters used for the alate nymph and minor soldier follows Roonwal (1970). Microphotographs were taken as multi-layer montages using a Leica M205C stereomicroscope controlled by Leica Application Suite version 3 software. Preserved specimens were suspended in a pool of Purell Hand Sanitizer to position the specimens on a transparent Petri dish background.

Taxonomy

Acorhinotermes claritae Castro & Scheffrahn, sp. nov.

<http://zoobank.org/92519036-1333-4086-9485-BBF1D8A33B3E>

Type material. *Holotype*. Minor soldier from colony CATAC 2722.

Type-locality. COLOMBIA: Amazonas, Leticia (-4.08975, -69.92705).

Paratypes. COLOMBIA, Amazonas, Leticia, (-4.08975, -69.92705): 12.VII.2018, James Chase col., 87 m, 1 alate nymph, 45 minor soldiers, 156 workers (CATAC 2722); 12.VII.2018, Daniela Manso col., 87 m, 11 minor soldiers, 56 workers (CATAC 2723); (-4.08900, -69.92497): 12.VII.2018, James Chase col., 91 m, 5 minor soldiers, 2 workers (CATAC 2724); (-4.04875, -70.00527): 13.VII.2018, Daniela Manso col., 106 m, 33 minor soldiers, 41 workers (CATAC 2750); (-4.04972, -69.92704): Daniel Castro col, 97 m, 5 minor soldiers, 4 workers (UF no. CO 918).

Diagnosis. Minor soldier head with concave lateral margins forming a posterior constriction, with prominent mandibular points extend beyond the fontanelle.

Description. *Alate nymph*. (Fig. 1A, B) Head capsule yellowish-brown, widely oval with numerous long bristles. Antennae with 20 articles, 2<3=4. Dorsum of body concolorous with head capsule. Compound eyes subcircular, eye margins wide and broadly separated from antennal sockets. Ocelli of small size, oval, well separated from eyes. Clypeus linguiform, not buttressed by frontal projection. Pronotum margin with numerous long bristles; rounded lateral margins. Mandibles with M1 more prominent than apical teeth. Right mandible with M1 more projected than left mandible. Left mandible with M2 projected to half the length of M1, M2 and M3 forms an obtuse angle, M3 and molar tooth projected at same distance.

Measurements (mm) for a single alate nymph: head length with labrum 1.27, head length to postclypeus 1.46, maximum width of the head with eyes 1.39, width of head

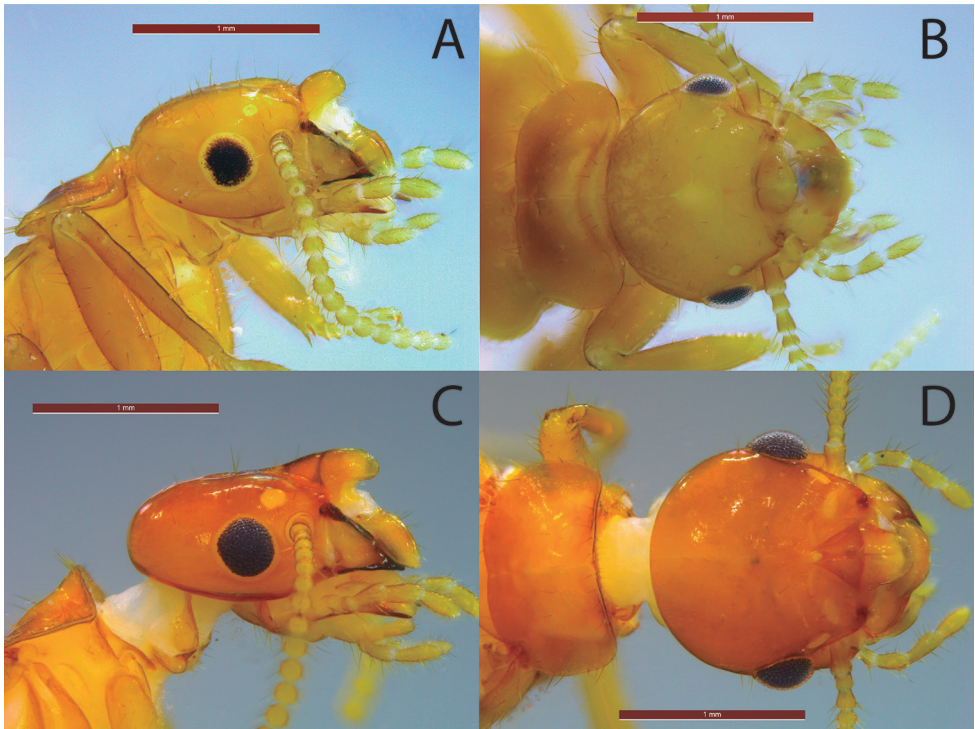


Figure 1. *Acorhinotermes* spp. **A, B** alate nymph of *Acorhinotermes claritae* sp. nov., lateral and dorsal view **C, D** imago of *Acorhinotermes subfusciceps*, lateral and dorsal view. Scale bar: 1 mm.

without eyes 1.21, diameter of eye 0.25, ocellus diameter 0.08, length of pronotum 0.78, width of pronotum 1.36, total body-length without wings 6.81.

Comparisons. *Acorhinotermes claritae* sp. nov. has more abundant bristles in lateral view. The ocelli and eyes are smaller than the *A. subfusciceps* imago, and the clypeal projection projects more acutely in *A. claritae* sp. nov. and it is not buttressed by a frontal projection as in *A. subfusciceps* (Fig. 1C).

Minor soldier. (Fig. 2; Table 1) Head capsule, in dorsal view, with concave lateral margins forming posterior constriction 10–12 long erect bristles, without microscopic hairs. Antennae with 15 or 16 articles, formula 2=3<4=5. Mandible vestigial, point long, straight and sharp. Labrum hyperelongate, broadening apically; tip bilobed; nearly in same plane as vertex in lateral view. Fontanelle at basal one-fifth of labrum. Pronotum concolorous with head, with 4–8 dispersed bristles, 2–4 in anterior margin and 2–4 in surface, pronotum without microscopic hairs. Tergites pale yellow, margins covered by dense layer of hairs. Legs with many long and short bristles; thick bristles on foretibia.

Comparisons. *Acorhinotermes claritae* sp. nov. is smaller and has longer mandibular points than *A. subfusciceps*. In profile, the dorsa of the occiput, vertex, and labrum of *A. claritae* sp. nov. form a nearly straight line, while in *A. subfusciceps* this profile

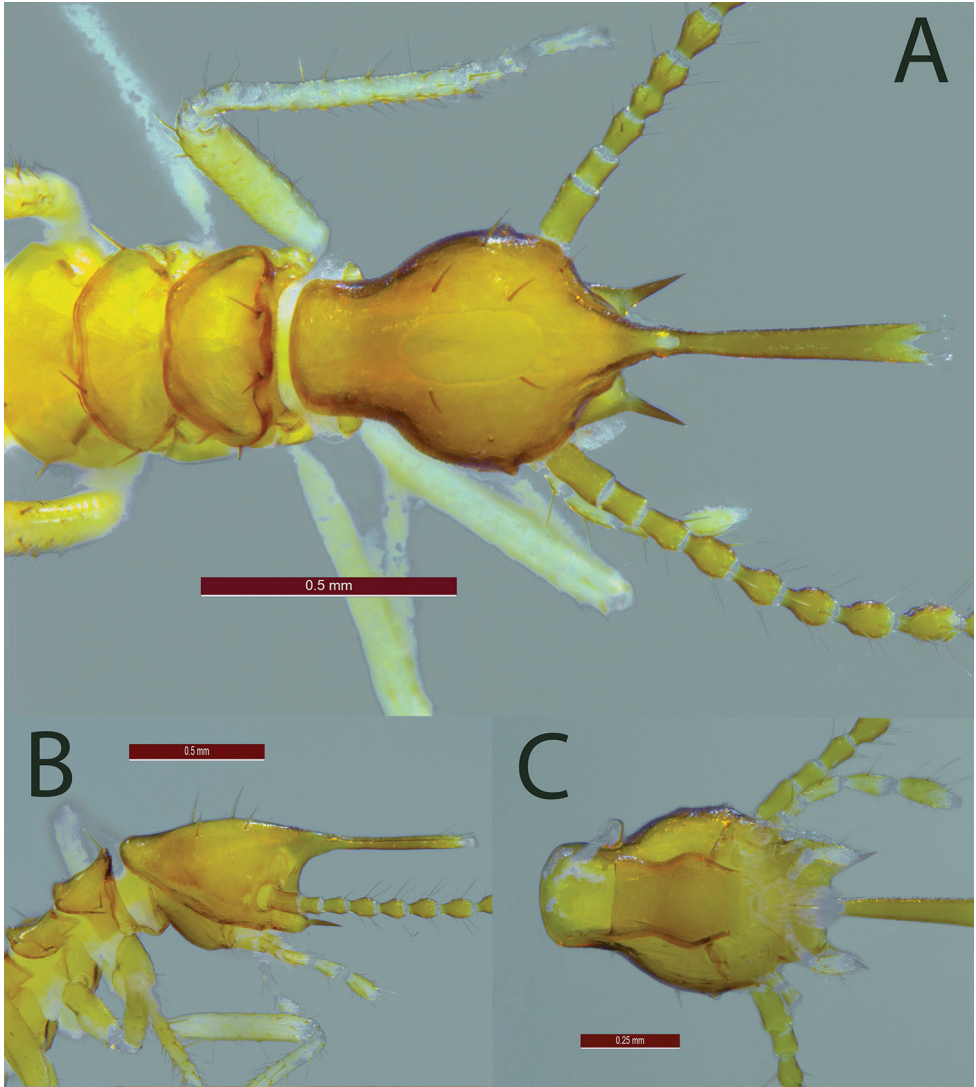


Figure 2. *Acorhinotermes claritae* sp. nov., minor soldier **A** head in dorsal view **B** head in lateral view **C** head in ventral view.

Table 1. Measurements (mm) of 10 minor soldiers from three colonies of *Acorhinotermes claritae* sp. nov.

	Holotype	CATAC 2722		CATAC 2723		CATAC 2724	
		Range	Mean ± SD	Range	Mean ± SD	Range	Mean ± SD
Max head width	0.53	0.45–0.58	0.53±0.05	0.53–0.63	0.58±0.03	0.55–0.66	0.59±0.03
Length head with labrum	1.30	1.18–1.36	1.31±0.06	1.23–1.38	1.32±0.05	1.23–1.40	1.28±0.05
Length of labrum	0.66	0.57–0.68	0.63±0.05	0.59–0.73	0.66±0.07	0.60–0.69	0.63±0.03
Pronotum width	0.42	0.39–0.46	0.43±0.03	0.43–0.49	0.47±0.02	0.44–0.56	0.48±0.04
Pronotum length	0.28	0.24–0.33	0.29±0.03	0.25–0.37	0.31±0.03	0.29–0.34	0.31±0.02
Length of hind tibia	0.84	0.81–0.89	0.85±0.03	0.77–0.88	0.82±0.03	0.80–0.93	0.84±0.04

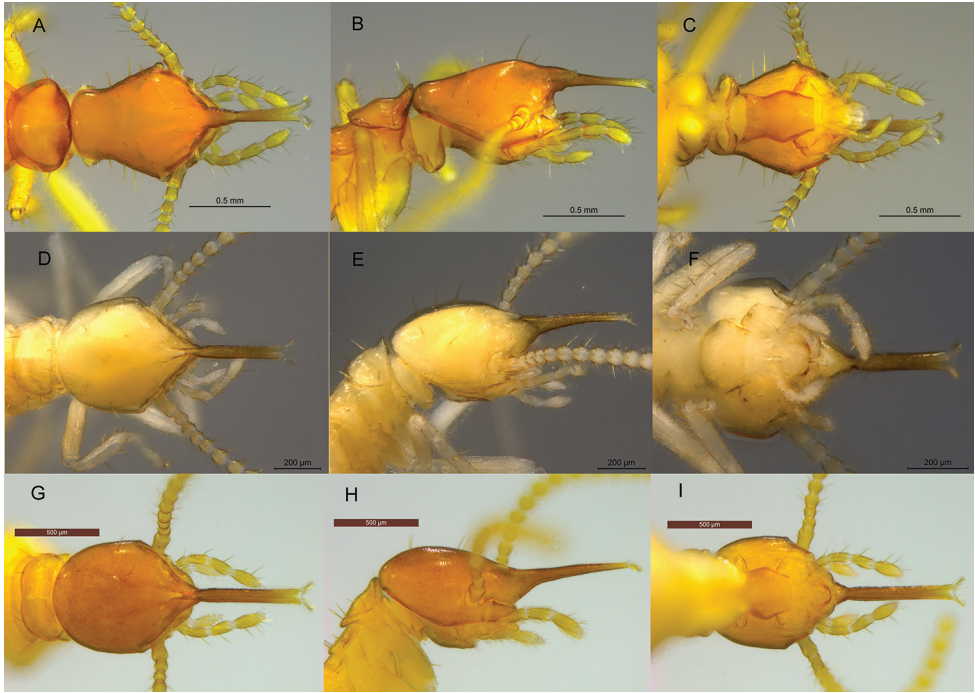


Figure 3. Minor soldiers of Neotropical Rhinotermitinae deposited in UF and CATAc termite collections **A–C** *Acorhinotermes subfusciceps* **D–F** *Dolichorhinotermes longidens* **G–I** *Dolichorhinotermes lanciarius*.

forms an obtuse angle (Fig. 3A, B). All minor soldiers of *Dolichorhinotermes* and *Rhinotermes* have the labrum tip bifurcated (forked or divided into two parts or branches), and it is much more bilobed in *A. subfusciceps* than in *A. claritae* sp. nov.

Biological notes. *Acorhinotermes claritae* sp. nov. was collected in a secondary rain forest near the Tacana river, close to a “chagra” (indigenous agricultural production system). During the wet season, these areas are in flood zones. The colonies were found in trunks of dead trees and in big dry branches on the ground. One particular colony of this species was found in a same dead branch together with *Heterotermes tenuis* (Hagen, 1858) and *Cylindrotermes parvignatus* Emerson, 1949, and another colony with *Silvestritermes gnomus* (Constantino, 1991). *Acorhinotermes claritae* sp. nov. was collected in a unique locality near the city of Leticia, although we did surveys in other two sites of a radius no greater than 15 km, it was not collected.

Distribution. The genus *Acorhinotermes* is distributed in the Amazon basin, Guiana shield and Caatinga (Fig. 5). *A. claritae* sp. nov. is restricted to the Amazon basin.

Etymology. The species is named in honor of Dr. Clara (Clarita) Peña-Venegas, who has supported and promoted the knowledge and inventories of termites and other terrestrial arthropods from the Colombian Amazon in the SINCHI Institute.

Key to the species of Neotropical Rhinotermitinae based on minor soldiers*

- 1 In dorsal view, fontanelle anterior to mandibular lobes (bases of mandibular points) (Figs 2B, 3A) (*Acorhinotermes*)..... **2**
 – In dorsal view, fontanelle at or posterior to mandibular lobes (Figs 3D, 4A, D) **3**
- 2 Mandibular points extend beyond the fontanelle (Fig. 2A) ***A. claritae* sp. nov.**
 – Mandibular points do not extend beyond the fontanelle (Fig. 3A–C)
 ***A. subfusciceps***
- 3 Mandibles points reduced to minute points on basal lobes (Fig. 3F, I) **4**
 – Long mandible points prominent, directed upward and forward (Fig. 4B, D, H)
 **5**
- 4 Smaller species: head length less than 1.10 mm. Panama (Fig. 3D–F)
 ***D. longidens***
 – Larger species: head length more than 1.47 mm. South America (see Engel and Krishna 2007: fig. 2) ***D. lanciarius***
- 5 Length of head to tip of labrum 1.35 mm or less **6**
 – Length of head to tip of labrum 1.45 mm or more..... **7**
- 6 Middle of anterior margin of pronotum with numerous short bristles, small mandibles do not exceed the base of the labrum, not visible from the dorsal view (see Constantino 1990: fig. 8)..... ***D. japuraensis***
 – Middle of anterior margin of pronotum smooth, without numerous short bristles, large mandibles reaching up to the middle of the labrum, visible from the dorsal view (Fig. 4A–C) ***D. longilabius*****
- 7 In lateral view, about 4–10 setae visible on vertex, labrum very elongated and narrow with a slight depression at its base (Fig. 4G) **8**
 – In lateral view, about 20–30 setae visible on vertex, labrum elongated and width without depression at its base (Fig. 4D) **9**
- 8 Head in dorsal view with a defined constriction behind antennae (Fig. 4G)
 ***R. marginalis*, *R. nasutus******
 – Head in dorsal view without constriction behind antennae, posterior margin of the head rounded (see Emerson 1925: fig. 42C)..... ***D. tenebrosus***
- 9 Head length to labrum tip 1.70–1.93 mm (Fig. 4D–F) ***R. hispidus***
 – Head length to labrum tip 2.20–2.35 mm (See: Snyder (1926). Plate 1, fig. 2)...
 ***R. manni***

* The key does not include the fossil species *Dolichorhinotermes apopnus* Engel & Krishna, 2007, *Dolichorhinotermes dominicanus* Schlemmermeyer & Canello, 2000, and *Rhinotermes miocenicus* Nel & Paicheler, 1993.

** The species *Dolichorhinotermes latilabrum* (Snyder, 1926) and *Dolichorhinotermes neli* Ensaf & Betsch, 2002 were not included in this key because we suspect they are junior synonyms of *Dolichorhinotermes longilabius* (Emerson, 1924).

*** These species cannot be separated only with the minor soldier. It is necessary the imago or the major soldier caste.

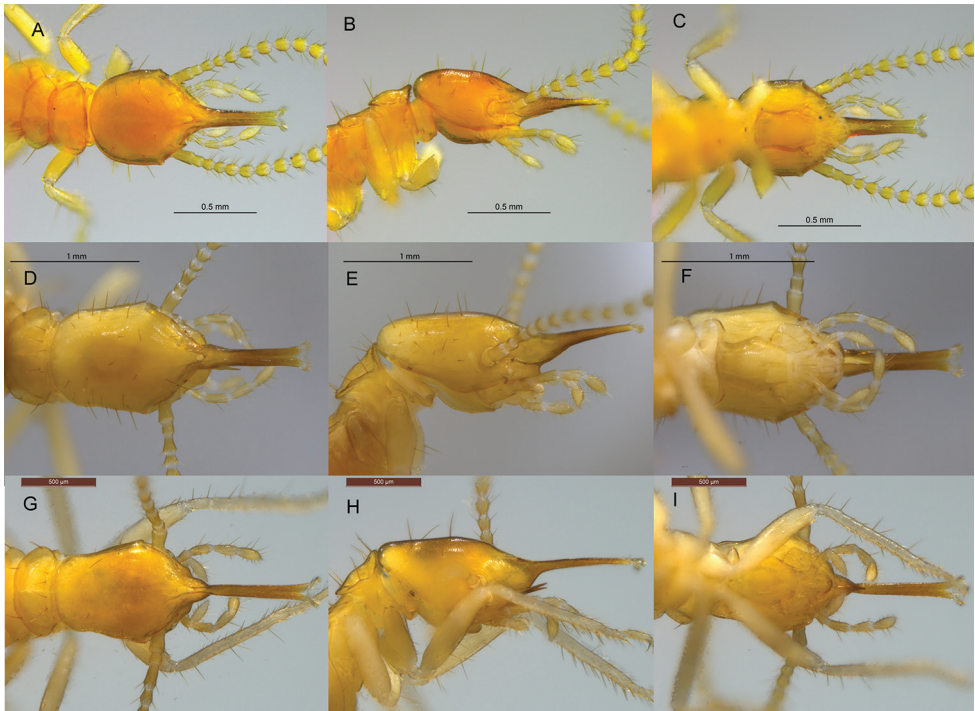


Figure 4. Minor soldiers of Neotropical Rhinotermitinae deposited in UF and CATAc termite collections **A–C** *Dolichorhinotermes longilabius* **D–F** *Rhinotermes hispidus* **G–I** *Rhinotermes marginalis*.

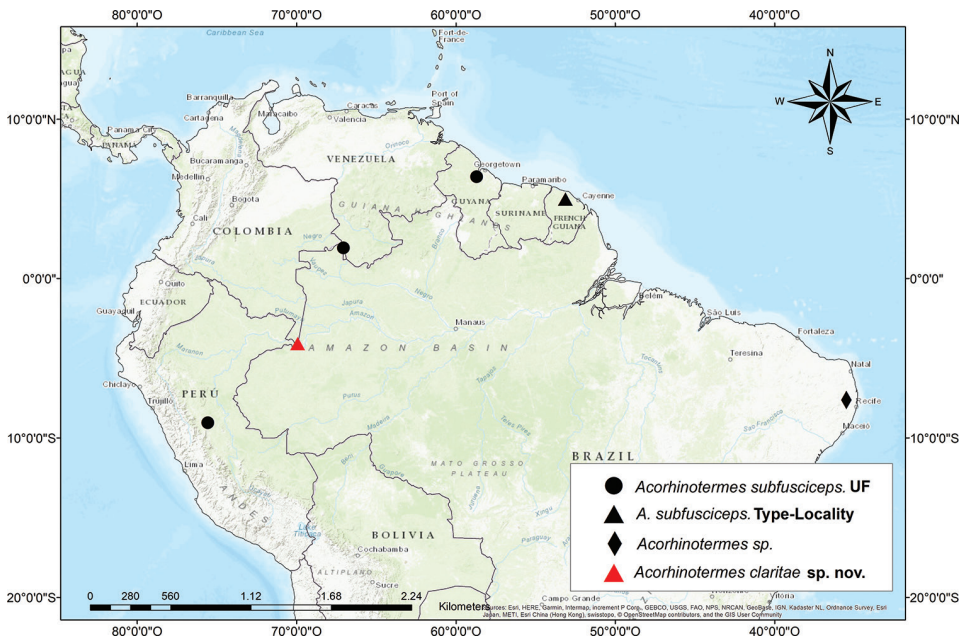


Figure 5. Distribution map of *Acorhinotermes* spp. Black circles are records from University of Florida termite collection and the black diamond is the record of Silva et al. (2019).

Discussion

In our Colombian survey, about 102 minor soldiers were collected without a single major soldier reinforces our belief that the latter caste is absent from *A. claritae* sp. nov. Among genera of the subfamily Rhinotermitinae, *Dolichorhinotermes* has been the most common in the Amazon region surveys, followed by *Rhinotermes* and then *Acorhinotermes* (Castro unpubl. data; Constantino 1991; de Souza and Brown 1994; Palin et al. 2011). However, *R. marginalis* is found in the West Indies while *D. longilabius* has not been reported from there, with the exception of the islands of Trinidad and Tobago where the latter species is common and the former has not been collected (Scheffrahn unpubl. data). *A. claritae* sp. nov. is the first record for the genus in Colombia.

In the key to genera of Neotropical termites, Constantino (2002) differentiated *Dolichorhinotermes* minor soldiers from *Rhinotermes* minor soldiers by the length of the head to the tip of the labrum, less than 1.2 mm, but *D. tenebrosus* and *D. lanciarius* measures greater than 1.2 mm. To differentiate these genera, the major soldier or imago caste is preferred. Major soldiers of *Dolichorhinotermes* have a narrow long labrum reaching near tips of mandibles while the major soldiers of *Rhinotermes* have a short wide labrum that extends no more than half the length of the mandibles when extended. Also, the known imagos of *Dolichorhinotermes* head width range is 1.18–1.29 mm while the *Rhinotermes* imago head width range is 1.90–2.18 mm.

Acknowledgments

A special thanks to James A. Chase for sponsoring the field trip. Thanks to Instituto Amazónico de Investigaciones Científicas SINCHI and to Dr. Clara Peña-Venegas for the logistics support to collect the material. We also thank to the survey team: James Chase, Daniela Manso and Lewis Pinedo. We heartily thank Dr. Mauricio Rocha, Dr. Carolina Cuezco and anonymous reviewer for their useful comments and suggestions on the manuscript.

References

- Constantino R (1990) Two new species of termites (Insecta, Isoptera) from western Brazilian Amazonia. *Boletim do Museu Paraense Emílio Goeldi* 6: 3–9.
- Constantino R (1991) Termites (Isoptera) from the lower Japurá River, Amazonas State, Brazil. *Boletim do Museu Paraense Emílio Goeldi* 7: 189–224.
- Constantino R (1992) Abundance and diversity of termites (Insecta: Isoptera) in Two Sites of Primary Rain Forest in Brazilian Amazonia. *Biotropica* 24: 420–430. <https://doi.org/10.2307/2388613>
- Constantino R (2002) An illustrated key to Neotropical termite genera (Insecta: Isoptera) based primarily on soldiers. *Zootaxa* 67: 1–40. <https://doi.org/10.11646/zootaxa.67.1.1>

- Constantino R (2019) Termite Database. University of Brasília. <http://www.termitologia.net/termite-database> [June 18, 2019]
- Constantino R, Canello EM (1992) Cupins (Insecta, Isoptera) da Amazônia Brasileira: distribuição e esforço de coleta. *Revista Brasileira de Biologia* 52: 401–413.
- Davies RG, Hernández LM, Eggleton P, Didham RK, Fagan LL, Winchester NN (2003) Environmental and spatial influences upon species composition of a termite assemblage across Neotropical forest islands. *Journal of Tropical Ecology* 19: 509–524. <https://doi.org/10.1017/S0266467403003560>
- Desneux J (1904) Notes termitologiques. *Annales de la Société Entomologique de Belgique* 48: 146–151.
- Emerson AE (1925) The termites of Kartabo, Bartica District, British Guiana. *Zoologica* 6: 291–459.
- Engel MS, Krishna K (2007) New *Dolichorhinotermes* from Ecuador and in Mexican Amber (Isoptera: Rhinotermitidae). *American Museum Novitates* 3592: 1–8. [https://doi.org/10.1206/0003-0082\(2007\)3592\[1:NDFEAI\]2.0.CO;2](https://doi.org/10.1206/0003-0082(2007)3592[1:NDFEAI]2.0.CO;2)
- Krishna K, Grimaldi DA, Krishna V, Engel M (2013) Treatise on the Isoptera of the world: 2. Basal Families. *Bulletin of the American Museum of Natural History* 377: 625–2704. <https://doi.org/10.1206/377.2>
- Maiti P (2011) A taxonomic monograph on the world species of termites of the family Rhinotermitidae (Isoptera: Insecta). *Memoirs of the Zoological Survey of India* 20: 1–272.
- Palin OF, Eggleton P, Malhi Y, Girardin CAJ, Rozas-Dávila A, Parr CL (2011) Termite Diversity along an Amazon-Andes Elevation Gradient, Peru. *Biotropica* 43: 100–107. <https://doi.org/10.1111/j.1744-7429.2010.00650.x>
- Pinzón OP, Baquero L, Beltran M (2017) Termite (Isoptera) diversity in a gallery forest relict in the Colombian eastern plains. *Sociobiology* 64: 92–100. <https://doi.org/10.13102/sociobiology.v64i1.1184>
- Roonwal ML (1970) Measurements of termites for taxonomic purposes. *Journal of Zoological Society of India* 21: 9–66.
- Salick J, Herrera R, Jordan CF, Url S, Salick J, Jordan CF (2013) Termitaria: Nutrient patchiness in nutrient-deficient Rain Forests. *Biotropica* 15: 1–7. <https://doi.org/10.2307/2387990>
- Silva I, Vasconcellos A, Moura FM (2019) Termite assemblages (Blattaria, Isoptera) in two montane forest (Brejo de Altitude) areas in northeastern Brazil. *Biota Neotropica* 19: 1–8. <https://doi.org/10.1590/1676-0611-bn-2018-0519>
- Snyder TE (1924) An extraordinary new *Rhinotermes* from Panama. *Proceedings of the Biological Society of Washington* 37: 83–85.
- Snyder TE (1926) Termites collected on the Mulford biological exploration to the Amazon Basin, 1991–1992. *Proceedings of the US National Museum* 68: 1–76. <https://doi.org/10.5479/si.00963801.68-2615.1>
- Snyder TE (1949) Catalog of the termites (Isoptera) of the world. *Smithsonian Miscellaneous Collections* 112: 9–378.
- de Souza OFF, Brown VK (1994) Effects of habitat fragmentation on Amazonian termite communities. *Journal of Tropical Ecology* 10: 1–197. <https://doi.org/10.1017/S0266467400007847>

Morphometric analysis of fossil bumble bees (Hymenoptera, Apidae, Bombini) reveals their taxonomic affinities

Manuel Dehon¹, Michael S. Engel^{2,3}, Maxence Gérard¹, A. Murat Aytekin^{1,4}, Guillaume Ghisbain¹, Paul H. Williams⁵, Pierre Rasmont¹, Denis Michez¹

1 Laboratory of Zoology, Research Institute of Biosciences, University of Mons, Place du parc 20, 7000 Mons, Belgium **2** Division of Invertebrate Zoology, American Museum of Natural History, Central Park West at 79th, New York, NY 10024-5192, USA **3** Division of Entomology, Natural History Museum, and Department of Ecology and Evolutionary Biology, University of Kansas, 1501 Crestline Drive – Suite 140, Lawrence, KS 66045, USA **4** Pamukkale Sitesi, B Blok, Çayyolu, Ankara, Turkey **5** Department of Life Sciences, Natural History Museum, Cromwell Road, London SW7 5BD, UK

Corresponding author: Denis Michez (denis.michez@umons.ac.be)

Academic editor: M. Ohl | Received 30 November 2018 | Accepted 28 September 2019 | Published 21 November 2019

<http://zoobank.org/8C9F49DC-20A7-46B1-B864-B41869F1A2F3>

Citation: Dehon M, Engel MS, Gérard M, Aytekin AM, Ghisbain G, Williams PH, Rasmont P, Michez D (2019) Morphometric analysis of fossil bumble bees (Hymenoptera, Apidae, Bombini) reveals their taxonomic affinities. ZooKeys 891: 71–118. <https://doi.org/10.3897/zookeys.891.32056>

Abstract

Bumble bees (*Bombus* spp.) are a widespread corbiculate lineage (Apinae: Corbiculata: Bombini), mostly found among temperate and alpine ecosystems. Approximately 260 species have been recognized and grouped recently into a simplified system of 15 subgenera. Most of the species are nest-building and primitively eusocial. Species of *Bombus* have been more intensely studied than any other lineages of bees with the exception of the honey bees. However, most bumble bee fossils are poorly described and documented, making their placement relative to other *Bombus* uncertain. A large portion of the known and presumed bumble bee fossils were re-examined in an attempt to better understand their affinities with extant Bombini. The taxonomic affinities of fossil specimens were re-assessed based on morphological features and previous descriptions, and for 13 specimens based on geometric morphometrics of forewing shape. None of the specimens coming from Eocene and Oligocene deposits were assigned within the contemporary shape space of any subgenus of *Bombus*. It is shown that *Calyptapis florissantensis* Cockerell, 1906 (Eocene-Oligocene boundary, Florissant shale, Colorado, USA) and *Oligobombus cuspidatus* Antropov, 2014 (Late Eocene, Bembridge Marls) likely belong to stem-group Bombini. *Bombus anacolus* Zhang, 1994, *B. dilectus*

Zhang, 1994, *B. luianus* Zhang, 1990 (Middle Miocene, Shanwang Formation), as well as *B. vetustus* Rasnitsyn & Michener, 1991 (Miocene, Botchi Formation) are considered as species inquirenda. In the Miocene, affinities of fossils with derived subgenera of *Bombus* s. l. increased, and some are included in the shape space of contemporary subgenera: *Cullumanobombus* (i.e., *B. pristinus* Unger, 1867, *B. randeckensis* Wappler & Engel, 2012, and *B. trophonius* Prokop, Dehon, Michez & Engel, 2017), *Melanobombus* (i.e., *B. cerdanyensis* Dehon, De Meulemeester & Engel, 2014), and *Mendacibombus* (i.e., *B. beskonakensis* (Nel & Petrulevičius, 2003), new combination), agreeing with previous estimates of diversification.

Keywords

Bombus, evolution, fossil, geometric morphometrics, review, taxonomy

Introduction

Bumble bees (Bombini: *Bombus* Latreille, 1802) are a lineage of corbiculate bees (Apidae: Apinae) dominant in many temperate and alpine ecosystems (Williams 1998; Michener 2007). Like almost all bees, they feed entirely on pollen for protein and lipid resources, and nectar for carbohydrates. *Bombus* are valuable for agricultural pollination (e.g., Pouvreau 1984; Plowright and Lavery 1987), and have been domesticated since the 1970s (Röseler 1973), resulting in commercial rearing with probably several millions of colonies produced per year (Velthuis and Doorn 2006; Goulson 2010). Approximately 260 species have been recognized (Williams 1998) and grouped into a simplified system of 15 subgenera (Williams et al. 2008). Most of the species are nest-building (i.e., females collect pollen using a corbicula) and primitively eusocial, meaning that the life cycle includes a solitary queen stage (Heinrich 1979). However, several species are social parasites: all species of the subgenus *Psithyrus* Lepeletier, 1832, and the species *Bombus* (*Thoracobombus*) *inexpectatus* (Tkalčů, 1963), *B. (Alpinobombus) hyperboreus* Schoenherr, 1809, and *B. (Alpinobombus) natvigi* Richards 1931 (Hines and Cameron 2010; Brasero et al. 2018; Williams et al. 2019). Morphologically, the genus *Bombus* is characterized by an intermediate to very large body size (9–22 mm long), often with conspicuous color patterns (Williams 2007), the presence of outer mandibular grooves, an apically closed forewing marginal cell, the presence of an auricle at the metatibia-metabasitarsus junction, the presence of a supra-alar carina, the hamuli not reduced on the hind wing margin, the absence of a jugal lobe, and glabrous compound eyes (Engel 2001; Michener 1990, 2007; Engel and Rasmussen in press). In females, the pretarsal claws are cleft, with a small arolium present, and the metatibial spurs are present (Engel 2001; Michener 1990, 2007; Engel and Rasmussen in press). Both wings have strong and complete venation (Michener 1990, 2007). In the forewing, the marginal cell is longer than the distance from its apex to the forewing tip; the pterostigma is small, scarcely longer than the prestigma; r-rs arises near or beyond the middle of the pterostigma; and the margin within the marginal cell is straight or commonly concave. *Bombus* s. l. display interspecific diversity in structures like male genitalia, female sting, color pattern, and mandibular shape (Engel 2001; Michener 1990, 2007).

Bumble bees have been more intensely studied than other lineages of bees with the exception of the honey bees (Apini: *Apis* L., 1758) (Michener 2007). Those studies include taxonomic and cladistic investigations, many of them focusing on the recovery of a robust hypothesis of phylogenetic relationships among and within the subgenera (e.g., Vogt 1911; Milliron 1961, 1973a, b; Tkalců 1972; Pekkarinen 1979; Pekkarinen et al. 1979; Obrecht and Scholl 1981; Ito 1985; Williams 1985; Pamilo et al. 1987; Cameron et al. 2007). Bumble bees exhibit higher species diversity in cooler climates of the Holarctic region, with more species and subgenera in Eurasia than in North America (Williams 1998). Historical patterns of dispersal among the continents and climatic associations of bumble bee origins were described by Skorikov (1923), Williams (1985), Kawakita et al. (2004), and Williams et al. (2018). Hines (2008) recently estimated divergence times using fossil calibrations and molecular rates derived from the literature. However, she purposefully excluded fossils of *Bombus* s. l. for her analyses, and instead considered that reliable bumble bee fossils were too poorly preserved to reveal good morphological synapomorphies for placement within *Bombus* s. l. Hines (2008) therefore decided to use outgroup fossils and subfossils as calibration points [i.e., the subfossil stingless bees *Liotrigona vetula* Moure & Camargo, 1978, *Hypotrigona gribodoi* (Magretti, 1884), and fossil meliponines *Liotrigonopsis rozeni* Engel, 2001, *Kelneriapis eocenica* (Kelner-Pillault, 1969), and *Proplebeia dominicana* (Wille & Chandler, 1964)]. Those analyses estimated that the crown group of extant *Bombus* s. l. originated in the Upper Eocene to Middle Oligocene, i.e., 40.0–25.0 Ma, perhaps near the Eocene-Oligocene boundary (i.e., 34.0 Ma). It is unclear whether the purposeful exclusion of *Cretotrigona prisca* (Michener & Grimaldi, 1988), from 70 Ma, as an outgroup calibration point impacted the overall estimated divergence times obtained by Hines (2008). Regardless, the Eocene-Oligocene transition is a well-documented global cooling period that resulted in significant extinctions, particularly across the Northern Hemisphere (Zachos et al. 2008; Hansen et al. 2013). An Old World ancestor of extant *Bombus* s. l. was supported, with early dispersal events from the Old World into the New World and North America to South America (Williams 1985; Hines 2008). In the phylogenetic tree presented in Cameron et al. (2007) and Hines (2008), *Mendacibombus* is sister to all other clades, while extant species of this subgenus are estimated to have diverged in the last 10 Ma (Williams et al. 2016). A global revision of available bumble bee fossils is needed to corroborate or reject temporal hypotheses proposed by Hines (2008), and more critically the discovery of more and better-preserved fossil bombines is needed as the record of this interesting tribe is quite scant.

Bombus is the only contemporary genus of the tribe Bombini but additional fossils have been associated with this tribe, and these have either been proposed within the genus, or in putatively extinct genera. Overall, the fossil record of bees is comparatively scarce, with only around 200 described species (e.g., Kotthoff et al. 2011; Michez et al. 2012; Wappler et al. 2012; Engel and Michener 2013a; Engel and Breitkreuz 2013; Engel et al. 2013, 2014, 2018; Dewulf et al. 2014; Dehon et al. 2014, 2017; Engel 2014, 2019a, b; Prokop et al. 2017). In total, 14 bombine fossil species have been described,

each described from a single specimen with the exception of *Calyptapis florissantensis* Cockerell which was documented from two specimens (Table 1). Most of these are poorly described and documented, making their placement relative to extant *Bombus* uncertain. The majority of the specimens were found in Miocene sediments and have been described in the genera *Bombus* Latreille, 1802, *Oligoapis* Nel & Petrulevičius, 2003, *Oligobombus* Antropov, 2014, *Paraelectrobombus* Nel & Petrulevičius, 2003, and *Calyptapis* Cockerell, 1906 (Table 1). The aim of the present study is to provide a taxonomic overview of the available fossil bumble bees and to evaluate their affinities with extant taxa. Using landmark-based geometric morphometric analyses of the forewing shape and morphology, we estimate the similarity/dissimilarity of the fossil wing shape with extant and extinct bee taxa, particularly other corbiculate bees (Apinae: Corbiculata). Based on the results of the forewing shape comparisons, we propose a new taxonomic arrangement for many of the fossils. Based on our revised system we re-examined whether these few occurrences have any impact on understanding the diversification and extinction patterns of bumble bees.

Materials and methods

Type revision, morphological terminology, and classification

We examined all of the fossils described in the literature as bumble bees or as closely allied extinct genera (Table 1), corresponding to 15 specimens representing 14 described species. For all species, we tried to locate the type material to check against the original description and to better illustrate the fossil, if needed. We contacted the potential repositories of the fossils and were able to locate 13 specimens for review (Fig. 1). Information about museum repositories is included in the “Results” section. Overall, we gathered pictures and/or drawings of the forewings of 13 specimens representing 12 of 14 species (Table 1).

The morphological terminology follows that of Engel (2001) and Michener (2007), while the higher classification (i.e., subfamily, tribe) follows that of Michener (2007) (i.e., seven families: Andrenidae, Apidae, Colletidae, Halictidae, Megachilidae, Melittidae, and Stenotritidae). For bumble bees, we used the subgeneric system of Williams et al. (2008) where 15 subgenera were proposed. A complete list of extant species with their nomenclature is available at the following link (updated from Williams 1998): (<http://www.nhm.ac.uk/research-curation/research/projects/bombus/groups.html>).

Geological settings

Fossils of bumble bees have been described from eleven deposits from the Late Eocene to the Upper Miocene: Brembridge Marls, Florissant, BesKonak, Latah, Bílina Mine, Krotensee, Randeck Maar, Shandong, Botchi River, Euboea, and La Cerdanya (Table 1).

Table 1. All known fossils described as bumble bees (genus *Bombus*) or as closely allied genera. Linear Discriminant Analysis (LDA) 1–3 are based on dataset 1. LDA 4 is based on dataset 2. LDA 5 is based on dataset 3. Key: * = fossil specimen without forewing picture/drawing available for geometric morphometric analyses. Abbreviations: Ap. = Apidae, B = Bombini, E = Electrapini, H = Holotype, S2: second specimen described by Cockerell (1908). B. = *Bombus*, C. = *Calyptapis*, O. = *Oligapis*, Ol. = *Oligobombus*, P. = *Paraelectrobombus*, ° = the specimen was included in the shape space of the most similar clade, a = Jiménez-Moreno et al. (2010), b = Bachmayer et al. (1971), c = Akhmetjev (1973), d = Yang et al. (2007), e = Heizmann (1983), f = J. Prokop, pers. comm. (Wappler et al. 2012), g = Knor et al. (2012), h = Gray and Kirtleman (1967), i = Paichelt et al. (1978), j = Evanoff et al. (2001), k = Antropov et al. (2014).

Taxon	Reference	Age (Ma)	Locality	LDA1	LDA2	LDA3	LDA4	LDA5	New taxonomic hypothesis
<i>B. cerdanyensis</i>	Dehon et al. (2014)	10.0 ^a	La Cerdanya ES	Ap.	Apinae	Bombini	Bombini [°]	<i>Melanobombus</i> [°]	<i>B. (Melanobombus) cerdanyensis</i>
<i>B.?</i> <i>pristinus</i>	Unger (1867)	11.2–7.1 ^b	Euboea GR	Ap.	Apinae	Bombini	Bombini [°]	<i>Cullumanobombus</i> [°]	<i>B. (Cullumanobombus) pristinus</i>
<i>B. vetustus</i>	Rasnitsyn and Michener (1991)	11.2–7.1 ^c	Bochi River RU	Ap.	Eucerinae	Bombini	Bombini	<i>Bombus</i>	<i>B. vetustus</i> sp. inq.
<i>B. anacolus</i>	Zhang et al. (1994)	17.0–15.2 ^d	Shandong CN	Ap.	Apinae	Bombini	Bombini	<i>Mendacibombus</i>	<i>B. anacolus</i> sp. inq.
<i>B. dilectus</i>	Zhang et al. (1994)	17.0–15.2 ^d	Shandong CN	Ap.	Apinae	Tetrapediini	Bombini	<i>Bombus</i>	<i>B. dilectus</i> sp. inq.
<i>B. luianus</i>	Zhang (1990)	17.0–15.2 ^d	Shandong CN	Ap.	Apinae	Bombini	Bombini [°]	<i>Melanobombus</i>	<i>B. luianus</i> sp. inq.
<i>B. randedkensis</i>	Wappler et al. (2012)	18.0–16.0 ^e	Randeck Maar DE	Ap.	Apinae	Bombini	Bombini [°]	<i>Cullumanobombus</i> [°]	<i>B. (Cullumanobombus) randedkensis</i>
<i>B.?</i> <i>craspipes</i> *	Novák (1877)	18.0–17.0 ^f	Krottensee CZ	–	–	–	–	–	<i>B. craspipes</i>
<i>B. trophonius</i>	Prokop et al. (2003)	20.0 ^g	Bilina Mine CZ	Ap.	Apinae	Bombini	Bombini [°]	<i>Cullumanobombus</i> [°]	<i>B. (Cullumanobombus) trophonius</i>
<i>B. proavus</i> *	Cockerell (1931)	21.3–12.1 ^h	Latah US	–	–	–	–	–	<i>B. proavus</i>
<i>O. beskonakensis</i>	Nel and Petrulevičius (2003)	22.5 ⁱ	Bes-Kornak TR	Ap.	Apinae	Bombini	Bombini [°]	<i>Mendacibombus</i>	<i>B. (Mendacibombus) beskonakensis</i> comb.n.
<i>P. patriciae</i>	Nel and Petrulevičius (2003)	22.5 ⁱ	Bes-Kornak TR	Ap.	Apinae	Bombini	Bombini	<i>Mendacibombus</i>	<i>B. (Paraelectrobombus) patriciae</i> comb.n.
<i>C. florissantensis</i>	Cockerell (1906)	37.0–33.9 ^j	Florissant shale US	Ap.	H; Apinae; S2: Eucerinae	Electrapini	H; B; S2; E	<i>Bombus</i>	<i>C. florissantensis</i>
<i>Ol. cuspidatus</i>	Antropov et al. (2014)	36.0 ^k	Isle of Wight UK	Ap.	Apinae	Electrapini	Bombini	<i>Bombus</i>	<i>Ol. cuspidatus</i>

The Insect Bed of the Bembridge Marls from the Late Eocene (i.e., 36.0 Ma) is located on the Isle of Wight (UK). Two bee fossils were recorded from the deposit: the presumed bumble *Oligobombus cuspidatus* Antropov, 2014 and specimen NHMUK In.10012 (Megachilidae, incertae sedis) (Antropov et al. 2014).

The Florissant shale of Colorado (USA) (Swisher and Prothero 1990), situated near the Eocene-Oligocene boundary is approximately 34.0 Ma in age (Epis and Chapin 1974; Evanoff et al. 2001; Boyle et al. 2008; Mustoe 2008; Veatch and Meyer 2008). It produced a large number of the known bee fossils, most of which were described in the early part of the 20th Century, with 36 specimens representing 34 species in 19 genera (Zeuner and Manning 1976; Michez et al. 2012). One possible bumble bee fossil was recorded: *Calyptapis florissantensis* Cockerell, 1906.

The deposits of BesKonak are from the Lower Miocene (Aquitania, i.e., 22.5 Ma) and located in Anatolia, north of Ankara Province, Turkey (Paichelier et al. 1978). The only bumble bee fossils discovered in the deposits of BesKonak are *Oligoapis beskonakensis* Nel & Petrulėvičius, 2003 and *Paraelectrobombus patriciae* Nel & Petrulėvičius, 2003.

The Latah Formation encompasses the Lower to Middle Miocene (i.e., 21.3–12.1 Ma) of eastern Washington and northwestern Idaho (USA) (Berry 1929; Kirkham and Melville 1929; Gray and Kittleman 1967; Lewis 1969; Robinson 1991; Derkey et al. 2003). The only known bee fossils from this deposit are *Bombus proavus* Cockerell, 1931 and an undetermined megachiline specimen (Cockerell 1931; Engel 2004).

The deposits of the Most Formation at Břilina Mine date from the Lower Miocene (i.e., 20.0 Ma), in northern Bohemia (Czech Republic) (Kvaček 1998; Prokop and Nel 2000; Prokop et al. 2003; Kvaček et al. 2004; Knor et al. 2012). Two bee fossils have been reported from the deposits of the Most Formation: undetermined specimens of *Apis* and the bumble bee *B. trophonius* Prokop, Dehon, Michez & Engel, 2017 (Prokop et al. 2003; Prokop et al. 2017; Engel pers. obs.).

Krottensee, also in the Czech Republic, dates from the Lower Miocene (i.e., 18.0–17.0 Ma), and is also referred to as Mokřina (Bůžek et al. 1996; Mlíkovský 1996; Rojčík 2004). A single bumble bee has been recovered from the deposits, *B. crassipes* Novák, 1878 (Novák 1878; Krzemiński and Prokop 2011).

The Randeck Maar deposits of the Lower-Middle Miocene (i.e., 18.0–16.0 Ma) are located in southwestern Germany, southeast of Stuttgart at the escarpment of the Swabian Alps (Heizmann 1983), and is the largest ancient Maar in that region (Köppen and Geiger 1928; Gregor 1986; Krautter and Schweigert 1991; Schweigert 1998; Lutz et al. 2000; Kottek et al. 2006). This fossil Lagerstätte contains exceptionally well-preserved flora and fauna (e.g., Armbruster 1938; Gregor 1986; Schawaller 1986; Ansoerge and Kohring 1995; Kotthoff 2005; Kotthoff and Schmid 2005; Kotthoff et al. 2011). Several prominent bee fossils have been reported from Randeck Maar – *Apis armbrusteri* Zeuner, 1931 (Kotthoff et al. 2011), *B. randeckensis* Wappler & Engel, 2012 (Wappler et al. 2012), and *Halictus schemppi* (Armbruster, 1938) – and while those of *Bombus* and *Halictus* are each from single specimens, a plethora of honey bee workers have been recorded (Kotthoff et al. 2011).

The Middle Miocene sediments of the Shanwang Formation (17.0–15.2 Ma) are located in Linqu County, Shandong Province, China (Yang et al. 2007). Many insects have been listed from this deposit, including bees (Megachilidae, Apidae), and specifically the bumble bees *B. anacolus* Zhang, *B. luianus* Zhang, and *B. dilectus* Zhang (Zhang 1990; Zhang et al. 1994).

The Botchi Formation is from the Upper Miocene (i.e., 11.2–7.1 Ma) and is located on the left bank of the Botchi River in Russia (Khabarovsk Region) (Akhmetjev 1973). This formation has yielded various plants, fishes, Crustacea, and insects, including *B. vetustus* Rasnitsyn & Michener, 1991.

The deposit of Kumi (Euboea, Greece) is from the Middle-Upper Miocene (i.e., 11.2–7.1 Ma). Insects from the orders Coleoptera, Diptera, and Hymenoptera were discovered in the Kumi deposit, and these included *B. pristinus* Unger, 1867.

The Spanish deposit of La Cerdanya corresponds to Upper Miocene lacustrine beds (i.e., 10.0 Ma) located in Spain (Lleida, Bellver-en-Cerdaña) (Diéguez et al. 1996; Jiménez-Moreno et al. 2010). The flora and entomofauna are quite abundant and diverse (Peñalver-Molla et al. 1999; Arillo 2001) with a rather high occurrence of bees, although nearly all specimens belong to *Apis* (Nel et al. 1999). *Bombus cerdanyensis* Dehon, De Meulemeester & Engel, 2014 was described from this deposit (Dehon et al. 2014).

Geometric morphometric analyses of forewing shape

We performed geometric morphometric analyses of the forewing shape in order to assess the taxonomic affinities of 12 bumble bee fossil species (13 specimens) showing well-preserved forewings (Fig. 1). This tool is useful in insect taxonomy for discriminating and diagnosing taxa at different levels (e.g., Pretorius 2005; Petit et al. 2006; Francoy et al. 2009, 2012; Sadeghi et al. 2009; Perrard et al. 2014; Van Cann et al. 2015), as well as in paleontology for assessing taxonomic affinities of fossils with contemporary and extinct taxa (e.g., Kennedy et al. 2009; Michez et al. 2009a; De Meulemeester et al. 2012; Wappler et al. 2012; Dehon et al. 2014, 2017; Dewulf et al. 2014; Perrard et al. 2016; Prokop et al. 2017). Several studies have demonstrated the utility of forewing shape analyses for diagnosing subgenera, species, and populations of bumble bees, depending on rearing conditions (e.g., Aytekin et al. 2007; Wappler et al. 2012; Barkan and Aytekin 2013; Gérard et al. 2018).

We used three different datasets to assess the taxonomic affinities of the fossils at different taxonomic levels. All three datasets represent a sampling of contemporary and extinct tribes with three submarginal cells, were largely assembled and analyzed in previous studies (i.e., Dehon et al. (2017) for the first dataset and Prokop et al. (2017) for the second and third datasets). We only (i) modified the classification of the species in the different datasets based on Bossert et al. (2019) and (ii) added the 13 fossils in each of these datasets. The first dataset included a comprehensive sampling of bee tribes in order to ensure correct tribal placement of the 13 fossils. This dataset consisted

of 50 tribes representing 226 species and 979 specimens (refer to Dehon et al. (2017) for full details; Suppl material 1: Table S1). It also uncovered a group of six tribes (i.e., Ancylaini, Electrapini, Emphorini, Euglossini, Melikertini, and Tetrapediini) showing similar wing shapes to Bombini. We then used a second dataset with more extensive sampling within Bombini and these six similar tribes. This second dataset was assembled and tested by Prokop et al. (2017). It includes 841 specimens and represents all 15 subgenera and 210 species of extant bumble bees (80% of the total species diversity) as well as tribes Ancylaini, Electrapini, Emphorini, Euglossini, Melikertini, and Tetrapediini, representing a further 18 genera, 43 species, and 132 specimens altogether (Suppl material 2: Table S2). Finally, fossils confirmed to belong to Bombini using the first and second datasets were compared to a third dataset that only consists of the bumble bee specimens of the second dataset in order to assess the taxonomic affinities of the specimens with extant subgenera of *Bombus*. Dehon et al. (2017) (Suppl materials 3–5: Tables S3–S5) and Prokop et al. (2017) (Suppl materials 6–7: Tables S6–S7) demonstrated reliability for these datasets in classifying bee specimens based on forewing shape similarity relative to the reference datasets of forewings. Hence, the cross-validation allows us to be confident in the discrimination.

The potential effect of sexual dimorphism on subgeneric assignment using wing morphometry was tested by Wappler et al. (2012) for the subgenus *Bombus* s. str. For this subgenus, the results showed that sexual dimorphism had limited impact on subgeneric assignment. We tested it on four additional subgenera (based on 82 specimens from 12 species of four subgenera: *Bombias*, *Cullumanobombus*, *Melanobombus*, and *Mendacibombus*); the identification of the subgenera based on wing shape was again highly supported (Suppl material 7: Table S7). Therefore, to limit intraspecific variability in our dataset, we sampled female specimens only. We selected females because Bombini are mostly social species and workers (i.e., females) are the most abundant caste. Moreover, most of the known fossil specimens are females, although the holotype of *B. vetustus* is a male as evidenced by the lack of a corbicula, male flagellomeres, etc. (Rasnitsyn and Michener 1991).

Left forewings were photographed using an Olympus SZH10 microscope combined with a Nikon D200 camera. Photographs were then uploaded in the software tpsUTIL 1.69 (Rohlf 2013a). The forewing shape was captured by digitizing two-dimensional Cartesian coordinates of 18 landmarks on the wing veins and cells (Fig. 4) with the software tpsDIG version 2.27 (Rohlf 2013b). Position of the landmarks was based on Owen (2012) and other studies like De Meulemeester et al. (2012), Wappler et al. (2012), Dewulf et al. (2014), Dehon et al. (2014, 2017), Gérard et al. (2015), and Prokop et al. (2017). The two-dimensional configurations of the landmarks were superimposed using the GLS Procrustes superimposition in the software R version 3.0.2 (Rohlf and Slice 1990; Bookstein 1991; Adams and Otárola-Castillo 2013; R Development Core Team 2013). The closeness of the tangent space to the curved shape space was analyzed by calculating the least-squares regression slope and the correlation coefficient between the Procrustes distances (in the shape space) and the Euclidean distances (in the tangent space) (Rohlf 1999). This was calculated using the software tpsSMALL v1.25 (Rohlf 2013c).

Shape discrimination at different taxonomic levels

Variation of shape in the dataset was explored with PCA analyses to visualize clustering and detect outliers (Fig. 5). Discrimination of the wing shape of the different taxa was assessed by Linear Discriminant Analyses (LDA) of the projected aligned configuration of landmarks like in Prokop et al. (2017). We performed three LDAs with the first dataset (Dehon et al. 2017, Suppl material 1: Table S1) with different levels a priori grouping (i.e., the groups are known a priori by the analysis): family, subfamily and tribe (LDA 1–3, Tables 1, Suppl materials 3–5). We did a fourth LDA analysis with the second dataset (i.e., bumble bees + six similar tribes, Suppl material 2: Table S2) with tribe level as a priori grouping (LDA 4, Table 1, Suppl material 6). Finally, we used a comprehensive sampling of extant bumble bees (i.e., third dataset, Suppl material 2: Table S2) for a fifth LDA considering the subgenus level as a priori grouping (LDA 5, Tables 1, Suppl material 7: Table S7). The LDA effectiveness was assessed by the percentages of individuals correctly classified to their original taxon (hit-ratio, HR) in a leave-one-out (LOO) cross-validation procedure based on the posterior probabilities of assignment (Suppl materials 3–7: Tables S3–S7). Given the observed scores of an “unknown”, the posterior probability (pp) equals the probability of the unit to belong to one group compared to all others. The unit is consequently assigned to the group for which the posterior probability is the highest (Huberty and Olejnik 2006). All discriminant analyses were performed using the R software (R Development Core Team 2013).

Assignment of the bee fossils

Taxonomic affinities of the fossils were assessed based on the score in the predictive discriminant space of shapes. Aligned coordinates of the specimens from the three datasets (including the fossils) were used to calculate the same five LDA as presented in the previous section. Assignment of the fossils was estimated by calculating the Mahalanobis Distance between each fossil and group mean of each taxon and then assigning it to the nearest group in the discriminant shape of the LDA (Suppl materials 7–12: Tables S7–S12). Principal Component Analyses (PCA) were also computed to visualize shape affinities between the fossils and the extant groups in the second dataset (Fig. 5). Mahalanobis Distance is well suited for dealing with large datasets of close-relative taxa (Claude 2008).

Results

Geometric morphometric analyses

The assignment of each fossil was assessed in each dataset. When using the first dataset, all fossils were assigned to Apidae, more specifically to Apinae (except for the second specimen of *C. florissantensis* described by Cockerell (1908) and *B. vetustus*, both assigned to Eucerinae) and to Bombini (except for *B. dilectus* assigned to Tetrapediini,

and *Oligobombus cuspidatus* and both specimens of *C. florissantensis*, all three assigned to Electrapini) (see LDA 1–3, Tables 1, Suppl materials 9–11). We then specifically assessed the assignment of each fossils based on the second and the third dataset. *Oligobombus cuspidatus* and both specimens of *C. florissantensis* were close to the shape space of contemporary Bombini, while being placed outside of contemporary Bombini and fossil Electrapini (Dataset 2, LDA 4). Among bombine subgenera, *Bombias* was most similar in forewing shape to *Oligobombus* and *Calyptapis* (Dataset 3, LDA 5). Based on our discriminant analyses, *Paraelectrobombus patriciae* was also similar to extant Bombini while being just outside of its shape space (Dataset 2, LDA 4). *Bombus beskonakensis* clustered within the shape space of extant Bombini (Dataset 2, LDA 4) and was similar to the subgenus *Mendacibombus* but outside the modern shape space of that subgenus (Dataset 3, LDA 5). The assignment of *B. trophonius* based on wing shape was already assessed in Prokop et al. (2017), this fossil clustered within contemporary *Cullumanobombus* (Dataset 3, LDA 5). The forewing shape of *B. randeckensis* was previously analyzed by Wappler et al. (2012) who proposed that the specimen was close to the subgenus *Bombus* s. str. Our analyses found a close similarity with *Cullumanobombus* (Dataset 3, LDA 5), while in Wappler et al. (2012) this subgenus was the fourth most similar subgenus to the fossil. This discrepancy may be explained by the fact that we used a larger and more diverse dataset, or possibly also because forewings were digitized by different experimenters in both studies. *Bombus luianus* clustered within Bombini based on its forewing shape (Dataset 2, LDA 4). Moreover, its forewing shape was similar to, but outside of modern *Melanobombus*, suggesting this fossil might be sister to extant *Melanobombus* (Dataset 3, LDA 5). *Bombus dilectus* did not cluster within the shape space of Bombini, but the tribe was the most similar (Dataset 2, LDA 4), but it is possible the published drawings are not entirely accurate. The most similar subgenus was the subgenus *Bombias* (Dataset 2, LDA 4), one of the most basal subgenera of the genus (Fig. 5). *Bombus anacolus* clustered just outside of crown-group Bombini while being quite similar to this tribe based on its forewing shape (Dataset 2, LDA 4), but again the published drawing is rather poor. Nonetheless, its forewing shape was similar to modern *Mendacibombus* (Dataset 3, LDA 5). *Bombus vetustus*, which is a male, was most similar to the tribe Bombini based on forewing shape but was placed outside of the shape space of modern Bombini (Dataset 2, LDA 4). Despite this, the most similar subgenus was *Bombias* (Dataset 3, LDA 5). There is only one specimen available of *B. pristinus*, which has incomplete wings. However, all landmarks are available except for number 16, whose position could be accurately estimated by the extension of cu-a and portion of vein A. We decided therefore to apply the same LDA analyses to the specimen, with the 18 landmarks. Our results found that this fossil clustered inside the shape space of Bombini (Dataset 2, LDA 4) and was similar to the subgenus *Cullumanobombus* (Dataset 3, LDA 5), although it would be worth reanalyzing this specimen with a dataset encompassing males from extant species in order to have greater confidence. Finally, the wing shape of *B. cerdanyensis* was first analyzed in Dehon et al. (2014). This specimen has incomplete wings; nonetheless, all landmarks are available except for numbers 17 and 18, but the position of the latter could be accurately estimated by the extension of cu-a and portion of vein A. Assignment of the fossil in the discriminant space did not allow a reliable subgeneric attribution. Herein, *B. cerdanyensis*

is assigned to *Melanobombus* (Dataset 3, LDA 5). The subgeneric assignment of each fossil within *Bombus* s. l. through geometric morphometric analyses is summarized in Table 1.

Systematics

In the following account of fossil bombyne species, we have organized the taxa by general age, proceeding from oldest to youngest.

Family Apidae Latreille

Subfamily Apinae Latreille

Clade Corbiculata Engel

Stem-group Bombini Latreille

Late Eocene

Genus *Oligobombus* Antropov, 2014

Type species. *Oligobombus cuspidatus* Antropov, 2014, by original designation.

Diagnosis. Sex unknown. Forewing distinctly pointed apically (apparently taphonomically altered); three submarginal cells of approximately equal sizes; marginal cell elongate, longer than distance between its apex and forewing tip, with apex roundly truncate; forewing distal membrane papillate; pterostigma short, with margin within marginal cell straight, approximately 4.0 times as long as prestigma; r-rs arising from distal part of pterostigma after its midpoint; 1rs-m straight; 2rs-m with posterior half curved apically; angle between 1rs-m and part of M inside third submarginal cell obtuse; first submarginal cell with an oblique translucent vein rs and not wider than second submarginal cell; second submarginal cell shorter than third marginal cell; third submarginal cell widest; 1m-cu slightly curved anteriorly, reaching second submarginal cell in its midpoint; 2m-cu curved anteriorly, reaching M basad 2rs-m; distance between anterior ends of 1m-cu and 2m-cu exceeding their length; basal vein slightly basad cu-a. See Antropov et al. (2014) for original diagnosis.

Oligobombus cuspidatus Antropov, 2014

Holotype. Sex unknown. NHMUK In.17349 (part and counterpart), Smith collection of the Natural History Museum (NHM, London, UK). Type specimen has been located and revised (Figs 1A, 3A).

Type strata and locality. Late Eocene (i.e., 36.0 Ma), Insect Bed of the Bembridge Marls from the Isle of Wight, UK.

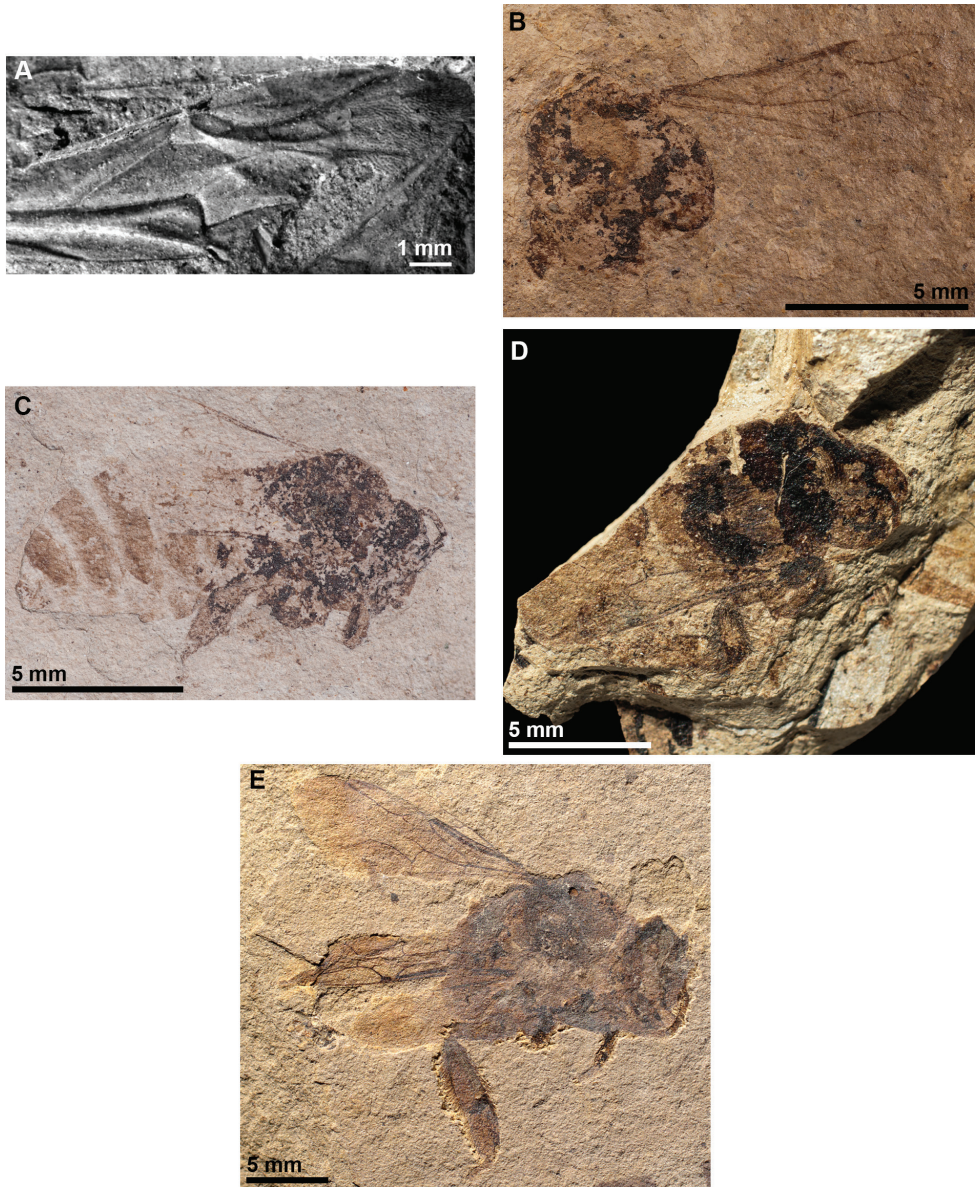


Figure 1. Representative fossil bumble bees **A** *Oligobombus cuspidatus* (photograph by Antropov et al. (2014)) **B** Holotype of *Calyptapis florissantensis* (photograph by Manuel Dehon) **C** *C. florissantensis* (photograph by Talia S. Karim) **D** *Bombus (Paraelectrobombus) patriciae* (photograph by Gaëlle Doitteau) **E** *B. (Mendacibombus) beskonakensis* (photograph by Gaëlle Doitteau).

Diagnosis. Owing to monotypy, the diagnosis for the species is identical to that of the genus (vide supra).

Description. Part consists in middle and apical parts of right forewing; counterpart consists of middle part of right forewing; forewing distal membrane papillate; complete venation preserved; total forewing length 13.3 mm, maximum width 4.0 mm as pre-

served; basal vein length 2.3 mm, relatively straight and basad cu-a; cu-a length 0.3 mm; marginal cell length 4.0 mm, width 0.9 mm, apex roundly truncate; prestigma 0.2 mm; pterostigma length 0.8 mm; 1st abscissa of Rs straight; 2nd abscissa of Rs almost straight; 3Rs length approximately same as r-rs; 4Rs slightly longer than 3Rs; M+Rs length 1.2 mm; three submarginal cells; first submarginal cell length 1.5 mm (as measured from origin of Rs+M to juncture of r-rs and Rs), width 0.6 mm (as measured from Rs+M to pterostigma); second submarginal cell length 1.3 mm (as measured from juncture of Rs+M and M to juncture of Rs and 1rs-m), width 0.7 mm (as measured from midpoint on M between 1m-cu and 1rs-m to juncture of r-rs and Rs); third submarginal cell length 1.4 mm (as measured from juncture of 1rs-m and M to juncture of M and 2rs-m), width 1.0 mm (as measured from juncture of M and 2m-cu to juncture of 2rs-m and Rs); 1rs-m straight; 2rs-m posterior half curved apically; 1m-cu anterior half curved apically, reaching M approximately at midpoint between 2nd abscissa of Rs and 1rs-m; 2m-cu basad 2rs-m. See Antropov et al. (2014) for original description.

Comments. There is only one specimen, the holotype NHMUK In.17349, consisting of a part and counterpart. Antropov et al. (2014) described the specimen and considered it as possibly a member of Bombini. According to the original author, the forewing shape displays mixed features of Bombini, Electrapini, Electrobombini, Euglossini, and Melikertini (e.g., the forewing distal membrane being papillate is characteristic of Bombini, Electrobombini, and Euglossini, the shape of vein Rs displays mixed features reminiscent of the corbiculate tribes Bombini, Electrobombini, Electrapini (i.e., *Thaumastobombus* Engel, 2001), Euglossini, and Melikertini (i.e., *Melikertes* Engel, 1998 and *Succinapis* Engel, 2001), the submarginal cells are reminiscent of Electrapini, Electrobombini, and Euglossini, 1m-cu is reminiscent of Electrapini and Electrobombini, 2m-cu is reminiscent of Electrapini, Euglossini, and Melikertini). All in all, the specimen has a forewing venation with features that can be found in different extinct and extant tribes of Corbiculata, but that taken together do not occur in any of them. According to the Antropov et al. (2014), the fossil forewing venation is generally similar to extant species of Bombini, but the lack of features from the pro-, meso-, and metasoma prevents identification of its exact taxonomic affinities. Based on the general morphology and forewing shape affinities, *Oligobombus* is perhaps a stem-group bumble and we consider it as such for the moment. Further material and additional characters, ideally analyzed in a cladistic framework, are needed to corroborate this placement, or the species could have phylogenetic affinities with Electrobombini or Electrapini.

Eocene-Oligocene boundary

Genus *Calyptapis* Cockerell, 1906

Type species. *Calyptapis florissantensis* Cockerell, 1906, by original designation.

Diagnosis. Three submarginal cells; third submarginal cell longest, shorter than combined length of first and second submarginal cells; first and second submarginal cells of more or less same size; first submarginal cell rounded; marginal cell wide,

apex rounded and scarcely offset from anterior forewing margin; basal vein long and straight, slightly curved in its base, meeting M+Cu near juncture of cu-a with M+Cu; cu-a slightly curved; 1m-cu meeting M at middle of second submarginal cell; 2m-cu slightly curved and not in line with 2rs-m, positioned before crossing between 2rs-m and M; 2rs-m strongly arched; 2Rs scarcely arched basally; pterostigma relatively small. Pro- and mesosoma black; corbicula preserved; no alar papillae (or, more likely, not visible as preserved); forewing not colored. Similar in forewing venation to *Bombus* s. l. but differing from most species in the combination of a simultaneously distally bulging third submarginal cell (i.e., 2rs-m strongly arched), with a relatively unmodified second submarginal cell (i.e., 2Rs scarcely arched basally, a putatively plesiomorphic trait and somewhat similar to many euglossines), and broad marginal cell apex that is scarcely offset from anterior wing margin.

Calyptapis florissantensis Cockerell, 1906

Holotype. Sex unknown. MCZPALE 2008, collections of the Museum of Comparative Zoology (Harvard University, Cambridge, USA). Samuel Hubbard Scudder collection. Type specimen has been located and revised (Figs 1B, 3B).

Type strata and locality. Eocene-Oligocene boundary (i.e., 34.0 Ma), the Florissant shale of Colorado, USA.

Diagnosis. Owing to monotypy, the diagnosis for the species is identical to that of the genus (*vide supra*).

Description. Integument of body black to dark brown as preserved (taphonomically altered); forewing venation brown to dark brown, membrane hyaline as preserved; forewing length 7.6 mm; maximum width approximately 2.5 mm as preserved; basal vein (1M) faintly arched at base, straight along length, basad 1cu-a by about twice vein width, faintly angled relative to 1Rs; Rs+M originating anteriorly, 1Rs about as long as r-rs; pterostigma short, slightly longer than wide, border inside marginal cell slightly concave, pterostigma very short, scarcely present, about as long as 2.5–3 times width of 1Rs; marginal cell length 2.2 mm, width 0.5 mm, tapering slightly across its length, free portion of cell subequal to portion bordering submarginal cells, apex rounded and offset from anterior wing margin by about vein width, not appendiculate; 2Rs weakly arched basally, comparatively straight; r-rs about as long as 3Rs; 4Rs slightly longer than 3Rs; three submarginal cells of comparatively similar sizes, albeit third slightly larger than first or second, but slightly shorter than combined lengths of first and second submarginal cells; first submarginal cell length 0.9 mm (as measured from origin of Rs+M to juncture of r-rs and Rs), width 0.4 mm (as measured from Rs+M to pterostigma); second submarginal cell length 0.7 mm (as measured from juncture of Rs+M and M to juncture of Rs and 1rs-m), width 0.4 mm (as measured from midpoint on M between 1m-cu and 1rs-m to juncture of r-rs and Rs); third submarginal cell length 0.9 mm (as measured from juncture of 1rs-m and M to juncture of M and 2rs-m), width 0.6 mm (as measured from juncture of M and 2m-cu to juncture of 2rs-m and Rs);

1rs-m weakly arched; 2rs-m strongly arched distally in posterior half, such that third submarginal cell is greatly bulged distally; 1m-cu distinctly angulate anteriorly near M, entering second submarginal cell slightly before cell's midlength; 2m-cu weakly and gently arched apically, meeting third submarginal cell near cell's apex, basad 2rs-m by about 2.5 times vein width; mesosoma length 4.4 mm as preserved; metasoma length 8.8 mm as preserved; total body length 15.2 mm as preserved. Specimen UCM 4415: left lateral view; pro-, meso-, and metasoma preserved, both forewings preserved; parts of right hindleg and foreleg preserved; forewing venation preserved; part of one antenna preserved. Specimen MCZPALE-2008: mesosoma preserved, as well as part of prosoma; right forewing visible. See Cockerell (1906, 1908c) for original description.

Comments. *Calyptapis florissantensis* was first described based on a poorly preserved specimen collected by Samuel H. Scudder (MCZPALE 2008), and was first attributed to Eucerini by Cockerell (1906). The well-preserved second specimen (UCM 4415) was described by Cockerell (1908) and this permitted him to attribute both specimens to Bombini. However, he stated that the fossil differed from extant *Bombus* in the form of the second and third submarginal cells, thus suggesting it to be a member of a genus close to *Bombus* (Cockerell 1906, 1908; Zeuner and Manning 1976). Based on the general morphology and forewing shape affinities, *Calyptapis* is perhaps a stem-group bombine and we consider it as such for the moment, although a cladistic analysis encompassing additional characters is needed for a more definitive clarification of its phylogenetic affinities.

Oligocene-Miocene boundary

Tribe Bombini Latreille

Genus *Bombus* Latreille

Subgenus *Paraelectrobombus* Nel & Petrulevičius, 2003, nomen translatum

Type species. *Paraelectrobombus patriciae* Nel & Petrulevičius, 2003.

Diagnosis. Bombiform bee; pterostigma larger than prestigma; vein 1m-cu curved apically in its anterior half; vein r-rs reaching pterostigma at midpoint; second abscissa of Rs relatively straight; vein 2rs-m curved apically in its posterior half; vein 2m-cu slightly curved at midpoint, reaching M basad to 2rs-m; two tibial spurs; corbicula with setae longer than metatibia width. See Nel and Petrulevičius (2003) for original diagnosis.

Bombus (Paraelectrobombus) patriciae (Nel & Petrulevičius, 2003), comb. nov.

Holotype. Female. MNHN-LP-R. 11187 (coll. Paichelier 1977), deposited in the Laboratoire de Palaeontologie, Muséum national d'Histoire naturelle, Paris, France. The type specimen was located, examined, and revised (Figs 1D, 3D).

Type strata and locality. Oligocene-Miocene boundary, 22.5 Ma, volcano-sedimentary paleolake deposit, BesKonak Basin, Anatolia, Turkey.

Diagnosis. Owing to monotypy, the diagnosis for the species is identical to that of the subgenus (vide supra).

Description. Body poorly preserved and covered with long setae; forewing membrane hyaline and covered with small pilosity, venation similar to that of extant species of *Bombus* s. l.; forewing length 9.0 mm, maximum width approximately 3.4 mm as preserved; basal vein slightly curved at base, and slightly basad cu-a, length 1.9 mm; prestigma length 0.3 mm, width 0.2 mm; pterostigma length 0.6 mm, width 0.3 mm; marginal cell length 2.8 mm, width 0.6 mm, with apex narrowly rounded and detached from margin of forewing; 1st abscissa of Rs straight; 2nd abscissa of Rs curved basally in its last posterior part; r-rs almost straight; 3Rs smaller than r-rs; 4Rs approximately as long as r-rs; Rs+M straight and longer than r-rs; three submarginal cells of approximately equivalent size; first submarginal cell length 1.4 mm (as measured from origin of Rs+M to juncture of r-rs and Rs), width 0.6 mm (as measured from Rs+M to pterostigma); second submarginal cell length 1.1 mm (as measured from juncture of Rs+M and M to juncture of Rs and 1rs-m), width 0.6 mm (as measured from midpoint on M between 1m-cu and 1rs-m to juncture of r-rs and Rs); third submarginal cell length 1.0 mm (as measured from juncture of 1rs-m and M to juncture of M and 2rs-m), width 0.8 mm (as measured from juncture of M and 2m-cu to juncture of 2rs-m and Rs); 1rs-m almost straight; 2rs-m with anterior half curved apically; 1m-cu with anterior half curved apically, reaching M slightly before midlength between 2nd abscissa of Rs and 1rs-m; 2m-cu slightly curved near midpoint, reaching M basad 2rs-m; prosoma length 3.0 mm as preserved; mesosoma length 4.5 mm as preserved; metatibia without basal plate, length 2.2 mm, width 0.6 mm; corbicula with long setae; metabasitarsus length 2.0 mm; width 1.0 mm, with auricle at base; metasoma not preserved. The taphonomy of the specimen does not allow us to ascertain the presence or absence of a transector. See Nel and Petrulevičius (2003) for original description.

Comments. There is only one specimen, the holotype MNHN-LP-R. 11197. The fossil was initially described as *Paraelectrobombus patriciae* within the extinct tribe Electrobombini by Nel and Petrulevičius (2003), and was described as a bombine-like species with a wing venation similar to those of Bombini and Electrobombini. However, these authors stated that it was not possible to determine its exact relationship relative to Bombini and Electrobombini owing to the lack of information on its body structures such as the pretarsal claws and arolia. Based on the specimen's forewing shape affinities, *Paraelectrobombus* is assuredly an extinct taxon of Bombini, and likely within the genus *Bombus*. Based on our results, we hypothesize that this group may be sister to extant *Bombus* or a stem group to *Bombus*.

Subgenus *Mendacibombus* Skorikov, 1914

= *Oligoapis* Nel & Petrulevičius, 2003, syn. nov.

***Bombus (Mendacibombus) beskonakensis* (Nel & Petrulevičius, 2003), comb. nov.**

Holotype. Female worker. MNHN-LP-B.47780 (BK349, coll. Paichelier, in 1977), part and counterpart, deposited in the Laboratoire de Palaeontologie, Muséum national d'Histoire naturelle, Paris, France. Type specimen has been located and revised (Figs 1E, 3E).

Type strata and locality. Oligocene-Miocene boundary, 22.5 Ma, volcano-sedimentary paleolake, BesKonak Basin, Anatolia, Turkey (Paichelier et al. 1978).

Diagnosis. Habitus and hind and forewing venation similar to those of extant Bombini, with pterostigma short but longer than prestigma, and metatibial spurs not visible as preserved (seemingly obscured by leg orientation). Short process of proximal posterior corner of metabasitarsus apparently preserved. See Nel and Petrulevičius (2003) for original diagnosis.

Description. Wing membrane red-brown, setose throughout; forewing length 15.0 mm; maximum width 5.2 mm as preserved; pterostigma slightly longer than prestigma, with posterior margin aligned with vein Sc+R; marginal cell with apex closed by strong vein; three submarginal cells of approximately same size; basal vein long, oblique and slightly curved in its base, slightly basad cu-a; cu-a straight; 1m-cu strongly curved apically in its anterior half, reaching second submarginal cell near midpoint; 2m-cu curved apically, reaching M basad to 2rs-m; second abscissa of Rs slightly double-curved; 1rs-m almost straight; 2rs-m with posterior half curved apically; prosoma length 6.3 mm, covered with long and dark hair; mouthparts not preserved, except for galea which is elongate; antennae approximately 3.5 mm long, with nine or ten visible flagellomeres, scape and pedicel poorly preserved; mesosoma length 8.0 mm, height 5.0 mm; metafemur length 4.2 mm, width 1.4 mm, with long curved hair; metatibia length 4.5 mm, width 1.8 mm, with corbicula; metabasitibial plate absent; metatibial spurs not visible as preserved (apparently owing to leg orientation); metabasitarsus length 2.7 mm, width 1.7 mm, with auricle preserved; arolia and claws not visible as preserved; metasoma length 9.0 mm, height 4.5 mm, covered with short setae. See Nel and Petrulevičius (2003) for original description.

Comments. The fossil was first described as *Oligoapis beskonakensis* by Nel and Petrulevičius (2003). The specimen is remarkably similar to extant Bombini in terms of its habitus and wing venation. However, the authors decided to place it in a separate genus of an undetermined corbiculate tribe owing to its pterostigma smaller than the prestigma, and by the putative absence of metatibial spurs. The absence of metatibial spurs is merely due to the lack of preservation and not to the definitive absence of spurs, and therefore this character cannot be evaluated. The metatibia is preserved with its outer surface exposed and the presence of spurs (particularly if they were reduced in size) on the inner anterior angle could not be observed in this orientation. In extant species of *Mendacibombus*, females are characterized by a few long bristles emerging from the outer surface of the metatibia, by a metatibia with the outer surface imbricate, i.e. coarsely sculptured, as well as by an unusually short (i.e., for *Bombus* s. l.) process of the proximal posterior corner of the metabasitarsus (Williams et al. 2008, 2016).

In the fossil, the long bristles emerging from the outer surface of the metatibia are not visible, while the short process of the proximal posterior corner of the metabasitarsus appears to be present. Furthermore, it is challenging to assess if the metatibia outer surface is coarsely sculptured due to the taphonomy of the specimen.

We consider the fossil as a stem group within *Mendacibombus* and thus synonymize *Oligoapis* under that subgenus. Like *Oligoapis*, *Mendacibombus* has a relatively reduced pterostigma, further emphasizing the similarity between these groups. Interestingly, this species from the Oligocene-Miocene boundary (i.e., 22.5 Ma) comes from a deposit near the estimated Old World origin of this subgenus (Williams et al. 2016). Because of the overall morphological assessment we place the species as a stem group within *Mendacibombus*.

Lower Miocene

Subgenus *Cullumanobombus* Vogt, 1911

Bombus (*Cullumanobombus*) *trophonius* Prokop, Dehon, Michez & Engel, 2017

Holotype. Female. ZD0003 (coll. Bílina mine). Type specimen has been located and revised (Figs 2A, 3F).

Type strata and locality. Lower Miocene (i.e., 20.0 Ma), Clayey Superseam Horizon, Bílina mine, Czech Republic.

Diagnosis. The fossil has a wing pattern most similar to *B.* (*Cullumanobombus*) *rufocinctus* Cresson (Milliron 1973; Williams et al. 2014). Moreover, both species display a similar combination of 3Rs about as long as r-rs but shorter than 4Rs, a basal vein basad 1cu-a, a vein 2Rs arched posteriorly but not as greatly prolonged proximally as in several other species of *Cullumanobombus* (e.g., Milliron 1971), and a vein 1m-cu entering second submarginal cell near midpoint. However, the convex pterostigmal border within the marginal cell, less apically narrowed marginal cell, and less arched 2rs-m minimally serve to distinguish the fossil species from *B. rufocinctus*. See Prokop et al. (2003) and Prokop et al. (2017) for original diagnosis.

Description. Wings and integument black as preserved; forewing total length 14.6 mm; maximum width 5.10 mm; basal vein weakly arched basally, comparatively straight along length, basad cu-a by about vein width, in line with 1Rs; M+Rs originating anteriorly, 1Rs slightly shorter than r-rs; pterostigma short, slightly longer than wide, tapering inside of marginal cell, border inside marginal cell convex, prestigma nearly as long as pterostigma; marginal cell length 5.1 mm, width 1.1 mm, free portion slightly shorter than portion bordering submarginal cells, apex rounded and offset from anterior wing margin by much more than vein width, not appendiculate; 2Rs strongly arched basally and slightly arched outward; r-rs about as long as 3Rs; 4Rs slightly longer than 3Rs; three submarginal cells of approximately same sizes, albeit third slightly larger than first or second; first submarginal cell length 0.9 mm (as meas-

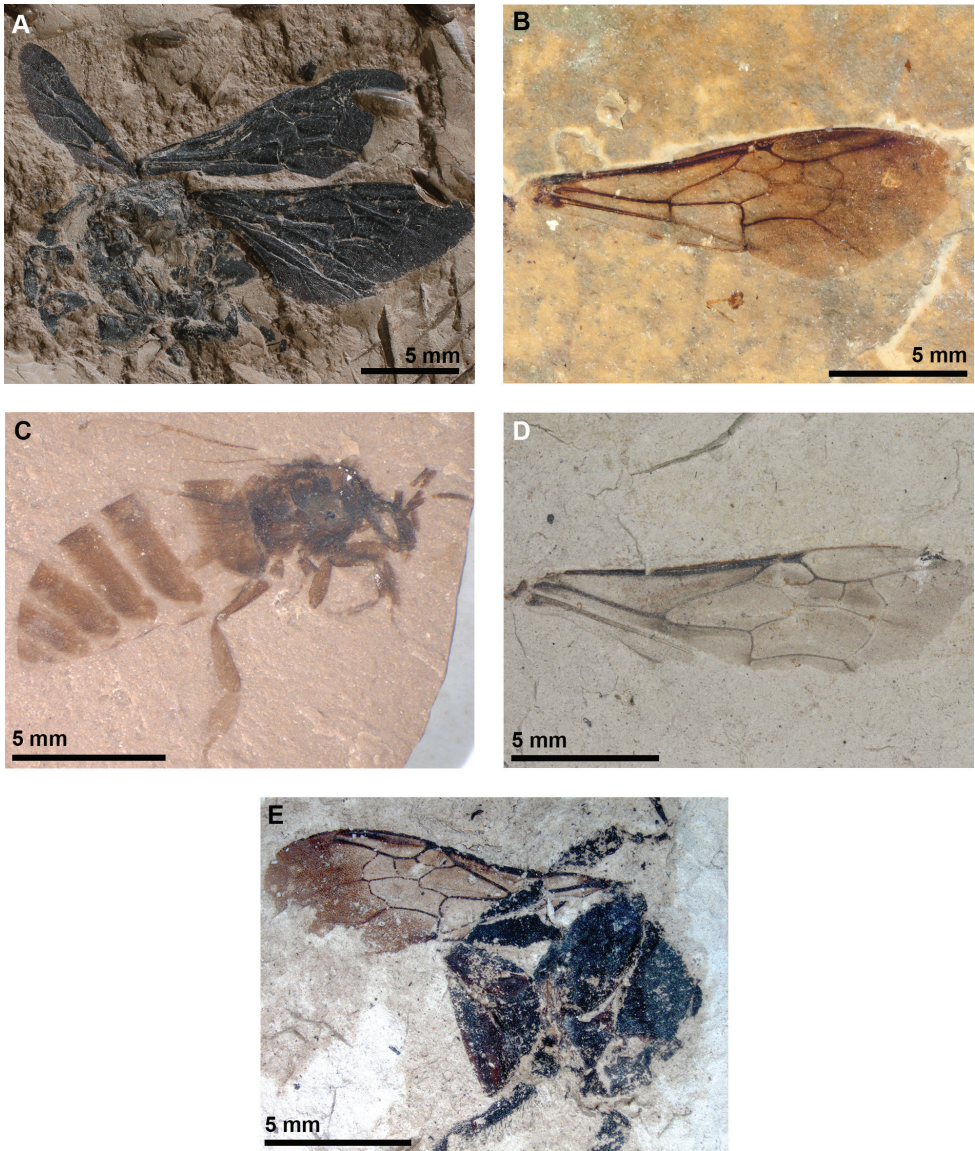


Figure 2. Representative fossil bumble bees **A** *Bombus (Cullumanobombus) trophoniuss* (photograph by Jakup Prokop) **B** *B. (Cullumanobombus) randeckensis* (photograph by Torsten Wappler) **C** *B. vetustus* (photograph by Alexandr P. Rasnitsyn) **D** *B. (Cullumanobombus) pristinus* (photograph by Irene Zorn and Monika Brüggeman-Ledolter) **E** *B. (Melanobombus) cerdanyensis* (photograph by Thibaut De Meulemeester).

ured from origin of M+Rs to juncture of r-rs and Rs), width 1.0 mm (as measured from Rs+M to pterostigma); second submarginal cell length 1.3 mm (as measured from juncture of Rs+M and M to juncture of Rs and 1rs-m), width 0.9 mm (as measured from midpoint on M between 1m-cu and 1rs-m to juncture of r-rs and Rs); third submarginal cell length 1.6 mm (as measured from juncture of 1rs-m and M to

junction of M and 2rs-m), width 1.2 mm (as measured from juncture of M and 2m-cu to juncture of 2rs-m and Rs); 1rs-m straight; 2rs-m arched distally in posterior half; 1m-cu distinctly angulate anteriorly near M, entering second submarginal cell near cell's midlength; 2m-cu slightly arched apically, meeting third submarginal cell at cell's apical fifth of length. Hind wing length 9.4 mm, width 2.6 mm. Preserved portion of mesosoma and legs difficult to describe, although portion of metatibial corbicula preserved (basal quarter to third), and sclerites with numerous, long setae. See Prokop et al. (2003) and Prokop et al. (2017) for original description.

Comments. The specimen was first reported as *Bombus* sp. in Prokop et al. (2003). Prokop et al. (2017) demonstrated that the fossil clustered within contemporary *Cullumanobombus* and formally described the species. Although the majority of contemporary species of *Cullumanobombus* are found in the New World and a few species in the Old World, Hines (2008) estimated that the subgenus originated around 20.0–15.0 Ma in the Palearctic. Our result, as well as that of Prokop et al. (2017), is consistent with Hines (2008) as the fossil specimen was found in the Lower Miocene (i.e., 20.0 Ma) deposits of Bilina Mine in northern Bohemia (Czech Republic).

***Bombus (Cullumanobombus) randeckensis* Wappler and Engel in Wappler et al. (2012)**

Holotype. Sex unknown. The fossil consists of an isolated forewing. SMNS 68000/28 (old Armbruster collection No. A5119). Conserved in the Staatliches Museum für Naturkunde, Stuttgart, Germany. Type specimen has been located and revised (Figs 2B, 3G).

Type strata and locality. Randeck Maar, southeast of Stuttgart, Swabian Alb; Early Miocene, i.e., 16.0–18.0 Ma (Burdigalian, Karpatian, MN 5).

Diagnosis. Bombiform bee; infusate area in marginal cell extends entire length of anterior half of marginal cell; forewing venation strictly similar to that of an extant bumble bee, with transector visible on both forewings. See Wappler et al. (2012) for original diagnosis.

Description. Forewing length 14.3 mm, maximum width 5.0 mm; marginal cell length 3.9 mm; basal vein almost straight, slightly curved in its base, slightly basad cu-a; vein cu-a straight; three submarginal cells; first submarginal cell length 1.7 mm (as measured from origin of M+Rs to juncture of r-rs and Rs), width 0.8 mm (as measured from M+Rs to pterostigma); second submarginal cell width 0.7 mm (as measured from midpoint on M between 1m-cu and 1rs-m to juncture of r-rs and Rs); third submarginal cell length 1.3 mm (as measured from juncture of 1rs-m and M to juncture of M and 2rs-m), width 1.1 mm (as measured from juncture of M and 2m-cu to juncture of 2rs-m and Rs); height of second medial cell 1.1 mm (as measured from Cu1 to juncture of 1m-cu and M); 1st abscissa of Rs almost straight; 2nd abscissa of Rs with anterior half curved apically; r-rs almost straight; M+Rs straight and longer than r-rs; 3Rs almost as long as r-rs; 4Rs slight smaller than M+Rs; 1rs-m almost straight; 2rs-m with posterior half curved apically; 1m-cu curved apically in last anterior part,

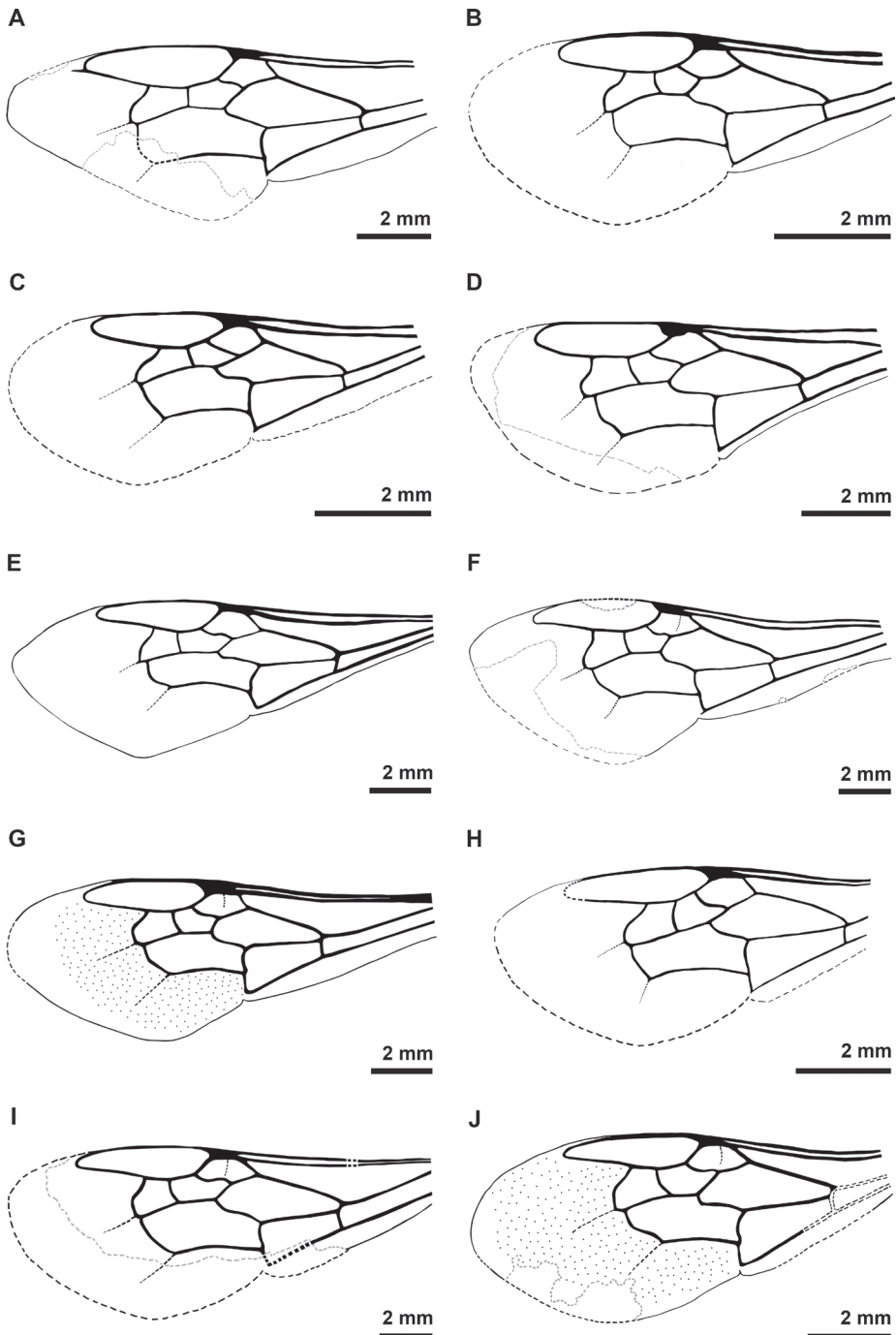


Figure 3. Forewing drawings of the fossil bumble bees studied herein. Some forewings were mirrored to enable comparison across all specimens **A** *Oligobombus cuspidatus* (mirrored) **B** Holotype of *Calyptrapis florissantensis* (mirrored) **C** *C. florissantensis* **D** *Bombus* (*Paraelectrobombus*) *patriciae* (mirrored) **E** *B.* (*Mendacibombus*) *beskonakensis* **F** *B.* (*Cullumanobombus*) *trophonius* (mirrored) **G** *B.* (*Cullumanobombus*) *randedeckensis* (mirrored) **H** *B. vetustus* **I** *B.* (*Cullumanobombus*) *pristinus* (mirrored) **J** *B.* (*Melanobombus*) *cerdanyensis*.

reaching second submarginal cell before midpoint; 2m-cu slightly curved, reaching M basad to 2rs-m. See Wappler et al. (2012) for original description.

Comments. The fossil was discovered in the Lower Miocene (i.e., 18.0–16.0 Ma) deposits of Randeck Maar, Germany, an age and locality in general accord with the estimate that *Cullumanobombus* originated between 20.0–15.0 Ma in the Old World. Based on the forewing shape affinities and the general morphological assessment, *B. randeckensis* is likely an extinct species of *Cullumanobombus*, like *B. trophonius*.

Middle-Lower Miocene

“*Bombus*” *luianus* Zhang, 1990, species inquirenda

Holotype. Female. Specimen n°82771. Plate XXXIII-1, fig. 164 from Zhang et al. (1994), plate I-1, 2 from Zhang (1990). The type material from Shanwang was not available for study and we have, therefore, had to base our information on this and the following two species (vide infra) on the original Chinese descriptions, the rather poor original photographs, and the tenuously accurate line drawings in these publications. Accordingly, our evaluation of *B. luianus*, *B. dilectus*, and *B. anacolus* has been considerably hampered.

Type strata and locality. Middle Miocene (i.e., 17.0–15.2 Ma), deposit of the Shanwang Formation, large lacustrine and lithified deposit, with diatomaceous and tuffaceous mudstone. Located in Linqu County, Shanwang Province, China.

Description. Taken from Zhang (1990) and Zhang et al. (1994): Prosoma poorly preserved; meso- and metasoma preserved; mesosoma stout, setose, and dark; metasoma dark, reddish-brown near apex, displaying five segments, suboval in shape, little longer than wide, distinctly narrower than mesosoma; forewing membrane brown and transparent, venation dark brown; metatibia widening posteriorly, displaying two strong spurs, outer margin covered with strong coarse setae; metabasitarsus flat, rectangular, truncated at both ends, nearly as wide as distal part of metatibia; tarsomere IV displaying pair of spur-like bristles distally; inner margin of pretarsal claw displaying single tooth at midlength; forewing length approximately 14.0 mm, maximum width approximately 4.5 mm as preserved; basal vein relatively straight and almost in line with cu-a; cu-a almost straight; 1st abscissa of Rs straight; 2nd abscissa of Rs curved anteriorly; r-rs curved; Rs+M straight and shorter than r-rs; 3Rs almost straight and as long as r-rs; 4Rs almost straight and longer than r-rs; marginal cell length approximately 4.0 mm, width 0.8 mm; three submarginal cells; 1rs-m slightly curved apically near midpoint; 2rs-m curved apically in its posterior half; 1m-cu almost straight and reaching M near midpoint between 2nd abscissa of Rs and 1rs-m; 2m-cu slightly curved and reaching M basad to 2rs-m; hind wing length 8.6 mm; total body length approximately 13.0 mm, width approximately 8.0 mm as preserved. The original description and figure do not display a transector vein. See Zhang (1990) and Zhang et al. (1994) for original descriptions.

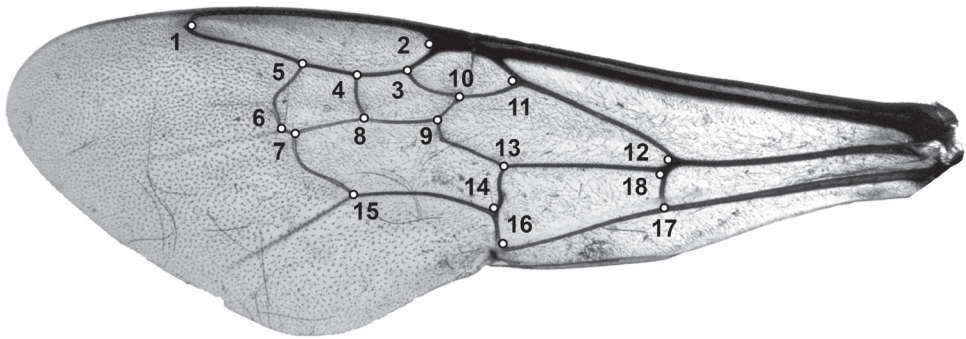


Figure 4. Left forewing of *Bombus (Bombus) terrestris* (Linnaeus, 1758) with the 18 landmark points indicated on the veins to describe the shape (photograph by Michaël Terzo). The names of the veins and cells can be found in Dehon et al. (2017).

Comments. According to Zhang (1990), the fossil species is closely similar to *B. (Bombus) tunicatus* Smith, 1852 (extant species distributed in Himalaya), but differs from it in that the mesosoma is narrower than the mesosoma, and not so massive as is usual for the genus; the spurs becoming shorter; vein 1m-cu meeting second submarginal cell at midlength; and veins M+Cu and M of hind wing aligned in a straight line. The validity of these features for distinguishing the species remains unclear. Our morphometric study showed a similar shape with the subgenus *Melanobombus*. It is estimated that *Melanobombus* originated between the Lower and Middle Miocene, while the fossil was discovered in the Middle Lower Miocene (i.e., 17.0–15.2 Ma) deposits of Shandong, China (Zhang 1990; Zhang et al. 1994). The results based on geometric morphometric analyses for this species could be wrong, since they were based on Zhang’s drawings and not on a picture or on examination of the holotype. Given this, we consider the fossil as species inquirenda.

“*Bombus*” *dilectus* Zhang, 1994, species inquirenda

Holotype. Female. Plate XXXIII-3, figs 168, 169 from Zhang et al. (1994). We were not able to study the holotype (see comment under *B. luianus*, vide supra).

Type strata and locality. Middle Miocene (i.e., 17.0–15.2 Ma), deposit of the Shanwang Formation, large lacustrine and lithified deposit, with diatomaceous and tuffaceous mudstone. Located in Linqu County, Shanwang Province, China.

Description. Taken from Zhang et al. (1994): Forewing and hind wing membrane papillate distally; forewing membrane dark brown; forewing length more than 15.0 mm, maximum width more than 6.0 mm as preserved; basal vein slightly curved, basad cu-a; cu-a very slightly curved apically; marginal cell length approximately 5.0 mm; 1st abscissa of Rs slightly curved apically near midpoint; 2nd abscissa of Rs curved apically near midpoint; r-rs straight; Rs+M straight and longer than r-rs; 3Rs straight and smaller than r-rs; 4Rs almost as long as Rs+M; three submarginal cells; 1rs-m

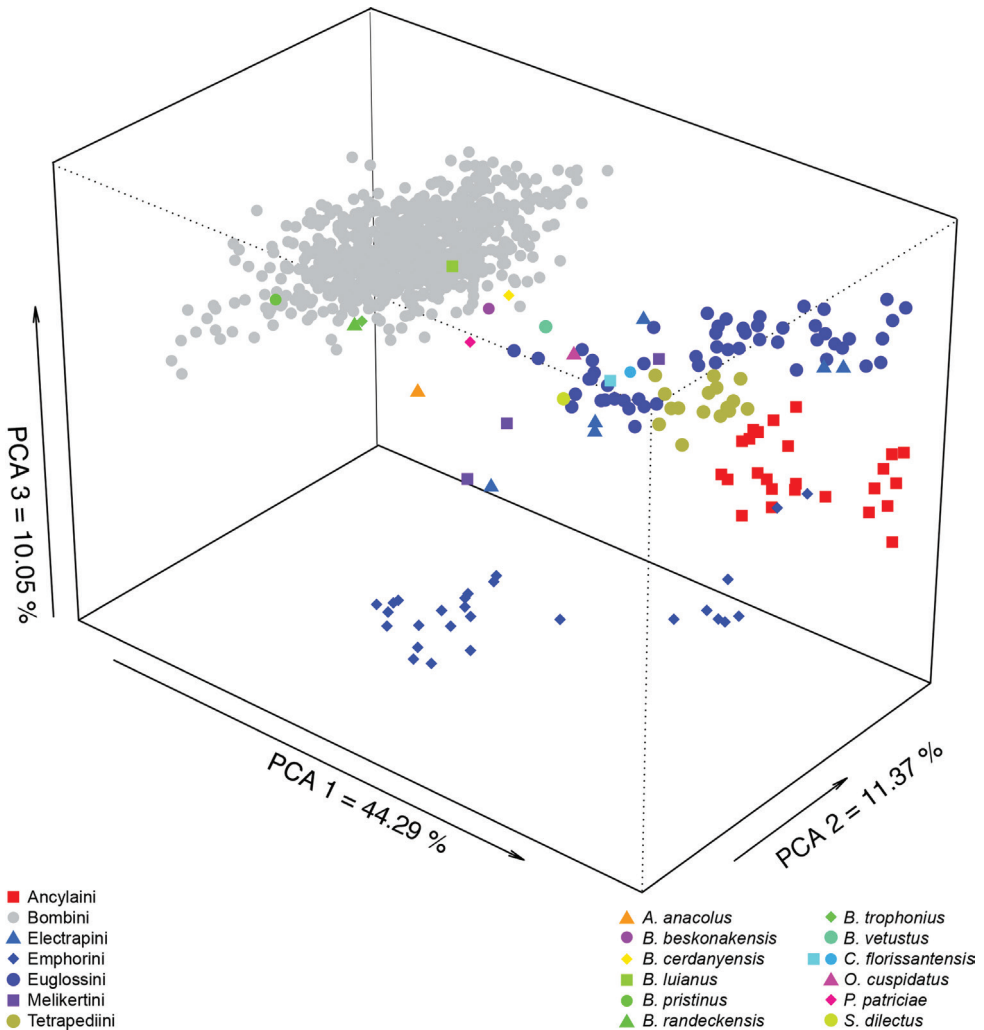


Figure 5. Ordination of the fossils along the three first axes of the PCA (PC1 = 44.29%, PC2 = 11.37%, PCA3 = 10.05%) in subgeneric dataset of *Bombus* s. l.

straight; 2rs-m curved apically in its posterior half; 1m-cu straight, reaching M near midpoint between 2nd abscissa of Rs and 1rs-m; 2rs-m curved and reaching M basad to 2rs-m; total body length approximately less than 20.0 mm as preserved. The original description and figure do not display a transector vein. See Zhang et al. (1994) for original description.

Comments. The specimen was first described as *B. dilectus* by Zhang et al. (1994) and was stated to be similar to *B. anacolus* in that the wing color of both fossil species is rather dark and not transparent, or at most semi-transparent at the wing margins, a character differing from that of living species. However, some extant species display fairly dark wings (e.g., *B. (Melanobombus) simillimus* Smith, 1852). The authors also stated that the wings and body color of *B. dilectus* are darker than *B. anacolus*. As ob-

served for *B. luianus*, results based on geometric morphometric analyses for this species (i.e., similarity to subgenus *Bombus*) could be wrong, since it was based on Zhang's drawings. Given this, we consider this fossil as species inquirenda.

“*Bombus*” *anacolus* Zhang, 1994, species inquirenda

Holotype. Female. Plate XXXIII-2, figs 165, 166, 167 in Zhang et al. (1994). We were not able study the holotype (see comment under *B. luianus*, vide supra).

Type strata and locality. Middle Miocene (i.e., 17.0–15.2 Ma), deposit of the Shanwang Formation, large lacustrine and lithified deposit, with diatomaceous and tuffaceous mudstone. Located in Linqu County, Shanwang Province, China.

Description. Taken from Zhang et al. (1994): Forewing blackish brown, opaque; forewing and hind wing papillate distally; forewing length approximately 15.0 mm, maximum width approximately 6.00 mm as preserved; basal vein relatively straight and basad cu-a; cu-a almost straight; marginal cell length almost 5.0 mm, width 1.1 mm; 1st abscissa of Rs almost straight; 2nd abscissa of Rs slightly curved near midpoint; r-rs straight; Rs+M straight and longer than r-rs; 3Rs straight and smaller than r-rs; 4Rs straight and approximately as long as Rs+M; three submarginal cells, second smallest; 1rs-m straight; 2rs-m curved apically in its posterior half; 1m-cu relatively straight, reaching M near midpoint between 2nd abscissa of Rs and 1rs-m; 2m-cu curved apically, reaching M basad to 2rs-m; total body length approximately 13.0 mm as preserved (large part of metasoma missing). See Zhang et al. (1994) for original description.

Comments. The specimen was described as *B. anacolus* by Zhang et al. (1994), and considered to be close to *B. luianus*, a species collected from the same deposit. Based on geometric morphometric analyses this species is similar to *Mendacibombus*, and it could be a relative of this subgenus. This hypothesis is supported by the fact that *Mendacibombus* is estimated to have originated around the Eocene-Oligocene boundary (i.e., 34 Ma) in the Old World (Hines 2008), while the fossil was discovered in the Middle Lower Miocene (i.e., 17.0–15.2 Ma) deposit of Shandong in China (Zhang 1990; Zhang et al. 1994). Moreover, the crown age of extant members of *Mendacibombus* apparently diversified during the Late Miocene (i.e., 8 Ma). As observed for *B. luianus* and *B. dilectus*, results based on geometric morphometric analyses for this species could be wrong since it was based on Zhang's drawings. Given this, we consider the fossil as species inquirenda.

Upper Miocene

“*Bombus*” *vetustus* Rasnitsyn & Michener, 1991, species inquirenda

Holotype. Male. #2054/229, part and counterpart impressions of an entire male, deposited in the Palaeontological Institute, Russian Academy of Science, Moscow. Type specimen was located and revised (Figs 2C, 3H).

Type strata and locality. Upper Miocene (i.e., 11.2–7.1 Ma), Botchi Formation, located on the left bank of the Botchi River, Russia.

Description. Male: Forewing length 10.4 mm as preserved; basal vein long and slightly basad cu-a; cu-a straight; marginal cell length approximately 3.3 mm, width approximately 0.7 mm as preserved; 1st abscissa of Rs straight; 2nd abscissa of Rs relatively straight; r-rs almost straight; Rs+M slightly curved and slightly longer than r-rs; 3Rs smaller than r-rs; 4Rs slightly longer than Rs+M; three submarginal cells; first submarginal cell length 1.3 mm (as measured from origin of Rs+M to juncture of r-rs and Rs), width 0.6 mm (as measured from Rs+M to pterostigma); second submarginal cell length 1.1 mm (as measured from juncture of Rs+M and M to juncture of Rs and 1rs-m), width 0.6 mm (as measured from midpoint on M between 1m-cu and 1rs-m to juncture of r-rs and Rs); third submarginal cell length 1.2 mm (as measured from juncture of 1rs-m and M to juncture of M and 2rs-m), width 0.9 mm (as measured from juncture of M and 2m-cu to juncture of 2rs-m and Rs); 2rs-m with posterior half curved apically, 1m-cu reaching M near midpoint; 2m-cu curved and reaching M basad to 2rs-m; prosoma length 3.9 mm; profemur length 1.9 mm; protibial length 1.8 mm; basitarsus length 1.6 mm; setae of pro- and mesosoma dark; total body length 19.2 mm as preserved. See Rasnitsyn and Michener (1991) for original description.

Comments. Given that this is a male specimen, further work is needed with comparisons of its forewing shape with a diverse dataset based on males. In addition, the venation is incompletely preserved and so hopefully further and more complete material will be discovered.

Subgenus *Cullumanobombus* Vogt, 1911

Bombus (*Cullumanobombus*) *pristinus* Unger, 1867

Holotype. Inventory number GBA 1867/004/0004. Sex unknown. The holotype is currently deposited in the Geologische Bundesanstalt (Vienna, Austria). Type specimen has been located and revised (Figs 2D, 3I).

Type strata and locality. Upper Miocene (i.e., 11.2–7.1 Ma), Kumi deposit, Euboea Island (Euboea, Greece).

Diagnosis. Basal vein long and almost straight, basad to apically curved cu-a; pterostigma slightly longer than prestigma; second abscissa of Rs with anterior half curved apically; three submarginal cells of approximately same size; 1rs-m almost straight; 2rs-m posterior half curved apically; 1m-cu with anterior half curved apically, reaching second submarginal cell slightly before midpoint; 2m-cu very slightly curved, reaching M basad to 2rs-m.

Description. Forewing length approximately 16.0 mm, maximum width 4.3 mm as preserved; forewing membrane hyaline, venation black becoming grey when reaching apex of forewing; marginal cell length 4.9 mm, width 1.2 mm; basal vein long and almost straight, basad cu-a; vein cu-a curved apically; pterostigma slightly longer than

prestigma; three submarginal cells; first submarginal cell length 2.1 mm (as measured from origin of Rs+M to juncture of r-rs and Rs), width 0.9 mm (as measured from Rs+M to pterostigma); second submarginal cell length 2.2 mm (as measured from juncture of Rs+M and M to juncture of Rs and 1rs-m), width 0.9 mm (as measured from midpoint on M between 1m-cu and 1rs-m to juncture of r-rs and Rs); third submarginal cell length 1.6 mm (as measured from juncture of 1rs-m and M to juncture of M and 2rs-m), width 1.3 mm (as measured from juncture of M and 2m-cu to juncture of 2rs-m and Rs); second abscissa of Rs with anterior half curved apically; 1rs-m almost straight; 2rs-m posterior half curved apically; 1m-cu with anterior half curved apically, reaching second submarginal cell slightly before midpoint; 2m-cu very slightly curved, reaching M basad to 2rs-m. It seems that a transector vein is visible on the first submarginal cell, but it might be an artefact created by the taphonomic alteration of the specimen. See Unger (1867) for original description.

Comments. The type of *B. pristinus* consists of just one right forewing. The specimen was described and illustrated by Unger (1867). The illustration, displaying a left forewing, is reversed left to right. Unger attributed the species to Regenhofer but, according to Rasnitsyn and Michener (1991), the latter appears not to have written the comments or prepared the illustration of Unger's work, thus making them conclude that the name must be attributed to Unger. Based on morphological and geometric morphometric analyses, it is likely that this fossil is an extinct species of *Cullumanobombus*.

Subgenus *Melanobombus* Dalla Torre, 1880

Bombus (Melanobombus) cerdanyensis Dehon, De Meulemeester & Engel, 2014

Holotype. Sex unknown. Conserved in the Paleontology department collection, Muséum national d'Histoire naturelle, Paris, France. The fossil consists of a part and counterpart. Type specimen has been located and revised (Figs 2E, 3I).

Type strata and locality. Late Miocene (i.e., 10.0 Ma), lacustrine beds of Cerdanya, Spain.

Diagnosis. Forewing membrane with alar papillae beyond apical crossveins; membrane infusate, particularly in area beyond apical crossveins and along anterior borders of radial and marginal cells; pterostigma small, trapezoidal, not larger relative to prestigma and width not much shorter than length; marginal cell longer than distance from apex to forewing tip, tapering in width across its length, with apex acutely rounded and slightly offset from forewing margin; three submarginal cells of approximately same size, anterior borders of second and third submarginal cells subequal; 1m-cu angulate anteriorly, meeting second submarginal cell near midpoint; 2m-cu slightly arched, meeting third submarginal cell in apical fifth; mesotibia five times longer than wide; transector vein visible in the first submarginal cell. See Dehon et al. (2014) for original diagnosis.

Description. Fossil compressed in apparently dorsal oblique view, with left forewing outstretched; right forewing not preserved; hind wings not preserved; prosoma

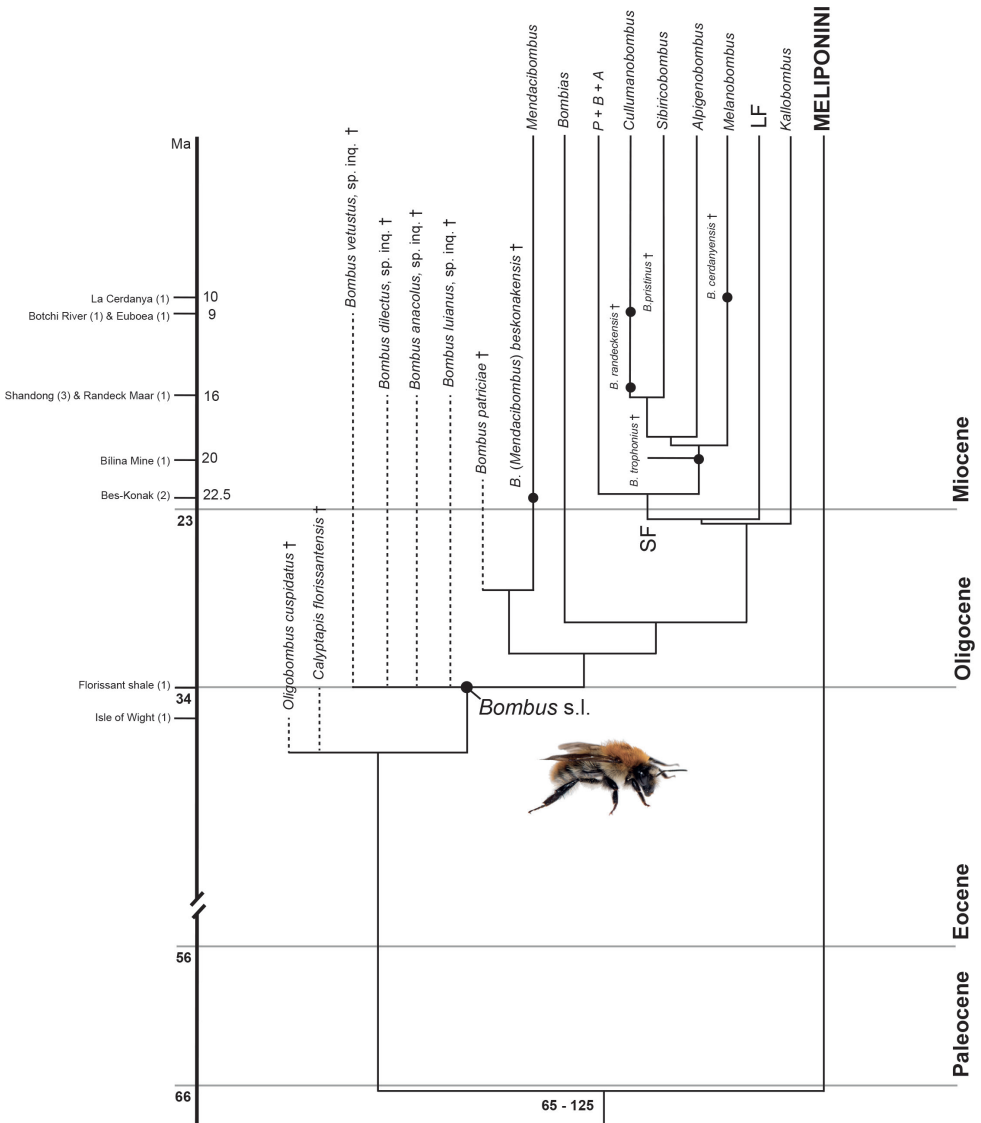


Figure 6. Hypothesis of bumble bee evolution according to the branching dates of Hines (2008) along with the subgeneric system of Williams et al. (2008). Fossils are mapped onto the clade according to our hypotheses based on our wing morphometry/shape results. Geometric morphometric analyses should be considered as a heuristic tool given the absence of other forms of pertinent data (e.g., absence of information on mandibular form, pretarsal structure, genitalic characters, etc.). A = *Alpinobombus*. B = *Bombus* s.str. LF = clade with mostly long-faced species. P = *Pyrobombus*. SF = clade with mostly short-faced species.

not preserved; mesosoma and metasoma incomplete and damaged; mid and hind legs preserved, partially overlapping forewing; right profemur length 1.4 mm, width 0.8 mm as preserved; left mesofemur length 3.6 mm, width 0.9 mm; mesotibia length 3.0 mm, width 0.6 mm; mesobasitarsus length 3.2 mm, width 0.9 mm; remaining tarsomeres

and pretarsal claws well preserved; pretarsal claws apparently not toothed as preserved; right mesofemur length 3.5 mm, width 0.5 mm; mesotibia length 2.0 mm, width 0.4 mm as preserved; left forewing length 13.3 mm, maximum width 4.6 mm; three submarginal cells of similar size; first submarginal cell length 1.5 mm (as measured from origin of Rs+M to juncture of r-rs and Rs), height 0.7 mm (as measured from Rs+M to pterostigma); second submarginal cell length 1.5 mm (as measured from juncture of Rs+M and M to juncture of Rs and 1rs-m), height 0.8 mm (as measured from midpoint on M between 1m-cu and 1rs-m to juncture of r-rs and Rs); third submarginal cell length 1.3 mm (as measured from juncture of 1rs-m and M to juncture of M and 2rs-m), height 1.1 mm (as measured from juncture of M and 2m-cu to juncture of 2rs-m and Rs); first medial cell length 3.4 mm (as measured from juncture of M+Cu and Cu to juncture of 1m-cu and M), height 1.2 mm (as measured from juncture of M and Rs+M to midpoint on Cu between M+Cu and 1m-cu); pterostigma length 0.9 mm; marginal cell length 3.4 mm with apex rounded, offset from anterior wing margin, not appendiculate; 1m-cu strongly curved, meeting second submarginal cell near midpoint; 2m-cu slightly arched, meeting third submarginal cell in apical fifth; metasoma width 5.8 mm as preserved; first two segments visible, first segment length 1.8 mm, second segment length 1.2 mm as preserved. See Dehon et al. (2014) for original description.

Comments. The attribution based on geometric morphometric analysis (i.e., *Melanobombus*) is consistent with the timing and geographic origin of the subgenus proposed by Hines (2008). Indeed, the fossil was found in the Upper Miocene (i.e., 10.0 Ma) deposit of La Cerdanya in Spain, while *Melanobombus* is estimated to have originated between 20.0–15.0 Ma in the Old World. The relative sizes of the prestigma and pterostigma exclude a placement in the Electrobombini (although the presence or absence of a jugal lobe in the hind wing cannot be determined in the holotype). The forewing is apically papillate (as in Bombini), and the marginal cell is not appendiculate and 1m-cu is strongly angulate together suggesting the species does not belong to the Electrapini or Melikertini (although some melikertines have 1m-cu more angulate, such as *Melissites trigona* Engel, 1m-cu is always much shorter and not as long as in Bombini or Euglossini; a long 1m-cu is more plesiomorphic among Corbiculata). Indeed, the forewings of the present fossil are distinctly *Bombus*-like: presence of papillae, general infuscation of the membrane, three submarginal cells of relatively similar size (albeit the latter character is assuredly plesiomorphic). Based on the specimen morphology and forewing shape affinities, the fossil is likely an extinct species of *Melanobombus*.

Discussion

Geometric morphometrics of forewing shape to discriminate taxa

As shown in Michez et al. (2009b), De Meulemeester et al. (2012), Wappler et al. (2012), Dehon et al. (2014, 2017), Dewulf et al. (2014), and Prokop et al. (2017), geometric morphometric analyses of forewing shape provide a robust tool for assessing the taxo-

onomic affinities of bee fossils with contemporary taxa and insights into bee evolution. We additionally demonstrate herein that the Hit Ratios for subgeneric level assessments were high for the genus *Bombus*. However, we need to combine geometric morphometrics of forewing shape with morphological features (e.g., pilosity, leg morphology, head and mouthpart characters, etc.) to get more powerful results, but such morphological characters are either limited or lacking with the current impression fossils.

Taxonomic affinities of *Calyptapis florissantensis* and *Oligobombus cuspidatus*

When using the first dataset with tribe a priori grouping, the most similar tribe to *C. florissantensis* (i.e., both specimens) and *O. cuspidatus* is Electrapini, while Tetrapediini is the second most similar tribe to *C. florissantensis* and Tetrapediini is the second most similar tribe to *O. cuspidatus* (LDA 3; Suppl material 10: Table S10). When using the second dataset, the most similar tribe to the holotype of *C. florissantensis* is Bombini, while the most similar tribe to the specimen described by Cockerell (1908) is Electrapini (the second most similar tribe being Bombini). The most similar tribe to *O. cuspidatus* is Bombini when using the second dataset (LDA 4; Suppl material 12: Table S12). Those results might be explained by the fact that when using the first dataset, only 20 specimens (i.e., four species, with five specimens per species) were chosen to represent Bombini, compared to 841 specimens (i.e., 210 species) in the second dataset and thereby more fully encompasses the breadth of morphospace represented among modern bombines. Furthermore, the species used to represent Bombini in the first dataset do not represent early-branching subgenera, which were found to be the most similar subgenera to *C. florissantensis* and *O. cuspidatus* in the third dataset (i.e., *Bombias*) (LDA 5; Suppl material 13: Table S13). The similarity of *O. cuspidatus* with Electrapini when using the first dataset is concordant with Antropov et al. (2014), who considered it as a possible member of Bombini with mixed features of Bombini and other corbiculate tribes (i.e., the extinct Electrapini, Electrobombini, Melikertini, and the extant Euglossini). This fossil may represent an extinct stem-group to Bombini and it would explain the different results obtained with the different datasets; those similarities across Bombini and the other tribes representing symplesiomorphic features encompassing the clade. Based on morphological features (i.e., presence of a corbicula, the forewing venation similar to *Bombus* s. l.) and forewing shape similarities, *C. florissantensis* could also belong to a stem-group bombine (Cockerell 1906, 1908; Zeuner and Manning 1976). Based on the available evidence, the conservative position is to consider both species as possible stem-group Bombini. It would be highly desirable to verify this hypothesis using cladistic analyses of new morphological characters in the future.

Origin and diversification of bumble bees

Our results generally support the timing of divergence of extant species proposed by Williams (1985) and Hines (2008) (Fig. 5), noting that the meager record available for

Bombini means such corroboration is minimal at best, albeit non-contradictory. The record of fossil bumble bees is sufficiently scant that at its best we can conclude that the available record does not contradict prior estimates, and falls in line with those for the subgenera *Cullumanobombus*, *Melanobombus*, and *Mendacibombus*. Unfortunately, fossils of most lineages within *Bombus* and certainly from more numerous and refined slices of time are simple lacking, meaning that the current record of fossil bumble bees lacks resolution for determining the timing of most diversification events (e.g., most fossils are clustered within a few deposits representing widely disparate slices in the Oligocene and Miocene). Nonetheless, none of the specimens from Eocene and Oligocene deposits were assigned within the shape space of any contemporary subgenus of *Bombus*, which is not surprising when looking at more completely preserved bees from, for example, the Eocene amber deposits (Baltic, Cambay, Rovno) (e.g., Engel 2001). On the other hand, most specimens coming from Miocene deposits were assigned within the contemporary shape space of *Bombus* s. l., and for some of them within contemporary subgenera (i.e., *Cullumanobombus*, *Melanobombus*, and *Mendacibombus*), again a pattern consistent with more completely preserved bees from other Miocene deposits (e.g., Dominican, Mexican amber) (e.g., Engel et al. 2012). This pattern mirrors the hypothesis that there were significant changes in the bee fauna between Eocene and Oligocene epochs and again at the Paleogene-Neogene transition (e.g., Engel 2001, 2004, 2019a, b). Contemporary species of *Melanobombus* and *Mendacibombus* are restricted to the Old World. On the other hand, most species of *Cullumanobombus* (excluding *B. cullumanus*, *B. semenoviellus*, *B. unicus*) occur in the New World (Williams 1998; Williams et al. 2014). *Cullumanobombus* and *Melanobombus* are estimated to have originated between 20.0–15.0 Ma, while the basal subgenus *Mendacibombus* has been estimated to have originated around 34.0–30.0 Ma (Hines 2008). All fossils having affinities to extant subgenera have an age that is posterior to the stem age of subgenera (Hines 2008), and therefore our assignments are coincident with the estimated origin and divergence times of *Bombus* s. l. and extant subgenera (Hines 2008).

Other fossil specimens that were assigned to extant subgenera of *Bombus* s. l. are in accordance with the estimated stem age of those groups. In occurrence, our analyses are concordant with the ages of *Cullumanobombus* and *Melanobombus* (i.e., between 20.00–15.00 Ma), as well as *Mendacibombus* (i.e., between 34.0–30.0 Ma) (Hines 2008). These species highlight that Bombini had diversified significantly by the Miocene and that these limited fossil data are concordant with dating estimates. Continued paleontological exploration will only further refine our understanding based on direct evidence for dating bumble bee evolution.

Cenozoic extinctions of Corbiculata

Corbiculata are the most represented bees in the fossil record, especially in terms of number of specimens found in amber deposits, with workers of certain stingless bees (Meliponini) numbering into the tens of thousands of individuals (Michez et al. 2012; Engel and Michener 2013b; Engel pers. obs.). Corbiculata appeared in the Late Cre-

taceous based on the occurrence of a crown-group meliponine in Maastrichtian-aged Raritan amber (Michener and Grimaldi 1988; Engel 2000). This indicates that the divergence events among the tribes, at least among their stem groups, extend back to at least the latest Cretaceous. The three extinct tribes of corbiculate bees Electrapini, Electrobombini, and Melikertini are known from the Eocene (Baltic amber, Cambay amber, various impression fossil deposits such as Messel and Eckfeld), and some of these were assuredly advanced eusocial like Apini and Meliponini based on the presence of morphologically specialized workers (Engel 2001). Dehon et al. (2014) described a new corbiculate species, *Euglossopteryx biesmeijeri* De Meulemeester, Michez & Engel, 2014 discovered in the Parachute Creek Member of the Green River Formation (Utah, USA), and had phenetic similarities in wing shape to Euglossini, but it remains to be determined whether this was symplesiomorphic similarity or indicative of a cladistic relationship.

During the Paleocene-Eocene (the Paleocene-Eocene Thermal Maximum and Eocene Thermal Optimum), the concentration of greenhouse gases and the mean global temperature was higher than at present, with poles with little to no ice (Zachos et al. 2001; Royer 2006). The Early Eocene was marked by the EECO (Early Eocene Climatic Optimum) 51–53 million years ago, with a high pCO₂ and the global temperature reaching a long-term maximum. This was likely caused in part by differences in volcanic emissions, particularly high during parts of the Paleocene-Eocene periods (i.e., 40.0–60.0 Ma) (Walker et al. 1981). The PETM (Paleocene Eocene Thermal Maximum, i.e., 55.0 Ma) is the most prominent and best-studied hyperthermal episode, during which the global temperature increased by more than 5°C in less than 10,000 years (Zachos et al. 2001, 2008). A global cooling that most certainly caused the large-scale extinction of many plant and animal species marked the Eocene-Oligocene transition (i.e., 34.0 Ma) (Zachos et al. 2008; Hansen et al. 2013). Although still speculative at this time, it could be hypothesized that the latter event was related to the extinction of the group of Bombini to which *Calyptapis florissantensis* and *Oligobombus cuspidatus* might have belonged. Similarly, Dehon et al. (2014) suggested that *E. biesmeijeri* could also be consistent with the hypothesis that global climates, particularly cooling and drying events, were somehow related to the loss of corbiculate diversity (Engel 2001, 2002; Engel et al. 2013a), and that this was perhaps a global phenomenon impacting similar bee lineages in the New World (Dehon et al. 2014). It is noticeable that extant bumble bees appear especially sensitive to hyperthermal crises (Kerr et al. 2015; Rasmont et al. 2015). These climatic events resulted in significantly floral turnovers and these florist changes certainly could have influenced ancient lineages of bees (Collinson 1992). Those events of successive changes in temperature might have played a role in the appearance or extinction of species studied herein.

Acknowledgements

The first author is a grant holder of the funds of the University of Mons. For access to pertinent collections we are grateful to the curators and collection managers of the following museums: P.D. Perkins, Museum of Comparative Zoology (Cambridge,

MA, USA); J.G. Rozen, Jr. and C. Smith, American Museum of Natural History (New York, NY, USA); L. Packer, York University (Toronto, Canada); D. Notton, The Natural History Museum (London, UK); F. Bakker, Naturalis Biodiversity Center (Leiden, The Netherlands); J. Bortels, University of Liège (Gembloux, Belgium); E. De Coninck, Royal Museum of Central Africa (Tervuren, Belgium); W. Dekoninck, Royal Belgian Institute of Natural Sciences (Brussels, Belgium); S. Schmidt, Zoologische Staatssammlung München (Munich, Germany); F. Gusenleitner, Oberösterreichisches Landesmuseum (Linz, Austria); C. Praz, University of Neuchâtel (Neuchâtel, Switzerland); J. Litman, Muséum d'Histoire Naturelle de Neuchâtel (Neuchâtel, Switzerland). For additional assistance in the collections of the University of Kansas Natural History Museum (Lawrence, KS, USA) we are thankful to Z.H. Falin and J.C. Thomas. For providing us pictures of *B. beskonakensis* and *Paraelectrobombus patriciae* we are grateful to Gaëlle Doitteau (MNHN, Paris, France), photographs of *B. vetustus* were graciously provided by Prof. Alexandr P. Rasnitsyn (Russian Academy of Sciences, Moscow, Russia), while images of *B. pristinus* were provided courtesy of Dr Irene Zorn and Monika Brüggemann-Ledolter (Geologische Bundesanstalt, Vienna, Austria). This research was supported by the Belgian Science Policy (project BR/132/A1/BELBEES). Lastly, we thank C. Praz and an anonymous referee for reviewing the paper. This is a contribution of the Division of Entomology, University of Kansas Natural History Museum.

References

- Adams DC, Otárola-Castillo E (2013) Geomorph: An R package for the collection and analysis of geometric morphometric shape data. *Methods in Ecology and Evolution* 4: 393–399. <https://doi.org/10.1111/2041-210X.12035>
- Akhmetjev MA (1973) Sikhote-Alin Miocene flora (Botchi River). *Transactions of the Geological Institute of the Academy of Sciences of the USSR* 247: 1–124.
- Ansorge J, Kohring R (1995) Insekten aus dem Randecker Maar. *Fossilien* 2:80–90.
- Antropov AV, Belokobylskij SA, Compton SG, Dlussky GM, Khalaim AI, Kolyada VA, Kozlov MA, Perfilieva KS, Rasnitsyn AP (2014) The wasps, bees and ants (Insecta: Vespida = Hymenoptera) from the Insect Limestone (Late Eocene) of the Isle of Wight, UK. *Earth and Environmental Science Transactions of the Royal Society of Edinburgh* 104: 335–446. <https://doi.org/10.1017/S1755691014000103>
- Arillo A (2001) Presencia de la familia Pompilidae (Insecta, Hymenoptera) en el Mioceno superior de la Cuenca de la Cerdaña (Lleida, NE de España). *Coloquios de Paleontología* 52: 79–83.
- Armbruster L (1938) Versteinerte Honigbienen aus dem obermiocänen Randecker Maar. *Archiv für Bienenkunde* 19: 1–48.
- Aytekin AM, Terzo M, Rasmont P, Cagatay N (2007) Landmark based geometric morphometric analysis of wing shape in *Sibircobombus* Vogt (Hymenoptera: Apidae: *Bombus* Latreille). *Annales de la Société Entomologique de France* 43: 95–102. <https://doi.org/10.1080/00379271.2007.10697499>

- Bachmayer F, Symeonidis N, Theodoropoulos D (1971) Einige Insektenreste aus den Jungtertiären Süßwasserablagerungen von Kumi (Insel Euboea, Griechenland). *Annales Géologiques des Pays Helléniques* 23: 165–174.
- Barkan, NP, Aytekin AM (2013) Systematical studies on the species of the subgenus *Bombus* (*Thoracobombus*) (Hymenoptera: Apidae, *Bombus* Latreille) in Turkey. *Zootaxa* 3737: 167–183. <https://doi.org/10.11646/zootaxa.3737.2.5>
- Berry EW (1929) A revision of the flora of the Latah Formation. United States Geological Surveys Professional Paper 154: 225–265. <https://doi.org/10.3133/pp154H>
- Bookstein FL (1991) Morphometric tools for landmark data: geometry and biology. Cambridge University Press, Cambridge, 435 pp. <https://doi.org/10.1017/CBO9780511573064>
- Bossert S, Murray EA, Almeida EAB, Brady SG, Blaimer BB, Danforth BN (2019) Combining transcriptomes and ultraconserved elements to illuminate the phylogeny of Apidae. *Molecular Phylogenetics and Evolution* 130: 121–131. <https://doi.org/10.1016/j.ympev.2018.10.012>
- Boyle B, Meyer HW, Enquist B, Salas S (2008) Higher taxa as paleoecological and paleoclimatic indicators: A search for the modern analog of the Florissant fossil flora. In: Meyer HW, Smith DM (Eds) *Paleontology of the Upper Eocene Florissant Formation, Colorado*, Geological Society of America Special Paper, 435 pp. [https://doi.org/10.1130/2008.2435\(03\)](https://doi.org/10.1130/2008.2435(03))
- Brasero N, Martinet B, Lecocq T, Lhomme P, Biella P, Valterová I, Urbanová K, Cronalba M, Hines H, Rasmont P (2018) The cephalic labial gland secretions of two socially parasitic bumblebees *Bombus hyperboreus* (*Alpinobombus*) and *Bombus inexpectatus* (*Thoracobombus*) question their inquiline strategy. *Insect Science* 25: 75–86. <https://doi.org/10.1111/1744-7917.12408>
- Bůžek Č, Holý F, Kvaček Z (1996) Early Miocene flora of the Cypris Shale (western Bohemia). *Acta Musei Nationalis Pragae, Series B, Historia Naturalis* 52: 1–72.
- Cameron SA, Hines HM, Williams PH (2007) A comprehensive phylogeny of the bumblebees (*Bombus*). *Biological Journal of the Linnean Society* 91: 161–188. <https://doi.org/10.1111/j.1095-8312.2007.00784.x>
- Cardinal S, Packer L (2007) Phylogenetic analysis of the corbiculate Apinae based on morphology of the sting apparatus (Hymenoptera: Apidae). *Cladistics* 23: 99–118. <https://doi.org/10.1111/j.1096-0031.2006.00137.x>
- Claude J (2008) *Morphometrics with R*. Springer, New York, New York, USA, 317 pp.
- Cockerell TDA (1906) Fossil Hymenoptera from Florissant, Colorado. *Bulletin of the Museum of Comparative Zoology* 50: 33–58. <https://doi.org/10.2307/2478887>
- Cockerell TDA (1908) Descriptions and records of bees – XX. *Annals and Magazine of Natural History* 8: 323–334. <https://doi.org/10.1080/00222930808692489>
- Cockerell TDA (1931) II Hymenoptera and Hemiptera. Insects from the Miocene (Latah) of Washington. *Annals of the Entomological Society of America* 24: 307–322. <https://doi.org/10.1093/aesa/24.2.309>
- Collinson ME (1992) Vegetational and floristic changes around the Eocene/Oligocene boundary in western and central Europe. In: Prothero DR, Berggren WA (Eds) *Eocene-Oligocene climatic and biotic evolution*. Princeton University Press, Princeton, NJ, 437–450. <https://doi.org/10.1515/9781400862924.437>

- Dehon M, Michez D, Nel A, Engel MS, De Meulemeester T (2014) Wing shape of four new bee fossils (Hymenoptera: Anthophila) provides insights to bee evolution. *PLoS ONE* 9(10): e108865. <https://doi.org/10.1371/journal.pone.0108865>
- Dehon M, Perrard A, Engel MS, Nel A, Michez D (2017) Antiquity of cleptoparasitism among bees revealed by morphometric and phylogenetic analysis of a Paleocene fossil nomadine (Hymenoptera: Apidae). *Systematic Entomology* 42(3): 543–554. <https://doi.org/10.1111/syen.12230>
- De Meulemeester T, Michez D, Aytakin AM, Danforth BN (2012) Taxonomic affinity of halictid bee fossils (Hymenoptera: Anthophila) based on geometric morphometrics analyses of wing shape. *Journal of Systematic Palaeontology* 10(4): 755–764. <https://doi.org/10.1080/14772019.2011.628701>
- Derkey RE, Hamilton MM, Stradling DF (2003) Geologic Map of the Nine Mile Falls 7.5-minute Quadrangle, Spokane and Stevens Counties, Washington. Washington Division of Geology and Earth Resources Open File Report 2003-8.
- Dewulf A, De Meulemeester T, Dehon M, Engel MS, Michez D (2014) A new interpretation of the bee fossil *Melitta willardi* Cockerell (Hymenoptera, Melittidae) based on geometric morphometrics of the wing. *ZooKeys* 389: 35–48. <https://doi.org/10.3897/zookeys.389.7076>
- Diéguez C, Nieves-Aldrey J, Barrón E (1996) Fossil galls (zoocecid) from the Upper Miocene of La Cerdaña (Lérida, Spain). *Review of Palaeobotany Palynology* 94: 329–343. [https://doi.org/10.1016/S0034-6667\(96\)00004-8](https://doi.org/10.1016/S0034-6667(96)00004-8)
- Engel MS (2000) A new interpretation of the oldest fossil bee (Hymenoptera: Apidae). *American Museum Novitates* 3296: 1–11. [https://doi.org/10.1206/0003-0082\(2000\)3296%3C0001:ANIOTO%3E2.0.CO;2](https://doi.org/10.1206/0003-0082(2000)3296%3C0001:ANIOTO%3E2.0.CO;2)
- Engel MS (2001) A monograph of the Baltic amber bees and evolution of the Apoidea (Hymenoptera). *Bulletin of the American Museum of Natural History* 259: 1–192. [https://doi.org/10.1206/0003-0090\(2001\)259<0001:AMOTBA>2.0.CO;2](https://doi.org/10.1206/0003-0090(2001)259<0001:AMOTBA>2.0.CO;2)
- Engel MS (2004) Notes on a megachiline bee (Hymenoptera: Megachilidae) from the Miocene of Idaho. *Transactions of the Kansas Academy of Sciences* 107: 97–100. [https://doi.org/10.1660/0022-8443\(2004\)107\[0097:NOAMBH\]2.0.CO;2](https://doi.org/10.1660/0022-8443(2004)107[0097:NOAMBH]2.0.CO;2)
- Engel MS (2014) An orchid bee of the genus *Eulaema* in Early Miocene Mexican amber (Hymenoptera: Apidae). *Novitates Paleontologicae* 7: 1–15. <https://doi.org/10.17161/np.v0i7.4726>
- Engel MS (2019a) Die Entwicklungsgeschichte unserer Bienen. Teil I. *Lëtzebuurger Beien-Zeitung* 130(6): 198–204.
- Engel MS (2019b) Die Entwicklungsgeschichte unserer Bienen. Teil II. *Lëtzebuurger Beien-Zeitung* 130(8): 266–273.
- Engel MS, Breitzkreuz LCV (2013) A male of the bee genus *Agapostemon* in Dominican amber (Hymenoptera: Halictidae). *Journal of Melittology* 16: 1–9. <https://doi.org/10.17161/jom.v0i16.4572>
- Engel MS, Michener CD (2013a) A minute stingless bee in Eocene Fushan [sic] amber from northeastern China (Hymenoptera: Apidae). *Journal of Melittology* 14: 1–10. <https://doi.org/10.17161/jom.v0i14.4560>

- Engel MS, Michener CD (2013b) Geological history of the stingless bees (Apidae: Meliponini). In: Vit P, Roubik DW (Eds) *Stingless Bees Process Honey and Pollen in Cerumen Pots*, 1–7. Facultad de Farmacia y Bioanálisis, Universidad de Los Andes, Mérida, Venezuela, 170 pp.
- Engel MS, Rasmussen C (in press) Corbiculate bees. In: Starr CK (Ed.) *Encyclopedia of Social Insects*. Springer, Berlin.
- Engel MS, Grimaldi DA, Gonzalez VH, Hinojosa-Díaz IA, Michener CD (2012) An exomolopsine bee in Early Miocene amber from the Dominican Republic (Hymenoptera: Apidae). *American Museum Novitates* 3758: 1–16. <https://doi.org/10.1206/3758.2>
- Engel MS, Ortega-Blanco J, Nascimbene PC, Singh H (2013) The bees of Early Eocene Cambay amber (Hymenoptera: Apidae). *Journal of Melittology* 25: 1–12. <https://doi.org/10.17161/jom.v0i25.4659>
- Engel MS, Breitzkreuz LCV, Ohl M (2014) The first male of the extinct bee tribe Melikertini (Hymenoptera: Apidae). *Journal of Melittology* 30: 1–18. <https://doi.org/10.17161/jom.v0i30.4698>
- Engel MS, Wang B, Alqarni AS, Jia L-B, Su T, Zhou Z-K, Wappler T (2018) A primitive honey bee from the middle Miocene deposits of southeastern Yunnan, China (Hymenoptera, Apidae). *ZooKeys* 775: 117–129. <https://doi.org/10.3897/zookeys.775.24909>
- Epis RC, Chapin CE (1974) Stratigraphic nomenclature of the Thirty-nine Mile volcanic field, central Colorado. *U.S. Geological Survey Bulletin*, Washington 1395(c): 1–23.
- Evanoff E, McIntosh WC, Murphey PC (2001) Stratigraphic summary and $^{40}\text{Ar}/^{39}\text{Ar}$ geochronology of the Florissant Formation, Colorado. *Proceedings of the Denver Museum of Nature & Science Series* 4: 1–16.
- Francoy TM, Silva RAO, Nunes-Silva P, Menezes C, Imperatriz-Fonseca VL (2009) Gender identification of five genera of stingless bees (Apidae, Meliponini) based on wing morphology. *Genetics and molecular research* 8: 207–214. <https://doi.org/10.4238/vol8-1gmr557>
- Francoy TM, De Faria Franco F, Roubik DW (2012) Integrated landmark and outline-based morphometric methods efficiently distinguish species of *Euglossa* (Hymenoptera, Apidae, Euglossini). *Apidologie* 43: 609–617. <https://doi.org/10.1007/s13592-012-0132-2>
- Gérard M, Michez D, Fournier D, Maebe K, Smagghe G, Biesmeijer JC, De Meulemeester T (2015) Discrimination of haploid and diploid males of *Bombus terrestris* (Hymenoptera; Apidae) based on wing shape. *Apidologie* 46: 644–653. <https://doi.org/10.1007/s13592-015-0352-3>
- Gérard M, Michez D, Debat V, Fullgrabe L, Meeus I, Piot N, Sculfort O, Vastrade M, Smagghe G, Vanderplanck M (2018) Stressful conditions reveal decrease in size, modification of shape but relatively stable asymmetry in bumblebee wings. *Scientific Reports* 8: 15169. <https://doi.org/10.1038/s41598-018-33429-4>
- Goulson D (2010) *Bumblebees: Behaviour, Ecology, and Conservation*. Oxford University Press, Oxford, 317 pp.
- Gray J, Kittleman R (1967) Geochronometry of the Columbia River Basalt and associated floras of eastern Washington and western Idaho. *American Journal of Science* 26: 251–291. <https://doi.org/10.2475/ajs.265.4.257>
- Gregor HJ (1986) *Zur Flora des Randecker Maares (Miozän, Baden-Württemberg)*. *Stuttgarter Beiträge zur Naturkunde, Serie B (Geologie und Paläontologie)* 122: 1–24.

- Hansen J, Sato M, Russell G, Kharecha P (2013) Climate sensitivity, sea level and atmospheric carbon dioxide. *Philosophical Transactions of the Royal Society of London A* 371: 20120294. <https://doi.org/10.1098/rsta.2012.0294>
- Heinrich B (1979) *Bumblebee Economics*. Harvard University Press, Cambridge, Massachusetts, 288 pp.
- Heizmann EPJ (1983) Die Gattung *Cainotherium* (Cainotheriidae) im Orleanium und Astracium Süddeutschlands. *Eclogae Geologicae Helvetiae* 76: 781–825.
- Hines HM (2008) Historical biogeography, divergence times, and diversification patterns of bumblebees (Hymenoptera: Apidae: *Bombus*). *Systematic Biology* 57: 58–75. <https://doi.org/10.1080/10635150801898912>
- Hines HM, Cameron SA (2010) The phylogenetic position of the bumblebee inquiline *Bombus inexpectatus* and implications for the evolution of social parasitism. *Insectes Sociaux* 57: 379–383. <https://doi.org/10.1007/s00040-010-0094-1>
- Huberty CJ, Olejnik S (2006) *Applied MANOVA and discriminant analysis*. Second Edition, New Jersey, 488 pp. <https://doi.org/10.1002/047178947X>
- Ito M (1985) Supraspecific classification of bumblebees based on the characters of male genitalia. *Contributions from the Institute of Low Temperature Science, Series B* 20: 1–143.
- Jiménez-Moreno G, Fauquette S, Suc J-P (2010) Miocene to Pliocene vegetation reconstruction and climate estimates in the Iberian Peninsula from pollen data. *Review of Palaeobotany and Palynology* 162: 403–415. <https://doi.org/10.1016/j.revpalbo.2009.08.001>
- Kawakita A, Sota T, Ito M, Asher JS, Tanaka H, Kato M, Roubik DW (2004) Phylogeny, historical biogeography, and character evolution in bumble bees (*Bombus*: Apidae) based on simultaneous analysis of three nuclear gene sequences. *Molecular Phylogenetics and Evolution* 31: 799–804. <https://doi.org/10.1016/j.ympev.2003.12.003>
- Kennedy WJ, Reymont RA, Macleod N, Kriege J (2009) Species discrimination in the lower cretaceous (Albian) ammonite genus. *Palaeontographica, Abteilung A: Palaeozoologie – Stratigraphie* 290: 1–63. <https://doi.org/10.1127/pala/290/2009/1>
- Kerr JT, Pindar A, Galpern P, Packer L, Potts SG, Roberts SM, Rasmont R, Schweiger O, Colla SR, Richardson LL, Wagner DL, Gall LF, Sikes DS, Pantoja A (2015) Climate change impacts on bumblebees converge across continents. *Science* 349: 177–180. <https://doi.org/10.1126/science.aaa7031>
- Kirkham V, Melville M (1929) The Latah Formation. *The Journal of Geology* 37: 483–504. <https://doi.org/10.1086/623639>
- Knor S, Prokop J, Kávček Z, Janovský Z, Wappler T (2012) Plant–arthropod associations from the Early Miocene of the Most Basin in North Bohemia – Palaeoecological and palaeoclimatological implications. *Palaeogeography, Palaeoclimatology, Palaeoecology* 321–322: 102–112. <https://doi.org/10.1016/j.palaeo.2012.01.023>
- Köppen W, Geiger R (1928) *Klimakarte der Erde* [Wall Map 150 cm X 200 cm]. Verlag Justus Perthes, Gotha.
- Kottek M, Grieser J, Beck C, Rudolf B, Rubel F (2006) World map of the Köppen-Geiger climate classification updated. *Meteorologische Zeitschrift* 15: 259–263. <https://doi.org/10.1127/0941-2948/2006/0130>

- Kotthoff U (2005) Über einige Hymenoptera (Insecta) aus dem Unter-Miozän des Randecker Maars (Schwäbische Alb, Südwestdeutschland). Stuttgartar Beiträge zur Naturkunde, Serie B (Geologie und Paläontologie) 355: 1–25.
- Kotthoff U, Schmid U (2005) A new fossil hoverfly (Insecta, Diptera: Syrphidae) from the Randeck Maar (Early Miocene, southwest Germany). Palaeontology 48: 1091–1096. <https://doi.org/10.1111/j.1475-4983.2005.00500.x>
- Kotthoff U, Wappler T, Engel MS (2011) Miocene honey bees from the Randeck Maar of southwestern Germany (Hymenoptera, Apidae). ZooKeys 96: 11–37. <https://doi.org/10.3897/zookeys.96.752>
- Krautter M, Schweigert G (1991) Bemerkungen zur Sedimentation, Flora und dem Paläoklima des Randecker Maars (Unter-/Mittel-Miozän, Schwäbische Alb). Neues Jahrbuch für Geologie und Paläontologie, Monatshefte 1991: 505–514.
- Kvaček Z (1998) Bílina: a window on Early Miocene marshland environments. Review of Palaeobotany and Palynology 101: 111–113. [https://doi.org/10.1016/S0034-6667\(97\)00072-9](https://doi.org/10.1016/S0034-6667(97)00072-9)
- Kvaček Z, Böhme M, Dvořák Z, Konzalová M, Mach K, Prokop J, Rajchl M (2004) Early Miocene freshwater and swamp ecosystems of the Most Basin (northern Bohemia) with particular reference to the Bílina mine section. Journal of the Czech Geological Society 49: 1–40.
- Krzemiński W, Prokop J (2011) *Ptychoptera deleta* Novák, 1877 from the Early Miocene of the Czech Republic: redescription of the first fossil attributed to Ptychopteridae (Diptera). ZooKeys 130: 299–305. <https://doi.org/10.3897/zookeys.130.1401>
- Lewis S (1969) Fossil insects of the Latah Formation (Miocene) of Eastern Washington and Northern Idaho. Northwest Science 43: 99–115.
- Lutz H, Neuffer FO, Harms F-J, Schaal S, Micklich N, Gruber G, Schweigert G, Loren V (2000) Tertiäre Maare als Fossilagerstätten: Eckfeld, Messel, Randeck, Höwenegg, Öhning. Mainzer naturwissenschaftliches Archiv, Beiheft 24: 125–160.
- Michener CD (1990) Classification of the Apidae (Hymenoptera). University of Kansas Science Bulletin 54: 75–163.
- Michener CD (2007) The bees of the world, second edition. The Johns Hopkins University Press, Baltimore, 953 pp. [20 pls.]
- Michener CD, Grimaldi DA (1988) A Trigona from Late Cretaceous amber of New Jersey (Hymenoptera: Apidae: Meliponinae). American Museum Novitates 2917: 1–10.
- Michez D, Patiny S, Danforth BN (2009a) Phylogeny of the bee family Melittidae (Hymenoptera: Anthophila) based on combined molecular and morphological data. Systematic Entomology 34: 574–597. <https://doi.org/10.1111/j.1365-3113.2009.00479.x>
- Michez D, De Meulemeester T, Rasmont P, Nel A, Patiny S (2009b) New fossil evidence of the early diversification of bees: *Paleohabropoda oudardi* from the French Paleocene (Hymenoptera, Apidae, Anthophorini). Zoologica Scripta 38: 171–181. <https://doi.org/10.1111/j.1463-6409.2008.00362.x>
- Michez D, Vanderplanck M, Engel MS (2012) Fossil bees and their plant associates. In: Patiny S (Ed.) Evolution of Plant-Pollinator Relationships. Cambridge University Press, Cambridge, 103–164. <https://doi.org/10.1017/CBO9781139014113.006>
- Milliron HE (1961) Revised classification of the bumblebees – A synopsis. Journal of the Kansas Entomological Society 34: 49–61.

- Milliron HE (1971) A monograph of the western hemisphere bumblebees (Hymenoptera: Apidae; Bombinae). I. The genera *Bombus* and *Megabombus* subgenus *Bombias*. Memoirs of the Entomological Society of Canada 82: 1–80. <https://doi.org/10.4039/entm10382fv>
- Milliron HE (1973a) A monograph of the western hemisphere bumblebees (Hymenoptera: Apidae; Bombinae). II. The genus *Megabombus* subgenus *Megabombus*. Memoirs of the Entomological Society of Canada 89: 81–237. <https://doi.org/10.4039/entm10589fv>
- Milliron HE (1973b) A monograph of the western hemisphere bumblebees (Hymenoptera: Apidae; Bombinae). III. The genera *Pyrobombus* subgenus *Cullumanobombus*. Memoirs of the Entomological Society of Canada 91: 238–333.
- Mlíkovský J (1996) Tertiary avian localities of the Czech Republic. Acta Universitatis Carolinae Geologica 39: 551–557.
- Moure JS, Camargo JMF (1978) A fossil stingless bee from copal (Hymenoptera: Apidae). Journal of the Kansas Entomological Society 51(4): 560–566.
- Mustoe GE (2008) Mineralogy and geochemistry of late Eocene silicified wood from Florissant Fossil Beds National Monument, Colorado. In: Meyer HW, Smith DM (Eds) Paleontology of the Upper Eocene Florissant Formation, Colorado: Geological Society of America Special Paper 435: 127–140. [https://doi.org/10.1130/2008.2435\(09\)](https://doi.org/10.1130/2008.2435(09))
- Nel A, Petrulėvičius JF (2003) New Palaeogene bees from Europe and Asia. Alcheringa 27: 227–293. <https://doi.org/10.1080/03115510308619108>
- Nel A, Martínez-Delclòs X, Arillo A, Peñalver E (1999) The fossil *Apis* Linnaeus, 1758 (Hymenoptera, Apidae). Palaeontology 42: 243–285. <https://doi.org/10.1111/1475-4983.00073>
- Novák O (1878) Fauna der Cyprisschiefer des Egerer Tertiärbeckens. Sitzungsberichte der Mathematisch-Naturwissenschaftlichen Classe der Kaiserlichen Akademie der Wissenschaften 76: 71–96.
- Obrecht E, Scholl A (1981) Enzymelektrophoretische Untersuchungen zur Analyse der Verwandtschaftsgrade zwischen Hummel- und Schmarotzerhummelarten (Apidae, Bombini). Apidologie 12: 257–268. <https://doi.org/10.1051/apido:19810303>
- Owen RE (2012) Applications of morphometrics to the Hymenoptera, particularly bumblebees (*Bombus*, Apidae). In: Wahl C (Ed.) Morphometrics. IntechOpen, London, 1–30. <https://doi.org/10.5772/34745>
- Paichelier J-C, De Broin F, Gaudant J, Mourer-Chauvire C, Rage JC, Vergnaud-Grazzini C (1978) Le bassin lacustre de Bes-Konak (Anatolie, Turquie). Géologie et introduction à la paléontologie des vertébrés. Geobios 11: 43–65. [https://doi.org/10.1016/S0016-6995\(78\)80018-7](https://doi.org/10.1016/S0016-6995(78)80018-7)
- Pamilo P, Pekkarinen A, Varvio S-L (1987) Clustering of bumblebee subgenera based on interspecific genetic relationships (Hymenoptera, Apidae: *Bombus* and *Psithyrus*). Annales Zoologici Fennici 24: 19–27.
- Pekkarinen A (1979) Morphometric, colour and enzyme variation in bumblebees (Hymenoptera, Apidae, *Bombus*) in Fennoscandia and Denmark. ACTA Zoologica Fennica 158: 1–60.
- Pekkarinen A, Varvio-Aho SL, Pamilo P (1979) Evolutionary relationships in northern European *Bombus* and *Psithyrus* species (Hymenoptera: Apidae) studied on the basis of allozymes. Annales Entomologici Fennici 45: 77–80.

- Peñalver-Molla E, Martínez-Delclòs X, Arillo A (1999) Yacimientos con insectos fósiles en España. *Revista Española de Palaeontología* 14: 231–245.
- Perrard A, Baylac M, Carpenter JM, Villemant C (2014) Evolution of wing shape in hornets: why is the wing venation efficient for species identification? *Journal of Evolutionary Biology* 27: 2665–2675. <https://doi.org/10.1111/jeb.12523>
- Perrard A, Lopez-Osorio F, Carpenter JM (2016) Phylogeny, landmark analysis and the use of wing venation to study the evolution of social wasps (Hymenoptera: Vespidae: Vespinae). *Cladistics* 32: 406–425. <https://doi.org/10.1111/cla.12138>
- Petit D, Picaud F, Elghadraoui L (2006) Géométrie morphologique des ailes des Acrididae (Orthoptera : Caelifera) : sexe, stridulation, caractère. *Annales de la société entomologique de France* 42: 63–73. <https://doi.org/10.1080/00379271.2006.10697450>
- Plowright RC, Lavery TM (1987) Bumblebees and crop pollination in Ontario. *Proceedings of the Entomological Society of Ontario* 118: 155–160.
- Pouvreau A (1984) Biologie et écologie des bourdons. In: Pesson P, Louveaux J (Eds) *Pollinisation et Production Végétales*. INRA, Paris, 595–630.
- Pretorius E (2005) Using geometric morphometrics to investigate wing dimorphism in males and females of Hymenoptera – a case study based on the genus *Tachysphex* Kohl (Hymenoptera: Sphecidae: Larrinae). *Australian Journal of Entomology* 44: 113–121. <https://doi.org/10.1111/j.1440-6055.2005.00464.x>
- Prokop J, Nel A (2000) *Merlax bohemicus* gen. n., sp. n., a new fossil dragonfly from the Lower Miocene of northern Bohemia (Odonata: Aeshnidae). *European Journal of Entomology* 97: 427–431. <https://doi.org/10.14411/eje.2000.065>
- Prokop J, Fleck G, Nel A (2003) New dragonflies from the Lower Miocene (Ottomanian/Karpatian) of the Cyprius Shale in western Bohemia (Odonata: Libellulidae). *Neues Jahrbuch für Geologie und Paläontologie, Monatshefte* 2003: 561–576.
- Prokop J, Dehon M, Michez D, Engel MS (2017) An Early Miocene bumble bee from northern Bohemia (Hymenoptera, Apidae). *ZooKeys* 710: 43–63. <https://doi.org/10.3897/zookeys.710.14714>
- R Development Core Team (2013) *A language and environment for statistical computing, version 3.0.2*, ISBN 3-900051-07-0, R Foundation for Statistical Computing, Vienna, Austria.
- Rasmont P, Franzen M, Lecocq T, Harpke A, Roberts SPM, Biesmeijer K, Castro L, Cederberg B, Dvorak L, Fitzpatrick U, Gonseth Y, Haubruge E, Mahé G, Manino A, Michez D, Neumayer J, Odegaard F, Paukkunen J, Pawlikowski T, Potts SG, Reemer M, Settele J, Straka J, Schweiger O (2015) *Climatic Risk and Distribution Atlas of European Bumblebees*. Pensoft Publishers, Sofia, 246 pp. <https://doi.org/10.3897/biorisk.10.4749>
- Rasnitsyn AP, Michener CD (1991) Miocene fossil bumblebee from the Soviet far east with comments on the chronology and distribution of fossil bees (Hymenoptera: Apidae). *Annals of Entomological Society of America* 84: 583–589. <https://doi.org/10.1093/aesa/84.6.583>
- Robinson JD (1991) *Stratigraphy and sedimentology of the Latah Formation, Spokane County, Washington*. Master of Science thesis, Washington, Eastern Washington University.
- Rohlf FJ (1999) Shape statistics: Procrustes superimpositions and tangent spaces. *Journal of classification* 16: 197–223. <https://doi.org/10.1007/s003579900054>
- Rohlf FJ (2013a) tpsUTIL Version 1.56. Department of Ecology and Evolution, State University of New York at Stony Brook, New York.

- Rohlf FJ (2013b) tpsDIG Version 2.17. Department of Ecology and Evolution, State University of New York at Stony Brook, New York.
- Rohlf FJ (2013c) tpsSMALL Version 1.25. Department of Ecology and Evolution, State University of New York at Stony Brook, New York.
- Rohlf FJ, Slice D (1990) Extensions of the Procrustes method for the optimal superimposition of landmarks. *Systematic Zoology* 39: 40–59. <https://doi.org/10.2307/2992207>
- Rojík P (2004) New stratigraphic subdivision of the Tertiary in the Sokolov Basin. *Journal of the Czech Geological Society* 49: 173–185.
- Röseler P-F (1973) Die Anzahl der Spermien im Receptaculum seminis von Hummelköniginnen (Hym., Apoidea, Bombinae). *Apidologie* 4: 267–274. <https://doi.org/10.1051/apido:19730303>
- Royer DL (2006) CO₂-forced climate thresholds during the Phanerozoic. *Geochimica et Cosmochimica Acta* 70(23 SPEC. ISS.): 5665–5675. <https://doi.org/10.1016/j.gca.2005.11.031>
- Sadeghi S, Adriaens D, Dumont HJ (2009) Geometric morphometric analysis of wing shape variation in ten European populations of *Calopteryx splendens* (Haris, 1782) (Zygoptera: Odonata). *Odonatologica* 38(4): 343–360.
- Schawaller W (1986) Fossile Käfer aus miozäne Sedimenten des Randecker Maars in Südwestdeutschland (Insecta: Coleoptera). *Stuttgarter Beiträge zur Naturkunde, Serie B (Geologie und Paläontologie)* 126: 1–9.
- Schweigert G (1998) Das Randecker Maar – ein fossiler Kratersee am Albtrauf. *Stuttgarter Beiträge zur Naturkunde, Serie C (Wissen für Alle)* 43: 1–70.
- Skorikov AS (1923) Palaearctic bumblebees. Part I. General biology (including zoogeography). *Izvestiya Severnoi oblastnoi stantsii zashchity rastenii ot vreditelei* 4(1922): 1–160.
- Swisher CC, Prothero DR (1990) Single-crystal ⁴⁰Ar/³⁹Ar dating of the Eocene-Oligocene transition in North America. *Science* 249: 760–762. <https://doi.org/10.1126/science.249.4970.760>
- Tkalců B (1972) Arguments contre l'interprétation traditionnelle de la phylogénie des abeilles. *Bulletin de la Société Entomologique de Mulhouse* 1972: 17–28.
- Unger F (1867) Die Fossile Flora Von Kumi Auf Der Insel Euboea. *Denkschriften der Kaiserlichen Akademie der Wissenschaften in Wien, Mathematisch-Naturwissenschaftlichen Classe* 27: 27–90.
- Van Cann J, Virgilio M, Jordaens K, De Meyer M (2015) Wing morphometrics as a possible tool for the diagnosis of the *Ceratitis fasciventris*, *C. anonae*, *C. rosa* complex (Diptera, Tephritidae). *ZooKeys* 540: 489–506. <https://doi.org/10.3897/zookeys.540.9724>
- Veatch SW, Meyer HW (2008) History of paleontology at the Florissant fossil beds, Colorado. In: Meyer HW, Smith DM (Eds) *Paleontology of the Upper Eocene Florissant Formation, Colorado*. Geological Society of America Special Paper, 1–18. [https://doi.org/10.1130/2008.2435\(01\)](https://doi.org/10.1130/2008.2435(01))
- Velthuis HHW, Doorn A (2006) A century of advances in bumblebee domestication and the economic and environmental aspects of its commercialization for pollination. *Apidologie* 37: 421–451. <https://doi.org/10.1051/apido:2006019>
- Vogt O (1911) Studien über das Artproblem. 2. Mitteilung. Über das Variieren der Hummeln. 2. Teil (Schluss). *Schriften der berlinischen Gesellschaft Naturforschender, Freunde, Berlin* 1911: 31–74.

- Walker JCG, Hays PB, Kasting JFA (1981) A negative feedback mechanism for the longterm stabilization of Earth's surface-temperature. *Journal of Geophysical Research* 86: 9776–9782. <https://doi.org/10.1029/JC086iC10p09776>
- Wappler T, De Meulemeester T, Aytekin AM, Michez D, Engel MS (2012) Geometric morphometric analysis of a new Miocene bumble bee from the Randeck Maar of southwestern Germany (Hymenoptera: Apidae). *Systematic Entomology* 37(4): 784–792. [https://doi.org/10.1666/0022-3360\(2003\)077<0908:TMEBFO>2.0.CO;2](https://doi.org/10.1666/0022-3360(2003)077<0908:TMEBFO>2.0.CO;2)
- Wille A, Chandler L (1964) A new stingless bee from the Tertiary amber of the Dominican Republic (Hymenoptera; Meliponini). *Revista de Biología Tropical* 12: 187–195.
- Williams PH (1985) A preliminary cladistic investigation of relationships among the bumblebees (Hymenoptera, Apidae). *Systematic Entomology* 10: 239–255. <https://doi.org/10.1111/j.1365-3113.1985.tb00529.x>
- Williams PH (1998) An annotated checklist of bumblebees with an analysis of patterns of description (Hymenoptera: Apidae, Bombini). *Bulletin of The Natural History Museum (Entomology)* 67(1): 79–152.
- Williams PH (2007) The distribution of bumblebee colour patterns world-wide: possible significance for thermoregulation, crypsis and warming mimicry. *Biological Journal of the Linnean Society* 92: 97–118. <https://doi.org/10.1111/j.1095-8312.2007.00878.x>
- Williams PH, Cameron SA, Hines HM, Cederberg B, Rasmont P (2008) A simplified subgeneric classification of the bumblebees (genus *Bombus*). *Apidologie* 39: 46–74. <https://doi.org/10.1051/apido:2007052>
- Williams PH, Thorp RW, Richardson LL, Colla SR (2014) *Bumblebees of North America. An identification guide*. Princeton University Press, Princeton, New Jersey, 208 pp.
- Williams PH, Huang J, Rasmont P, An J (2016) Early-diverging bumblebees from across the roof of the world: the high-mountain subgenus *Mendacibombus* revised from species' gene coalescence and morphology (Hymenoptera, Apidae). *Zootaxa* 4204(1): 1–72. <https://doi.org/10.11646/zootaxa.4204.1.1>
- Williams PH, Lobo JM, Meseguer AS (2018) Bumblebees take the high road: climatically integrative biogeography shows that escape from Tibet, not Tibetan uplift, is associated with divergences of present-day *Mendacibombus*. *Ecography* 41: 461–477. <https://doi.org/10.1111/ecog.03074>
- Williams PH, Berezin MV, Cannings SG, Cederberg B, Odegaard F, Rasmussen C, Richardson LL, Rykken J, Sheffield CS, Thanosing C, Byvaltsev AM (2019) The arctic and alpine bumblebees of the subgenus *Alpinobombus* revised from integrative assessment of species gene coalescence and morphology (Hymenoptera, Apidae, *Bombus*). *Zootaxa* 4625: 1–68. <https://doi.org/10.11646/zootaxa.4625.1.1>
- Yang J, Wang Y-F, Spicer RA, Mosbrugger V, Li C-S, Sun Q-G (2007) Climatic reconstruction at the Miocene Shanwang Basin, China, using leaf margin analysis, CLAMP, coexistence approach, and overlapping distribution analysis. *American Journal of Botany* 94: 599–608. <https://doi.org/10.3732/ajb.94.4.599>
- Zachos J, Pagani M, Sloan L, Thomas E, Billups K (2001) Trends, rhythms, and aberrations in global climate 65 Ma to present. *Science* 292 (5517): 686–693. <https://doi.org/10.1126/science.1059412>

- Zachos JC, Dickens GR, Zeebe RE (2008) An early Cenozoic perspective on greenhouse warming and carbon-cycle dynamics. *Nature* 451: 279–283. <https://doi.org/10.1038/nature06588>
- Zeuner FE, Manning FJ (1976) A monograph on fossil bees (Hymenoptera: Apoidea). *Bulletin of the British Museum (Natural History), Geology* 27: 149–268.
- Zhang JF (1990) New fossil species of Apoidea (Insecta: Hymenoptera). *Acta Zootaxonomica Sinica* 15: 83–91.
- Zhang JF, Sun B, Zhang XY (1994) *Miocene Insects and Spiders from Shanwang, Shandong*. Science Press, Beijing, 298 pp.

Supplementary material 1

Table S1. First dataset for the geometric morphometric analyses

Authors: Manuel Dehon, Michael S. Engel, Maxence Gérard, A. Murat Aytekin, Guillaume Ghisbain, Paul H. Williams, Pierre Rasmont, Denis Michez

Data type: species data

Explanation note: This sampling includes 988 specimens from 233 species, 141 genera, 53 tribes, 19 subfamilies, and 7 families of Apoidea Anthophila. N1 = number of species. N2 = number of specimens.

Copyright notice: This dataset is made available under the Open Database License (<http://opendatacommons.org/licenses/odbl/1.0/>). The Open Database License (ODbL) is a license agreement intended to allow users to freely share, modify, and use this Dataset while maintaining this same freedom for others, provided that the original source and author(s) are credited.

Link: <https://doi.org/10.3897/zookeys.891.32056.suppl1>

Supplementary material 2

Table S2. Second dataset for the geometric morphometric analyses

Authors: Manuel Dehon, Michael S. Engel, Maxence Gérard, A. Murat Aytekin, Guillaume Ghisbain, Paul H. Williams, Pierre Rasmont, Denis Michez

Data type: species data

Explanation note: This sampling includes 973 specimens from 252 species, 19 genera, and five tribes of Apidae. N = number of specimens.

Copyright notice: This dataset is made available under the Open Database License (<http://opendatacommons.org/licenses/odbl/1.0/>). The Open Database License (ODbL) is a license agreement intended to allow users to freely share, modify, and use this Dataset while maintaining this same freedom for others, provided that the original source and author(s) are credited.

Link: <https://doi.org/10.3897/zookeys.891.32056.suppl2>

Supplementary material 3

Table S3. Specimen assignment in families using the cross-validation procedure in the LDA of forewing shape in first dataset

Authors: Manuel Dehon, Michael S. Engel, Maxence Gérard, A. Murat Aytekin, Guillaume Ghisbain, Paul H. Williams, Pierre Rasmont, Denis Michez

Data type: statistical data

Explanation note: Original groups are along the rows, predicted groups are along the columns. The hit ratio (HR%) is given for each family.

Copyright notice: This dataset is made available under the Open Database License (<http://opendatacommons.org/licenses/odbl/1.0/>). The Open Database License (ODbL) is a license agreement intended to allow users to freely share, modify, and use this Dataset while maintaining this same freedom for others, provided that the original source and author(s) are credited.

Link: <https://doi.org/10.3897/zookeys.891.32056.suppl3>

Supplementary material 4

Table S4. Specimen assignment in subfamilies using the cross-validation procedure in the LDA of forewing shape in first dataset

Authors: Manuel Dehon, Michael S. Engel, Maxence Gérard, A. Murat Aytekin, Guillaume Ghisbain, Paul H. Williams, Pierre Rasmont, Denis Michez

Data type: statistical data

Explanation note: Original groups are along the rows, predicted groups are along the columns. The hit ratio (HR%) is given for each subfamily.

Copyright notice: This dataset is made available under the Open Database License (<http://opendatacommons.org/licenses/odbl/1.0/>). The Open Database License (ODbL) is a license agreement intended to allow users to freely share, modify, and use this Dataset while maintaining this same freedom for others, provided that the original source and author(s) are credited.

Link: <https://doi.org/10.3897/zookeys.891.32056.suppl4>

Supplementary material 5

Table S5. Specimen assignment in tribes using the cross-validation procedure in the LDA of forewing shape in first dataset

Authors: Manuel Dehon, Michael S. Engel, Maxence Gérard, A. Murat Aytekin, Guillaume Ghisbain, Paul H. Williams, Pierre Rasmont, Denis Michez

Data type: statistical data

Explanation note: Original groups are along the rows, predicted groups are along the columns. The hit ratio (HR%) is given for each tribe.

Copyright notice: This dataset is made available under the Open Database License (<http://opendatacommons.org/licenses/odbl/1.0/>). The Open Database License (ODbL) is a license agreement intended to allow users to freely share, modify, and use this Dataset while maintaining this same freedom for others, provided that the original source and author(s) are credited.

Link: <https://doi.org/10.3897/zookeys.891.32056.suppl5>

Supplementary material 6

Table S6. Specimen assignment in tribes using the cross-validation procedure in the LDA of forewing shape in the second dataset

Authors: Manuel Dehon, Michael S. Engel, Maxence Gérard, A. Murat Aytekin, Guillaume Ghisbain, Paul H. Williams, Pierre Rasmont, Denis Michez

Data type: statistical data

Explanation note: Original groups are along the rows, predicted groups are along the columns. The hit ratio (HR%) is given for each tribe.

Copyright notice: This dataset is made available under the Open Database License (<http://opendatacommons.org/licenses/odbl/1.0/>). The Open Database License (ODbL) is a license agreement intended to allow users to freely share, modify, and use this Dataset while maintaining this same freedom for others, provided that the original source and author(s) are credited.

Link: <https://doi.org/10.3897/zookeys.891.32056.suppl6>

Supplementary material 7

Table S7. Specimen assignment in subgenera using the cross-validation procedure in the LDA of forewing shape in the third dataset

Authors: Manuel Dehon, Michael S. Engel, Maxence Gérard, A. Murat Aytekin, Guillaume Ghisbain, Paul H. Williams, Pierre Rasmont, Denis Michez

Data type: statistical data

Explanation note: Original groups are along the rows, predicted groups are along the columns. The hit ratio (HR%) is given for each subgenus.

Copyright notice: This dataset is made available under the Open Database License (<http://opendatacommons.org/licenses/odbl/1.0/>). The Open Database License (ODbL) is a license agreement intended to allow users to freely share, modify, and use this Dataset while maintaining this same freedom for others, provided that the original source and author(s) are credited.

Link: <https://doi.org/10.3897/zookeys.891.32056.suppl7>

Supplementary material 8

Table S8. Specimen assignment in subgenera using the cross-validation procedure in the LDA of forewing shape based on male wing shapes

Authors: Manuel Dehon, Michael S. Engel, Maxence Gérard, A. Murat Aytekin, Guillaume Ghisbain, Paul H. Williams, Pierre Rasmont, Denis Michez

Data type: statistical data

Explanation note: Original groups are along the rows, predicted groups are along the columns. The hit ratio (HR%) is given for each family.

Copyright notice: This dataset is made available under the Open Database License (<http://opendatacommons.org/licenses/odbl/1.0/>). The Open Database License (ODbL) is a license agreement intended to allow users to freely share, modify, and use this Dataset while maintaining this same freedom for others, provided that the original source and author(s) are credited.

Link: <https://doi.org/10.3897/zookeys.891.32056.suppl8>

Supplementary material 9

Table S9. Mahalanobis distances (MD) between family centroids and the 988 specimens, and the fossil and family centroids in the first dataset

Authors: Manuel Dehon, Michael S. Engel, Maxence Gérard, A. Murat Aytekin, Guillaume Ghisbain, Paul H. Williams, Pierre Rasmont, Denis Michez

Data type: statistical data

Copyright notice: This dataset is made available under the Open Database License (<http://opendatacommons.org/licenses/odbl/1.0/>). The Open Database License (ODbL) is a license agreement intended to allow users to freely share, modify, and use this Dataset while maintaining this same freedom for others, provided that the original source and author(s) are credited.

Link: <https://doi.org/10.3897/zookeys.891.32056.suppl9>

Supplementary material 10

Table S10. Mahalanobis distances (MD) between subfamily centroids and the 988 specimens, and the fossil and subfamily centroids in the first dataset

Authors: Manuel Dehon, Michael S. Engel, Maxence Gérard, A. Murat Aytekin, Guillaume Ghisbain, Paul H. Williams, Pierre Rasmont, Denis Michez

Data type: statistical data

Copyright notice: This dataset is made available under the Open Database License (<http://opendatacommons.org/licenses/odbl/1.0/>). The Open Database License (ODbL) is a license agreement intended to allow users to freely share, modify, and use this Dataset while maintaining this same freedom for others, provided that the original source and author(s) are credited.

Link: <https://doi.org/10.3897/zookeys.891.32056.suppl10>

Supplementary material 11

Table S11. Mahalanobis distances (MD) between tribe centroids and the 988 specimens, and the fossil and tribe centroids in the first dataset

Authors: Manuel Dehon, Michael S. Engel, Maxence Gérard, A. Murat Aytekin, Guillaume Ghisbain, Paul H. Williams, Pierre Rasmont, Denis Michez

Data type: statistical data

Copyright notice: This dataset is made available under the Open Database License (<http://opendatacommons.org/licenses/odbl/1.0/>). The Open Database License (ODbL) is a license agreement intended to allow users to freely share, modify, and use this Dataset while maintaining this same freedom for others, provided that the original source and author(s) are credited.

Link: <https://doi.org/10.3897/zookeys.891.32056.suppl11>

Supplementary material 12

Table S12. Mahalanobis distances (MD) between tribe centroids and the 973 specimens, and the fossil and tribe centroids in the second dataset

Authors: Manuel Dehon, Michael S. Engel, Maxence Gérard, A. Murat Aytekin, Guillaume Ghisbain, Paul H. Williams, Pierre Rasmont, Denis Michez

Data type: statistical data

Copyright notice: This dataset is made available under the Open Database License (<http://opendatacommons.org/licenses/odbl/1.0/>). The Open Database License (ODbL) is a license agreement intended to allow users to freely share, modify, and use this Dataset while maintaining this same freedom for others, provided that the original source and author(s) are credited.

Link: <https://doi.org/10.3897/zookeys.891.32056.suppl12>

Supplementary material 13

Table S13. Mahalanobis distances (MD) between subgenus centroids and the 841 specimens, and the fossils and subgenus centroids in the third dataset

Authors: Manuel Dehon, Michael S. Engel, Maxence Gérard, A. Murat Aytekin, Guillaume Ghisbain, Paul H. Williams, Pierre Rasmont, Denis Michez

Data type: statistical data

Copyright notice: This dataset is made available under the Open Database License (<http://opendatacommons.org/licenses/odbl/1.0/>). The Open Database License (ODbL) is a license agreement intended to allow users to freely share, modify, and use this Dataset while maintaining this same freedom for others, provided that the original source and author(s) are credited.

Link: <https://doi.org/10.3897/zookeys.891.32056.suppl13>

Taxonomic review of *Gasterophilus* (Oestridae, Gasterophilinae) of the world, with updated nomenclature, keys, biological notes, and distributions

Xin-Yu Li^{1,2}, Thomas Pape², Dong Zhang¹

1 School of Ecology and Nature Conservation, Beijing Forestry University, Qinghua east road 35, Beijing 10083, China **2** Natural History Museum of Denmark, University of Copenhagen, Universitetsparken 15, Copenhagen, Denmark

Corresponding author: Dong Zhang (ernest8445@163.com)

Academic editor: R. Meier | Received 6 August 2019 | Accepted 22 October 2019 | Published 21 November 2019

<http://zoobank.org/84BE68FC-AA9D-4357-9DA0-C81EEBA95E13>

Citation: Li X-Y, Pape T, Zhang D (2019) Taxonomic review of *Gasterophilus* (Oestridae, Gasterophilinae) of the world, with updated nomenclature, keys, biological notes, and distributions. ZooKeys 891: 119–156. <https://doi.org/10.3897/zookeys.891.38560>

Abstract

A taxonomic review of *Gasterophilus* is presented, with nine valid species, 51 synonyms and misspellings for the genus and the species, updated diagnoses, worldwide distributions, and a summary of biological information for all species. Identification keys for adults and eggs are elaborated, based on a series of new diagnostic features and supported by high resolution photographs for adults. The genus is shown to have its highest species richness in China and South Africa, with seven species recorded, followed by Mongolia, Senegal, and Ukraine, with six species recorded.

Keywords

biology, distribution, horse stomach bot fly, identification, nomenclature, taxonomy

Introduction

The oestrids or bot flies (Oestridae) are known as obligate parasites of mammals in their larval stage. They are often highly host specific, and the short-lived, non-feeding adult flies may show remarkable patterns of camouflage or mimicry (Zumpt 1965; Grunin

1965, 1966, 1969; Guimarães and Papavero 1999; Colwell et al. 2006). Species of *Gasterophilus* Leach (Diptera: Oestridae, Gasterophilinae) are commonly known as horse stomach bot flies (from Greek: *gaster* for stomach, *-philus* indicating love or fondness). They have adapted to a larval life in the alimentary tract of Equidae (Zumpt 1965; Grunin 1969; Colwell et al. 2006), and their presence can lead to serious injuries or even death of the host (Hall and Wall 1995; Sequeira et al. 2001; Colwell et al. 2006; Bezdekova et al. 2007; Getachew et al. 2012). Because of their great veterinary importance, *Gasterophilus* species have received considerable attention since the early 1800s (Clark 1815; Dove 1918; Patton 1937; Zumpt and Paterson 1953; James 1974; Otranto et al. 2005a, b; Colwell et al. 2006, 2007; Zhang et al. 2016; Liu et al. 2016; Huang et al. 2017; Li et al. 2018). A total of more than 40 species-group names have been proposed for what is here recognized as nine valid species because of extensive intraspecific variation (Zumpt 1965; Grunin 1969; Pont 1980; Soós and Minář 1986; Cogley 1991a), and a series of misidentifications can be ascribed to their similar larval morphology (Colwell et al. 2007; Li et al. 2018). Zumpt (1965) and Grunin (1969) provided the basis of *Gasterophilus* taxonomy, and further taxonomic studies have been successively published, such as the recognition of *G. lativentris* (Brauer) as a synonym of *G. pecorum* (Fabricius) (Cogley 1991b) and the resurrection of *G. flavipes* (Olivier) [from synonymy with *G. haemorrhoidalis* (Linnaeus)] as a valid species (Li et al. 2019). Consequently, an update of the taxonomy, biology and distribution of *Gasterophilus* species was in demand.

Gasterophilus species were restricted to the Palearctic and Afrotropical Regions, along with their equid hosts (Zumpt 1965; Leite et al. 1999), before becoming near cosmopolitan due to the association of several species with domestic hosts (Brauer 1863; Dove 1918; Zumpt 1965; Grunin 1969; Pont 1973; James 1974; Soós and Minář 1986; Wood 1987; Xue and Wang 1996; Colwell et al. 2006). Nonetheless, *G. meridionalis* (Pillers & Evans) and *G. ternicinctus* Gedoelst appear to be endemic to the Afrotropics, apparently exclusively associated with Burchell's zebra (*Equus quagga burchellii* Gray) (Zumpt 1965); and *G. nigricornis* (Loew) is only recorded from eastern Europe and Central Asia in the Palearctic Region (Zumpt 1965; Grunin 1969; Soós and Minář 1986; Xue and Wang 1996; Huang et al. 2017; Li et al. 2018). Records of *G. meridionalis* larvae in domestic horses from the Palearctic Region (i.e., Iran, Italy, and Turkey) (Özdal et al. 2010; Mashayekhi and Ashtari 2013; Pilo et al. 2015) are suspected to be misidentifications (Li et al. 2018).

The life history of *Gasterophilus* species has been extensively investigated (Clark 1815; Dove 1918; Hadwen and Cameron 1918; Zumpt 1965; Grunin 1969; Catts 1979; Cogley and Cogley 2000; Anderson 2006; Colwell et al. 2006). The adults are known to live only 3–5 days, hovering around the host for ovipositing or gathering at hilltop aggregation sites for mating (Catts 1979). Females lay eggs directly on the host, attaching their eggs to the hairs of the lips, chin, cheeks, or forelegs, depending on the species (Dove 1918; Hadwen and Cameron 1918; Anderson 2006; Colwell et al. 2006; Wood 2006). One exception is *G. pecorum*, which attaches eggs to the tips of grass blades (Zumpt 1965; Grunin 1969). Larvae hatch spontaneously within 5–8 days, or when they are stimulated by moisture and friction associated with host lick-

ing, feeding or grooming. First instar larvae quickly penetrate into the host around the hatching site and migrate subcutaneously to the hosts' mouth except for *G. nasalis*, which migrates on the mucosal surface to reach the inter-dental spaces (Zumpt 1965; Anderson 2006; Colwell et al. 2006). Each species of *Gasterophilus* has a specific site of penetration of the skin and route of migration to the stomach or intestine, where the second and third instar larval development is completed (Cogley et al. 1982; Colwell et al. 2006). It takes about 11 months for the larva to develop, with the third instar taking around 9–10 months in temperate climates. Mature larvae will be excreted with the feces and pupate in the soil (Zumpt 1965; Grunin 1969). The adults eclose after about 2–5 weeks and mate very soon after (Zumpt 1965; Anderson 2006).

Here, we take the opportunity to present an updated catalogue of all nine *Gasterophilus* species, including revised keys for eggs and adults, and updated diagnoses, host data, distributions, and original as well as major secondary literature for each species. This will be a help for entomologists, veterinarians, and other researchers with an interest in *Gasterophilus* to familiarize themselves more rapidly and more confidently in the taxonomy, biology, distribution, and literature on this group.

Materials and methods

Specimens

Label data provided under 'Material examined' are given in a standardized notation, with country names in capital letters and Chinese provinces in bold. Specimens studied or otherwise referred to are deposited in the following institutions:

IOZ	Institute of Zoology, Chinese Academy of Sciences, Beijing, China
KZNM	KwaZulu-Natal Museum, Pietermaritzburg, South Africa
MBFU	Beijing Forestry University, Beijing, China
MNHN	Museum national d'Histoire naturelle, Paris, France
NHMUK	Natural History Museum, London, United Kingdom
NHMD	Natural History Museum of Denmark, University of Copenhagen, Denmark
NHMW	Naturhistorisches Museum Wien, Austria
ZIN	Zoological Institute, Russian Academy of Sciences, St. Petersburg, Russia

Imaging and terminology

A Visionary Digital Imaging System, with a Canon EOS 7D camera (Canon, Inc., Tokyo, Japan) was used to take series of photographs at the Natural History Museum of Denmark. Superimposed photographs were stacked using the Zerene Stacker software and composed using Adobe Photoshop CS6 (Adobe Systems, Inc., San Jose, CA, U.S.A.) on a Windows 10 platform.

Photographs are provided for *G. intestinalis* (De Geer), *G. meridionalis*, *G. nasalis* (Linnaeus), *G. nigricornis*, *G. ternicinctus*, and *G. pecorum*. High resolution photographs of *G. flavipes*, *G. haemorrhoidalis* and *G. inermis* (Brauer) were recently provided by Li et al. (2019).

Morphological terminology follows Cumming and Wood (2009) for adults and Ferrar (1987) for eggs.

Distribution

A worldwide species diversity map was produced using the non-commercial version of StatPlanet (StatSilk 2018).

Format of catalog

Regional catalogues (Pont 1973, 1980; Soós and Minář 1986) are followed with regard to synonyms as the valid names for species of *Gasterophilus* are accepted throughout current literature and the synonymies appear stable. All original proposals of available and unavailable names and first occurrences of misspellings were checked and updated for information on type locality. Generic synonyms are given with author, year: page, type species and mode of designation. The most important taxonomic, morphological, biological, distributional and evolutionary studies of *Gasterophilus* are selected and listed chronologically.

Valid species are treated in alphabetic order, with the valid name given in bold followed by a list of all synonyms in their original generic combination with author, year and page plus type locality given in modern English (with an original quotation where considered relevant, e.g., France, Pyrenees, “Dans les Pyrénées”). Precise localities provided by early authors are cited as well [e.g. Democratic Republic of the Congo (as “Zaire”), 11.5 km W of Luapula river (as “6 milles W. du Luapula”)]. Synonyms are listed chronologically for each species, followed by all published misspellings known to us. Most important references about taxonomic, morphological, biological, distributional and evolutionary studies of species in *Gasterophilus* are selected and listed chronologically.

Host records and distribution are given based on information from specimens examined for the present study (directly or from photos) and data from Brauer (1863), Zumpt (1965), Guimarães (1967), Grunin (1969), Pont (1973), James (1974), Kaboret et al. (1986), Soós and Minář (1986), Pearse et al. (1989), Pandey et al. (1992), Escartin and Bautista (1993), Xue and Wang (1996), Güiris et al. (2010), Özdal et al. (2010), Tavassoli and Bakht (2012), Mashayekhi and Ashtari (2013), Pape (2013), Ganjali and Keighobadi (2016), Huang et al. (2016), Hoseini et al. (2017), Muller and Ranwashe (2017), Tähtinen and Lahti (2017), van Noort and Ranwashe (2017). Host data is listed alphabetically, with both common name and scientific name. Distribution is given with countries listed alphabetically in their respective biogeographical regions, i.e., Afrotropi-

cal, Australasian, Nearctic, Neotropical, Palearctic and Oriental Regions with boundaries as applied in Pape (1996). Further information, like Provinces or States, were given for countries with large continental area (i.e. Argentina, Australia, Brazil, Canada, Chile, China, United States of America), if applicable. Large islands (i.e., Corsica, Sardinia and Sicily) are listed together with their mainland countries. Non-vouchered literature records of *G. flavipes* obtained from Li et al. (2019) were retained with a question mark.

Biological information provided for eggs, larvae and adults is summarized and presented in Table 1.

The generic diagnosis is provided for adults, eggs and larvae, while species diagnoses are provided only for adults. Keys are modified from already existing keys and updated with more diagnostic characters for both adults and eggs. Comprehensive identification keys to first instar larvae were published by Grunin (1969) and Zumpt (1965), and to third instar larvae by Li et al. (2018).

Catalogue

Genus *Gasterophilus*

Figs 1–19; Table 1

Gasterophilus Leach, 1817: 2. Type species: *Oestrus equi* Clark, 1797 [= *Oestrus intestinalis* De Geer, 1776], by subsequent designation of Curtis (1826: 146).

Gastrus Meigen, 1824: 174. Type species: *Oestrus intestinalis* De Geer, 1776, by subsequent designation of Coquillett (1910: 546).

Gastrophilus Agassiz, 1846: 160. Unjustified emendation of *Gasterophilus* Leach, 1817. Type species: *Oestrus equi* Clark, 1797 [= *Oestrus intestinalis* De Geer, 1776] (automatic).

Enteromyza Rondani, 1857: 20. Unnecessary new replacement name for *Gastrus* Meigen, 1824 and *Gasterophilus* Leach, 1817. Type species: *Oestrus equi* Clark, 1797 [= *Oestrus intestinalis* De Geer, 1776] (automatic).

Rhinogastrophilus Townsend, 1918: 152. Type species: *Oestrus nasalis* Linnaeus, 1758, by original designation.

Enteromyia Enderlein, 1934: 425. Type species: *Oestrus haemorrhoidalis* Linnaeus, 1758, by original designation.

Stomachobia Enderlein, 1934: 425. Type species: *Oestrus pecorum* Fabricius, 1794, by original designation.

Haemorrhoestrus Townsend, 1934: 406. Type species: *Oestrus haemorrhoidalis* Linnaeus, 1758, by original designation.

Progastrophilus Townsend, 1934: 406. Type species: *Oestrus pecorum* Fabricius, 1794, by original designation.

Selected references. Brauer (1863: 53); Zumpt (1965: 111); Grunin (1969: 21); Pont (1973: 698); James (1974: 92); Kettle (1974); Papavero (1977: 19); Wood (1987:

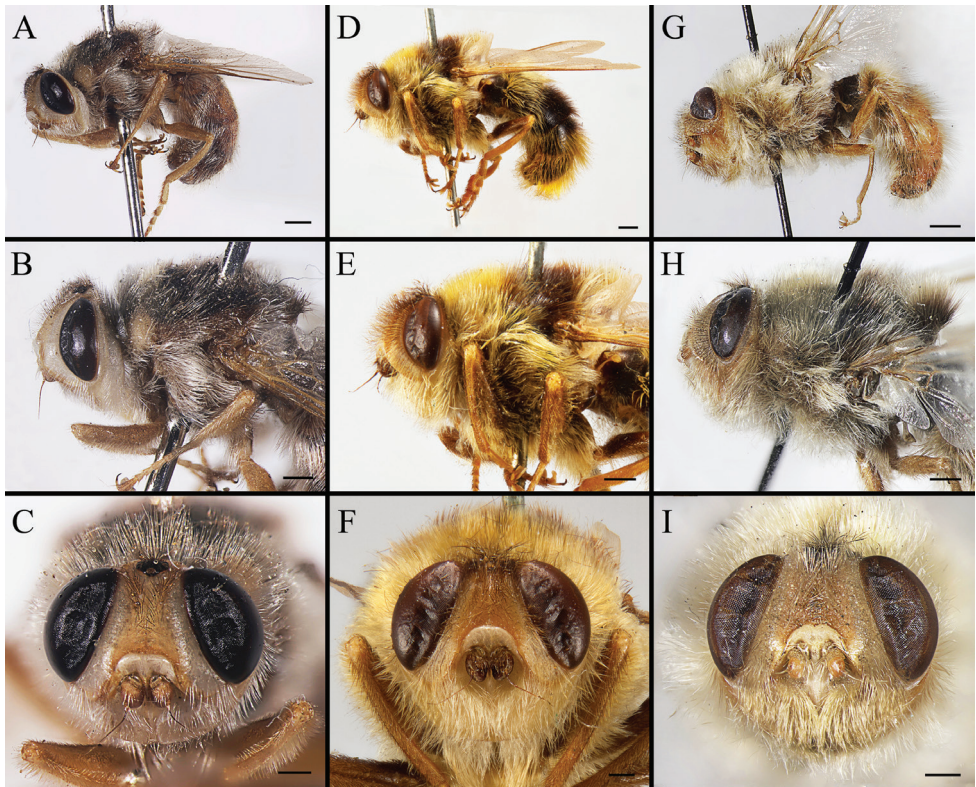


Figure 1. Left lateral view of habitus (**A, D, G**), head and thorax (**B, E, H**), and head in frontal view (**C, F, I**) of male *Gasterophilus* species, modified from Li et al. (2019) **A–C** *G. flavipes* (Olivier); Morocco (in IOZ) **D–F** *G. haemorrhoidalis* (Linnaeus); China (in MBFU) **G–I** *G. inermis* (Brauer); Germany (in NHMD). Scale bars: 1 mm (**A, D, G**); 0.5 mm (**B, C, E, F, H, I**).

1148); Soós and Minář (1986: 238); Xue and Wang (1996: 2209); Pape (2001); Pape et al. (2017); Otranto et al. (2005); Colwell et al. (2006: 5); Colwell et al. (2007); Felix et al. (2007); Zhang et al. (2012); Huang et al. (2016); Zhang et al. (2016); Li et al. (2018, 2019); Yan et al. (2019).

Diagnosis. Body covered with dense, yellowish hair-like setae, variously interrupted by reddish-yellow or dark brown (or black) bands (Figs 1–10). Facial plate with a narrow median keel. Antennal arista long, slender, gradually tapered and slightly flattened, with short, sparse microtrichia (Figs 1C, F, I, 2C, F, I, 3C, F, I, 7C, F, I, 8C, F, I, 9C, F, I). Proboscis and palpus vestigial, visible as small, yellow or brown knobs. Thorax ground color mainly dark brown or black (Figs 4–6, 7A, D, G, 8A, D, G, 9A, D, G). Notopleuron weakly defined. Posterior spiracle open, with short, hair-like fringes, lappets oriented obliquely at an angle of about 45 degrees. Wing vein M almost straight, very slightly curved posteriorly; vein $A_1 + CuA_2$ extending to wing margin (Fig. 10). Upper and lower calypters yellowish, fringed with long, whitish, hair-like setae along the external margin. Abdomen ground color yellow, dark brown

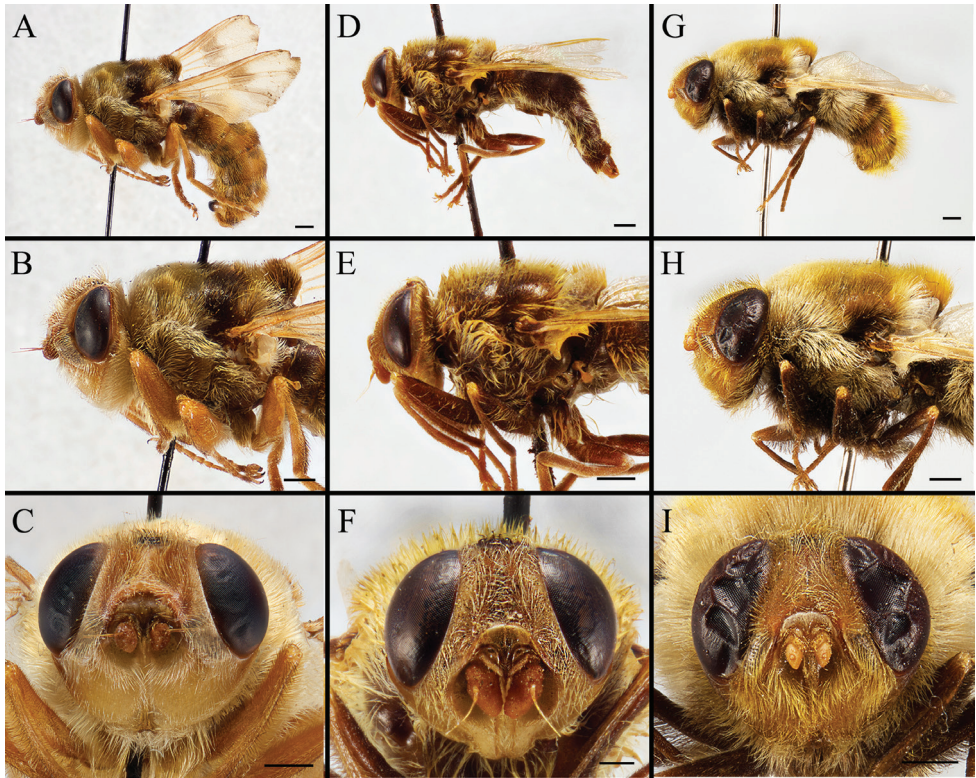


Figure 2. Left lateral view of habitus (**A, D, G**), head and thorax (**B, E, H**), and head in frontal view (**C, F, I**) of *Gasterophilus* species **A–C** Male *G. intestinalis* (De Geer) China (in MBFU) **D–F** Female *G. meridionalis* (Pillers & Evans); South Africa (in KZNM) **G–I** Male *G. nasalis* (Linnaeus) China (in MBFU). Scale bars: 1 mm (**A–E, I**); 0.5 mm (**F**).

or black, sometimes with several irregular dark spots (Figs 1A, D, G, 2A, D, G, 3A, D, G, 4A, C, E, 5A, C, E, 6A, C, E, 7A, B, D, E, 8A, B, D, E, 9A, B, D, E, G, H). Male cercus (Figs 11–13) broadly connected to its counterpart by a membrane at the base, with a long or short free apex (Figs 11C, F, I, 12C, F, 13C, F, I); surstylus with a rounded or gradually tapered apex (Figs 11B, E, H; 12B, E; 13B, E, H); phallus short, dorsolateral processes of distiphallus reduced, epiphallus absent; pregonite tuberculous; postgonite falcate (Figs 11A, D, G, 12A, D, 13A, D, G); processi longi (remnants of sternite 10) setose, tubercular or elongated (Patton 1937, Grunin 1969). Female terminalia (Figs 14–16) gradually tapered, either short and straight (Fig. 9E) or long and curved forward (Figs 7B, E, H, 8B, E, 9B, H); segment 7 modified, fully sclerotized, tube-shaped, dorsally with a longitudinal suture, without separation of tergite and sternite 7; tergite 8 laterally expanded downwards; sternite 8 either with a longitudinal concavity in the middle and with a keel-shaped apex (Fig. 16F), or longitudinally ridged in the middle and with a scallop-shaped apex (Figs 14C, F, L, 15C, F, L, 16C); tergite 10 (epiproct) composed of two approximately triangular sclerites

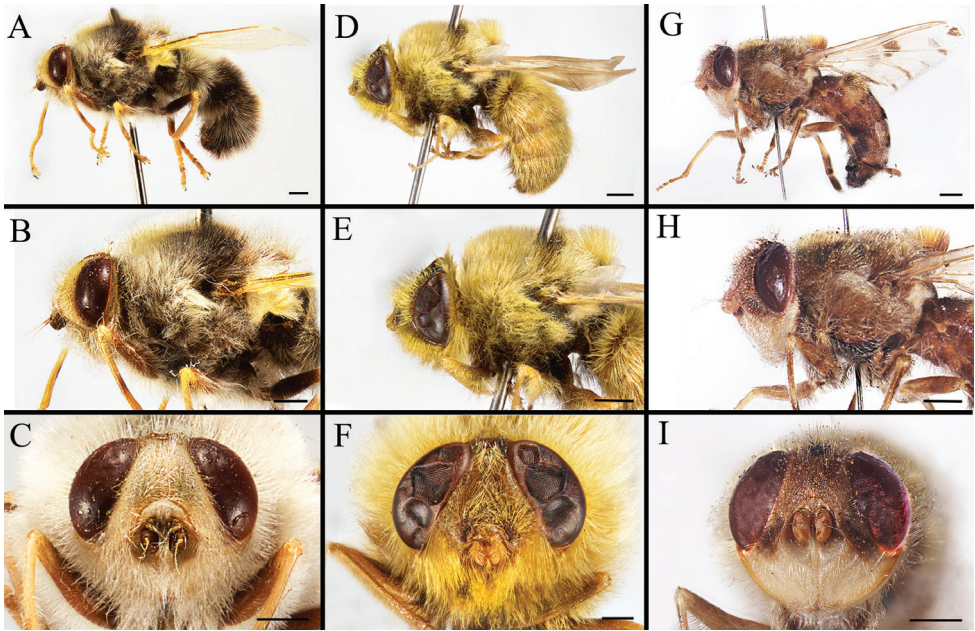


Figure 3. Left lateral view of habitus (**A, D, G**), head and thorax (**B, E, H**), and head in frontal view (**C, F, I**) of male *Gasterophilus* species **A–C** *G. nigricornis* (Loew); China (in MBFU) **D–F** *G. pecorum* (Fabricius); China (in MBFU) **G–I** *G. ternicinctus* Gedoelst; South Africa (in MBFU). Scale bars: 1 mm (**A–I**).

(Figs 14B, E, H, 15B, E, H, 16B, E); cercus long and narrow, narrowly connected to its counterpart by membrane and with a very short prolongation (Figs 14A, D, G, 15A, D, G, 16A, D). Eggs with an attachment organ, short and posteriorly located or elongated and situated ventrally (Figs 17–18). The larva with a bilobed, highly constricted pseudocephalon, three thoracic segments, seven abdominal segments, and the anal division divided into three subdivisions (Zumpt 1965; Grunin 1969; Li et al. 2018). The freshly hatched larva fusiform, anteriorly encircled with strong body spinose; posterior spiracles slightly or distinctly elongated, fully exposed, with two serrated margined slits (Zumpt 1965; Grunin 1969). The second and third instar larva sub-cylindrical, with mouth hooks posterolaterally curved and sharply pointed, and a pair of oral plates between mouth hooks; most of the body segments circled anteriorly by strong, posteriorly directed spines arranged in one, two or three rows (Zumpt 1965; Grunin 1969; Li et al. 2018). The third instar larva distinctively colored in red, yellow or green (Li et al. 2018).

Hosts. Known exclusively from the genus *Equus* Linnaeus (Perissodactyla: Equidae). So far, no records have been made from the species *E. grevyi* Oustalet (Grévy's zebra) and *E. kiang* Moorcroft (kiang or Tibetan wild ass).

Distribution and diversity. Native distribution matches that of the horse family, currently with highest diversity in China and South Africa, with 7 species recorded, followed by Mongolia, Senegal and Ukraine, with 6 species recorded (Fig. 19). Introduced with domestic hosts to most parts of the world.

Key to adults of *Gasterophilus* spp.

- 1 Wing with darkened patches (Fig. 10C, D, H, I) **2**
 – Wing entirely hyaline (Fig. 10A, B, E–G)..... **5**
- 2 Wing patches sharply demarcated (Fig. 10I); hind tibia and tarsus distinctly flattened (to a lesser degree in female), tarsomeres 2–4 shortened, as broad as long or broader than long (Figs 3D, 9G, H) ***Gasterophilus ternicinctus***
 – Wing patches with ill-defined edges (Figs 10C, D, H); hind tibia and tarsus unmodified, tarsomeres 2–4 long and narrow, distinctly longer than broad **3**
- 3 Antennal pedicel elongated, length/width ratio more than 0.8 (Figs 3E, 9F); facial plate setose; abdomen ground color yellow in male (Fig. 3D), mainly black in female (Fig. 9E); female terminalia short (Fig. 9E), abdominal sternite 8 with a keel-shaped apex (Fig. 16F) ***Gasterophilus pecorum***
 – Antennal pedicel short, length/width ratio less than 0.5; facial plate bare; abdomen ground color mainly yellow; female terminalia elongated, abdominal sternite 8 with a scallop-shaped apex (Figs 15C, F, I, 16C) **4**
- 4 Hind trochanter ventrally with a spatulate process in male or a tubercle in female (Grunin 1969: fig. 95); male surstylus yellow, with a black apex (Fig. 12A–C); female abdominal segment 7 longer than broad (Fig. 8B) ***Gasterophilus intestinalis***
 – Hind trochanter without a process or tubercle; male surstylus entirely yellow (Grunin 1969: fig. 86); female abdomen abdominal segment 7 broader than long (Fig. 7H) ***Gasterophilus inermis***
- 5 Crossvein dm-cu present; antennal postpedicel yellow or brownish; meral setae unmodified **6**
 – Crossvein dm-cu absent (Fig. 10G); antennal postpedicel red-brown to blackish (Figs 3C, 9C); meral setae with tip swollen ***Gasterophilus nigricornis***
- 6 Crossvein dm-cu distinct; antennal postpedicel globular **7**
 – Crossvein dm-cu extremely faint (Fig. 10E); antennal postpedicel long-oval (Fig. 2F) ***Gasterophilus meridionalis***
- 7 Distance between crossveins r-m and dm-cu at least twice as long as r-m; male cercus short and broad, length/width ratio equal to or less than 1.0, surstylus much longer than cercus **8**
 – Distance between crossveins r-m and dm-cu less than length of r-m (Fig. 10F); male cercus long and narrow, length/width ratio more than 3.0, surstylus and cercus of similar length (Fig. 12D–F) ***Gasterophilus nasalis***
- 8 Postsutural scutum with a light (yellowish), rectangular area near scutoscutellar suture (Fig. 4A); legs yellow; abdomen ground color yellow, covered with yellow setae (Figs 1A, 4A, 7A–B); male with surstylus gradually tapered proximally and distally, surstylar setae long, reaching the sagittal plane (Fig. 11A–C) ***Gasterophilus flavipes***
 – Postsutural scutum with ground color uniformly brown or black (Figs 4C, D, 7D); legs yellowish brown, with femora distinctly darkened; abdomen ground color dark brown or black, with reddish-yellow or orangish setae posteriorly (Figs 1D, 7E); male with surstylus abruptly tapered distally, surstylar setae short, reaching at most halfway to the sagittal plane (Fig. 11D–F) ***Gasterophilus haemorrhoidalis***

Key to eggs of *Gasterophilus* spp.

- 1 Posteriorly with an elongated pedicel (a continuation of the broad chorionic flanges) (Fig. 17A, B, E, F)..... **2**
- Posteriorly with a very short pedicel or without a pedicel (Figs 17I, J, M, N, 18A, B, E, F, I, J)..... **3**
- 2 Pedicel short and thick, with width/length ratio around 1/4 in lateral view, accounting for 1/3 of the total egg length (Fig. 16A–D) ***Gasterophilus flavipes***
- Pedicel long and slender, with width/length ratio around 1/6 in lateral view, accounting for 2/5 of the total egg length (Fig. 17E–H).....
..... ***Gasterophilus haemorrhoidalis***
- 3 Chorion brownish black, posteriorly with a short attachment organ, accounting for 1/6 of egg length (Fig. 18I–L) ***Gasterophilus pecorum***
- Chorion yellowish, ventrally with a long attachment organ, accounting for at least 1/2 of egg length **4**
- 4 Egg gradually tapered, anterior half distinctly broader than posterior half (Fig. 17M–P) ***Gasterophilus intestinalis***
- Egg fusiform, swollen in the middle, anteriorly and posteriorly tapered **5**
- 5 Attachment organ around half the length of the egg (Cogley 1991b: fig. 8)
..... ***Gasterophilus ternicinctus***
- Attachment organ almost the same length as the egg..... **6**
- 6 Operculum placed apically (parallel to the egg's cross section) (Fig. 18A)
..... ***Gasterophilus nasalis***
- Operculum placed sub-apically (distinctly angled relative to the egg's cross section) (Figs 17I, 18E) **7**
- 7 Micropylar position apical (on top surface) (Cogley 1991b: fig. 9).....
..... ***Gasterophilus meridionalis***
- Micropylar position sub-apical (on ventral surface) **8**
- 8 Operculum length/width ratio about 2.0 (Fig. 18E) ***Gasterophilus nigricornis***
- Operculum length/width ratio about 4.0 (Fig. 17I)..... ***Gasterophilus inermis***

***Gasterophilus flavipes* (Oliver, 1811)**

Figs 1A–C, 4A, B, 7A–C, 10A, 11A–C, 14A–C, 17A–D; Table 1

Oestrus flavipes Olivier, 1811: 467. Type locality: France, Pyrenees (“Dans les Pyrénées”).

Selected references. Brauer (1863: 80); Patton (1937); Li et al. (2019).

Diagnosis. Facial plate bare. Postsutural scutum of light color (yellowish), with rectangular area near scutoscuteellar suture. Wing completely hyaline. Distance between crossveins r-m and dm-cu at least twice as long as r-m. Meron with unmodified setae. Legs yellow; hind tarsus with long, strong and dense setae ventrolaterally. Abdomen ground color yellow. Male cercus short and broad, length/width ratio equal or less

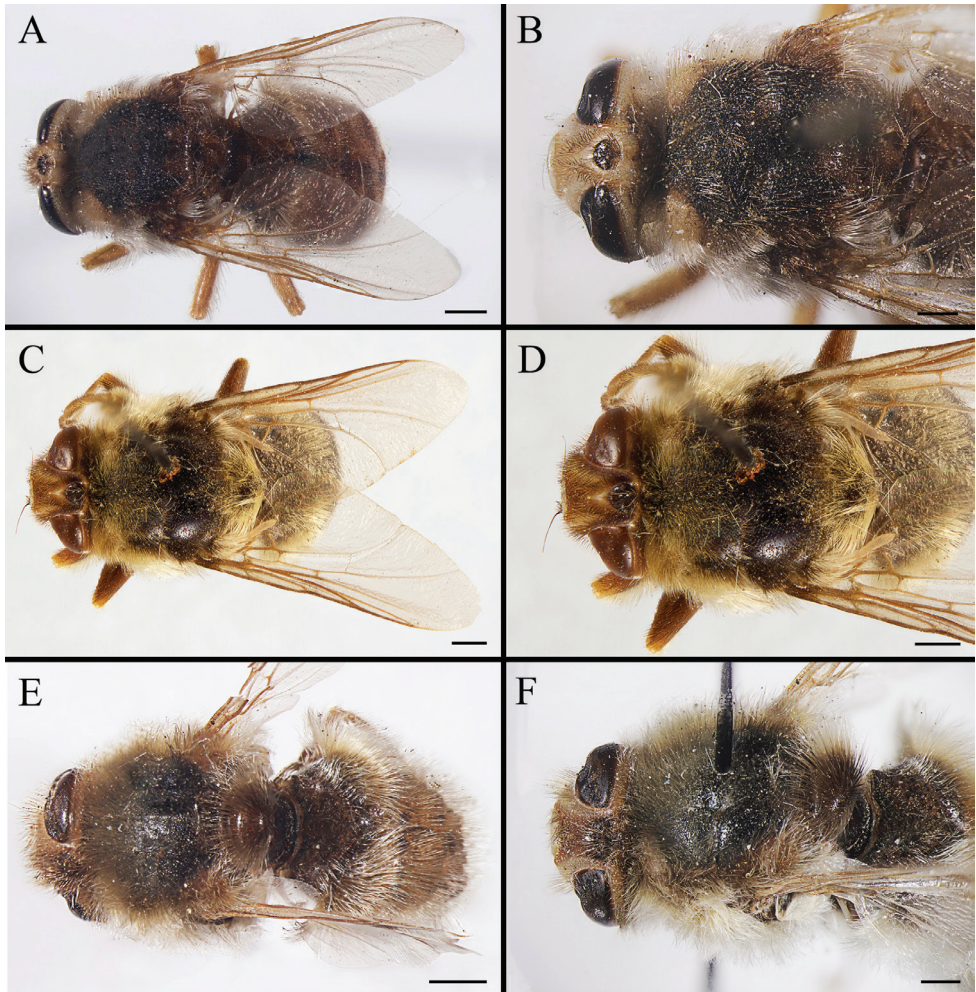


Figure 4. Dorsal view of habitus (**A, C, E**) and head and thorax (**B, D, F**) of male *Gasterophilus* species, modified from Li et al. (2019) **A, B** *G. flavipes* (Olivier) **C, D** *G. haemorrhoidalis* (Linnaeus) **E, F** *G. inermis* (Brauer). Scale bars: 1 mm (**A, C–D, E**); 0.5 mm (**B, F**).

than 1.0; surstylus yellow, gradually tapered proximally and distally, with a gradually tapered apex; surstylar setae long, reaching the sagittal plane; processus longi tubercular. Female sternite 8 longitudinally ridged in the middle and with a scallop-shaped apex.

Material examined. CHINA – Xinjiang Uyghur Autonomous Region • 10♂♂, 14♀♀; Kalamaili, Qiaomuxibai water reservoir; 45°13.8'N, 89°3.0'E (DDM); 1000 m; 26 Jun 2017; Y.Q. Ge & W.Y. Pei leg.; MBFU • 1♂, 1♀; same data as for preceding; NHMD. – Inner Mongolia • 1♂; Chifeng; 1 Jul. 1960, collector unknown; IOZ • 1♂; same collection locality as for preceding; 3 Jul. 1960; collector unknown; IOZ. CYPRUS • 1♂; no further data; NHMUK. MOROCCO • 1♂; no further data; 1897; G. Buchet leg.; MNHN • 1♂; Haute Moulouya; 1918; Thullet leg.; MNHN

Table 1. Natural history of *Gasterophilus* species.

Species	Embryonic development /days	Hatching strategy	First instar development	Second and third instar development	Pupal period /days	Host
<i>G. flavipes</i>	NA	NA	NA	NA	NA	· Domestic donkey (<i>Equus africanus asinus</i> Linnaeus) [speculated by Brauer (1863) without evidence].
<i>G. haemorrhoidalis</i>	2	Stimulated by moisture from licking or feeding of hosts.	· Penetrate epidermis of the lips of hosts and migrate into mouth.	· Second instar move to stomach and duodenum; · Third instar larvae become detached after some time and then pass to the rectum and re-attach themselves.	15–26	· Burchell's zebra (<i>E. quagga burchellii</i> Gray); · Domestic horse (<i>E. ferus caballus</i> Linnaeus) · Domestic donkey; · Mongolian wild ass (<i>E. hemionus hemionus</i> Pallas); · Mountain zebra [<i>E. zebra</i> Linnaeus]; × Wild horse (<i>E. przewalskii</i> Poliakov)
<i>G. inermis</i>	NA	Spontaneous.	· Penetrate skin of hosts at hatching site; · Migrate firstly under epidermis to the corner of mouth and then under the mucous membrane inside cheek.	· Second and third instar larvae found in the rectum.	21–26	· Burchell's zebra; · Domestic horse; · Mongolian wild ass; · Wild horse.
<i>G. intestinalis</i>	5	Stimulated by moisture and friction supplied by rubbing and licking of hosts.	· Penetrate hosts' dorsal mucosa of tongue; · Burrow from the anterior to posterior end; the migration route is almost parallel to the right or left lateral margin of tongue.	· Young second instar larvae attach to the pharynx and the sides of the epiglottis, and then pass to the stomach; · Third instar larvae are generally found clustered near the boundary of the nonglandular and glandular epithelia.	22–28	· Domestic donkey; · Domestic horse; · Mongolian wild ass; · Wild horse.
<i>G. meridionalis</i>	NA	NA	NA	· Attached to stomach mucosa.	28–31	· Burchell's zebra.
<i>G. nasalis</i>	5–10	Spontaneous.	· Migrate on surface to inter-dental spaces of hosts.	· Moults to second instar at inter-dental sites; · Migrate to duodenum and attach near pylorus.	16–24	· Burchell's zebra; · Domestic donkey; · Domestic horse; · Mongolian wild ass; · Wild horse.
<i>G. nigricornis</i>	3–9	Spontaneous.	· Penetrate hosts and migrate firstly under epidermis to the corner of mouth and then under the mucous membrane inside the cheek.	· Molt to the second stage in the central part of the cheek; · Migrate to duodenum, attach to mucosa and become encysted; · Third instar larvae leave the cyst and become attached superficially to the mucous membrane.	31–34	· Domestic donkey; · Domestic horse; · Mongolian wild ass; · Wild horse.

• 1♂; Moyen Atlas; Hun. 1949; L. Chopard leg.; MNHN • 1♀; LIBYA • Zuwarah; no further data; NHMUK • 1♂; SUDAN • Ed Dueim; 1937; collector unknown; NHMUK • 1♂; no further data; NHMUK.

Hosts. Donkey (*E. africanus asinus* Linnaeus) [speculated by Brauer (1863) without evidence].

Distribution. **Afrotropical** – Sudan. **Palaeartic** – China (Inner Mongolia, Xinjiang), Croatia?, Cyprus, Egypt?, France, Iran?, Kazakhstan?, Libya, Morocco, Spain?, Turkey?

Gasterophilus haemorrhoidalis (Linnaeus, 1758)

Figs 1D–F, 4C, D, 7D–F, 10B, 11D–F, 14D–F, 17E–H; Table 1

Oestrus haemorrhoidalis Linnaeus, 1758: 584 (as “hæmorrhoidalis”). Type locality: not given, probably Sweden, Germany, and France (through reference to *Fauna Svecica* and unspecified works by Johann Leonhard Frisch and Antoine Ferchault de Réaumur).

Oestrus salutiferus Clark, 1816: 3. Type locality: England.

Oestrus duodenalis Schwab, 1840: 35. Type locality: Europe. Proposed in synonymy with *Oestrus salutiferus* Clark, 1816, made available from subsequent use as a valid name for a taxon by Gistel (1848: 153).

Gastrophilus pallens Bigot, 1884: 4. Type locality: Sudan, Suakin (as “Suakim? Soudan oriental”).

Gasterophilus pseudohaemorrhoidalis Gedoelst, 1923: 272 (as “pseudo-hæmorrhoidalis”). Type locality: Eritrea, Asmara (as “Erythre: Asmara”); Republic of the Congo, Katanga Province, Biano (as “Katanga: Biano”) and Zambia (as “Zambi”).

Oestrus hemorrhoidalis Clark, 1815: 71; incorrect subsequent spelling of *haemorrhoidalis* Linnaeus, 1758.

Oestrus haemorrhoidales Clark, 1816: [1]; incorrect subsequent spelling of *haemorrhoidalis* Linnaeus, 1758.

Oestrus hemorroidalis Guérin-Méneville, 1827: 96; incorrect subsequent spelling of *haemorrhoidalis* Linnaeus, 1758.

Oestrus aemorrhoidalis Rondani, 1857: 21; incorrect subsequent spelling of *haemorrhoidalis* Linnaeus, 1758.

Selected references. Brauer (1863: 83); Zumpt (1965: 122); Grunin (1969: 40); Pont (1973: 698); James (1974: 97); Soós and Minář (1986: 238); Cogley (1991b); Xue and Wang (1996: 2209); Otranto et al. (2005); Colwell et al. (2006: 9); Colwell et al. (2007); Zhang et al. (2016); Li et al. (2018, 2019); Yan et al. (2019).

Diagnosis. Facial plate bare. Wing completely hyaline. Distance between cross-veins r-m and dm-cu at least twice as long as r-m. Meron with unmodified setae. Legs yellowish brown, with femora distinctly darkened; hind tarsus with long, strong and dense setae ventrolaterally. Abdomen ground color dark brown or black. Male cercus short and broad, length/width ratio equal or less than 1.0; surstylus yellow, with an abruptly swollen lobe near base and a rounded apex; surstylar setae short, reaching at

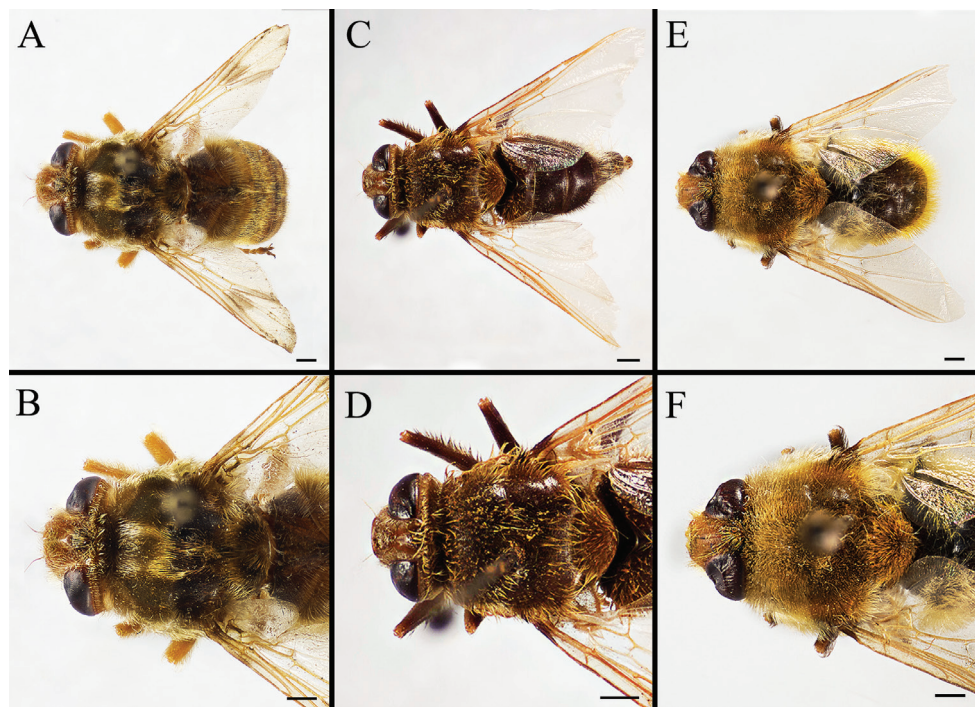


Figure 5. Dorsal view of habitus (**A, C, E**) and head and and thorax (**B, D, F**) of male *Gasterophilus* species **A, B** Male *G. intestinalis* (De Geer) **C, D** Female *G. meridionalis* (Pillers & Evans) **E, F** Male *G. nasalis* (Linnaeus). Scale bars: 1 mm (**A–F**).

most halfway to the sagittal plane; processus longi tubercular. Female sternite 8 longitudinally ridged in the middle and with a scallop-shaped apex.

Material examined. CHINA – **Inner Mongolia** • 20♂♂, 11♀♀; Chifeng, Zhaowuda League, Right Banner; 20 May–17 Sep. 1960; collector unknown; IOZ • 1♂; Ulanqab; Temurtei; 5 Jun. 1971; collector unknown; IOZ • 1♀; Xilingol League, Dongwu Banner; 24 Aug. 1971; collector unknown; IOZ. – **Heilongjiang Prov.** • 1♂; Anda; 26 Jul. 1965; collector unknown; IOZ • 1♀; Qiqihar; Fuyu County; 8 Aug. 1966; collector unknown; IOZ. – **Xinjiang Uyghur Autonomous Region** • 1♂; Wusu; 2000 m; 11 Jun. 1971; IOZ • 1♀; Kalamaili; 3 Apr. 2011; D. Zhang leg.; MBFU • 1♂; Kalamaili; 6 May 2011; D. Zhang leg.; MBFU.

Hosts. Burchell's zebra (*E. quagga burchellii*), domestic horse (*E. ferus caballus* Linnaeus), donkey (*E. africanus asinus*), Mongolian wild ass (*E. hemionus hemionus* Pallas), Mountain zebra (*E. zebra* Linnaeus), wild horse (*E. przewalskii* Poliakov).

Distribution. **Afrotropical** – Burkina Faso, Democratic Republic of the Congo, Eritrea, Ethiopia, Kenya, Namibia, Republic of the Congo, Senegal, South Africa, Sudan, Tanzania, Zambia. **Australasian** – Australia (New South Wales, Queensland, Victoria), Hawaii, New Zealand, Tasmania. **Nearctic** – Canada (Alberta, British Columbia, Manitoba, Saskatchewan), Mexico (no further data), USA (Colorado, Idaho, Illinois, Iowa, Kansas, Minnesota, Missouri, Montana, Nebraska, North Dakota, Or-

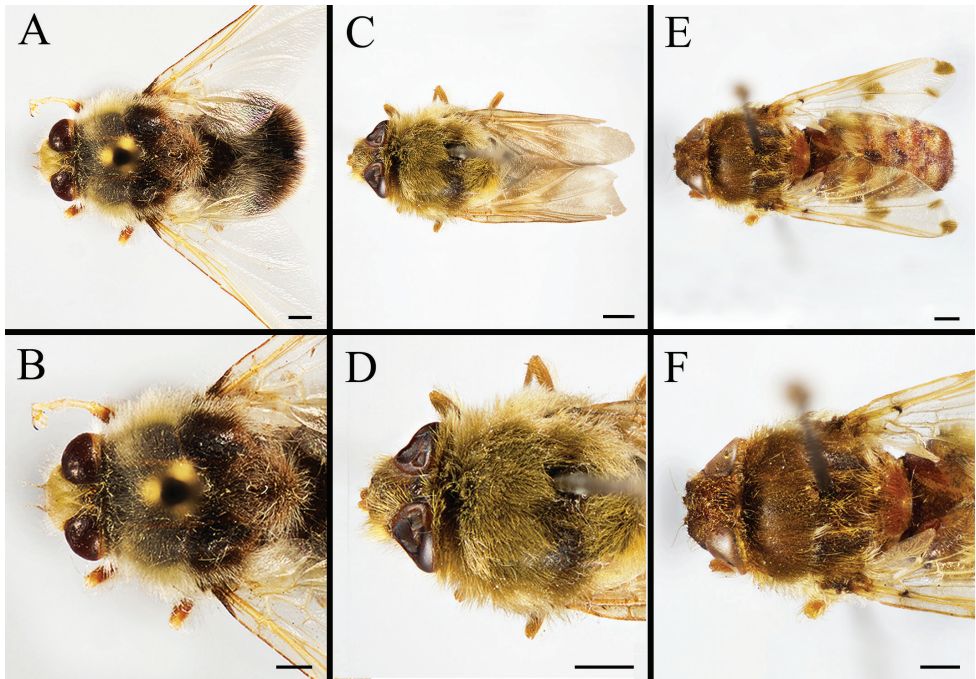


Figure 6. Dorsal view of habitus (A, C, E) and head and thorax (B, D, F) of male *Gasterophilus* species A, B *G. nigricornis* (Loew) C, D *G. pecorum* (Fabricius) E, F *G. ternicinctus* Gedoelst. Scale bars: 1 mm (A–F).

egon, South Dakota, Utah, Virginia, Washington, Wisconsin, Wyoming). **Neotropical** – Argentina (no further data), Venezuela. **Oriental** – India. **Palaeartic** – Austria, Azerbaijan, Belgium, Bulgaria, China (Heilongjiang, Inner Mongolia, Qinghai, Shaanxi, Tibet, Xinjiang), Czech Republic, Denmark, Finland, France (incl. Corsica), Germany, Hungary, Iran, Iraq, Italy, Kazakhstan, Kyrgyzstan, Lithuania, Malta, Mongolia, Morocco, Palestine, Poland, Romania, Russia (Tomsk, Transbaikal, Yakutsk, Yenisseisk), Slovak Republic, Sweden, Switzerland, Tajikistan, The Netherlands, Turkey, Turkmenistan, Ukraine, United Kingdom, Uzbekistan.

***Gasterophilus inermis* (Brauer, 1858)**

Figures 1G–I, 4E, F, 7G–I, 10C, 11G–I, 14G–I, 17I–L; Table 1

Gastrus inermis Brauer, 1858: 464. Type locality: Austria, Neusiedlersee, Jois (as “auf der Rosswiede bei Gyois am Neusiedlersee”).

Selected references. Brauer (1863: 73); Zumpt (1965: 124); Grunin (1969: 44); Soós and Minář (1986: 238); Cogley (1991b); Xue and Wang (1996: 2209); Otranto et al. (2005); Colwell et al. (2006: 36); Li et al. (2018, 2019); Yan et al. (2019).

Diagnosis. Facial plate bare. Wing partly infuscate, with darkened patches with ill-defined edges. Distance between crossveins r-m and dm-cu less than length of r-m.

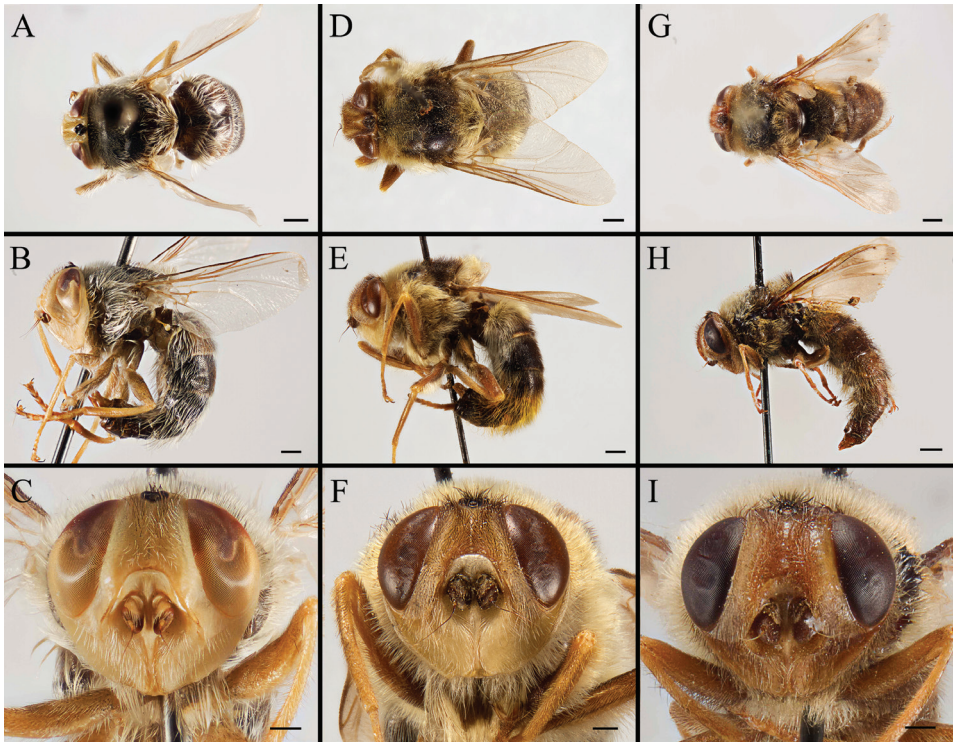


Figure 7. Dorsal view (**A, D, G**) and left lateral view (**B, E, H**) of habitus, and head in frontal view (**C, F, I**) of female *Gasterophilus* species, modified from Li et al. (2019) **A–C** *G. flavipes* (Olivier); China (in MBFU) **D–F** *G. haemorrhoidalis* (Linnaeus); China (in MBFU) **G–I** *G. inermis* (Brauer); Germany (in NHMD). Scale bars: 1 mm (**A, B, D, E, G, H**); 0.5 mm (**C, F, I**).

Merons bare. Legs yellowish brown, with femora distinctly darkened. Abdomen ground color yellow. Male cercus short and broad, length/width ratio equal or less than 1.0; surstylus yellow, with a rounded apex; processus longi tubercular. Female sternite 8 longitudinally ridged in the middle and with a scallop-shaped apex.

Type material examined. Syntypes of *Gastrus inermis* Brauer, 1858. AUSTRIA • 1♂, 1♀; no further data; NHMW [from photo].

Additional material examined. AUSTRIA • 1♀; no locality data; 31 Jul. 1986; Waldegg leg.; NHMW [from photo] • 1♂; 1892; no further data; NHMW [from photo]. ROMANIA • 1♂, 1♀; G. Dinulescu leg.; no further data; MNHN. GERMANY • 1♂, 1♀; 1918; Wüstnei leg.; no further data; NHMD. CHINA – **Inner Mongolia** • 1♂; Chifeng, Zhaowuda League, Right Banner; 16 Aug. 1969; collector unknown; IOZ • 1♀; locality as for preceding; 22 Aug. 1969; IOZ.

Hosts. Burchell's zebra (*E. quagga burchellii*), domestic horse (*E. ferus caballus*), Mongolian wild ass (*E. hemionus hemionus*), wild horse (*E. przewalskii*).

Distribution. **Afrotropical** – Senegal, South Africa. **Nearctic** – USA (Illinois). **Palearctic** – Austria, China (Inner Mongolia, Xinjiang), Germany, Hungary, Iran, Italy, Kazakhstan, Kyrgyzstan, Romania, Mongolia, Moldova, Slovak Republic, Tajikistan, Turkmenistan, Ukraine, Uzbekistan.

Remarks. Brauer (1858: 465) explicitly states that he examined “one pair” of adults that were hatched from puparia collected by the Austrian entomologist Alois Friedrich Rogenhofer in horse dung. 1♂, 1♀ in NHMW each carry two labels with the information “Oesterreich / Coll. Brauer” and “inermis / det Brauer”. A fragment of a puparium carries labels with “Gastrus / inermis / det Brauer” and “Coll. Brauer”. We consider the pair of adults to most probably represent original syntypes, but we are deliberately abstaining from designating a lectotype at this time.

***Gasterophilus intestinalis* (De Geer, 1776)**

Figs 2A–C, 5A, B, 8A–C, 10D, 12A–C, 15A–C, 17M–P; Table 1

Oestrus intestinalis De Geer, 1776: 292. Type locality: Sweden.

Oestrus equi Clark, 1797: 298. Junior primary homonym of *Oestrus equi* Fabricius, 1787. Type locality: England.

Oestrus gastricus major Schwab, 1840: 31. Unavailable name; proposed in synonymy with *Oestrus intestinalis* De Geer, 1776 and *Oestrus equi* Clark, 1797 and not made available from subsequent use as a valid name for a taxon before 1961.

Oestrus bengalensis Macquart, 1843: 182. Type locality: Bangladesh (as “Du Bengal”) and India.

Oestrus gastrophilus Gistel, 1848: 153 (as “*O. gastrophilus*, mihi. *O. Equi*. Linné.”). Type locality: not given, probably Germany.

Oestrus schwabianus Gistel, 1848: 153 (as “*Oestrus Schwabianus*, mihi. *O. gastric. major* Schwab”). Type locality: not given, probably Germany, Bavaria.

Gastrophilus equi var. *asininus* Brauer, 1863: 71. Type locality: Egypt and Sudan (“Egypten” & “Nubien”).

Gastrophilus aequi: Brauer 1863: 28; incorrect subsequent spelling of *equi* Clark, 1797.

Gasterophilus magnicornis Bezzi, 1916: 29. Type locality: Eritrea.

Selected references. Zumpt (1965: 125); Grunin (1969: 48); Pont (1973: 698); James (1974: 96); Kettle (1974); Soós and Minář (1986: 238); Cogley (1991b); Escartin and Bautista (1993); Xue and Wang (1996: 2210); Otranto et al. (2005); Colwell et al. (2006: 4); Colwell et al. (2007); Felix et al. (2007); Güiris et al. (2010); Ganjali and Keighobadi (2016); Zhang et al. (2016); Li et al. (2018); Yan et al. (2019).

Diagnosis. Facial plate bare. Wing partly infuscate, with darkened patches with ill-defined edges; crossvein dm-cu situated almost opposite of crossvein r-m. Meron with unmodified setae. Legs yellow, with more or less dark coloration on tarsus; hind trochanter with a spatulate process in male and a tubercle in female. Abdomen ground color yellow in both male and female. Male cercus elongated and broad, length-width ratio around 1.5; surstylus mainly yellow with black coloration apically, and a rounded apex; processus longi elongated. Female abdominal segment 7 distinctly longer than broad, sternite 8 longitudinally ridged in the middle and with a scallop-shaped apex.

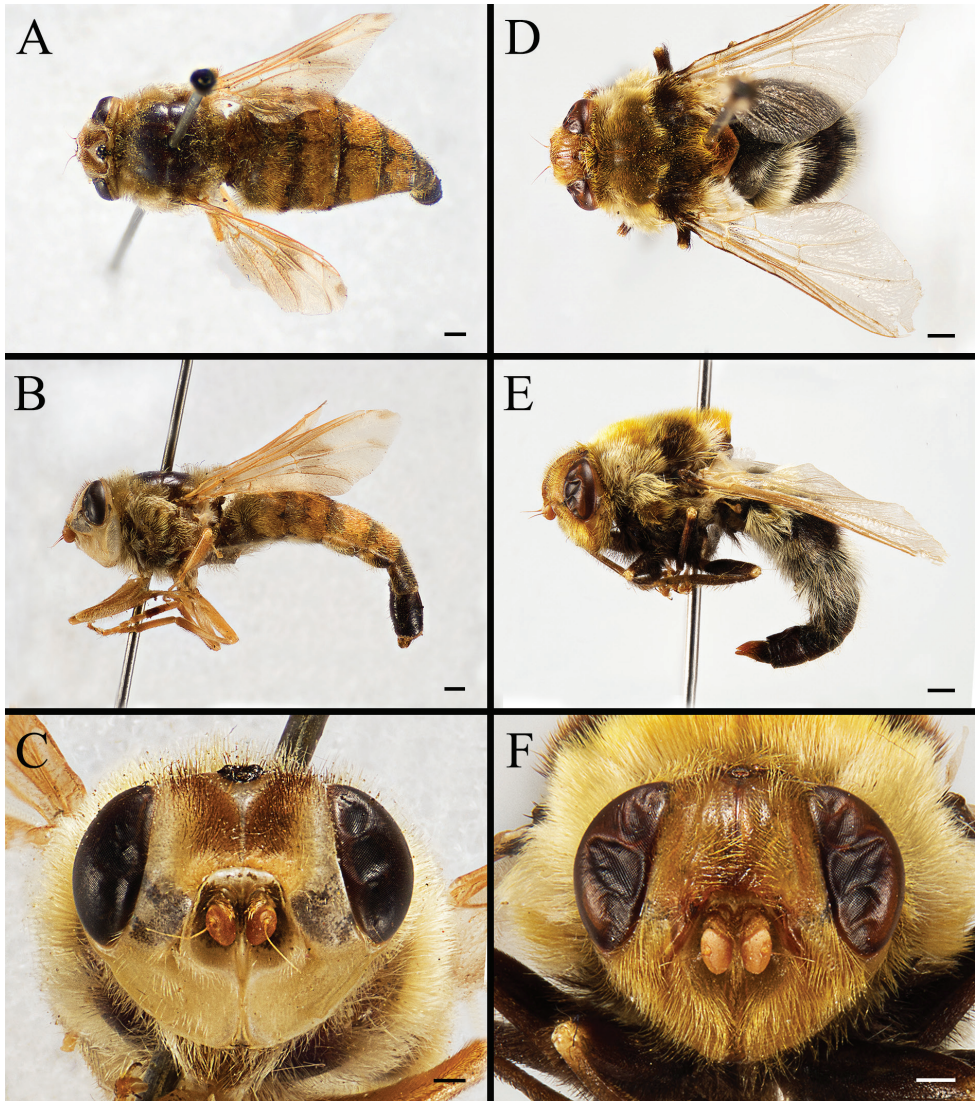


Figure 8. Dorsal view (**A, D, G**) and left lateral view (**B, E, H**) of habitus, and head in frontal view (**C, F, I**) of female *Gasterophilus* species **A–C** *G. intestinalis* (De Geer); China (in MBFU) **D–F** *G. nasalis* (Linnaeus); China (in MBFU). Scale bars: 1 mm (**A, B, D, E**); 0.5 mm (**C, F**).

Material examined. CHINA • – Inner Mongolia • 13♂♂, 26♀♀; Chifeng; Zhaowuda League, Right Banner; 13 Jun.–17 Sep. 1960; collector unknown; IOZ • 1♀; Hulunbeir; Genhe; 13 Aug. 1971; collector unknown; IOZ • 1♀; Hulunbeir; Yakeshi; 19 Aug. 1971; collector unknown; IOZ • 1♀; Hailaer; 23 Aug. 1971; collector unknown; IOZ • 1♀; Hulunbeir; Yakeshi; Boketu; 28 Aug 1971; collector unknown; IOZ • 1♀; Ulanqab; Temurtei; 29 Aug. 1971; collector unknown; IOZ • 7♂♂; Ulan-

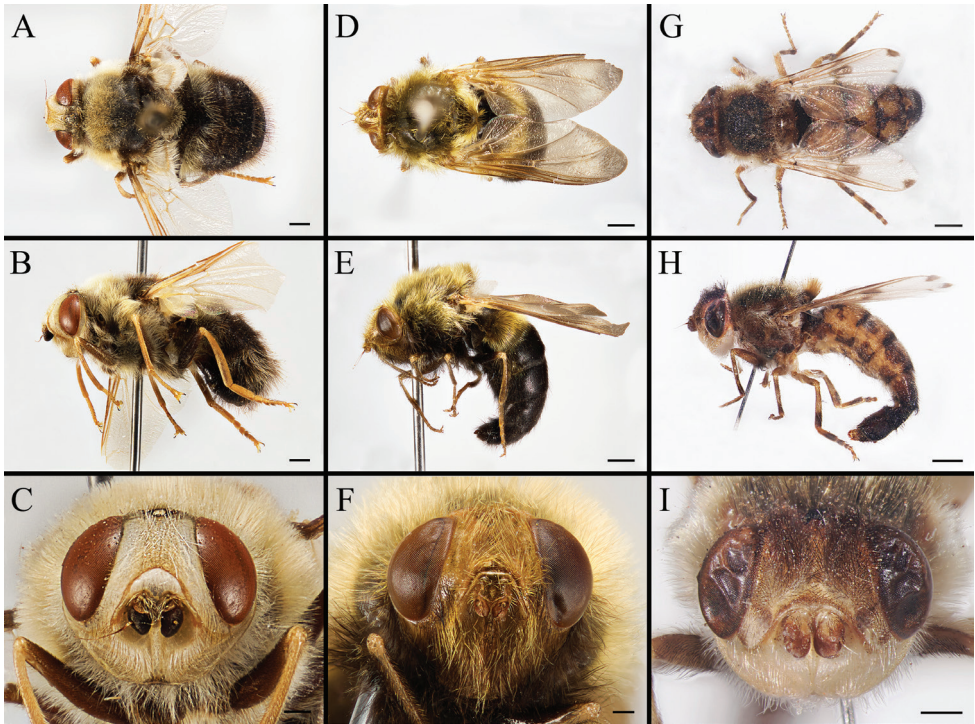


Figure 9. Dorsal view (**A, D, G**) and left lateral view (**B, E, H**) of habitus, and head in frontal view (**C, F, I**) of female *Gasterophilus* species **A–C** *G. nigricornis* (Loew); China (in MBFU) **D–F** *G. pecorum* (Fabricius); China (in MBFU) **G–I** *G. ternicinctus* Gedoelst; Kenya (in NHM). Scale bars: 1 mm (**A, B, D–E, G, H**); 0.5 mm (**C, F, I**).

qab; Temurtei; 29 Aug. 1971; collector unknown; IOZ • 2♀♀; Ulanqab, Temurtei; 30 Aug. 1971; collector unknown; IOZ. – **Heilongjiang Prov.** • 2♂♂, 2♀♀; Anda; 26–27 Aug. 1965; collector unknown; IOZ • 3♀♀; Qiqihar, Fuyu County; 15 Jun.–26 Aug. 1966; collector unknown; IOZ • 1♀; Daqing, Lamadian County; 15 Aug. 1969; collector unknown; IOZ • 1♀; locality as for preceding; 17 Sep. 1969; collector unknown; IOZ • 1♀; Qiqihar, Tailai County, Jiangning; 20 Jun. 1970; collector unknown; IOZ • 5♂♂, 1♀; Mudanjiang, Ning'an; 2 Sep. 1970; collector unknown; IOZ. – **Beijing** • 1♀; Yanqing County; 4 Aug. 1970; collector unknown; IOZ. – **Tibet Autonomous Region** • 1♂; Xinglin; 2550 m; 18 Aug. 1974; collector unknown; IOZ. – **Sichuan Prov.** • 1♀; Aba Autonomous Prefecture, Hongyuan County; 3700 m; 27 Aug. 1983; collector unknown; IOZ • 1♀; locality as for preceding; 3500 m; 28 Aug. 1983; collector unknown; IOZ • 1♂, 4♀♀; Ruergai County; 30 Aug.–1 Sep. 1983; collector unknown; IOZ. • 1♀; no further data; MNHN.

Hosts. Domestic horse (*E. ferus caballus*), donkey (*E. africanus asinus*), Mongolian wild ass (*E. hemionus hemionus*), wild horse (*E. przewalskii*).

Distribution. **Afrotropical** – Burkina Faso, Chad, Eritrea, Ethiopia, Ghana, Kenya, Morocco, Nigeria, Republic of the Congo, Senegal, South Africa, Sudan, Tanza-

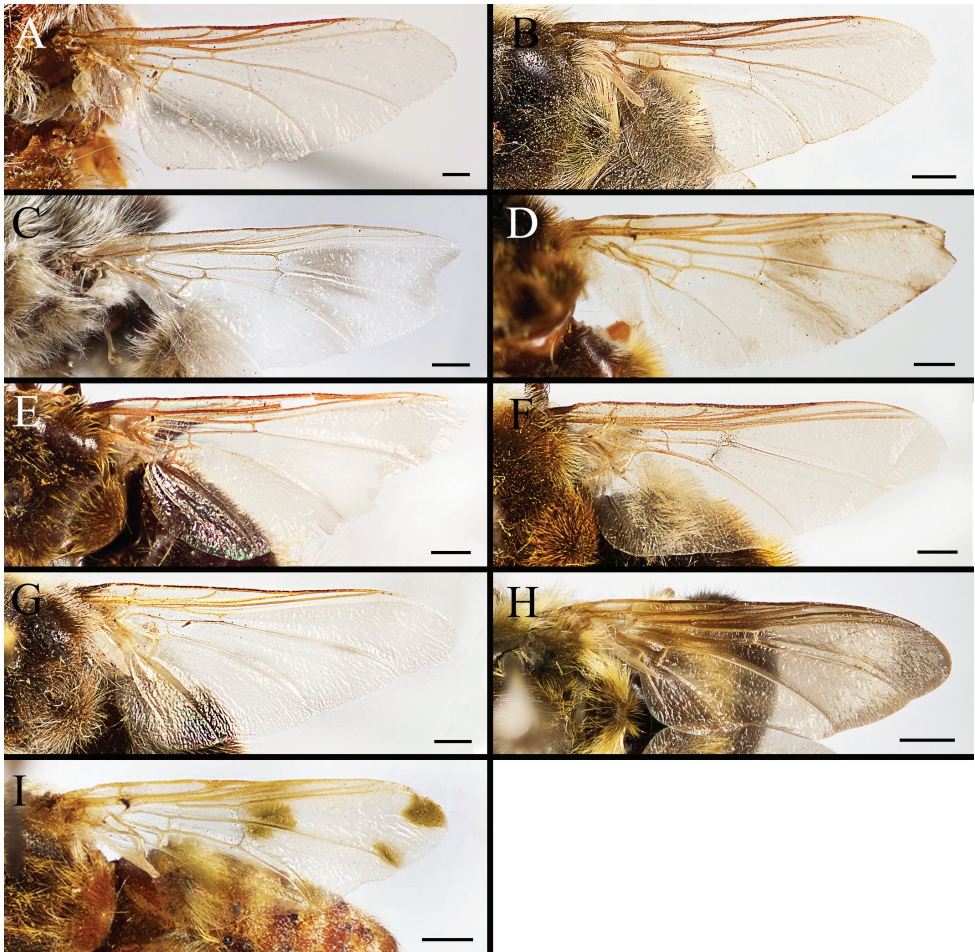


Figure 10. Wing of *Gasterophilus* species, with **A–C** modified from Li et al. (2019) **A** *G. flavipes* (Olivier) **B** *G. haemorrhoidalis* (Linnaeus) **C** *G. inermis* (Brauer) **D** *G. intestinalis* **E** *G. meridionalis* (Pillers & Evans) **F** *G. nasalis* (Linnaeus) **G** *G. nigricornis* (Loew) **H** *G. pecorum* (Fabricius) **I** *G. ternicinctus* Gedoelst. Scale bars: 0.5 mm (**A–C**); 1 mm (**D–I**).

nia. **Australasian** – Australia (New South Wales, Norfolk I, Tasmania), Hawaii, New Zealand. **Nearctic** – Canada (Alberta, British Columbia, Manitoba, New Brunswick, Ontario, Quebec, Saskatchewan), Mexico (Aguascalientes, Chiapas), USA (Arizona, California, Colorado, Connecticut, Idaho, Illinois, Iowa, Kansas, Maine, Maryland, Massachusetts, Michigan, Minnesota, Mississippi, Missouri, Montana, Nebraska, New Hampshire, New Jersey, New Mexico, New York, North Carolina, North Dakota, Ohio, Oklahoma, Oregon, South Dakota, Texas, Utah, Vermont, Virginia, Washington, Wisconsin, Wyoming). **Neotropical** – Argentina (no further data), Brazil (Rio Grande do Sul), Chile (Bío Bío Region), Jamaica, Venezuela. **Oriental** – India. **Palearctic** – Bangladesh, Belgium, China (Beijing, Gansu, Heilongjiang, Inner Mongolia, Qinghai, Shanxi, Shaanxi, Sichuan, Tibet, Xinjiang, Yunnan), Czech

Republic, Denmark, Egypt, Finland, France (incl. Corsica), Germany, Hungary, Ireland, Iran, Italy (incl. Sicily), Jordan, Lithuania, Mongolia, Norway, Pakistan, Poland, Romania, Slovak Republic, Sweden, Switzerland, The Netherlands, Turkey, Ukraine, United Kingdom.

***Gasterophilus meridionalis* (Pillers & Evans, 1926)**

Figs 2D–F, 5C, D, 11E, 15D–F; Table 1

Oestrus meridionalis Pillers & Evans, 1926: 264. Type locality: Zimbabwe (as “Rhodesia”).

Selected references. Zumpt (1965: 121); Cogley (1991b); Colwell et al. (2006: 36); Colwell et al. (2007: 256).

Diagnosis. Male unknown. Antennal postpedicel long-oval. Facial plate setose. Wing completely hyaline. Crossvein dm-cu extremely weak, with only a faint trace; distance between crossveins r-m and dm-cu equal or less than length of r-m. Meron with unmodified setae. Legs black or black-brown. Abdomen ground color dark brown. Female sternite 8 longitudinally ridged in the middle and with a scallop-shaped apex.

Material examined. SOUTH AFRICA • 2♀♀; Transvaal; Newington; 15 Aug. 1957; reared from third instar larvae by F. Zumpt; KZNM.

Hosts. Burchell’s zebra (*E. quagga burchellii*).

Distribution. Afrotropical – Botswana, Democratic Republic of the Congo, Mozambique, Namibia, Republic of the Congo, South Africa, Tanzania, Zambia, Zimbabwe.

***Gasterophilus nasalis* (Linnaeus, 1758)**

Figs 2G–I, 5E, F, 8D–F, 10F, 11F, 12D–F, 15G–I; Table 1

Oestrus nasalis Linnaeus, 1758: 584. Type locality: Sweden (through reference to *Fauna Svecica*).

Oestrus equi Fabricius, 1787: 321. Type locality: not given, probably Europe.

Oestrus veterinus Clark, 1797: 312. New replacement name for *Oestrus nasalis* Linnaeus, 1758 [“I have given it the name of *veterinus* in preference to the erroneous one of *nasalis*” (p. 313)].

Oestrus salutaris Clark, 1815: pl. 1. Nomen nudum.

Gasterophilus clarkii Leach, 1817: 2. Type locality: England, Bantham close to Kingsbridge (as “Habitat in Anglia Occidentali. Apud Bantham prope Kingsbridge a meipso captus”).

Gastrus jumentarum Meigen, 1824: 179. Type locality: not given, probably Denmark (as “Ein Weibchen in dem Koppenhagener Königl. Museum”).

Oestrus gastricus minor Schwab, 1840: 40. Unavailable name proposed in synonymy with *Oestrus nasalis* Linnaeus, 1758 and *Oestrus veterinus* Clark, 1797 and not made available from subsequent use as a valid name for a taxon before 1961.

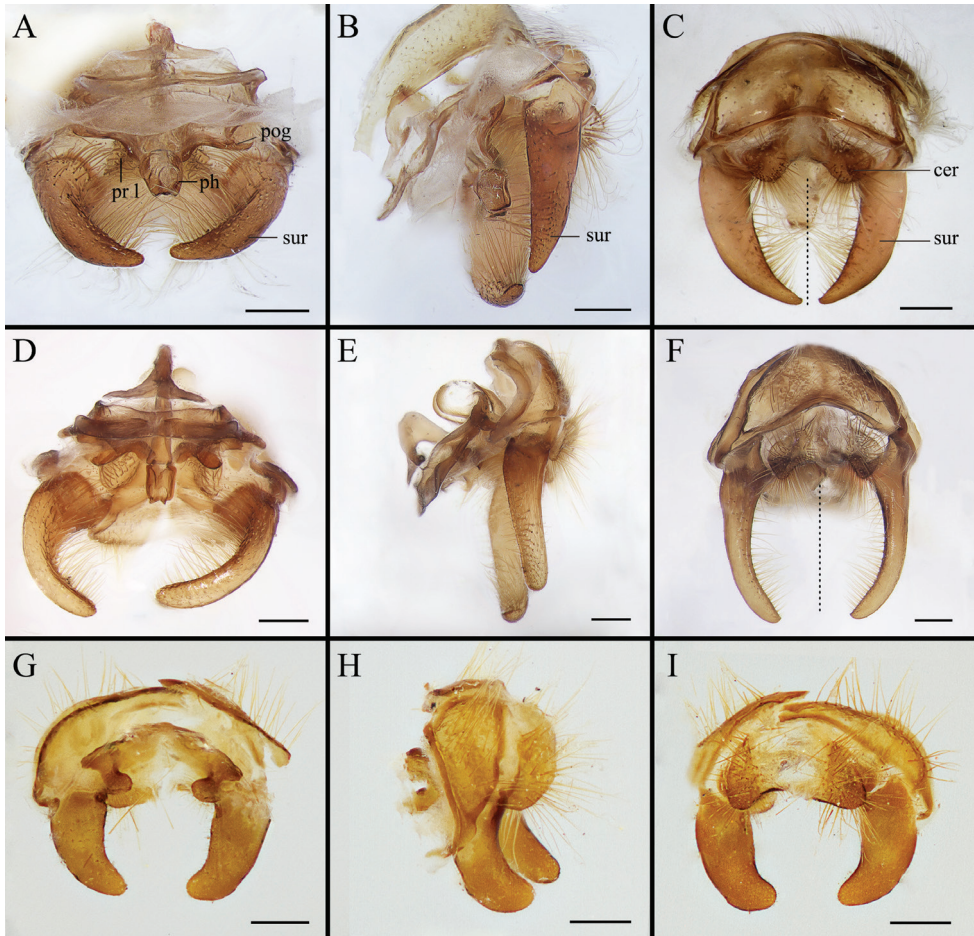


Figure 11. Anterior (**A, D, G**), left lateral (**B, E, H**) and posterior view (**C, F, I**) of male terminalia of *Gasterophilus* species, modified from Li et al. (2019) **A–C** *G. flavipes* (Olivier) **D–F** *G. haemorrhoidalis* (Linnaeus) **G–I** *G. inermis* (Brauer). Scale bars: 0.5 mm (**A–I**). The dotted line in **C** and **F** indicates the sagittal plane. Abbreviations: cer, cercus; ph, phallus; pog, postgonite; pr l, processi longi; sur, sustylus.

Gastrus subjacens Walker, 1849: 687. Type locality: Canada, Nova Scotia.

Oestrus stomachinus Gistel, 1848: 153. Type locality: not given, probably Germany, Bavaria.

Gasterophilus crossi Patton, 1924: 963. Type locality: India, Punjab.

Gasterophilus albescens Pleske, 1926: 228. Type locality: Egypt, Cairo (as “Il provient de l’Egypte des environs du Caire”).

Gasterophilus nasalis var. *nudicollis* Dinulescu, 1932: 28, 32. Type locality: not given.

Gasterophilus veterinus var. *aureus* Dinulescu, 1938: 315. Type locality: not given.

Gastrus jumentorum: Brauer 1863: 87, 280; incorrect subsequent spelling of *jumentorum* Meigen, 1824.

Oestrus nasulis: Fabricius 1787: 321; incorrect subsequent spelling of *nasalis* Linnaeus, 1758.

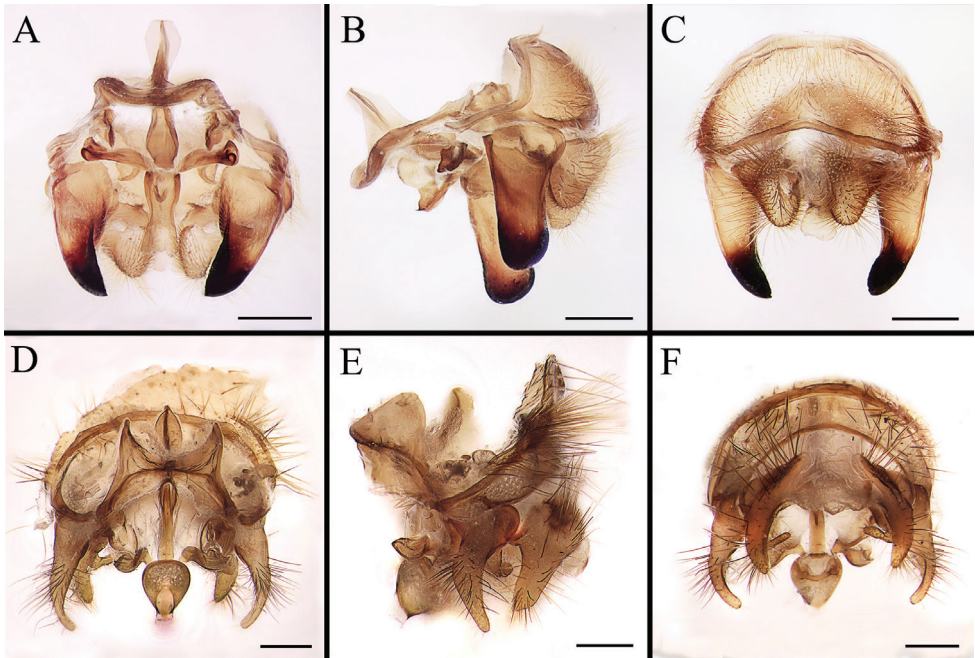


Figure 12. Dorsal (A, D), left lateral (B, E) and posterior (C, F) view of male genitalia of *Gasterophilus* species A–C *G. intestinalis* (De Geer) D–F *G. nasalis* (Linnaeus). Scale bars: 0.5 mm (A–F).

Selected references. Zumpt (1965: 117); Grunin (1969: 32); Pont (1973: 698); Kettle (1974); Soós and Minář (1986: 238); Cogley (1991b); Escartin and Bautista (1993); Xue and Wang (1996: 2210); Sequeira et al. (2001); Otranto et al. (2005); Colwell et al. (2006: 6); Colwell et al. (2007); Felix et al. (2007); Zhang et al. (2016); Li et al. (2018); Yan et al. (2019).

Diagnosis. Facial plate setose. Wing entirely hyaline; distance between crossveins r-m and dm-cu less than length of r-m. Meron with unmodified setae. Legs mainly black-brown. Abdomen ground color dark brown or black, with reddish-yellow hair-like setae on tergites 5–7 in male, pale yellow in female. Male cercus long and narrow, length/width ratio more than 3.0; surstylus yellow, with gradually a tapered apex; processus longi elongated and distinctly bent inwards. Female sternite 8 longitudinally ridged in the middle and with flattened and a scallop-shaped apex.

Type material examined. Holotype of *Gasterophilus albescens* Pleske, 1926. EGYPT • ♂; Cairo; no further information; ZIN.

Additional material examined. CHINA – Inner Mongolia • 2♂♂, 5♀♀; Chifeng; Zhaowuda League, Right Banner; 24 May–10 Aug. 1960; collector unknown; IOZ • 5♂, 1♀; Ulanqab, Temurtei County; 12–30 Aug. 1971; Y.R. Zhang leg.; IOZ. – Xinjiang Uyghur Autonomous Region • 1♂; Altay, Qinghe County; 6 Jul. 1960; S.Y. Wang leg.; IOZ • 1♀; Altyn-Tagh; 3850 m; 7 Aug. 1988; X.Z. Zhang leg.; IOZ • 1♂; locality as for preceding; 11 Aug. 1988; X.Z. Zhang leg.; IOZ • 3♂♂; Fuyun County; Qiakuertu; 25 May–3 Jun. 2010; F. Mo leg.; MBFU • 8♂♂, 1♀; Kalamaili;

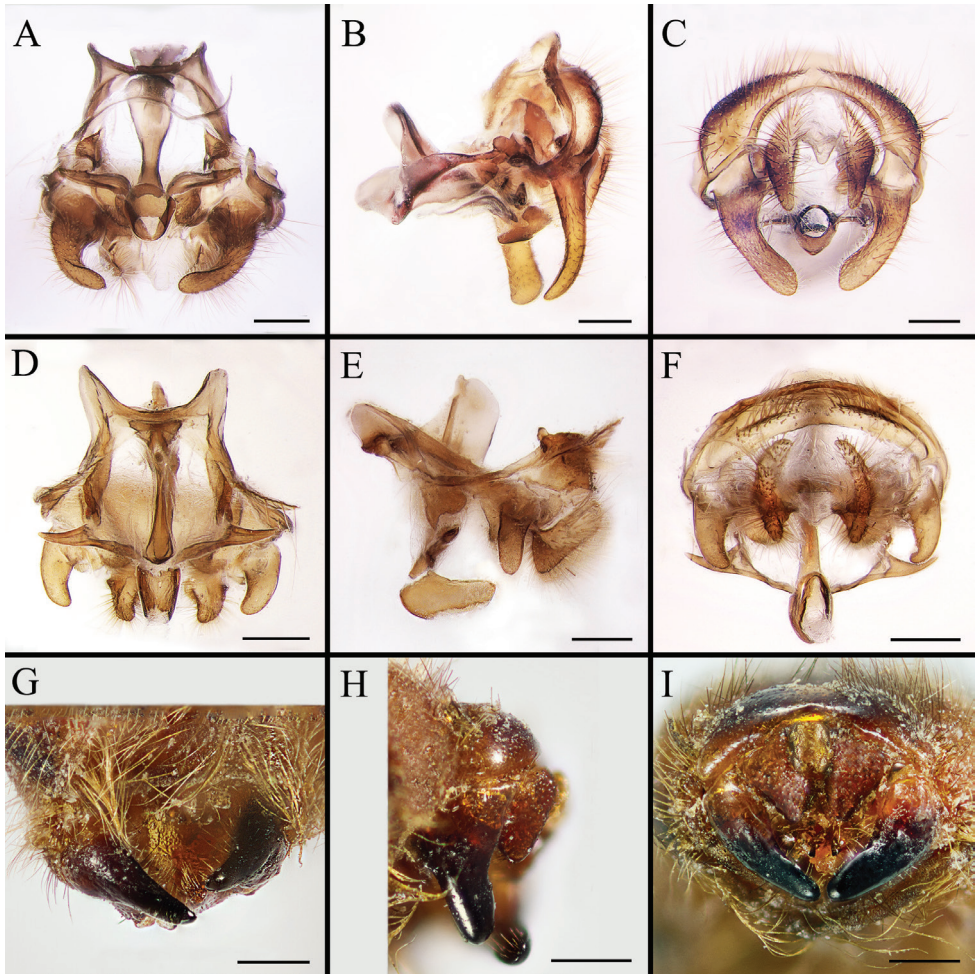


Figure 13. Dorsal (**A, D, G**), left lateral (**B, E, H**) and posterior (**C, F, I**) view of male genitalia of *Gasterophilus* species **A–C** *G. nigricornis* (Loew) **D–F** *G. pecorum* (Fabricius) **G–I** *G. ternicinctus* Gedoelst. Scale bars: 0.5 mm (**A–I**).

18 Apr.–25 Jun. 2010; D. Zhang leg.; MBFU • 1♂, 5♀; Kalamaili; 16 Apr.–8 May 2011; D. Zhang leg.; MBFU.

Hosts. Burchell's zebra (*E. quagga burchellii*), domestic horse (*E. ferus caballus*), donkey (*E. africanus asinus*), Mongolian wild ass (*E. hemionus hemionus*), wild horse (*E. przewalskii*).

Distribution. **Afrotropical** – Burkina Faso, Ethiopia, Kenya, Lesotho, Morocco, Namibia, Senegal, South Africa, Zambia, Zimbabwe. **Australasian** – Australia (Queensland, Tasmania), Fiji, Hawaii, New Zealand. **Nearctic** – Canada (Alberta, British Columbia, Manitoba, Northwestern, Nova Scotia, Quebec, Saskatchewan), Mexico (Aguascalientes, San Vicente Chicoloapan), USA (Arizona, California, Colorado, Illinois, Iowa, Kansas, Kentucky, Maryland, Michigan, Minnesota, Missouri,



Figure 14. Dorsal (**A, D, G**), left lateral (**B, E, H**) and ventral (**C, F, I**) view of female genitalia of *Gasterophilus* species, modified from Li et al. (2019) **A–C** *G. flavipes* (Olivier) **D–F** *G. haemorrhoidalis* (Linnaeus) **G–I** *G. inermis* (Brauer). Scale bars: 0.5 mm (**A–C**); 1 mm (**D–I**). Abbreviations: cer, cercus; epi, epiproct; sg 7, segment 7; sl, stalk-like pedicel; st 8, sternite 8; tg 8, tergite 8.

Montana, Nebraska, New Jersey, New Mexico, New York, North Dakota, Ohio, Oklahoma, Oregon, South Dakota, Texas, Washington, Wyoming). **Neotropical** – Antigua and Barbuda, Argentina, Brazil (Rio Grande do Sul, São Paulo), Chile (Bío Bío Region), Jamaica, Panama, Puerto Rico, Uruguay, Venezuela. **Oriental** – India, Malaysia, Myanmar, Thailand. **Palaeartic** – Afghanistan, Austria, Bulgaria, China (Heilongjiang, Inner Mongolia, Shaanxi, Tibet, Xinjiang), Cyprus, Denmark, Egypt, France, Germany, Hungary, Iraq, Italy (incl. Corsica and Sicily), Jordan, Kazakhstan, Kyrgyzstan, Lithuania, Mongolia, Morocco, Pakistan, Poland, Romania, Russia (Tomsk), Sweden, Switzerland, The Netherlands, Tajikistan, Turkey, Turkmenistan, Ukraine, United Kingdom, Uzbekistan.

Gasterophilus nigricornis (Loew, 1863)

Figs 3A–C, 6A, B, 9A–C, 10G, 13A–C, 16A–C, 18E–H; Table 1

Gastrus nigricornis Loew, 1863: 38. Type locality: Moldova, Bessarabia (as “Bessarabien”).

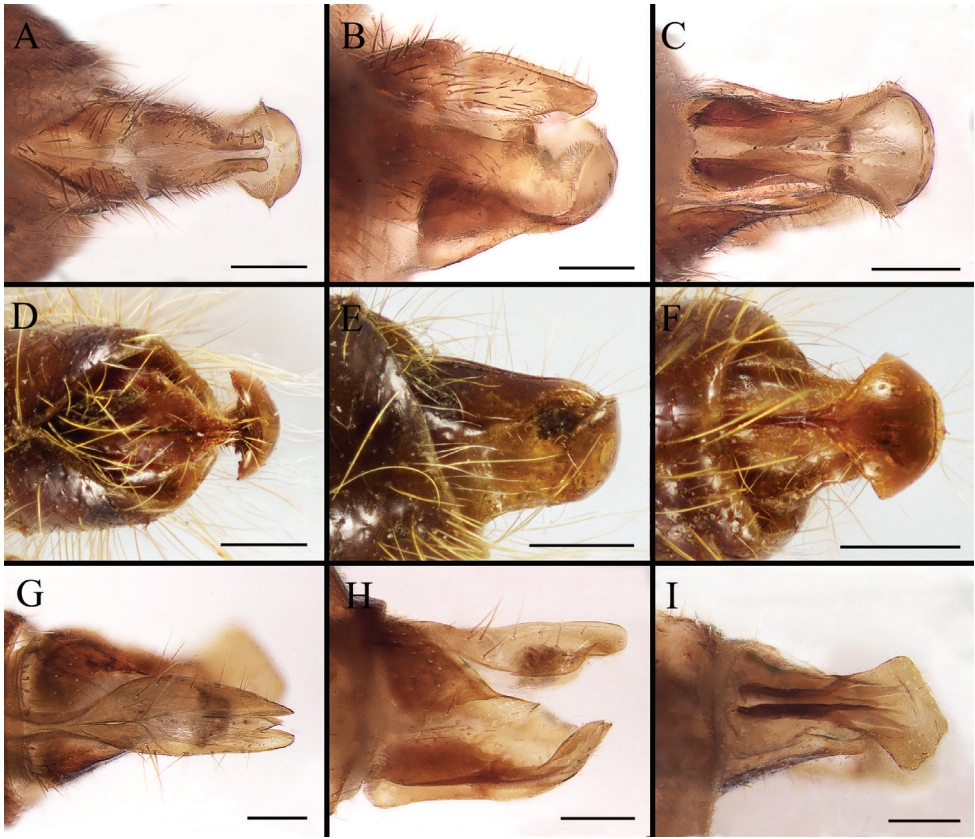


Figure 15. Dorsal (A, D, G), left lateral (B, E, H) and ventral (C, F, I) view of female genitalia of *Gasterophilus* species **A–C** *G. intestinalis* (De Geer) **D–F** *G. meridionalis* (Pillers & Evans) **G–I** *G. nasalis* (Linnaeus). Scale bars: 0.5 mm (A–I).

Gasterophilus viridis Sultanov, 1951: 41. Type locality: Kazakhstan, Kzyl-Ordinskaja, around Teren-Uzyakaskiy.

Gasterophilus migricornis: Colwell 2006: 291; incorrect subsequent spelling of *nigricornis* Loew, 1863.

Selected references. Zumpt (1965: 119); Grunin (1969: 36); Soós and Minář (1986: 239); Xue and Wang (1996: 2214); Colwell et al. (2006: 36); Zhang et al. (2012, 2016); Li et al. (2018); Yan et al. (2019).

Diagnosis. Antennal postpedicel red-brown to blackish. Facial plate setose. Meral setae with swollen tip. Wing completely hyaline. Crossvein dm-cu absent. Legs yellowish brown with femora distinctly darkened. Male cercus long and narrow, length/width ratio more than 3.0; surstylus yellow, with a rounded apex; processus longi elongated. Female sternite 8 longitudinally ridged in the middle and with a scallop-shaped apex.

Material examined. CHINA – Xinjiang Uyghur Autonomous Region • 1♂; Barköl Kazak Autonomous County, Saerqiaoke; 14 Aug. 1968; collector unknown;

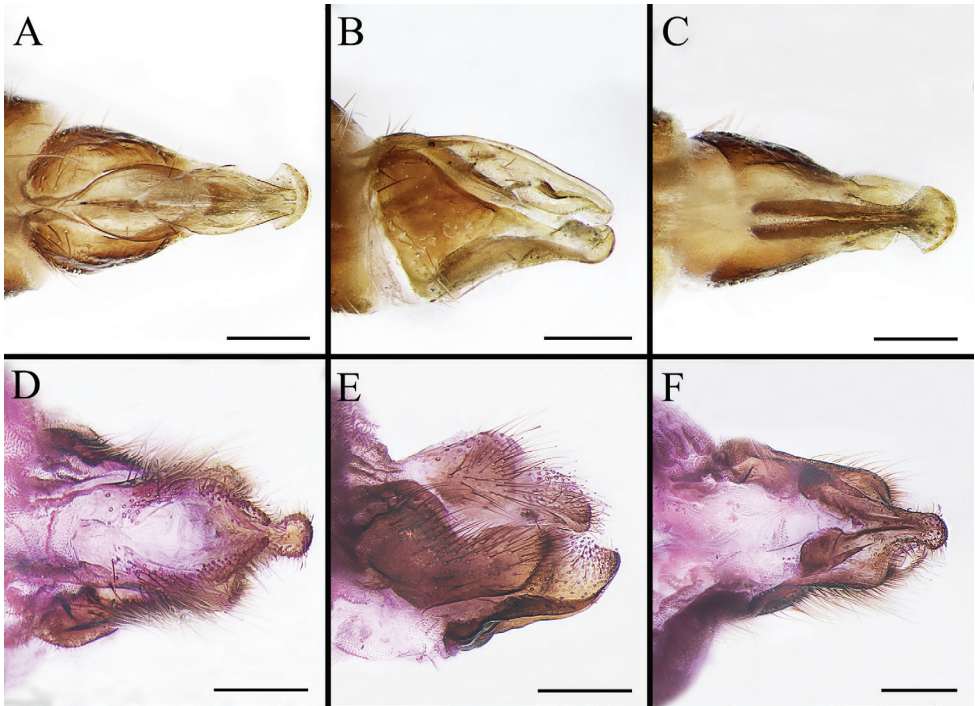


Figure 16. Dorsal (**A, D**), left lateral (**B, E**) and ventral (**C, F**) view of female genitalia of *Gasterophilus* species **A–C** *G. nigricornis* (Loew) **D–F** *G. pecorum* (Fabricius). Scale bars: 0.5 mm (**A–F**).

IOZ • 9♂♂, 1♀; Kalamaili; 3 Apr.–18 May 2009; D. Zhang leg.; MBFU • 27♂♂, 1♀; Fuyun County, Qiakuertu; 25 Apr.–13 May 2009; F. Mo leg.; MBFU.

Hosts. Domestic horse (*E. ferus caballus*), donkey (*E. africanus asinus*), Mongolian wild ass (*E. hemionus hemionus*), wild horse (*E. przewalskii*).

Distribution. **Palearctic** – China (Inner Mongolia, Qinghai, Xinjiang), Kazakhstan, Kyrgyzstan, Moldova, Mongolia, Tajikistan, Turkmenistan, Ukraine, Uzbekistan.

Remarks. The distribution of *G. nigricornis* appears to be limited to far eastern Europe and Central Asia. Thus, reports of *G. nigricornis* from western part of Europe [Spain: Lucientes (2002); Italy: Pape (2013)] are suspected to be misidentifications and the records are not included.

Gasterophilus pecorum (Fabricius, 1794)

Figs 3D–F, 6C, D, 9D–F, 10H, 13D–F, 16D–F, 18I–L; Table 1

Oestrus pecorum Fabricius, 1794: 230. Type locality: not given, probably Europe.

Oestrus vituli Fabricius, 1794: 231. Type locality: not given, but at least Sweden and France by reference to works of Linnaeus and Geoffroy.

Gastrus jubarum Meigen, 1824: 179, 180. Type locality: Austria.

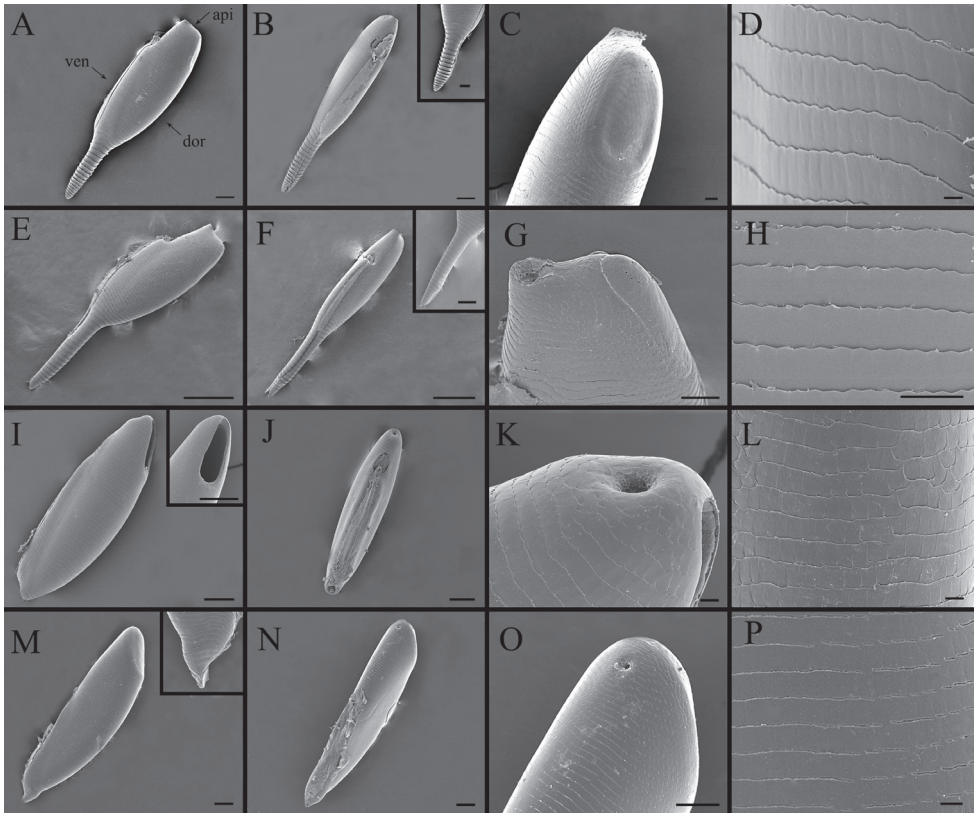


Figure 17. Right lateral (**A, E, I, M**) and ventral (**B, F, J, N**) view, micropyle (**C, G, K, O**) and ultrastructural details of plastron (**D, H, L, P**) of eggs in *Gasterophilus* species **A–D** *G. flavipes* (Olivier) **E–H** *G. haemorrhoidalis* (Linnaeus) **I–L** *G. inermis* (Brauer) **M–P** *G. intestinalis*. Abbreviations: api, apical; dor, dorsal; ven, ventral. Scale bars: 100 μm (**A, B, I–J, M, –N**), 50 μm (in box of **B**), 100 μm (in box of **I**); 20 μm (**C**); 5 μm (**D**); 250 μm (**E, F**), 20 μm (in box of **F**); 50 μm (**G, O**); 25 μm (**H**); 10 μm (**K, L, P**).

Gastrus lativentris Brauer, 1858: 465. Type locality: Latvia, Curland (as “in Kurland gefangen”).

Gastrus ferruginatus Zetterstedt, 1844: 978. Type locality: Sweden, Skåne, Tranås socken, Esperöd. (as “ad Esperöd in paröcia Tranås Scaniae”).

Gasterophilus pecorum var. *zebrae* Rodhain & Bequaert, 1920: 181. Type locality: Kenya and Tanzania.

Gasterophilus vulpecula Pleske, 1926: 227. Type locality: China, Inner Mongolia, Alxa League.

Gasterophilus gammeli Szilády, 1935: 140. Type locality: Hungary.

Gasterophilus hammeli: Paramonov 1940: 34, 46; incorrect subsequent spelling of *gammeli* Szilády, 1935.

Gasterophilus hummeli: Paramonov 194 “Dans les Pyrénées” 0: 32; incorrect subsequent spelling of *gammeli* Szilády, 1935.

Gastrus selysi Walker, 1849: 687. Nomen nudum.

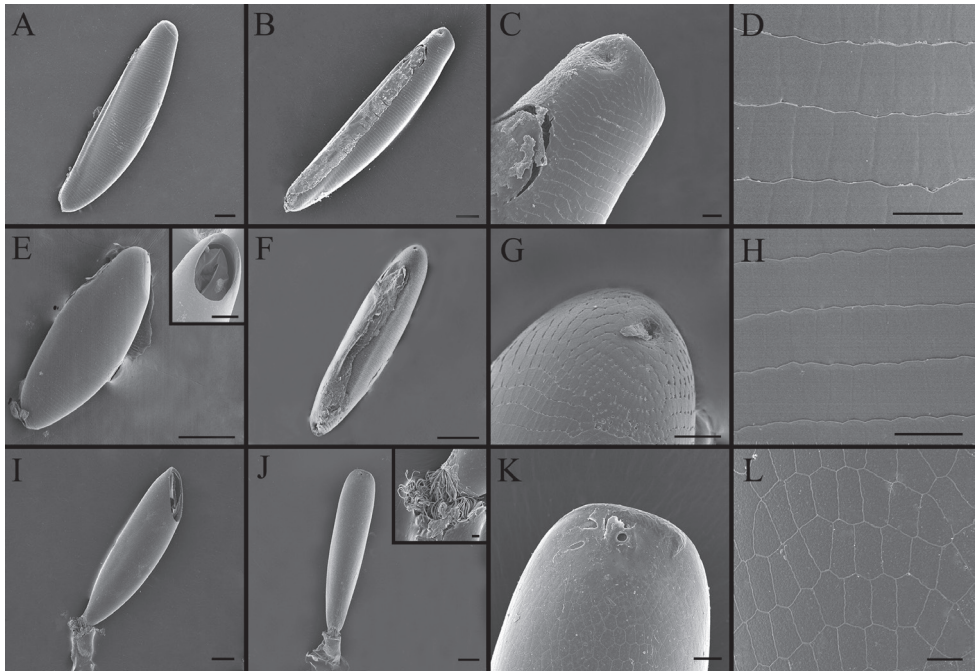


Figure 18. Right lateral (**A, E, I**) and ventral (**B, F, J**) view, micropyle (**C, G, K**) and ultrastructural details of plastron (**D, H, L**) of eggs in *Gasterophilus* species **A–D** *G. nasalis* (Linnaeus) **E–H** *G. nigricornis* (Loew) **I–L** *G. pecorum* (Fabricius). Scale bars: 100 μm (**A, B, I–J**), 10 μm (in the box of **J**); 20 μm (**C, H, K**); 15 μm (**D**); 20 μm (**E**), 50 μm (in the box of **E**); 150 μm (**F**); 25 μm (**G**); 10 μm (**L**).

Selected references. Zumpt (1965: 114); Grunin (1969: 25); Pont (1973: 698); Soós and Minář (1986: 239); Cogley (1991b); Xue and Wang (1996: 2210); Otranto et al. (2005); Colwell et al. (2006: 5); Colwell et al. (2007); Zhang et al. (2016); Hoseini et al. (2017); Li et al. (2018); Yan et al. (2019).

Diagnosis. Antennal pedicel elongated, with length/width ratio more than 0.8. Facial plate setose. Wing dark, with broad darkened patches with ill-defined edges; crossvein dm-cu absent. Meron with unmodified setae. Legs yellowish brown with femora distinctly darkened. Abdomen ground color yellow in male, mainly dark brown to black in female. Male cercus long and narrow, length/width ratio more than 3.0; surstylus yellow, with a rounded apex; processi longi elongated. Female sternite 8 with a longitudinal concavity in the middle and with a keel-shaped apex.

Material examined. CHINA – **Xinjiang Uyghur Autonomous Region** • 1♂; Akesu; 25 Sep. 1958; collector unknown; IOZ • 1♀; Bayingolin Mongol Autonomous Prefecture, Qiemo County; Aqiang; 3000 m; 20 Jul. 1988; X.Z. Zhang leg.; IOZ • 2♀♀; Fuyun County, Qiakuertu; 8–10 Jun. 2009, F. Mo leg.; MBFU • 9♂♂, 4♀♀; Kalamaili; 6 May–1 Jun. 2009; D. Zhang leg.; MBFU. – **Inner Mongolia** • 1♀; Chifeng, Zhaowuda League, Right Banner; 22 Aug.–28 Sep. 1959; collector unknown; IOZ • 2♂♂; Ulanqab, Temurtei, 4–27 Aug. 1971; collector unknown; IOZ • 1♂; Xisuqi; 1 Sep. 1971; collector unknown; IOZ.

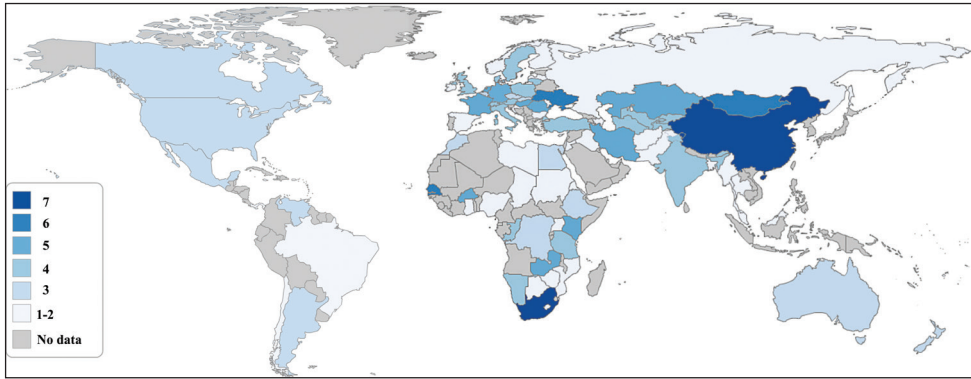


Figure 19. Species diversity map of all nine *Gasterophilus* species worldwide. Different colors represent the number of species recorded in a specific country. Interactive map showing the global distribution of all nine *Gasterophilus* species is available in Supplementary Information 1.

Hosts. Burchell's zebra (*E. quagga burchellii*), domestic horse (*E. ferus caballus*), donkey (*E. africanus asinus*), Mongolian wild ass (*E. hemionus hemionus*), Persian onager (*E. hemionus onager* Boddaert), wild horse (*E. przewalskii*).

Distribution. **Afrotropical** – Burkina Faso, Kenya, Namibia, Senegal, South Africa, Tanzania, Uganda, Zambia. **Oriental** – India. **Palearctic** – Austria, Belgium, China (Heilongjiang, Inner Mongolia, Xinjiang), Czech Republic, Denmark, France, Germany, Hungary, Iran, Italy (incl. Corsica and Sicily), Latvia, Lithuania, Mongolia, Poland, Romania, Sweden, Switzerland, The Netherlands, Turkey, Ukraine, United Kingdom.

Gasterophilus ternicinictus (Gedoelst, 1912)

Figs 3G–I, 6E, F, 9G–I, 10I, 13G–I; Table 1

Gasterophilus ternicinictus Gedoelst, 1912: 426. Type locality: Democratic Republic of the Congo (as “Zaire”), 11.5 km W of Luapula river (as “6 milles W. du Luapula”).

Gasterophilus gedoelsti Rodhain & Bequaert, 1920: 188. Type locality: Kenya.

Selected references. Zumpt (1965: 128); Cogley (1991b); Colwell et al. (2006: 36).

Diagnosis. Facial plate bare. Wing with darkened patches with demarcated edges. Distance between crossveins r-m and dm-cu less than length of r-m. Meron with unmodified setae. Legs yellowish brown, with tibiae and tarsi more or less darkened. Hind trochanter of male with a long, spatulate process, of female with a tubercle; hind tibia and tarsus flattened distinctly in male, slightly in female; tarsomeres 2–4 shortened in both sexes, broader than long. Abdomen ground color yellow in both male and female. Male cercus elongated and broad, length/width ratio around 1.5; surstylus mainly black with yellow coloration basally, and a rounded apex. Female abdominal segment 7 distinctly longer than broad, sternite 8 longitudinally ridged in the middle and with a scallop-shaped apex.

Material examined. SOUTH AFRICA • 1♂; KwaZulu; Hluhluwe-Imfolozi Park; 8 Mar. 1963; collector unknown; MBFU. KENYA • 1♂, 1♀; Kenplains, Athi river; 13 Mar. 1991; C.F. Dewhurst leg.; NHMUK.

Hosts. Burchell's zebra (*E. quagga burchellii*).

Distribution. **Afrotropical** – Burkina Faso, Democratic Republic of the Congo, Kenya, Republic of the Congo, Senegal, South Africa, Zambia.

Acknowledgements

We wish to thank Prof Jun Chen, Ms Hong Liu and Ms Kuiyan Zhang (Institute of Zoology, Chinese Academy of Sciences), Dr Olga Ovtshinnikova (Zoological Institute, Russian Academy of Sciences, St Petersburg) and Ms Tricia Pillay (KwaZulu-Natal Museum, Pietermaritzburg, South Africa) for kindly arranging for loans of *Gasterophilus* specimens, Mr Nigel Wyatt (Natural History Museum, London) and Mr Peter Sehnal (Naturhistorisches Museum Wien) for providing photos and locality details of particular specimens. This study was supported by the National Science Foundation of China (Nos. 31872964 and 31572305) and the Fundamental Research Funds for the Central Universities (No. 2019JQ0318) to D Zhang, Key Project of International Scientific and Technological Innovation Cooperation, National Key R&D Program of China (No. 2016YFE0203100), and by an award from the State Scholarship Fund of China Scholarship Council (No. 201806510006) to X.-y. Li to pursue her studies at the University of Copenhagen.

References

- Agassiz JLR (1846) Nomenclatoris zoologici index universalis: continens nomina systematica classium, ordinum, familiarum, et generum animalium omnium, tam viventium quam fossilium. Jent & Gassmann, Switzerland, 393 pp.
- Anderson JR (2006) Adult biology. In: Colwell DD, Hall MJR, Scholl PJ (Eds) The Oestrid Flies: Biology, Host-Parasite Relationships, Impact and Management. CABI, Wallingford, 140–166. <https://doi.org/10.1079/9780851996844.0140>
- Bezdekova B, Jahn P, Vyskocil M (2007) Pathomorphological study on gastroduodenal ulceration in horses: Localisation of lesions. *Acta Veterinaria Hungarica* 55: 241–249. <https://doi.org/10.1556/AVet.55.2007.2.10>
- Bezzi M (1916) Un nuova specie di Estride dell'Eritrea. *Bollettino del Laboratorio di zoologia generale e agraria della R. Scuola superiore d'agricoltura in Portici* 10: 27–32.
- Bigot JMF (1884) Descriptions de Diptères nouveaux récoltés par M. le professeur Magretti dans le Soudan oriental. *Annales de la Société entomologique de France ser. 6*, 4(2): 57–59.
- Brauer F (1858) Neue Beiträge zur Kenntniss der europäischen Oestriden. *Verhandlungen der Kaiserlich-Königliche Zoologisch-Botanischen Gesellschaft in Wien* 8: 464.

- Brauer F (1863) Monographie der Oestriden. W. Braumüller, Wien, 292 pp. <https://doi.org/10.5962/bhl.title.57896>
- Catts EP (1979) Hilltop aggregation and mating behavior by *Gasterophilus intestinalis* (Diptera: Gasterophilidae). *Journal of Medical Entomology* 16: 461–464. <https://doi.org/10.1093/jmedent/16.6.461>
- Clark B (1797) Observations on the genus *Oestrus*. *Transactions of the Linnean Society of London* 3: 289–329. <https://doi.org/10.1111/j.1096-3642.1797.tb00570.x>
- Clark B (1815) An Essay on the Bots of Horses and Other Animals. Old Bailey, London, 72 pp. <https://doi.org/10.5962/bhl.title.159664>
- Clark B (1816) Discovery of the fly of the white bot. Supplementary sheet. London, 4 pp.
- Cogley TP (1991a) Key to the eggs of the equid stomach bot flies *Gasterophilus* Leach 1817 (Diptera: Gasterophilidae) utilizing scanning electron microscopy. *Systematic Entomology* 16: 125–133. <https://doi.org/10.1111/j.1365-3113.1991.tb00681.x>
- Cogley TP (1991b) Status of the stomach bot fly *Gasterophilus lativentris* (Brauer) 1858 (Diptera: Gasterophilidae). *Systematic Entomology* 16: 135–136. <https://doi.org/10.1111/j.1365-3113.1991.tb00682.x>
- Cogley TP, Anderson JR, Cogley LJ (1982) Migration of *Gasterophilus intestinalis* larvae (Diptera: Gasterophilidae) in the equine oral cavity. *International Journal for Parasitology* 12: 473–480. [https://doi.org/10.1016/0020-7519\(82\)90079-0](https://doi.org/10.1016/0020-7519(82)90079-0)
- Cogley TP, Cogley MC (2000) Field observations of the host-parasite relationship associated with the common horse bot fly, *Gasterophilus intestinalis*. *Veterinary Parasitology* 88: 93–105. [https://doi.org/10.1016/S0304-4017\(99\)00191-0](https://doi.org/10.1016/S0304-4017(99)00191-0)
- Colwell DD, Hall MJR, Scholl PJ (2006) The Oestrid Flies: Biology, Host-Parasite Relationships, Impact and Management. CABI, Wallingford, 357 pp. <https://doi.org/10.1079/9780851996844.0000>
- Colwell DD, Otranto D, Horak IG (2007) Comparative scanning electron microscopy of *Gasterophilus* third instars. *Medical and Veterinary Entomology* 21: 255–264. <https://doi.org/10.1111/j.1365-2915.2007.00692.x>
- Coquillett DW (1910) The type-species of the North American genera of Diptera. *Proceedings of the United States National Museum, Washington*, 499–647. <https://doi.org/10.5479/si.00963801.37-1719.499>
- Colwell DD (2006) Life cycle strategies. In: Colwell DD, Hall MJR, Scholl PJ (Eds) *The Oestrid Flies: Biology, Host-Parasite Relationships, Impact and Management*. CABI, Wallingford, 67–77. <https://doi.org/10.1079/9780851996844.0067>
- Cumming JM, Wood DM (2009) Adult morphology and terminology. In: Brown BV, Borkent A, Cumming JM (Eds), *Manual of Central American Diptera Vol. 1*. NRC Research Press, Ottawa, 9–50.
- Curtis J (1826) *British entomology: being illustrations and descriptions of the genera of insects found in Great Britain and Ireland: containing coloured figures from nature of the most rare and beautiful species, and in many instances of the plants upon which they are found*. Printed for the author, London, 146 pp.
- Dinulescu G (1932) Recherches sur la biologie des gastrophiles, anatomie, physiologie, cycle évolutif. *Annales des Sciences Naturelles Zoologie Série 10*: 183 pp.

- Dinulescu G (1938) *Gastrophilus veterinus* var. *aureus*. Archives Roumaines de Pathologie Expérimentale et de Microbiologie (Bucuresti) 11: 315–335.
- Dove WE (1918) Some biological and control studies of *Gastrophilus haemorrhoidalis* and other bots of horses. United States Department of Agriculture 597: 52 pp. <https://doi.org/10.5962/bhl.title.64448>
- Enderlein G (1934) Dipterologica. Sitzungsberichte der Gesellschaft naturforschender Freunde zu Berlin 1933: 416–429.
- Escartin P, Bautista G (1993) Comparison of five tests for the serologic diagnosis of myiasis by *Gasterophilus* spp. larvae (Diptera: Gasterophilidae) in horses and donkeys: a preliminary study. Medical and Veterinary Entomology 7: 233–237. <https://doi.org/10.1111/j.1365-2915.1993.tb00682.x>
- Fabricius JC (1787) Mantissa insectorum sistens eorum species nuper detectas adiectis characteribus genericis, differentiis specificis, emendationibus, observationibus. Impensis Christian Gottlob Proft, Copenhagen, 382 pp. <https://doi.org/10.5962/bhl.title.36471>
- Fabricius JC (1794) Entomologia systematica emendata et aucta, Vol. 4: Secundum classes, ordines, genera, species. Impensis Christ Gottl Proft, Copenhagen, 472 pp.
- Felix SR, Silva CE, Schmidt E, Nizoli LQ, Götz MM, Silva SS (2007) Presence of *Gasterophilus* (Leach, 1817) (Diptera: Oestridae) in horses in Rio Grande do Sul State, Brazil. Parasitologia Latinoamericana 62: 122–126. <https://doi.org/10.4067/S0717-77122007000200004>
- Ferrari PA (1987) Guide to the breeding habits and immature stages of Diptera Cyclorrhapha. In: Lyneborg L (Ed.) Entomonograph, Vol. 8. Scandinavian Science Press, Copenhagen, 907 pp.
- Ganjali M, Keighobadi M (2016) A rare case of gastric Myiasis in a lion caused by *Gasterophilus intestinalis* (Diptera: Gasterophilidae)-case report. Journal of Arthropod-Borne Diseases 10: 423–425.
- Gedoelst LM (1912) Contribution à la faune des Oestrides du Congo belge. Revue Zoologique Africaine 1: 426–432.
- Gedoelst LM (1923) Note sur la larve du *Gasterophilus haemorrhoidalis* et description de la larve d'une nouvelle espèce africaine. Annales de Parasitologie 1: 269–275. <https://doi.org/10.1051/parasite/1923013269>
- De Geer C (1776) Mémoires pour servir à l'histoire des insectes. Tome sixième. P. Hesselberg, Stockholm, 523 pp.
- Getachew AM, Innocent G, Trawford AF, Reid SWJ, Love S (2012) Gasterophilosis: A major cause of rectal prolapse in working donkeys in Ethiopia. Tropical Animal Health and Production 44: 757–762. <https://doi.org/10.1007/s11250-011-9961-7>
- Gistel J (1848) Naturgeschichte des Thierreichs für höheren Schulen. R. Hoffmann, Stuttgart, 216 pp.
- Grunin KJ (1965) 64b. Hypodermatidae. In: Lindner E (Ed.) Die Fliegen der Paläarktischen Region 8. Schweizerbart'sche, Stuttgart, 153 pp.
- Grunin KJ (1966) 64a'. Oestridae. In: Lindner E (Ed.) Die Fliegen der Paläarktischen Region 8. Schweizerbart'sche, Stuttgart, 96 pp.
- Grunin KJ (1969) 64a. Gasterophilidae. In: Lindner E (Ed.) Die Fliegen der Paläarktischen Region 8. Schweizerbart'sche, Stuttgart, 66 pp.

- Guérin-Méneville FÉ (1827) Dictionnaire classique d'histoire naturelle. Paris, Rey et Gravier, Librairies-Editeurs, Auai des Augustins, no. 55; Baudouin FrèreS, Librairies-Editeurs, Imprimeurs de la société D'Histoire Naturelle, Rue de Vaugirard, no. 36, Paris, 634 pp.
- Guimarães JH (1967) Family Gasterophilidae. In: A Catalogue of the Diptera of the Americas South of the United States. Departamento de Zoologia, Secretaria da Agricultura, São Paulo, 1–2.
- Guimarães JH, Papavero N (1999) Myiasis in Man and Animals in the Neotropical Region; Bibliographic Database. Editora Plêiade, São Paulo, 306 pp.
- Güiris ADM, Rojas HNM, Berovides A V., Sosa PJ, Pérez EME, Cruz AE, Chávez HC, Mogueel AJA, Jimenez-Coello M, Ortega-Pacheco A (2010) Biodiversity and distribution of helminths and protozoa in naturally infected horses from the biosphere reserve “La Sierra Madre de Chiapas”, México. *Veterinary Parasitology* 170: 268–277. <https://doi.org/10.1016/j.vetpar.2010.02.016>
- Hadwen S, Cameron AE (1918) A contribution to the knowledge of the bot-flies, *Gasterophilus intestinalis*, DeG., *G. haemorrhoidalis*, L., and *G. nasalis*, L. *Bulletin of Entomological Research* 9: 91–106. <https://doi.org/10.1017/S0007485300037858>
- Hall M, Wall R (1995) Myiasis of humans and domestic animals. *Advances in parasitology* 35: 257–334. [https://doi.org/10.1016/S0065-308X\(08\)60073-1](https://doi.org/10.1016/S0065-308X(08)60073-1)
- Hoseini SM, Zaheri BA, Adibi MA, Ronaghi H, Moshrefi AH (2017) Histopathological study of esophageal infection with *Gasterophilus pecorum* (Diptera: Oestridae) in Persian Onager (*Equus hemionus onager*). *Journal of Arthropod-Borne Diseases* 11: 441–445.
- Huang H, Chu H, Cao J, Bu L, Hu D, Zhang D, Li K (2017) Distribution of *Gasterophilus* (Diptera, Gasterophilidae) Myiasis Foci in Arid Desert Steppe: a case study of Kalamaili Mountain Ungulate Nature Reserve. *Linye Kexue/Scientia Sinicae* 53. <https://doi.org/10.11707/j.1001-7488.20171116>
- Huang H, Zhang B, Chu H, Zhang D, Li K (2016) *Gasterophilus* (Diptera, Gasterophilidae) infestation of equids in the Kalamaili Nature Reserve, China. *Parasite* 23: 1–36. <https://doi.org/10.1051/parasite/2016036>
- James MT (1974) The flies that cause myiasis in man. United States Government Printing Office, Washington, 175 pp.
- Kaboret Y, Pangui LJ, Vercruysse J (1986) Note on gasterophilosis in donkeys in Burkina Faso. *Revue d'Elevage et de Médecine Vétérinaire des Pays Tropicaux* 39: 211–212.
- Kettle P (1974) The genus *Gasterophilus* in the horse in New Zealand. *New Zealand Veterinary Journal* 22: 43–45. <https://doi.org/10.1080/00480169.1974.34130>
- Leach WE (1817) On the arrangement of oestrideous insects. In: On the genera and species of eproboscideous insects, and on the arrangement of oestrideous insects. Neill & Co., Edinburgh, 1–20.
- Leite ACR, Scott FB, Evangelista LG (1999) Scanning electron microscope observations on third-instar *Gasterophilus nasalis* (Diptera: Oestridae). *Journal of Medical Entomology* 36: 643–648. <https://doi.org/10.1093/jmedent/36.6.643>
- Li XY, Chen Y, Wang Q, Li K, Pape T, Zhang D (2018) Molecular and morphological characterization of third instar Palaearctic horse stomach bot fly larvae (Oestridae: Gasterophilinae, *Gasterophilus*). *Veterinary Parasitology* 262: 56–74. <https://doi.org/10.1016/j.vetpar.2018.09.011>

- Li XY, Pape T, Zhang D (2019) *Gasterophilus flavipes* (Oestridae: Gasterophilinae): a horse stomach bot fly brought back from oblivion with morphological and molecular evidence. PLoS ONE 14(8): e0220820. <https://doi.org/10.1371/journal.pone.0220820>
- Linnaeus C (1758) Systema naturae per regna tria naturae :secundum classes, ordines, genera, species, cum characteribus, differentiis, synonymis, locis. Salvii, Stockholm, 824 pp. <https://doi.org/10.5962/bhl.title.542>
- Liu SH, Li K, Hu DF (2016) The incidence and species composition of *Gasterophilus* (Diptera, Gasterophilidae) causing equine myiasis in northern Xinjiang, China. Veterinary Parasitology 217: 36–38. <https://doi.org/10.1016/j.vetpar.2015.12.028>
- Loew H (1863) Zwei neue europäische Dipterengattungen. Wiener Entomologische Monatschrift 7: 38–40.
- Lucientes J (2002) Gasterophilidae. In: Carles-Tolrà M (Ed.) Catalogue of the Diptera of Spain, Portugal and Andorra (Insecta). Monografias SEA 8, 207 pp.
- Macquart PJM (1843) Diptères exotiques nouveaux ou peu connus. Tome deuxième, 3^{ème} partie. Roret, Paris, 460 pp.
- Mashayekhi M, Ashtari B (2013) Study of *Gasterophilus* role in Equine Gastric Ulcer Syndrome in Tabriz area. Bulletin of Environment, Pharmacology and Life Sciences 2: 169–172.
- Meigen JW (1824) Systematische Beschreibung der bekannten europäischen zweiflügeligen Insekten. Vierter Theil. Schulz-Wundermann'sche Buchhandlung, Hamm, 428 pp. [pls. 33–41]
- Muller B, Ranwashe F (2017) NMSA: Arthropod Collections (1900–2012). Version 1.1. South African National Biodiversity Institute. Occurrence dataset. <https://doi.org/10.15468/a4tpcb>
- van Noort DS, Ranwashe F (2017) IZIKO South Africa Museum Collection (1800–2013). Version 1.3. South African National Biodiversity Institute. Occurrence dataset. <https://doi.org/10.15468/vf3ko1>
- Olivier GA (1811) Encyclopédie méthodique. Histoire naturelle. Insectes. Vol. 8. H Agasse, Paris, 722 pp.
- Otranto D, Milillo P, Capelli G, Colwell DD (2005a) Species composition of *Gasterophilus* spp. (Diptera, Oestridae) causing equine gastric myiasis in southern Italy: Parasite biodiversity and risks for extinction. Veterinary Parasitology 133: 111–118. <https://doi.org/10.1016/j.vetpar.2005.05.015>
- Otranto D, Traversa D, Milillo P, De Luca F, Stevens J (2005b) Utility of Mitochondrial and Ribosomal Genes for Differentiation and Phylogenesis of Species of Gastrointestinal Bot Flies. Journal of Economic Entomology 98: 2235–2245. <https://doi.org/10.1603/0022-0493-98.6.2235>
- Özdal N, Biçek K, Orunç Ö, Değir S (2010) Presence of *Gasterophilus* species in horses in Van Region. YYU Veteriner Fakültesi Dergisi 21: 87–90.
- Pandey VS, Ouhelli H, Verhulst A (1992) Epidemiological observations on *Gasterophilus intestinalis* and *G. nasalis* in donkeys from Morocco. Veterinary Parasitology 41: 285–292. [https://doi.org/10.1016/0304-4017\(92\)90087-P](https://doi.org/10.1016/0304-4017(92)90087-P)
- Papavero N (1977) The World Oestridae (Diptera) Mammals and Continental Drift. Series Entomologica Vol. 14, 240 pp. <https://doi.org/10.1007/978-94-010-1306-2>

- Pape T (1996) *Memoires of Entomology*, Vol. 8. International Catalogue of the Sarcophagidae of the world. Stockholm, 558 pp.
- Pape T (2001) Phylogeny of Oestridae (Insecta: Diptera). *Systematic Entomology* 26: 133–171. <https://doi.org/10.1046/j.1365-3113.2001.00143.x>
- Pape T (2013) Fauna Europaea: *Gasterophilus*. Fauna Europaea version 2019.10. <https://fauna-eu.org>
- Pape T, Piwczynski M, Wyborska D, Akbarzadeh K, Szpila K (2017) A new genus and species of hypodermatine bot flies (Diptera: Oestridae). *Systematic Entomology* 42: 387–398. <https://doi.org/10.1111/syen.12220>
- Paramonov SJ (1940) *Gastrophilidae und ihre Bekämpfungen*. Kiew-Lwow, 128 pp.
- Patton WS (1924) *Gasterophilus crossi* sp. nov., parasitic in its larval stage in the stomach of the horse in the Punjab. *Indian Journal of Medical Research* 11: 963.
- Patton WS (1937) Studies on the higher Diptera of medical and veterinary importance. *Annals of Tropical Medicine & Parasitology* 31: 351–359. <https://doi.org/10.1080/00034983.1937.11684990>
- Pearse B, Peucker S, Cottam R (1989) Identification of *Gasterophilus haemorrhoidalis* in Queensland. *Australian Veterinary Journal* 66: 380. <https://doi.org/10.1111/j.1751-0813.1989.tb09745.x>
- Pillers AWN, Evans AM (1926) A new larva of *Oestrus* (*Gastrophilus*) from zebras. *Annals of Tropical Medicine & Parasitology* 20: 263–266. <https://doi.org/10.1080/00034983.1926.11684499>
- Pilo C, Altea A, Scala A (2015) Gasterophilosis in horses in Sardinia (Italy): effect of meteorological variables on adult egg-laying activity and presence of larvae in the digestive tract, and update of species. *Parasitology Research* 114: 1693–1702. <https://doi.org/10.1007/s00436-015-4352-z>
- Pleske T (1926) *Revue des espèces paléarctiques des Oestrides et catalogue raisonné de leur collection au Musée Zoologique de l'Académie des Sciences*. *Annuaire du Musée Zoologique de l'Académie Impériale des Sciences de Saint Pétersbourg* 26: 215–230.
- Pont AC (1973) Family Oestridae. In: Delfinado M, Hardy D (Eds) *A Catalog of the Diptera of the Oriental Region: Suborder Cyclorrhapha*. University Press of Hawaii, Honolulu, 700–701.
- Pont AC (1980) Family Gasterophilidae. In: Crosskey RW (Ed.) *Catalogue of the Diptera of the Afrotropical Region*. British Museum of Natural History, London, 883–884.
- Rodhain J, Bequaert J (1920) Oestrides d'antilopes et de zèbres recueillis en Afrique orientale avec un conspectus du genre *Gasterophilus*. *Revue Zoologique Africaine* 8: 169–228. <https://doi.org/10.5962/bhl.part.22396>
- Rondani C (1857) *Dipterologiae Italicae prodromus*. Vol. 2. Species Italicae ordinis dipterorum in genera characteribus definita, ordinatim collectae, methodo analitica distinctae, et novis vel minus cognitis descriptis. Pars prima: Oestridae, Syrphidae, Conopidae. Stocchi, Parmae, 264 pp. <https://doi.org/10.5962/bhl.title.8160>
- Schwab KC (1840) *Die Oestraciden – Bremsen – der Pferde, Rinder und Schafe*. Matthäus Pössenbacher, München, 83 pp.

- Sequeira JL, Tostes RA, Oliveira-Sequeira TCG (2001) Prevalence and macro- and microscopic lesions produced by *Gasterophilus nasalis* (Diptera: Oestridae) in the Botucatu Region, SP, Brazil. *Veterinary Parasitology* 102: 261–266. [https://doi.org/10.1016/S0304-4017\(01\)00536-2](https://doi.org/10.1016/S0304-4017(01)00536-2)
- Soós Á, Minář J (1986) Family Gasterophilidae. In: Soós Á, Papp L (Eds) *Catalogue of Palaearctic Diptera*, Vol. 11. Scathophagidae – Hypodermatidae. Elsevier, Amsterdam, 237–240.
- StatSilk (2018) StatPlanet Desktop: Interactive Data Visualization and Mapping Software <http://www.statsilk.com>
- Sultanov MA (1951) A new species of botflies from horse -- *Gasterophilus viridis sultanov* sp. nov. *Doklady Akademii Nauk Uzbekskoi SSR* 1951: 41–44.
- Szilády Z (1935) Die ungarischen Dasselfliegen. *Állattani Közlemények* 32: 136–140.
- Tähtinen M, Lahti T (2017) Finnish Entomological Database. Version 1.2. Finnish Biodiversity Information Facility. Occurrence dataset. <https://doi.org/10.15468/jlud8r>
- Tavassoli M, Bakht M (2012) *Gasterophilus* spp. myiasis in Iranian equine. *Scientia Parasitologica* 13: 83–86.
- Townsend CHT (1918) New muscoid genera, species and synonymy (Diptera). *Insector Inscitiae Menstruus* 6: 157–182.
- Townsend CHT (1934) New Neotropical oestromuscoid flies. *Revista de Entomologia [Rio De Janeiro]* 4: 201–212.
- Walker F (1849) List of the specimens of dipterous insects in the collection of the British Museum. Part III. British Museum (Natural History), London, 485–687.
- Wood DM (1987) Oestridae. In: McAlpine JF (Ed.) *Manual of Nearctic Diptera*, Vol. 2. Research Branch, Agriculture Canada, Ottawa, 1147–1158.
- Wood DM (2006) Morphology of Adult Oestridae. In: Colwell DD, Hall MJR, Scholl PJ (Eds) *The Oestrid Flies: Biology, Host-Parasite Relationships, Impact and Management*. CABI, Wallingford, 79–80.
- Xue WQ, Wang MF (1996) Gasterophilidae. In: Xue WQ, Zhao JM (Eds) *Flies of China*. Vol. 2. Liaoning Science and Technology Press, Shenyang, 2207–2215.
- Yan L, Pape T, Elgar MA, Gao Y, Zhang D (2019) Evolutionary history of stomach bot flies in the light of mitogenomics. *Systematic Entomology*. <https://doi.org/10.1111/syen.12356>
- Zetterstedt JW (1844) *Diptera Scandinaviae disposita et descripta*. Tomus 3. Officina Lundbergiana, Lundae, 895–1280.
- Zhang D, Li X, Liu X, Wang Q, Pape T (2016) The antenna of horse stomach bot flies: Morphology and phylogenetic implications (Oestridae, Gasterophilinae: *Gasterophilus* Leach). *Scientific Reports* 6. <https://doi.org/10.1038/srep34409>
- Zhang D, Wang QK, Hu DF, Li K (2012) Sensilla on the antennal funiculus of the horse stomach bot fly, *Gasterophilus nigricornis*. *Medical and Veterinary Entomology* 26: 314–322. <https://doi.org/10.1111/j.1365-2915.2011.01007.x>
- Zumpt F (1965) *Myiasis of Man and Animals in the Old World*. Butterworths Ltd., London, 264 pp.
- Zumpt F, Paterson HE (1953) Studies on the family Gasterophilidae, with keys to the adults and maggots. *Journal of the Entomological Society of Southern Africa* 16: 59–72.